OVERCOMING INTRACELLULAR BARRIERS IN NON-VIRAL GENE DELIVERY: CHROMATIN TARGETING, MESSENGER RNA AND NON-CODING DNA

HET OVERWINNEN VAN INTRACELLULAIRE BARRIÈRES BIJ NIET-VIRALE GENTHERAPIE: CHROMATINEGERICHTE BINDING, MESSENGER RNA EN NIET-CODEREND DNA

Nathalie SYMENS
bioscience engineer

Thesis submitted in fulfillment of the requirements for the degree of
Doctor (Ph.D.) in Pharmaceutical Sciences

Proefschrift voorgedragen tot het bekomen van de graad van
Doctor in de Farmaceutische Wetenschappen

2012

Promoter: Prof. dr. Stefaan De Smedt
Co-promoters: dr. Katrien Remaut and dr. Joanna Rejman

Laboratory of General Biochemistry and Physical Pharmacy, Harelbekestraat 72, 9000 Ghent, Belgium

©

The author and the promoters grant the authorization to consult and to copy parts of this thesis for personal use only. Any other use is limited by the laws of Copyright, especially the obligation to refer to the source whenever results from this thesis are cited.

De auteur en de promotoren geven de toelating dit proefschrift voor consultering beschikbaar te stellen en delen ervan te kopiëren voor persoonlijk gebruik. Elk ander gebruik valt onder de beperkingen van het auteursrecht, in het bijzonder met betrekking tot de verplichting uitdrukkelijk de bron te vermelden bij het aanhalen van resultaten uit dit proefschrift.

Ghent, 19th of June 2012

Promoter:
Prof. dr. Stefaan De Smedt

Author:
Nathalie Symens

Co-promoters:
dr. Katrien Remaut

dr. Joanna Rejman

DANKWOORD

"Whatever you do will be insignificant, but it is very important that you do it."
Mahatma Ghandi (1869-1948)

De interpretaties die dit citaat uitlokken passen precies bij wat ik voel bij het afleveren van dit proefschrift. Mijn doctoraat was vooral een persoonlijke uitdaging en leerproces, dat op de gepaste momenten werd ondersteund en bijgestuurd door heel wat mensen. De ene heeft al meer invloed gehad dan de andere. De andere heeft het van meer dichtbij meegemaakt dan de ene. Op dit moment, deze mijlpaal rest er me al die mensen te bedanken. Omdat ik bang ben iemand te vergeten, wil ik allereerst zeggen aan **iedereen die meer of minder betrokken was** bij mijn doctoraat: een welgemeende dankjewel!

Verder wil ik de **Gentse universiteit** bedanken voor m'n beurs gedurende de eerste vier maanden en het agentschap voor Innovatie door Wetenschap en Technologie (**IWT**) voor m'n beurs tot het einde van m'n doctoraat. Ook dank dat deze voor een periode kon worden opgeschort en later verder kon worden opgenomen.

Uiteraard wil ik m'n promotor professor **Stefaan De Smedt** en de professoren **Jo Demeester** en **Kevin Braeckmans** bedanken voor het vertrouwen en om me de kans te bieden een doctoraat te verwezenlijken in hun lab. Dank voor alle voorzieningen die mijn werk mogelijk maakten. Stefaan, ik zal ook je paraatheid en interventie op die dag in januari 2009 niet vergeten.

Katrien Remaut, je was m'n co-promotor sinds de start. Ik vind het geweldig dat je me de XNER reactie hebt doen gebruiken. Dank je voor ons bezoek aan de groep van professor Iain Mattaj op het EMBL in Heidelberg. Uiteraard wil ik ook hem en de mensen van zijn lab bedanken. Katrien, bedankt voor de experimenten die je deed en voor het corrigeren van onze onderzoeksartikels en onze review.

Joanna, je werd op het einde van de rit m'n extra co-promotor. Jouw ongeëvenaarde kennis, passie en ervaring is van onschatbare waarde. Je was dan ook m'n raadgever van dienst. Dank je voor je hulp bij experimenten, de interessante discussies, het corrigeren van onze publicaties en m'n proefschrift en voor alles wat ik van je geleerd heb. Ik kan je niet genoeg bedanken. Je was er als co-promotor, als wetenschapper 'pur sang' maar ook als vriendin…Het ga je goed!

Ook wil ik een woordje van dank brengen aan de andere leden van de **lees- en examencommissie**: prof. Dieter Deforce, dr. Christophe Stove, prof. Daisy Vanrompay, dr. Enrico Mastrobattista, prof. Niek Sanders, prof. Peter Dubruel en dr. Raymond Schiffelers. Dank voor het beoordelen van m'n doctoraat en de daarmee samenhangende interessante discussies.

Marie-Luce, je was er van begin tot einde. We hebben heel veel aan elkaar gehad en het voelt dan ook goed om samen én succesvol deze periode af te sluiten. Ik vind dat je supertrots kan zijn op jouw doctoraat met dat recordaantal publicaties. Marie-Luce, met zo'n 'down to earth' mentaliteit en intelligentie, weet ik zeker dat er een mooie wetenschappelijke carrière ligt te wachten.

Bart Lucas, onze vaste waarde op het lab en dan bedoel ik ook 'waarde'. Je bent er altijd om net datgene te helpen zoeken wat nodig is. Je kijkt ook net iets verder of vanuit een andere hoek naar de projecten zodat je soms een héél andere discussie over de onderwerpen toelaat. Ik ben ervan overtuigd dat dit al velen van ons heeft vooruit geholpen. Dankjewel waarde collega en vriend!

José and **Alejandro**, I want to thank you for our fruitful and perfect collaboration. I hope we can stay in touch and I wish you all the best. **Alejandro**, thanks again for your hostility!

Anneleen, we zijn samen gestart op de faculteit als buitenbeentjes en we deelden lief en leed tot het eind. Het is ook tof en speciaal dat we konden schrijven naar dezelfde faculteitsraad toe en dat we dit hoofdstuk tegelijkertijd kunnen afronden. Ik wens je het allerbeste toe met je project bij Johnson & Johnson!

Mijn (ex-)bureaugenootjes **Stefaan Derveaux**, **Kevin Buyens**, **Koen Raemdonck**, **Bart Geers** en **Koen Rombouts** verdienen ook een speciaal woordje. Jullie zag ik in verhouding meer dan m'n andere collega's. Merci voor de leuke tijd, de grappige momenten, je luisterend oor en 'our office bond'!

Stefaan Derveaux en **Geertrui,** jullie wil ik nog eens apart bedanken voor de veilige bureaustoeltocht door de gangen naar de auto op die dag in januari 2009. Ik ben blij dat ik er nu dankzij jullie al lachend aan kan terug denken.

Dries, ik moet nu denken aan jouw dankwoord en wil ook zeggen dat ik dat tennisslagveld ook niet zo vlug zal vergeten. Dankjewel!

Broes, wij zijn samen gestart. Dat schept ook een band, vind je niet? Merci voor je steun en begrip, tout court je goede karakter, het opvrolijken van de sfeer waar je was en ook voor je constante paraatheid bij experimenten of computerproblemen. Ook **Thomas** wil ik hier uiteraard voor bedanken. Jij hebt nog even te gaan, maar dat komt zeker goed!

Hendrik, **Oliwia** en **Geertrui**, dank je voor de minder en meer serieuze gesprekken, leuke tijden, kortom jullie aangename gezelschap! Jullie zijn de volgende afleveraars. Alvast veel succes!

Stefaan Soenen, jij kwam ons wat later vervoegen. Merci voor je steun en vertrouwen. Alsook voor de mopjes als we alweer alleen of vroeg in het cellab waren. Stefaan, ik wens je een mooie academische carrière.

Lynn, jij was een van de collega's die ik, sinds je in ons lab kwam doctoreren, gewoon het 'meeste' zag. Je was een toffe en lieve collega die ook altijd bezig was in het cellab. Het ga je goed, meid! Jij samen met **Katrien Forier**, **Heleen**, **Laura** en **Ine De Cock** vormen de nieuwe vrouwen van het lab. Ik weet dat jullie je mannetje kunnen staan en wens jullie veel succes met je doctoraat.

Roos, **Sofie**, **Ine Lentacker**, **Lies**, **Barbara** en **Farzaneh**, de ervaren vrouwen van het lab en daarbuiten toen ik als groentje toekwam. Dank je voor de zovele babbels, steun alsook voor de gezellige lunches in de souperette.

Chaobo, zelfs na je doctoraat kan ik je nog steeds vragen naar de pdf's van interessante publicaties. Dank je. **Ranhua**, ook jou wens ik succes met je onderzoek.

Ook de vele **bezoekers** en mijn thesisstudenten, **Tieme**, **Tinne** en **Maja**, maar ook alle andere **thesisstudenten** wil ik niet vergeten. Door jullie werd een dynamische en een meer internationale sfeer in het lab verzekerd.

Katharine, **Bruno** en **Ilse**, jullie verdienen ook een speciaal woordje van dank. Merci om me te verlichten van alle administratieve zorgen tijdens en op het eind van mijn doctoraat alsook voor de aangename gesprekjes en (schuine) mopjes!

Uiteraard wil ik ook **al m'n (ex)-collega's samen** nog eens bedanken voor de aangename tijd op het lab, de helpende handen, de leuke babbels en de gedenkwaardige activiteiten buiten het lab zoals de labweekends en feestjes. Merci!

Jurgen, jou wil ik speciaal bedanken voor het ontwerpen en schrijven van de tekst op de cover van mijn proefschrift.

Zonder de enorme steun en het vertrouwen van m'n stevige achterban zou dit proefschrift er niet uitzien zoals het nu is. Allemaal heel erg bedankt! **Dokters** en **therapeuten**, dankjewel voor de steun en hulp bij m'n revalidatie. **Vrienden bio-ingenieurs**, **vrienden vanuit Sint-Lodewijks**, **vrienden van de Chiro**, **vrienden via vrienden**, **vrienden van het FFW** en **alle andere vrienden**, ik wens jullie allemaal te bedanken voor de steun en de vele leuke ontspannende activiteiten, avonden, koffiekransjes... en enkelen onder jullie specifieker voor je hulp bij experimenten of het nalezen van de Nederlandse samenvatting. **Mamies**, **papies**, **tantes**, **nonkels**, **neven** en **nichten**, dankjewel voor je interesse, je medeleven en onze leuke samenkomsten. **Papie**, dank je voor het ontwerp van de cover van mijn proefschrift. Dit maakt het voor mij nog specialer. **Mama**, **papa**, **Liesbeth**, **Barbara** en **Isabel**, dank je voor je weet wel: alles! I love you!

Nathalie

"Minds are like parachutes... they only function when open."

Thomas R. Dewar (1864 - 1930)

TABLE OF CONTENTS

Table of contents		1
List of abbreviations and symbols		3
Study objectives		7
CHAPTER 1	Review on intracellular partitioning of cell organelles and exogenous nanoparticles during mitosis	9
CHAPTER 2	Nuclear inclusion of non-targeted and chromatin-targeted polystyrene beads and plasmid DNA-containing nanoparticles	75
CHAPTER 3	How does non-coding DNA influence lipofection efficiency in HeLa cells?	101
CHAPTER 4	Efficient transfection of hepatocytes mediated by mRNA complexed to galactosylated cyclodextrins	135
Summary and general conclusions		193
Samenvatting en algemene besluiten		197
Curriculum vitae		203

LIST OF ABBREVIATIONS AND SYMBOLS

AIBN	azobisisobutyronitrile
ASGPr	asialoglycoprotein receptor
ASV	avian sarcoma virus
AT	adenosine monophosphate thymidine monophosphate
ATP	adenosine triphosphate
BAF	barrier-to-autointegration factor
BET	bromodomain and extra-terminal
bp	base pair
BPV	bovine papillomavirus
Brd4	double bromodomain protein 4
BSA	bovine serum albumin
Bub1	kinetochore protein budding uninhibited by benzimidazole 1
CD	cyclodextrin
CDK	cyclin-dependent kinase
CDplexes	cyclodextrin/nucleic acid complexes
CF	cystic fibrosis
CFTR	cystic fibrosis transmembrane conductance regulator
CGN	*cis*-Golgi network
CLSM	confocal laser scanning microscopy
COSY	correlation spectroscopy
CpG	cytosine monophosphate guanine
Cy	cyanine
DAPI	4', 6-diamidino-2-phenylindole
DCM	dichloromethane
$DiIC_{18}$	1,1'-dioctadecyl-3,3,3',3'-tetramethylindocarbocyanine perchlorate
DMAEA	dimethylamine ethylamine
DMEM	Dulbecco's modified Eagle's medium
DMEM-F12	Dulbecco's modified Eagle's medium: nutrient mixture F-12
DMF	*N,N*-dimethylformamide
DNA	deoxyribonucleic acid
DOPE	1,2-dioleoyl-glycero-3-phosphoethanolamine
DOTAP	1,2-dioleoyl-3-trimethylammonium-propane
dsDNA	double stranded DNA
DTS	DNA nuclear-targeting sequence
EBNA1	Epstein Barr virus nuclear antigen 1
EBP2	nucleolar EBNA1 binding protein 2
EBV	Epstein Barr virus
ECM	extracellular side of the plasma membrane
E. coli	*Escherichia coli*
EDC	1-ethyl-3-(3-dimethylaminopropyl) carbodiimide hydrochloride

ELYS	embryonic large molecule derived from yolk sac
EMA	European Medicines Agency
ER	endoplasmic reticulum
ESIMS	electrospray mass spectra
FBS	fetal bovine serum
FDA	food and drug administration
FISH	fluorescent *in situ* hybridization
FRET	fluorescence resonance energy transfer
FV	foamy virus
G_0	postmitotic rest phase
G_1	growth phase
G_2	gap 2 phase
gaCDs	neutral glycoamphiphilic cyclodextrins
Gag	group-specific antigen
Gal10CDs	10% tri-antennary-galactose-bearing Hex-CD-N_{21}
Gal12CDs	12% tri-antennary-galactose-bearing Hex-CD-N_{21}
GalPEGCDs	10% thio-PEG5000-tri-antennary-galactose-bearing Hex-CD-N_{21}
GFP	green fluorescent protein
GPC	gel permeation chromatography
GST	glutathione-S-transferase
GTP	guanine triphosphate
H1	histone 1
H2A-H2B	histone 2A-histone 2B pocket
HeLa	human epithelial cervical cancer cells (Henrietta Lacks)
HEPES	4-(2-hydroxyethyl)-1-piperazineethanesulfonic acid
HepG2	human hepatoblastoma cells
Heptakis	[6-(2-(*N'*-(2-(*N,N*-bis-(2-aminoethyl)amino)ethyl)thioureido)ethylthio)-2,3-di-*O*-hexanoyl]cyclomaltoheptose
Hex-CD-N_{21}	a paCD: hexanoyl cyclodextrin with 21 protonable nitrogens
HHV	human herpesvirus
HIV	human immunodeficiency virus
HMG	high mobility group
HMGA2β	high mobility group AT-hook 2 isoform β
HMQC	heteronuclear multiple quantum correlation
HPV	human papillomavirus
HSQC	heteronulcear single quantum correlation
HVS	herpesvirus saimiri
ICM	intracellular side of the plasma membrane
IFN	interferon
IL-33	interleukin 33
IN	integrase
INM	inner nuclear membrane
IONP	iron oxide nanoparticle

kb	kilobase
kDa	kilodalton
KSHV	Kaposi sarcoma associated herpesvirus
LANA	latency associated nuclear antigen
LDLR	low density lipoprotein receptor
LEDGF/p75	endogenous lens epithelium derived growth factor/p75
LEM	Lap2, Emerin, Man1
M	mitosis
MA	matrix
Mel-28	maternal effect lethal 28
MHz	megahertz
MTOC	microtubule organizing center
mRNA	messenger RNA
MuLV	murine leukemia virus
mV	millivolt
NE	nuclear envelope
NEBD	nuclear envelope breakdown
NHS	N-hydroxysuccinimide
NLS	nuclear localization signal
nm	nanometer
NMR	nuclear magnetic resonance
N/P ratio	the ratio of moles of the amine groups of the specific cationic carrier to those of the phosphate groups of the nucleic acids
NPC	nuclear pore complex
NuSAP	nucleolar and spindle associated protein
ONM	outer nuclear membrane
oriP	origin of replication
paCD	polycationic amphiphilic cyclodextrin
PBS	phosphate buffered saline
PC	phosphatidylcholine
PCI	photochemical internalization
pDNA	plasmid DNA
PE	phosphatidylethanolamine
PEG	polyethylene glycol
PEGCDs	13% thio-PEG5000-bearing Hex-CD-N_{21}
PEI	polyethyleneimine
PFA	paraformaldehyde
pg	picogram
PhSen	photosensitizer
PIC	pre-integration complex
PolyA	poly adenine
PS	phosphatidylserine
QD	quantum dot

Reference CD	Hex-CD-N_{21} as a reference to evaluate the effect of galactose; this compound is not a reference for other paCDs
RER	rough endoplasmic reticulum
RNA	ribonucleic acid
ROS	reactive oxygen species
RT	room temperature
S	DNA synthesis phase
SAF-A	scaffold attachment factor A
S/MAR	scaffold/matrix attachment region
SNV	spleen necrosis virus
SV40	Simian vacuolating virus 40
Tf_2O	trifluoromethanesulfonic anhydride
TGN	*trans*-Golgi network
TLC	thin-layer chromatography
TLR	toll-like receptor
TOCSY	total correlation spectroscopy
TPP	triphenylphosphine
TRITC	tetramethyl rhodamine isothiocyanate
UTR	untranslated region
UV	ultraviolet
Vpr	viral protein R
VSV-G	vesicular stomatitis virus glycoprotein G
XNER	*Xenopus* nuclear envelope reassembly

LIST OF SYMBOLS

Å	Angström
λ_{em}	emission wavelength
λ_{ex}	excitation wavelength
µg	microgram
µl	microliter
µM	micromolair
ζ	zeta potential

STUDY OBJECTIVES

In principle, gene therapy could increase or restore the expression of virtually any protein in a cell. This in consequence could bring a cure for various inherited or acquired genetic diseases. In spite of years of extensive research, gene delivery by non-viral carriers has not met with these expectations. None of numerous polymeric and lipidic nucleic acid carriers has received approval from the Food and Drug Administration (FDA) and the European Medicines Agency (EMA), which indicates that existing carriers do not possess suitable properties to ensure safe and effective *in vivo* delivery of nucleic acids. One of the reasons is the low frequency at which plasmid DNA (pDNA) reaches its target, the nucleus. This is mostly due to the presence of multiple extracellular and intracellular barriers which have to be overcome before pDNA can be transcribed. For example, when particles carrying pDNA are administered systemically, they should be stable in the blood stream and be able to reach the target organ. Moreover, these particles should evade clearance by the immune system. Once the particles reach the organ of interest, they should be taken up only by desired cell subpopulations. The internalized particles should then timely escape the endosomal compartment. pDNA in the cytosol should be protected against degradation by nucleases and should be transported toward the nucleus. The nuclear envelope (NE) is one of the most difficult intracellular barriers to overcome. In non-dividing cells the only way for pDNA to enter the nucleus is via the nuclear pore complexes (NPCs). This process is very inefficient due to the size limit of the pores. In dividing cells, the NE is timely disassembled during mitosis allowing pDNA enclosure in the newly formed daughter nuclei. To ensure transfection, intranuclearly located pDNA should be able to reach transcription-active sites.

The research presented in this thesis focused on overcoming the intracellular barriers that limit non-viral delivery of pDNA. The **first chapter** provides a detailed overview on intracellular partitioning of cell organelles, foreign macromolecules and nanoparticles during mitosis. Moreover, it highlights how viruses take advantage of cell division to transfer or segregate their genetic information into the daughter nuclei. It also proposes strategies to enhance non-viral gene delivery in dividing cells. **Chapter 2** reports on one of these strategies. Specifically, the nuclear inclusion of fluorescent polystyrene nanospheres and pDNA-containing nanoparticles modified with chromatin-binding peptides was studied. Initially, the nuclear inclusion was followed in the cell-free *Xenopus* nuclear envelope reassembly (XNER) model in which artificial nuclei are formed. The same particles were also injected and followed in living cells. In **chapter 3**, the effect of non-coding DNA co-delivered with coding pDNA on transfection efficiency mediated by lipoplexes was studied. Non-coding pDNA in

supercoiled and linear form as well as non-coding salmon DNA were evaluated for their influence on transfection efficiency. It was further investigated at which level(s) of the transfection pathway the presence of non-coding DNA becomes essential. In **chapter 4**, polycationic amphiphilic cyclodextrins (paCDs) were assessed as nucleic acids carriers. mRNA-based transfection was presented as an alternative to pDNA-based transfection in slowly dividing cells. The specific uptake of complexes of galactosylated paCDs and mRNA via asialoglycoprotein receptors (ASGPr) on the surface of hepatocytes was also evaluated.

1

REVIEW ON INTRACELLULAR PARTITIONING OF CELL ORGANELLES AND EXOGENOUS NANOPARTICLES DURING MITOSIS

Parts of this chapter are published in:

Nathalie Symens, Stefaan J. Soenen, Joanna Rejman, Kevin Braeckmans, Stefaan C. De Smedt and Katrien Remaut. Intracellular partitioning of cell organelles and extraneous nanoparticles during mitosis. *Advanced Drug Delivery Reviews* **64** (1), 78-94 (2012).

Laboratory of General Biochemistry and Physical Pharmacy, Faculty of Pharmaceutical Sciences, Ghent University, Harelbekestraat 72, 9000 Ghent, Belgium.

ABSTRACT

The nucleocytoplasmic partitioning of nanoparticles as a result of cell division is highly relevant for the field of non-viral gene delivery. Therefore, we reviewed the literature on intracellular distribution of cell organelles (endosomal vesicles, Golgi apparatus, endoplasmic reticulum and nucleus), foreign macromolecules (dextrans and plasmid DNA) and inert nanoparticles (gold, quantum dot, iron oxide and polystyrene) during mitosis. Further, we describe how retroviruses and latent DNA viruses take advantage of mitosis to transfer their viral genome and to segregate their episomes into host daughter nuclei, respectively. Based on this knowledge we propose strategies to improve non-viral gene delivery in dividing cells with the ultimate goal to design non-viral gene delivery systems which are as efficient as their viral counterparts, but which are non-immunogenic, non-oncogenic and easy to prepare.

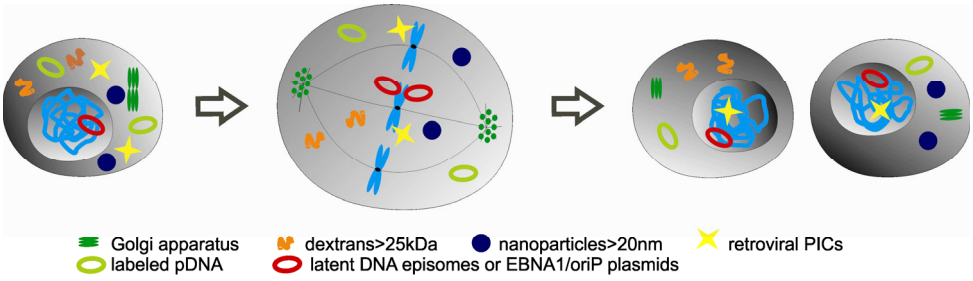

Abstract figure. Intracellular distribution of cell organelles (Golgi apparatus), macromolecules (dextrans, labeled pDNA and episomes) and nanoparticles (nanoparticles > 20 nm and retroviral PICs) during and after cell division.

1

INTRACELLULAR PARTITIONING OF CELL ORGANELLES AND EXOGENOUS NANOPARTICLES DURING MITOSIS

TABLE OF CONTENTS

1. General introduction 12
2. Breakdown and reassembly of the nuclear envelope during mitosis 14
   - 2.1. Nuclear envelope structure 14
   - 2.2. Nuclear envelope breakdown 16
   - 2.3. Nuclear envelope reassembly 17
3. Mitotic partitioning of cell organelles 18
   - 3.1. Early endosomes, late endosomes and lysosomes 18
   - 3.2. Golgi apparatus and endoplasmic reticulum 19
4. Mitotic partitioning of macromolecules 20
   - 4.1. Dextrans 20
   - 4.2. Free plasmid DNA 23

5. Mitotic partitioning of inert quantum dots, gold, polystyrene and iron oxide nanoparticles 25
6. Effect of cell division on non-viral gene delivery particles 29
7. Viruses taking advantage of mitosis 34
   7.1. Retroviruses 34
   7.2. Latent DNA viruses 38
8. Reflections on strategies for the improvement of nuclear inclusion of exogenous nucleic acids or other macromolecules 40
   8.1. Chromatin targeting 41
   8.2. Targeting non-chromatin nuclear elements 47
   8.3. Cell-division responsive nanoparticles 48
   8.4. *Xenopus* nuclear envelope reassembly assay to study nuclear envelope dynamics 49
9. Messenger RNA as an alternative to plasmid DNA 51
10. General conclusions 55

1. GENERAL INTRODUCTION

Gene therapy using plasmid DNA (pDNA) aims at inducing protein production by the administration of pDNA that encodes for the desired protein. To date, several hurdles still need to be overcome to allow highly efficient delivery of drugs or genes at the desired intracellular location. For gene therapy to be successful, pDNA should reach the transcription machinery in the nucleus of the target cells. Nucleic acids should also remain intact as their sequence ensures their biological activity. In recent years the notion that for maximal transfection the pDNA not just needs to reach the nucleus, but rather gain access to the right intranuclear compartment has been gaining increasing recognition[1-3]. Moreover, transfection efficiency can differ substantially between cell types, and within one cell type, between various phases of the cell cycle[4, 5].

The cell cycle can be divided into 4 phases: growth or G_1 phase, DNA synthesis or S phase, gap 2 or G_2 phase and mitosis or M phase. G_1/S/G_2 phases together are named the interphase, in which the cells prepare themselves for mitosis. During each cell cycle, the nuclear genome is doubled in S phase and the two identical genomic copies are subsequently separated into both daughter cells during M phase. The typical length of the cell cycle can differ substantially between species, but generally mitosis is completed within 1 - 1.5 hours and cells remain most of the time in interphase (e.g. approximately 8, 6 and 5 hours for G_1/S/G_2 in humans). Cells which do not divide are considered to be in a postmitotic rest phase or G_0 phase. Mitosis itself is divided into several distinct subphases: i) prophase, in which the chromatin condenses into chromosomes and the nuclear envelope breaks down (NEBD), ii) metaphase, in which the chromosomes align themselves along the metaphase plate iii) anaphase, in which the sister chromatids are separated by moving to the opposite poles and iv) telophase/cytokinesis in which the nuclear envelope (NE) is reassembled around the segregated chromatids and the cell divides into two daughter cells. The different stages of the cell cycle are controlled by subsequent phosphorylation and dephosphorylation reactions governed by cyclins and cyclin-dependent kinase (CDK) complexes, which are strictly controlled both in space and in time[6, 7]. Several checkpoints verify the completion of the processes at each phase of the cell cycle before progression into the next phase is allowed.

It has been shown that cells which do not go through M phase are difficult to transfect[5, 8]. The main reason for this is the NE, which consists of two phospholipid bilayers[9-11]. The outer nuclear membrane (ONM) and the inner nuclear membrane (INM) are connected in places to form the nuclear pore complexes (NPCs). In interphase, pDNA can only gain access to the nuclear interior through the small central channel of the NPCs, which is a very inefficient process. Although some gene delivery systems are cell cycle-independent[12], most of them profit from the process of cell division[5, 8, 13-18]. The majority of higher eukaryotes undergo 'open mitosis', characterized by the complete disassembly of the NE allowing the intermixing of

nucleoplasmic and cytoplasmic components. At the end of mitosis, the NE reconstitutes and the cytoplasm and nucleoplasm unmix again. It is likely that certain cytoplasmic components can gain access to the nucleoplasm during these mitotic mixing and unmixing events. In this review, we will first focus on the cellular machinery involved in NE breakdown and reassembly during mitosis. Secondly, we will review the fate of cell organelles, macromolecules and non-viral nanoparticles during mitosis. Further, we will focus on the mechanisms employed by certain viruses to deliver their genome into the cell nucleus or segregate their latent episomes to progeny cells during mitosis (**Table 1**). Based on this knowledge we will propose experimental approaches which could enhance the intranuclear delivery of non-viral gene delivery complexes during cell division. Moreover, we will discuss the application of messenger RNA (mRNA) instead of pDNA, that only needs to reach the cytosol to exert its biological function.

2. BREAKDOWN AND REASSEMBLY OF THE NUCLEAR ENVELOPE DURING MITOSIS

2.1. Nuclear envelope structure

In eukaryotic cells, the genetic material is kept inside the nucleus, surrounded by the NE which physically separates the nucleoplasm from the cytoplasm. It consists of two phospholipid bilayers composed of the ONM, which is continuous with the endoplasmic reticulum (ER), and the INM which interacts with the underlying lamina and chromatin through several integral and associated membrane proteins (**Fig. 1**)[19, 20]. The NE is equipped with NPCs which regulate traffic between the cytoplasm and the nucleus. These 125 kDa large multi-protein complexes contain an hydrophobic channel that permits passive transport of molecules up to 10 nm in size. Larger molecules require a nuclear localization signal (NLS) that can enlarge the central channel of the NPCs up to 40 nm[21]. NPCs are strongly anchored in the NE and are composed of strongly associated nucleoporin complexes[22]. NPCs are assumed to play a role in gene regulation since activated genes associate with the NPCs. Furthermore,

they can maintain a 'transcriptional memory': previously transcribed genes are retained at the NPCs and show an accelerated gene expression following reactivation. Interestingly, this transcriptional memory can be maintained even after cell division[23]. The 30 – 100 nm thick nuclear lamina is located in-between the chromatin and the INM. It provides mechanical strength and transcriptional regulation to the cell nucleus and is composed of type A and type B lamins and lamin-associated proteins which are often integral proteins of the INM[24]. Many of these INM proteins contain the LEM-domain (Lap2, Emerin, Man1), through which they bind the lamins, as well as other components such as the barrier-to-autointegration factor (BAF). BAF in turn can bind dsDNA, chromatin and transcription activators, thereby connecting the nuclear lamina to the peripheral chromatin[25, 26]. Due to multiple interactions between the lamina and the chromatin, the lamins play an important role in the regulation of transcription in response to a chemical or mechanical stimulus[23]. If the nuclear lamina is affected in so-called laminopathies, this can drastically alter the expression profile of the cell[27]. The most striking example is probably molecular aging in Hutchinson-Gilford progeria syndrome, which is the result of a single mutation in lamin A[28].

In the cell nucleus, DNA is packed with histones into chromatin. In interphase, at least two types of chromatin can be distinguished: a lightly packed form of chromatin (euchromatin) that has greater potential to be transcribed and highly condensed chromatin (heterochromatin) that is generally transcriptionally inactive. When the chromosomes are formed during mitosis, the chromatin is arranged into its most compact form. Euchromatin is generally found in the core of the nucleus, while heterochromatin is located closer to the lamina, suggesting that the nuclear interior promotes gene expression, whereas the nuclear periphery promotes gene silencing, except in the areas close to NPCs[23, 29].

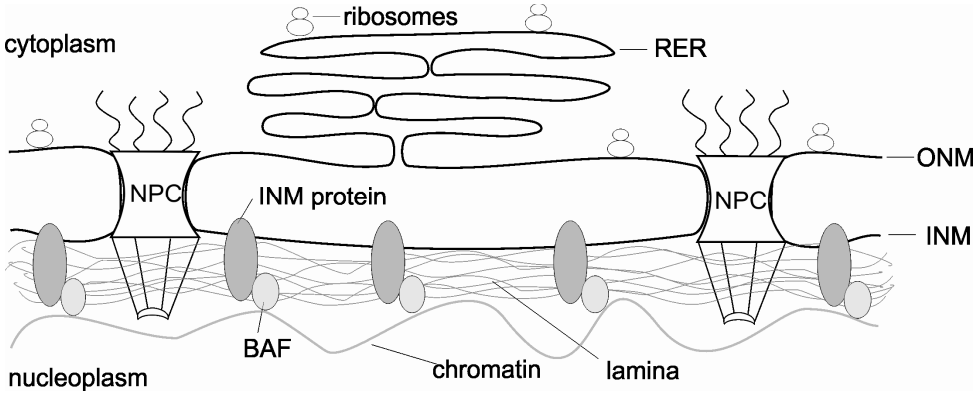

Figure 1. Structure of the nuclear envelope (NE). The NE consists of an outer nuclear membrane (ONM) continuous with the rough endoplasmic reticulum (RER), and the inner nuclear membrane (INM). ONM and INM are connected in places to form nuclear pore complexes (NPCs). Barrier-to-autointegration factor (BAF) is a chromatin-associated protein that also binds to the nuclear lamina and several nuclear envelope proteins.

2.2. Nuclear envelope breakdown

In the process called 'open mitosis', the NE completely disassembles, resulting in the intermixing of nucleoplasmic and cytoplasmic components. The stepwise process of NEBD is initiated at late prophase by a series of CDK1-dependent phosphorylations of nucleoporins, lamins and integral membrane proteins from the INM[30]. The initial step of NEBD is the partial disassembly of the NPCs. This increases the passive permeability of the NPCs to molecules up to about 40 nm, thereby promoting the nuclear import of larger cytoplasmic molecules such as tubulin, a major component of the mitotic spindle[31]. Subsequently, the core nucleoporins are released, resulting in the complete disassembly of the NPCs. The complete disassembly of the NPCs is a rapid process, which is completed in minutes. Initially the NE elements were thought to be distributed in the cytoplasm in vesicular form. Currently it is becoming more and more evident that most NE membranes and their associated proteins are resorbed in the ER[19]. As the final step in NEBD, the nuclear lamina depolymerizes and INM proteins dissociate from the lamins and the chromatin.

2.3. Nuclear envelope reassembly

During anaphase, the sister chromatids are moving to opposite poles by shortening of the microtubuli[32]. This results in the physical separation of two sets of identical chromosomes, around which a new NE is formed. This NE starts to reassemble in late anaphase and NE formation is completed at telophase/cytokinesis, when two daughter cells are formed. To prevent non-nuclear material to end up in the nucleus, it is important to securely unmix the cytoplasmic and nucleoplasmic elements. Also, all chromatin should be included in only one nucleus, avoiding the formation of a second so-called 'micronucleus' around chromosomes which were separated from the rest. To facilitate this process, chromatin is in its most condensed state when the NE has to reform[33]. The different phases of the NE reassembly include targeting of proteins to chromosomes, assembly of the NPCs, recruitment and fusion of membrane elements and nuclear import of lamins. In contrast to NEBD, which is triggered by a series of phosphorylation reactions, a series of dephoshorylation events coordinates the NE assembly.

Two different models exist for the NE assembly. In the 'insertion model', NPCs are inserted in the already formed NE. In the 'prepore' model, first the so-called prepores or pre-NPCs are formed, which is followed by the formation of the NE in-between these pores. It was previously thought that membrane elements could bind to chromatin in the form of membrane vesicles, which would ultimately fuse to form the NE[34-36]. Currently, however, it is thought that the NE reappears from the ER, where it is redistributed during NEBD. The binding of ER tubules to the chromatin most likely occurs through INM proteins. The ER tubule tips flatten then to form membrane sheets and eventually the closed NE. The holes which still exist could then be 'filled' with NPCs[37]. Very recently, Lu *et al*.[38] presented evidence that is in favor of the insertion model. The authors found that the NE reassembly primarily occurs by coordinated direct contact of ER cisternae with the chromosomes and that a functional NPC is only formed when NE formation at that site was completed. Both in the insertion and the prepore model, the final step in NE formation is the import of

lamins through the rebuilt NPCs and the assembly of the nuclear lamina through dephosphorylation of B-type lamins[7, 33]. It is not clear whether the nuclear lamina already binds to specific parts of the chromatin when it assembles or that it initially binds at random and rearranges according to the gene expression needs by detachment and rebinding afterwards[37].

3. MITOTIC PARTITIONING OF CELL ORGANELLES

As described above, the predominant function of cell division is to deliver a complete set of chromosomes to the two daughter cells. In addition, it should ensure appropriate distribution of key organelles located in the cytosol and prevent non-nuclear material to be included in the daughter nuclei. The latter can occur through exclusion from condensed chromatin throughout mitosis and completion of NE assembly before nuclear expansion[39]. Vesicular particles such as early or late endosomes and lysosomes are distributed in large numbers throughout the cytoplasm. On the other hand, the endoplasmic reticulum (ER) and Golgi apparatus exist as single or low-copy organelles. Therefore, it is conceivable that their partitioning during mitosis will display significant differences.

3.1. Early endosomes, late endosomes and lysosomes

Distinctive pathways of endocytosis serve to assure efficient uptake of macromolecules and (gene delivery) particulate formulations by cells. Early or late endosomes and lysosomes are prime players in this process. Bergeland *et al.*[40] studied mitotic partitioning of early and late endosomes and observed that none of the endocytic vesicles fragmented or fused during cell division. Even though the numbers of both types of endosomes in the two daughter cells were roughly the same, no evidence for a strict mechanism guaranteeing their equal distribution was found. This observation was confirmed by others[41], leading to a model in which the partitioning of vesicles in the cytoplasm occurs passively but equally between the two

daughter cells. In this model, it is assumed that the more vesicles are present in the cytoplasm, the more accurate their partitioning.

Dunster *et al.*[41] found that late endosomes and lysosomes were inherited by daughter cells in a different manner than early endosomes. It was shown that clustering of early endosomes occurs in a directed manner, which implies active partitioning of the organelles among the daughter cells, most likely dependent on the mitotic spindle and interphase microtubule scaffold[40, 41]. This was confirmed by the observation that soon after cytokinesis endosomal vesicles accumulate in the area of the microtubule organization center (MTOC)[40].

3.2. Golgi apparatus and endoplasmic reticulum

In mammalian interphase cells, the Golgi apparatus is typically positioned close to the centrosome, at one side of the nucleus[41, 42]. It consists of a stack of disk-shaped membranes (cisternae) surrounded on each side by dense tubular-reticular networks called the *cis*- (CGN) and *trans*-Golgi network. The Golgi apparatus accommodates the enzymes needed for specific modifications of protein- and lipid-bound oligosaccharides on their way from the ER to their ultimate destination. The CGN participates in the recycling of proteins between the Golgi apparatus and the ER[43]. The TGN plays a key role in protein and lipid sorting for different intracellular destinations[44].

Interestingly, it was observed already more than 100 years ago that the very characteristic stack-like organization of the Golgi apparatus changes remarkably at the onset of mitosis[45]. Electron microscopy studies published in the late 1980's clearly demonstrated that the number of Golgi stacks decreases considerably at the onset of cell division[46, 47]. This disappearance of Golgi stacks is accompanied by the appearance of large numbers of tubular and vesicular structures, which were proven to derive from the Golgi apparatus[47, 48]. The fragmentation of the Golgi apparatus into hundreds of tubular and vesicular structures (between 50 and 250 nm in size) is considered to facilitate its uniform distribution between the daughter cells[47, 49]. As for

the partitioning of endocytic vesicles, the partitioning of Golgi fragments is believed to be random and from a statistical point of view its accuracy depends on two factors: the number of organelle units and their distribution in the cytosol. The larger the number of units and the more evenly they are allocated in the cytosol, the more accurate is their partitioning[49]. This random partitioning has been challenged by Shima *et al.*[50] who demonstrated that the Golgi distribution between two daughter cells is too precise for a stochastic process. Later reports have demonstrated the involvement of the mitotic spindle in the organization of at least a part of Golgi-derived structures during cell division, suggesting some sort of active segregation mechanism for these cell organelles[41, 51].

In addition to the passive or active model of segregation of cell organelles, for the Golgi apparatus a third possible segregation mechanism has been proposed[52, 53]. This model assumes that the Golgi apparatus behaves more like the NE and during cell division temporary disappears and redistributes to the ER, from which it reappears when the daughter cells are formed. The ER can thus be considered as the storage for NE and Golgi apparatus elements during mitosis. The formation of the NE around the sister chromatids assures the equal partitioning of ER and NE elements between the two daughter cells. Likewise, the Golgi apparatus that is also resorbed into the ER, can reappear in the daughter cells, resulting in its efficient partitioning. At the end of mitosis the Golgi apparatus starts to reassemble again. The vesicles fuse with each other which results in the formation of several well defined stacks[48]. They are carried to the perinuclear region by a mechanism depending on microtubules[54].

4. MITOTIC PARTITIONING OF MACROMOLECULES SUCH AS DEXTRANS AND FREE PLASMID DNA

4.1. Dextrans

Dextrans are electroneutral hydrophilic D-glucose polymers. Therefore, they behave as relatively inert molecules inside cells: self-aggregation or binding to other cellular structures is negligible and they show no toxicity even at high concentrations and

over prolonged periods. Dextrans are commercially available in practically any molecular weight[55]. With increasing molecular weight, neither shape nor surface properties of dextrans change. Consequently, dextrans are perfectly suited as molecular standards to measure the permeability of pores and channels[31].

At first glance, nuclear entry during mitosis would appear to be a passive process, as NEBD would allow (exogenous) macromolecules to enter compartments which will be included in the nuclei when they reassemble. However, distribution of cellular components between the cytoplasm and the nucleoplasm is tightly controlled both during interphase and mitosis. As a result, there is only a small effect of cell division on the partitioning of exogenous macromolecules. Swanson and McNeil[39] and Benavente *et al*.[56] were the first to report that only the chromosomes themselves and the macromolecules physically associated with them (e.g. the perichromosomal layer[57-59]) are included in newly formed nuclei, while organelles (**as described in section 3**) and other large macromolecules which cannot pass the NPCs are excluded. Swanson and McNeil[39] have reported that after scratch-loading of the cells, the fluorescently labeled large dextrans (> 25 kDa) did not appear in the nuclei, even when cells went through mitosis. Dextrans smaller than 20 kDa, however, were observed in the nuclei of interphase cells regardless of cell division as they can enter the nucleus through the NPCs of the intact NE. These observations were confirmed by Ludtke *et al*.[60] (**Fig. 2**) who found that after cytoplasmic injection, the labeled large dextrans remained outside the nucleus regardless of mitosis. After nuclear injection, the labeled large dextrans were localized in the nucleus of cells which did not divide and outside the nucleus of cells which divided. Also Lenart *et al*.[31] found that labeled large dextrans were excluded from reassembled nuclei after mitosis. Thus, cellular compartmentalization at telophase appears to be a two-step process. First, the NE tightly encloses the condensed chromosomes, excluding non-selectively all macromolecules not associated with the chromosomes. Then, selective NPC-mediated import of nuclear proteins from the cytoplasm leads together with the decondensation of the chromosomes to nuclear expansion and the interphase

nuclear organization[39, 56]. It should be noted that Miyawaki *et al*.[61] identified that the NE barrier is more permeable during a short period directly after cytokinesis as a large molecule (210 kDa) diffused across the NE. They saw a subtle but substantial decrease in the diameter of the aqueous channels through the NE formation: it was ~10 nm immediately after cytokinesis and reduced to ~8 nm in 30 minutes. It remains to be elucidated whether the passive diffusion is due to incompleteness of the NE sealing or altered NPC functions after nuclear reassembly. According to the findings, at least a fraction of macromolecules which are normally not able to pass the NPCs should be able to reach the cell nucleus shortly after cytokinesis.

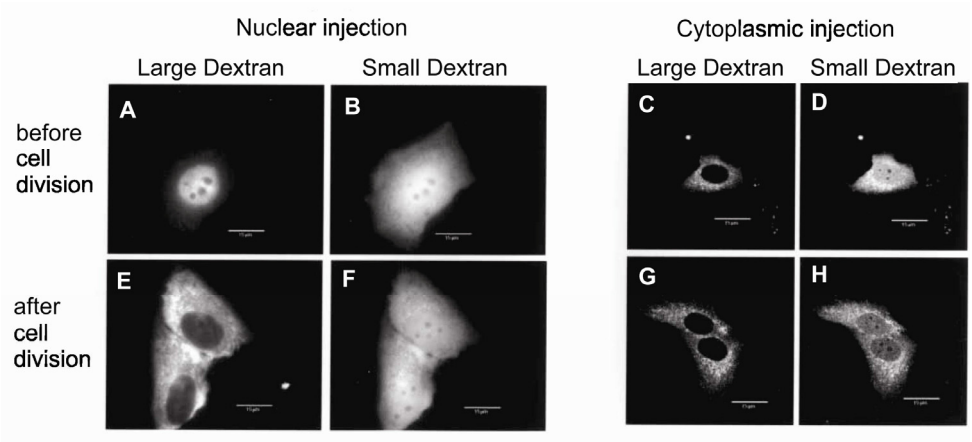

Figure 2. Subcellular distribution of dextrans. Cells were injected with rhodamine-labeled small dextran (11 kDa) and fluorescein-labeled large dextran (485 kDa). **(A, B, E, and F)** Nuclear injection. **(C , D, G and H)** Cytoplasmic injection. **(A - D)** Dextrans distribution before cell division. **(E - H)** Dextrans distribution after cell division. **(A), (B), (E),** and **(F)** are epifluorescent images. **(C), (D), (G)** and **(H)** are single optical sections of confocal images. Scale bars, 15 µm. (Reprinted by permission from Macmillan Publishers Ltd: [Molecular Therapy][60], copyright (2002), DOI: 10.1006/mthe.2002.0581, http://www.nature.com/mt/journal/v5/n5/full/mt200282a.html)

4.2. Free plasmid DNA

The use of non-viral vectors for gene therapy is hampered by poor transfection efficiencies, largely because of the metabolic instability of pDNA in the cytosol, the inability of pDNA to diffuse freely through the dense cytoplasm and to travel through the NPC[10, 62-64]. It has been reported that only 1 in 10^4 pDNA molecules is able to translocate from the cytoplasm to the nucleus[65]. Several attempts to improve the entry of pDNA into the nucleus have been reported. These include the use of electrostatic binding of DNA to cationic nuclear localization signal (NLS)-containing proteins or peptides[66], as well as covalent attachments of NLS peptides to DNA[67]. Additionally, the effect of inclusion of DNA nuclear-targeting sequences (DTSs) like the Simian vacuolating virus 40 (SV40) enhancer sequence in the pDNA was investigated[68]. Another strategy was to increase the permeability of the NPCs with *trans*-cyclohexane-1,2-diol[69]. All these attempts have met with limited success.

A few studies have focused on the fate of pDNA during cell division. Dowty *et al*.[70] reported an interesting study where electron microscopy was used to determine the precise intracellular localization of gold-labeled pDNA which was microinjected into the cytoplasm. The authors observed that the distance between the cytoplasmic site of delivery of pDNA and the nucleus is a key determinant for nuclear incorporation of DNA. Only when pDNA was injected close to the nucleus, nuclear translocation was observed, regardless of the cell cycle status. They have seen that pDNA entered postmitotic nuclei of primary rat myotubes and concluded that cell division-dependency for pDNA to enter the nucleus is also cell type-dependent. Remaut *et al*.[71] injected unlabeled pDNA in the nucleus or the cytoplasm of the cells. The authors observed expression of the supercoiled pDNA upon nuclear injection even at low pDNA concentrations. Cell division and a high concentration of supercoiled pDNA were required to reach comparable transfection efficiencies when pDNA was injected in the cytoplasm. More detailed studies on the intracellular behaviour of pDNA were performed by Ludtke *et al*.[60] and Gasiorowski and Dean[72]. Ludtke *et al*.[60] microinjected naked labeled pDNA into the cyto- or nucleoplasm. Randomly labeled

pDNA resembles the intracellular localization pattern of large dextrans as described in section 4.1 (**Fig. 2**). Following mitosis, the labeled pDNA was always localized in the cytosol, regardless of prior cyto- or nucleoplasmic microinjection. Gasiorowski and Dean[72], have shown that naked unlabeled plasmids microinjected directly into nuclei and later detected by FISH were found almost exclusively and in equal amounts within the nuclei of the daughter cells after mitosis. On the other hand, when plasmids were randomly labeled with several commercially available fluorescent DNA labeling kits and afterward injected into HeLa cell nuclei, the randomly modified plasmids were excluded from the daughter nuclei after cell division. Around the same time Shimizu *et al*.[73] reported similar findings, demonstrating that randomly labeled pDNA microinjected into the nucleus was not found in the nucleus after mitosis. However, they concluded that unlabeled pDNA microinjected into the nucleus rapidly forms intranuclear aggregates and that unlabeled pDNA was not detected (by FISH) in the nucleus anymore 24 hours after nuclear injection like labeled pDNA. The aggregates present in the cytoplasm resembled micronuclei, the nuclei formed by mixing purified DNA, the proteins and membranes present in *Xenopus* egg extracts[74, 75].

The results of Gasiorowski and Dean[72] suggest that naked, unmodified plasmids are retained in the nucleus following cell division and likely continue to be expressed in the daughter cells. The episomal pDNA localizes in the region of the cell which will be enclosed by the reforming NE at the end of mitosis, even in the absence of viral chromatin associating systems (**section 6.2**). Alternatively, the dividing cell may simply recognize the pDNA as a marker for NE reassembly as previous experiments in chromosome-free cellular extracts have shown that functional NEs are formed around extrachromosomal DNA[74, 75]. Consequently, unlabeled pDNA can end up in the nuclei or in the cytoplasm as micronuclei. A pDNA with randomly attached fluorophores, however, is likely to be recognized as a large, foreign molecule and not as a DNA molecule. Therefore, it will be no longer highly interactive with a range of cellular DNA-binding proteins, which likely interferes with the enclosure of the

modified pDNA within the new nuclei or micronuclei[72, 76]. A solution to this problem could be the fluorescent tagging of pDNA only at a specific sequence, leaving the rest of the pDNA sequence accessible to cellular proteins. This can be achieved with quantum dots as described by Srinivasan *et al*.[77]. However, the long term follow up of the intracellular fate and nuclear uptake of these plasmids has not been studied in detail yet. Moreover, toxicity concerns related to labeling with quantum dots have been raised.

5. MITOTIC PARTITIONING OF INERT QUANTUM DOTS, GOLD, POLYSTYRENE AND IRON OXIDE NANOPARTICLES

In the past two decades, rapid developments in the field of nanotechnology have led to a steady increase of applications in the area of nanomedicine[78]. Examples of frequently used nanoparticles are gold, silver or iron oxide nanoparticles (IONPs), quantum dots (QDs) or carbon nanotubes. Also in the area of drug and gene delivery, these particles exhibit several characteristics which make them highly interesting as carrier systems. Fluorescent polystyrene particles are mostly used for diagnostic purposes[79]. Nonetheless, they have been also used as models of gene delivery particles. Their homogenous size distribution, strong fluorescence and biological inertness are certainly favorable for these applications. Due to the small size (ranging between one and several tens of nanometers) and solid structure of all these nanoparticles, they are avidly taken up by cultured cells, while their large surface areas enable profound surface chemistry. The particles can thus be equipped with multiple functionalities allowing the combination of several different modalities (e.g. imaging, therapy and carrier systems) in one nanoparticle.

IONPs, QDs and gold particles have been used most frequently for drug and gene delivery. IONPs can be supplied with a cationic coating which allows DNA binding. Their cellular uptake can be strongly enhanced by applying a static magnetic field gradient over the target cells in a procedure which is known as 'magnetofection'[80]. QDs are fluorescent particles exhibiting high photostability, limited photobleaching,

high fluorescence emission intensities and narrow fluorescence emission spectra, which allow multi-colour analysis of complex localization, even *in vivo*[81]. Gold nanoparticles are considered to be the most biocompatible, allow easy surface chemistry and are able to strongly adsorb or scatter incident light at a certain resonance wavelength (often in the near Infra-Red region), a phenomenon called localized surface plasmon resonance, enabling microscopy-based long term tracking of complexes in cells and tissues[82].

One of the few studies focusing on the fate of nanoparticles during cell division was performed by Feldherr *et al*.[83]. They microinjected gold particles of different sizes (3-17 nm) in the cytoplasm of amoebas and studied the cytoplasmic/nucleoplasmic distribution by electron microscopy. Cells injected in interphase contained about 2.6 times more particles in the cytoplasm than in the nucleoplasm. Interestingly, mainly small gold particles (<14 nm) were able to reach the nucleus through the NPCs. When injections were performed in prophase or shortly after mitosis, about 7.3 times more particles could be found in the nucleoplasm when compared to the cytoplasm. Furthermore, the inclusion of larger gold particles (>14 nm) was also observed. Thus, higher relative uptake and incorporation of larger gold nanoparticles were observed in nuclei of dividing cells compared to non-dividing cells. According to Feldherr *et al*.[83], the gold particles enter the nuclei during and/or shortly after mitosis, what could be related to an increased permeability of the NE shortly after it was formed. Later on, Feldherr *et al*.[84] demonstrated that recently formed NEs with newly forming NPCs are more permeable than those of older cells with fully reconstituted mature NPCs. These studies indicate that the NEBD on itself is not of special importance with regard to the uptake of material into the nucleoplasm, but rather the increased permeability of the NPCs. The rates of diffusion across the NE are the highest during the first and fifth hour after the onset of anaphase[84]. This corresponds with the similar time pattern and non-uniform rate of NPC formation reported in HeLa cells[85]. These findings are consistent with electron microcopy studies of dividing cells[86-88] and the study of Swanson and McNeil[39] which have shown that the NE reforms at the

surface of the chromosomes, excluding cytoplasmic substances from the daughter nuclei at the time of reassembly. Therefore, small nanoparticles such as these gold particles are probably not included in the nuclei during mitosis, but are imported shortly afterwards through the more permeable NPCs. On the contrary, positively charged polystyrene nanoparticles of 100 nm, much bigger than the previous gold nanoparticles, were never seen in the nuclei of divided HeLa cells after they were microinjected in the cytoplasm of the cells. Instead, the polystyrene nanoparticles were colocalized with lysosomes (**chapter 2**)[89].

For IONPs or QDs, the focus has been put on the dilution of these particles due to cell division, rather than their nucleocytoplasmic distribution. It has been accepted that for these slowly or non-degrading particles, cell division usually results in an exponential decrease in the intracellular concentration of the particles, as in general both daughter cells receive approximately 50% of the particles. Several studies have recently questioned the general applicability of this finding[90, 91]. Walczak *et al*.[92] observed clear differences in endosomally located IONP turnover in C17.2 neural progenitor cells which were either left to proliferate and showed a uniform dilution of the IONPs or underwent differentiation, resulting in a large difference in numbers of particles per cell. The authors found that this effect was due to asymmetric cell division, a phenomenon quite common for stem cells, which occurs during simultaneously differentiation and renewal of stem cells. This results in a faster dilution of IONPs than in continuously proliferating cells undergoing symmetric cell division (**Fig. 3**)[92].

Also for cells dividing symmetrically, however, the dilution of nanoparticles can differ between the two daughter cells. The dilution of endocytosed QDs upon cell division leads to an asymmetric segregation of endosomes and thus of QDs[93]. Using a statistical model, the same group further showed that partitioning of nanoparticles upon cell division is a random and asymmetric event[94]. From a biological point of view, it has been suggested that large cell populations can proceed to asymmetric cell

divisions in order to be able to more effectively counteract the effects of the 'toxic' nanoparticles[95]. As one cell receives most of the particles, this cell is likely 'sacrificed' so that the remaining daughter cells with nearly no particles have a better chance to survive. Cellular responses to stress induced by nanosized materials can also lead to the induction of autophagy, a self-defense mechanism which can occur in all eukaryotic cells which contain lysosomes[96]. Typically, two membranes will be formed surrounding the region where the nanoparticles are located, to separate this region from the rest of the cytoplasm and then fuse with lysosomes in order to reduce cellular stress and degrade the particles[96]. Also gold nanoparticles, which are generally seen as quite biocompatible, induce oxidative stress upon cellular internalization which in turn activates autophagy[97]. It should be noted that in general, the above mentioned nanoparticles are actively endocytosed and remain within the endosomal compartment of the cell. This most likely explains why these nanoparticles are not frequently reported to be in the nucleus of the cells, although their small size could permit access to the nuclear interior through the NPCs.

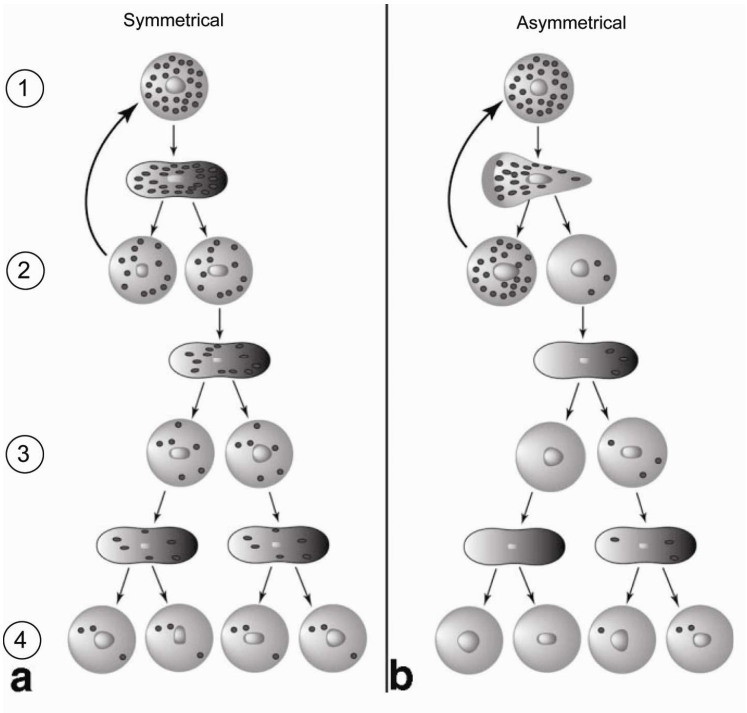

Figure 3. Schematic presentation of symmetrical versus asymmetrical cell division and dilution of Feridex particles. **(A)** In symmetrically dividing cells the contrast agent is distributed equally among daughter cells. **(B)** Asymmetric cell division, as commonly encountered in stem cells, leads to a unequal/uneven distribution of Feridex particles. This in turn can lead to a sharp decline in cell detectability. (Reprinted by permission from John Wiley and Sons: [Magnetic Resonance in Medicine][92], copyright (2007), DOI: 10.1002/mrm.21280, http://onlinelibrary.wiley.com/doi/10.1002/mrm.21280/abstract;jsessionid=D765ABF7E11FB97240148DDDE79FFA9E.d01t03)

6. EFFECT OF CELL DIVISION ON NON-VIRAL GENE DELIVERY PARTICLES

As naked pDNA molecules are only poorly internalized, they need a complexation partner to help them to reach the cytoplasm or the nucleus of the cells. Ideally, this carrier should also provide protection of the nucleic acids against enzymatic degradation during the different steps of the delivery process. In the field of non-viral gene delivery, lipid-based and polymeric delivery systems (known as lipoplexes and polyplexes, respectively) have a long history[98]. Compared to viral delivery systems,

both lipo- and polyplexes are generally easy to prepare, not or weakly immunogenic and allow the incorporation of larger DNA pieces as there is no intrinsic size limitation as with viral particles[13]. Typically, liposomal systems consist of at least two lipid types: a cationic lipid, which allows them to electrostatically interact with polyanionic DNA and facilitates cellular uptake through endocytosis, and an accompanying matrix lipid with long, unsaturated fatty acid chains, which mostly aid in the endosomal escape of these lipoplexes, resulting in the release of free pDNA in the cytosol of the cells[99, 100].

Polyplexes contain a polycationic polymer, such as polyethyleneimine (PEI), that binds to the anionic DNA. Also in this case a surplus of cationic charges allows for binding to the cells. Like lipoplexes, polyplexes are taken up by endocytosis and will therefore end up in the endosomal compartment from which they must be released to allow nuclear translocation of the DNA. In general, polyplexes with high buffering capacity are expected to finally escape out of the endosomes into the cell cytosol by an osmotic rupture according to the proton sponge hypothesis[101].

When compared to viral vectors, the overall transfection efficiency of lipo- and polyplexes is rather low, commonly resulting in transgene expression in less than 50% of all treated cells[14]. This low expression efficiency can be explained by taking into account several hurdles which are intrinsically associated with lipo- or polyplex-based gene delivery: 1) cellular uptake of the complexes, 2) the release of the complexes from the endosomal compartment, 3) dissociation of the DNA from the lipid or polymer carrier and 4) translocation of the DNA from the cytoplasm to the nuclear compartment[11, 102, 103]. Which one of these barriers limits the transfection efficiency in the most pronounced way is debatable. Likely, all barriers contribute to some extent to the lowering of the obtained gene expression. The transfer of free DNA from the cytoplasm to the nucleus has been reported to be a very inefficient process. Capecchi[10] and Escriou *et al*.[64] observed transgene expression in 50-100% of the cells microinjected with naked DNA directly into the nucleus but no significant expression upon DNA microinjection in the cytoplasm. Our recent results also indicate that the

NE is the main obstacle to pDNA delivery as we saw nearly no GFP-positive HepG2 cells transfected with pDNA complexed to polycationic amphiphilic cyclodextrins. In contrast, when the same cyclodextrin complexes were used to deliver mRNA, that only needs to reach the cytosol to display biological activity, up to 31% of GFP-positive HepG2 cells were detected (**chapter 4**)[104]. An even more pronounced difference was observed for HeLa cells[105]. Furthermore, although both lipo- and polyplexes are specifically designed to enable endosomal escape, the majority of the complexes remains entrapped within the acidic endosomes[64, 106]. The acidic environment of the endosomes and presence of degrading enzymes such as lipases will result in the degradation of most liposomes and polymers[107], where the non-degradable polymer backbones or cationic lipids are exocytosed or kept within the lysosomes. DNA molecules which do reach the cell cytosol are rapidly degraded by cytosolic nucleases and their cytosolic residence time should therefore be kept minimal[108].

The intracellular fate of non-viral gene delivery particles still remains obscure. As long as the lipo- or polyplexes have not escaped the endosomal compartment, they are expected to distribute within endocytic vesicles among daughter cells upon recurrent cell division. For lipoplexes, it is assumed that endosomal escape results in the delivery of naked pDNA into the cytosol of the cells. This dissociation seems to be necessary since it has been shown that pDNA is not transcriptionally active upon injection of the intact lipoplexes in the cytoplasm nor the nucleus[11, 65]. Therefore, upon cell division, the naked pDNA in the cytoplasm of the cells will most likely behave as described above **(section 4.2)**. Indeed, Keller *et al.*[109] reported the presence of labeled pDNA in the nuclei of dividing cells 30 to 45 minutes after transfecting them with lipoplexes. By contrast, pDNA was detected exclusively in the cytoplasm in growth-arrested cells. For polyplexes, however, it is still under debate whether or not pDNA has to dissociate from the polyplexes before nuclear translocation occurs. PEI polyplexes have been observed in the nuclei of transfected cells, suggesting that nuclear uptake of the polyplexes should be possible[110]. Also,

Pollard *et al*.[65] showed that PEI polyplexes injected in the nucleus were transcriptionally active, questioning the need for cytosolic pDNA unloading. In line with these speculations, Breuzard *et al*.[111] found evidence of nuclear polyplexes by FRET imaging. On the contrary, Bieber *et al*.[112] found no evidence of nuclear PEI polyplexes and mainly observed colocalization with lysosomes. Correspondingly, we did not observe PEI polyplexes in the daughter nuclei after they were microinjected in the cytoplasm of the mother cell. The polyplexes bearing labeled pDNA or the labeled pDNA only, co-localized with the lysosomal compartment (**chapter 2**)[89]. Also, Itaka *et al*.[113] observed fast release of pDNA from (linear) PEI polyplexes in the cytosol, questioning the long-term existence of cytosolic PEI polyplexes and their subsequent delivery to the nucleus. The nuclear localization of PEI polyplexes observed in the aforementioned studies could then result from a recomplexation of pDNA and PEI polymers, after both of them reached the nuclear interior independently. Overall, the presence of polyplexes in the nucleus of cells seems to be a very rare phenomenon.

Surprisingly, the long term intracellular fate of lipo- and polyplexes during cell division has never been investigated in detail. Consequently, little is known on the nuclear entry of nanoparticles during mitosis, although the nuclear inclusion appears a very simple concept to study. To address this question, only a detailed real-time analysis of the intracellular distribution of cytoplasmically microinjected nanoparticles would be needed. In living cells, however, the lack of information can partially be explained by the difficulties to inject particles which are larger than 200 nm because of problems of aggregation, needle clogging and long-term survival of the cells after injection. Therefore, most information on the nuclear delivery of pDNA to the nucleus upon lipid-based[5, 8, 13-17] or polymer-based[5, 8, 12] delivery comes from indirect evidence of nuclear entry, namely an increased gene expression, which was reported to be two- to several hundredfold higher in dividing than in non-dividing cells. As mentioned in section 2, the cell cycle can be roughly subdivided into five different phases, being: G_0, G_1, S, G_2 and M phase. A common finding is that the transfection efficiency for both lipo- and polyplexes is considerably higher during S, G_2 or M

phases than during G_0 or G_1 phases[5, 13, 16, 18]. Generally, it is believed that during M phase and associated NEBD, the larger complexes can reach the nuclear DNA[15]. Complexes which were taken up by cells in G_0 or G_1 phase are likely not retained long enough to still be fully functional when reaching the M phase[5]. Apart from NEBD, other events such as a cell cycle dependent internalization of the complexes may play a significant role as well. Although studies have indicated that the cell cycle status has no effect on the cellular uptake of the complexes[114], other studies point to a clear link between complex uptake efficiency and cell cycle status[14, 18]. Männisto *et al*.[18] linked their observations to previous studies in which it was shown that the rate of endocytosis, in general, increases gradually during the G_1, S and G_2 phases, but drops drastically at the beginning of mitosis. Of further interest is the study by Marenzi *et al*.[115] who linked reporter gene expression levels to the compaction state of transfected DNA at different cell cycle phases. For transfection of cells in G_0 or G_1 phase, the plasmid is packaged into a more compact form which inactivates reporter gene expression. This compact pDNA is not reactivated when cells are stimulated to cycle. Therefore, differences in gene expression are not directly linked to alterations in transfection efficiencies but rather to the inability of the pDNA to be transcribed when packaged into a more compact form.

Cell cycle independent gene transfer by using polyplexes composed of linear PEI has been reported as well[12]. Also, compact DNA particles were shown to transfect postmitotic cells, showing that at least some nanoparticle types are able to reach the nucleus of non-dividing cells[116]. Furthermore, Escriou *et al*.[15] although confirming that mitosis is an important upregulator of transfection efficiency, also observed expression in cells which had not divided, albeit to a lower extent. In line with these findings Dowty *et al*.[70] found that when pDNA was injected close to the nucleus, nuclear translocation was observed, regardless of the cell cycle status.

Overall, these data indicate a clear effect of cell cycle progression on transgene expression levels, but the variety of cell types and carrier systems used make it hard

to clearly define the exact mechanism underlying this effect. Likely, a combination of factors play a role, where cells in S or G_2 phase have the highest endocytic capacity, while in M phase facilitated nuclear transport by NEBD occurs and the pDNA is allowed to be packaged into a more open form, thus enabling high reporter gene expression levels.

7. VIRUSES TAKING ADVANTAGE OF MITOSIS

Viral vectors remain to have the best transfection efficiencies because for millions of years they have developed mechanisms to survive in the extracellular environment, stabilize virus-cell interactions, increase internalization, hijack intracellular transport systems, deliver their genomes into the appropriate subcellular compartment (cytosol or nucleus) of dividing and non-dividing cells and increase transcription. Most of these mechanisms involve introduction of specific proteins into the virus. Many viruses have evolved, gaining the ability to replicate and store their genome in the cell nucleus. These viruses aim at maintaining their genome in the infected cells until the host organism dies. They usually achieve this by integrating genomic DNA into the host chromosomes or segregating episomal DNA into daughter cells[117]. Two groups of viruses which take advantage of cell division during their life cycle, will be discussed in this section: certain retroviruses which depend on mitosis to integrate their genome and thus infect the host cells and some DNA viruses which use mitosis to partition their episomes in the progeny cells of latent infected host cells.

7.1. Retroviruses

Retroviral virions are enveloped particles of about 80-100 nm in diameter[118]. In retroviruses, the viral ssRNA is reverse transcribed in the cytosol via reverse transcriptase into dsDNA. This DNA together with viral integrase is organized into the pre-integration complex (PIC)[117, 119]. Also, host proteins such as the barrier-to-autointegration factor (BAF) or high mobility group (HMG) proteins can associate with the PIC[120]. Generally, viruses deliver their genome through the NE of the interphase

nucleus. This delivery mechanism permits infection of non-dividing cells and offers the opportunity to infect terminally differentiated cells. Some retroviruses, however, are dependent on mitosis for infection and their PIC waits in the cytosol until the cell undergoes mitosis. During the temporary NEBD, the PIC can associate with the chromosomes and enter a newly assembling nucleus after which the dsDNA integrates into the host genome (**Fig. 4A**)[119]. Many retroviruses infect cells exclusively, or more efficiently, if the host cell divides[121, 122]. These include murine leukemia virus (MuLV)[123, 124], human immunodeficiency virus (HIV)[125-127], spleen necrosis virus (SNV)[128], avian sarcoma virus (ASV)[128-134] and foamy virus (FV)[135, 136].

For example, gene transfer and expression of exogenous genes using retrovirus based vectors, such as MuLV, requires cell proliferation which limits their application to dividing cells. Why MuLV cannot work its way into non-dividing cell nuclei via nuclear pores is unclear. Yamashita *et al.*[137] indicated that the MuLV capsid protein that is closely associated with MuLV PICs, prevents PICs from migrating into the nucleus of non-dividing cells. MuLV PICs perhaps lack NLSs or fail to display NLSs due to MuLV capsid, preventing their NPC import. Alternatively, the MuLV capsid may sterically hinder NPC import[138]. For that reason, MuLV PICs bind the host chromosomes during mitosis and are subsequently enclosed together with them in the daughter nuclei. A particular factor with tethering activity to mitotic chromosomes has not yet been described for MuLV. However, phosphoprotein p12, a part of the MuLV PIC, bears a similar N-terminus as the histone H5 protein[139] and shows a close association with the chromatin. Taking this together, it is tempting to assume that p12 also functions in tethering the MuLV PIC to the chromatin[140]. It should be stressed here that the limited knowledge of PICs in general is caused by the difficulty of obtaining large amounts of material[141].

Contrary to MuLVs, lentiviruses such as HIV-1 infect dividing as well as non-dividing cells, like terminally differentiated macrophages[142, 143]. HIV-1 capsid is not strongly associated with HIV-1 PICs as opposed to MuLV capsid[137]. How HIV-1 PICs move

through NPCs remains unclear. For reviews about this controversial matter, the reader is referred to ref.[144-146]. Overall, transport of the HIV-1 PICs into the nucleus may require the combined action of three constituent proteins, namely matrix (MA), viral protein R (Vpr) and integrase (IN), in addition to specific DNA sequences. During transport, several factors such as virus uncoating, NLS signals and disruptions in NE integrity may play a significant role[117, 119]. The integration efficiency of HIV-1 is up to threefold higher in dividing cells than in non-dividing cells as a result of the balance of two opposite effects. While NEBD facilitates docking of the viral genome to the host chromatin, chromosome condensation directly antagonizes and therefore delays integration[147]. Also for lentiviruses, evidence of existence of a specific chromosome binding factor is lacking but the endogenous lens epithelium derived growth factor/p75 (LEDGF/p75) is an attractive candidate chromatin-tethering factor. LEDGF/p75 is a nuclear protein that binds integrase via its C-terminus and binds chromatin via its N-terminus, thereby tethering integrase and thus the PIC to the chromatin[148]. However, Katz *et al.*[149] reported that nuclear import of HIV-1 PICs may be mitosis-independent in dividing cells. This finding indicates that LEDGF/p75 as a chromatin-tethering factor is not necessary for nuclear entry of HIV-1 PICs, but that it is required for viral dsDNA integration in the host genome.

Aside from lentiviruses, also other retroviruses such as ASV and FV enter the nuclei of non-dividing cells, albeit less efficiently than of dividing cells[135, 138]. Recently, the FV group-specific antigen (Gag) was found to be the essential linker between the viral DNA in the PICs via its C-terminus and host chromosomes during mitosis through interaction with H2A/H2B histones via its N-terminus[150, 151]. The substitution of this chromatin-binding site with the chromatin-binding site of LANA (**section 6.2**) allows binding of the incoming PICs onto host chromosomes but it does not restore full infectivity[150]. For ASV, the factors which translocate their PICs into the nucleus of (non-)dividing cells are speculated or unknown e.g. an NLS in the ASV integrase protein may underlie PIC import[138]. In contrast to MuLV, lentiviruses and FV vectors showed a long-term persistence of a stable transduction intermediate in quiescent

cells, so that they efficiently transduced G_0 fibroblasts which were later stimulated to divide[135]. A mechanism envisioned for how retroviruses might deal with the potentially restrictive environment of non-dividing cells, is that the retroviruses themselves may induce cell cycle progression to create a more favorable environment[152, 153]. Studies have indicated that binding of some retroviruses to Toll-like receptors on the cell surface can stimulate the cell to enter into the cell cycle[152]. However, such stimulatory activities are unlikely to be universal[149].

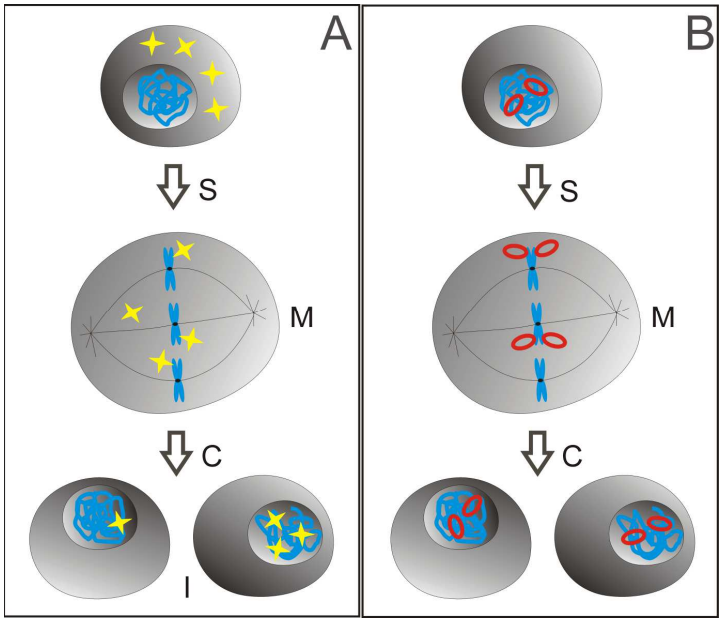

Figure 4. Schematic presentation of how retroviruses **(A)** and latent DNA viruses **(B)** take advantage of mitosis. **(A)** Infection by retroviruses. After reverse transcription, packages of viral DNA are assembled (pre-integration complexes: PICs). The PICs tether host chromosomes during methapase (M) and, following cytokinesis (C), are enclosed into the daughter nuclei, where integration (I) can take place. **(B)** Latent DNA virus episome or EBNA1/oriP plasmid maintenance and segregation. Episomes/oriP plasmids are bound to the host chromatin. Replication of host chromosomes and episomes/oriP plasmids and partitioning of episomes/oriP plasmids to sister chromatids take place during DNA synthesis (S) phase. Nuclear segregation of episomes/oriP plasmids to the daughter nuclei is achieved following mitosis (M+C).

7.2. Latent DNA viruses

Besides the retroviruses which make use of mitosis to integrate their genome into the host DNA, some latent dsDNA viruses associate their genome with the host mitotic chromosomes for persistence of viral episomes in infected cells and their progeny (**Fig. 4B**). This is achieved by attaching the viral circular dsDNA as an extrachromosomal element to the host genome. DNA viruses which use this strategy include certain herpesviruses such as Epstein Barr virus (EBV), Kaposi sarcoma-associated herpesvirus (KSHV) and herpesvirus saimiri (HVS) as well as latent papillomaviruses such as bovine papillomavirus (BPV-1) and human papillomavirus (HPV). The virions of herpesviruses are enveloped and rather big (180-200 nm) while papillomaviruses (53-57 nm) are very small and do not have an envelope[118].

Herpesviruses

EBV or human herpesvirus 4 (HHV-4) that is best known as the cause of infectious mononucleosis, can infect a number of cell types, including epithelial and B cells. During latency, EBV is stably maintained as a circular plasmid that is replicated once per cell cycle and partitioned at mitosis. The AT hook activity of a single viral protein named EBV nuclear antigen 1 (EBNA1) is required for both processes. AT hooks are DNA binding motifs found in a family of proteins which bind the minor groove of AT rich scaffold-associated regions on metaphase chromosomes[154, 155]. The stable circular episome carries only two EBV components: the *cis* acting origin of replication (oriP) and the latently expressed EBNA1 in *trans*. EBNA1 binds directly to viral DNA via its C-terminal domain and tethers the EBV genome to chromatin through its N-terminal domain, initially by direct interactions via its AT hooks, or afterward through association with the nucleolar EBNA1 binding protein 2 (EBP2). The latter is a part of the perichromosomal layer and the binding with EBNA1 may be required to stabilize the EBNA1-chromosome interaction[156].

Additionally, HVS which transforms T cells was seen to be closely related to EBV and has similarly a *cis* acting oriP that permits stable replication and the efficient persistence of episomes in HVS-infected cells[157].

KSHV, also known as human herpesvirus 8 (HHV-8), commonly occurs in AIDS patients and persists as a multi-copy episome in latently-infected tumor cells. KSHV latency associated nuclear antigen (LANA) is required for episome persistence in host cells during latent infection. LANA mediates viral genome attachment to mitotic chromosomes[158]. Previous studies have shown that LANA directly binds the viral episome via its C-terminal domain, nucleosomes via its N-terminal domain through the folded region of histones H2A-H2B[158, 159] and the mitotic chromosomes via its C-terminal domain through the double bromodomain protein 4 (Brd4)[159]. Brd4 has been identified as the first mitotic chromosome receptor for DNA viruses[160]. Recently, however, Xiao *et al*.[161] have reported that the molecular mechanism underlying the bridge between the virus, LANA and the host chromosome is likely complex, involving numerous proteins, such as the kinetochore protein budding uninhibited by benzimidazole 1 (Bub1), with which association throughout mitosis is maintained, making the LANA-Bub1 interaction likely critical for segregation to daughter nuclei[161].

Papillomaviruses

Besides the herpesviruses discussed above, also certain papillomaviruses use mitosis to persist in latently infected host cells. For example, HPV-16, together with type 18, causes most of the HPV-associated cancers (e.g. cervical cancer). By the same token, BPV-1 infects paragenital areas in cattle and provides an excellent model for studying papillomavirus molecular biology. A common strategy for papillomaviruses, is that the viral E2 proteins tether episomes to mitotic chromosomes so that the episomes are segregated and enclosed in the daughter nuclei. For example, HPV-8 E2, interacts via its flexible linker hinge region between the N- and C-terminus, with regions of ribosomal DNA repeats located on the short arm of human acrocentric chromosomes[162] and via its C-terminus with the episome[163]. Long term genome

maintenance and stable copy number require multiple E2 binding sites in the episome, which are used to tether the episomes to mitotic chromosomes[164]. Brd4 was previously identified as the mitotic chromosome anchor for BPV-1 and HPV-16 via the N-terminus of E2[160]. Recently, Silla *et al*.[165] have reported that the formation of the BPV-1 E2 segregation complex is Brd4 independent, which is also the case for all HPVs [166]. Silla *et al*.[165] additionally concluded that the formation of segregation-competent complexes depends on a certain protein level threshold and that multiple E2 molecules are present in a single segregation complex together with cellular proteins, including certain components of the transcription machinery. Therefore, it seems that the chromosome binding action and the transcriptional regulation mediated by the E2 protein are not operating independently. The E2 proteins have been observed to be associated with condensed chromatin at all stages of mitosis, even at times when many other transcription factors have been displaced from mitotic chromatin[167]. E2 proteins are multifunctional, as they are also involved in initiating viral DNA replication and regulating viral transcription, in addition to maintaining the genome as an extrachromosomal replicating element[162]. Also interesting to add is that it has been shown that the consensus sequence RXXS in the hinge region is important for chromosome binding by the HPV-8 E2 protein. The serine residue in this region is phosphorylated by CDKs and this phosphorylation most likely regulates the chromosome binding. Furthermore, the RXXS motif can be found in the N-terminal domain of LANA and in the AT hooks of EBNA1, suggesting that cell cycle-dependent phosphorylation could be a common strategy to regulate chromosome tethering during cell division[162].

8. REFLECTIONS ON STRATEGIES FOR THE IMPROVEMENT OF NUCLEAR INCLUSION OF EXOGENOUS NUCLEIC ACIDS OR OTHER MACROMOLECULES

We and many others are interested in delivery of pDNA to the nuclei of target cells. During interphase, pDNA has to access the nuclear interior via the NPCs. pDNA is however a large hydrophilic molecule which does not easily pass the hydrophobic

central channel of the NPCs. Efforts to increase the nuclear import of pDNA through NPCs by the use of NLSs have met with limited success, although this strategy initially seemed very promising[168, 169]. The use of NLSs to bring pDNA into the nucleus is not within the scope of this review and has been reviewed elsewhere[1, 21]. As described above, when cells undergo mitosis the NE is temporary disassembled, to reappear at the end of mitosis, when a new NE forms around the segregated sister chromatids. It has been shown that cell division greatly enhances the transfection efficiency of pDNA, presumably because of the intermixing of cytoplasmic and nucleoplasmic components during mitosis, followed by accidental retention of pDNA in the newly formed daughter nuclei[5, 8, 13, 14, 71]. We hypothesize that it should be possible to increase the nuclear inclusion of DNA during cell division by different strategies, which will be discussed here.

8.1. Chromatin targeting

The targeting of pDNA to chromatin is conducted such that pDNA is included in the nuclear interior as the NE is formed around it. Both the pDNA itself and the non-viral gene delivery particles containing the pDNA could be equipped with chromatin-binding factors. These factors should be able to bind the chromatin directly, or by the recruitment of endogenous proteins which mediate the binding to chromatin. Additionally, as indicated by the results of viral studies, the pDNA should be equipped with multiple chromatin-binding sites, to assure a strong anchoring of the chromatin during cell division. It should be noted that during mitosis, the chromatin is surrounded by the so-called perichromosomal layer[57-59]. The function of this protein layer is not completely understood. Possibly it plays a role in chromosome organization and/or compartmentalization of cells in prophase to telophase, serves as a binding site for chromosomal passenger proteins or just as a protective barrier around chromosomes. It is very likely that the presence of the perichromosomal layer prevents the attachment of exogenous pDNA to the chromatin unless correct targeting proteins are used. It should also be noted that the space between the

chromatin and the newly forming NE is very narrow, raising the question whether at all it will be possible to attach large pDNA molecules or nanoparticles to the chromatin, without disturbing the formation of a smooth NE. However, as described above both retroviruses (**section 7.1**) and latent DNA viruses (**section 7.2**) frequently use the chromatin-targeting strategy to bind their genome to the chromatin and assure its partitioning to the daughter cells (**Fig. 4**). Also, it was shown that large macromolecules such as dextrans or pDNA which do not interact with the chromatin, are not retained into the nuclei upon cell division[60, 72]. Therefore, we believe that the chromatin-targeting strategy has great potential in improving both the amount of pDNA that reaches the cell nucleus during cell division and the chance that the nuclear pDNA gets inherited by daughter cells during subsequent cell divisions.

Non-viral chromatin-tethering factors

All known chromosomal or DNA-binding proteins contain one or more AT hooks, suggesting that it may act as a universal chromosome-tethering factor. Therefore, coupling the AT hook region of proteins (consensus motif PRGRP), instead of the full length protein to pDNA or pDNA containing nanoparticles could be sufficient to mediate chromosome binding. Recently, we showed with the *Xenopus* nuclear envelope reassembly (XNER) assay that the nuclear inclusion of polystyrene beads and PEI/pDNA nanoparticles could be improved about threefold upon chromatin targeting with AT hooks derived from the endogenous Mel-28 (maternal effect lethal 28; ELYS in mammalian cells) and HMGA2β (high mobility group AT-hook 2 isoform β)[89]. This clearly shows that chromatin targeting indeed improves the nuclear inclusion of nanoparticles which are bound to the chromatin. In living cells, however, these microinjected nanoparticles seemed to be 'trapped' in the lysosomal compartment, causing their equal distribution to daughter cells upon cell division, without any apparent nuclear inclusion of the nanoparticles[89]. It should be noted that in this study the chromatin-binding peptides were bound to the pDNA-carrier and not to the pDNA itself. Consequently, as soon as the pDNA is released from the

nanoparticles, the chromatin-targeting properties are lost (**chapter 2**). In future it could be interesting to attach the chromatin-binding peptides directly to pDNA and observe if this results in an increased nuclear retention upon cell division.

Endogenous proteins such as members of the high mobility group proteins (HMG) and histones have also been used as pDNA delivery systems as such[170, 171] or in combination with conventional lipids and polymers[172] to increase transfection efficiency[173]. These proteins were able to enhance pDNA nuclear translocation and transfection efficiency to some extent, most likely due to their innate DNA binding and condensing properties, as well as their intrinsic NLSs. As the chromatin-binding domain (N-terminus) of EBNA1 can be replaced by those of either HMG-I or histone H1, with successful maintenance of daughter cell episomes after cell division, these motifs also have potential for mediating pDNA attachment to chromatin and pDNA segregation[174].

Additionally, already more than 10 years ago, a new episomal system has been described (pEPI-1) which possesses replication and episomal retention features through the function of a scaffold/matrix attachment region (S/MAR) isolated from the human β-interferon gene. S/MARs are associated with most of the characterized mammalian origins of replication[175, 176]. The 30 nm fiber of DNA, histones and chromatin proteins appears to be organized into loops by interaction of S/MARs with the nuclear matrix[177]. S/MARs have besides their structural function, also an important role in temporal and spatial organization of gene expression[178]. Recently, Lufino *et al*.[179] showed full functional recovery of low density lipoprotein receptor (LDLR) activity in a deficient cell line. *LDLR* transgene expression retained physiological regulation and was repressed by high sterol levels. They showed also a high mitotic stability of the vector by demonstrating long-term episomal retention in the absence of selection. The mitotic stability is provided by the specific interaction of the vector with the chromosome scaffold via scaffold attachment factor A (SAF-A) from the nuclear matrix. This enables co-segregation with the chromosomes during

cell division[180]. Moreover, Tessadori *et al*.[181] concluded that the regulatory mechanisms that act on episomal genes seem to be similar to those that control host genes. The episomal chromatin undergoes the same modifications as the host chromatin e.g. histone modifications and DNA methylation. The generation of artificial chromosomes with an optimal size with respect to stability as well as transfection efficiencies, may be promising for the future of non-viral gene therapy as it may be a perfect alternative for viral episomal gene vectors (**next paragraph**). This possibility is even more interesting in the context of possible immunogenic or oncogenic properties of viral vectors[182]. Additionally, the transgenes bear strong constitutive promoters, which result in nonphysiological overexpression. To achieve physiological conditions of expression, correct alternative splicing and promoter usage, an efficient vector should be based on sequences derived from the human genome, which include the native promoter and all regulatory sequences of a gene [183, 184].

Viral chromatin-tethering factors

AT hooks also occur in the chromosome-binding region of viral segregation proteins which mediate viral genome retention into the nuclei of the host cells. The most interesting features to this point are the chromosome-tethering factors of the latent DNA viruses, as the information of responsible chromosome-binding factors in the different retrovirus PICs is still limited. Proteins which are identified to have chromosome-binding properties are EBNA1, LANA and E2. In addition to sharing the common function of genome tethering, these proteins also play an important role in viral genome replication and transcriptional regulation[159]. Structurally, all three proteins form, or are predicted to form, a similar dimeric β-barrel C-terminal DNA binding structure, regardless of a lack of sequence homology[185]. However, Sekhar *et al*.[162] have shown that the HPV-8 E2 chromosome binding sequence has similarities with chromosome binding regions in EBNA1 and LANA tethering proteins. Although these proteins may have different chromosomal targets, a common mechanism of

regulation of chromosome binding function could be the phosphorylation by certain CDKs[162]. The recent discovery of the RXXS motif, that is a recognition target of several CDKs, in all three proteins is in favor of this hypothesis. As it has been shown that the segregation complex in papillomaviruses contains multiple E2 proteins and also the viral genome should contain at least 5 E2 protein recognition sites[165], it can be expected that a strong chromosomal binding is needed to assure efficient partitioning during cell division. Also, the local organization of chromatin is expected to greatly influence the ability of binding nanoparticles during mitosis. For the EBNA1 protein, for example, a possible chromosome binding place has been identified in chromosome 11, although only in 23 out of the 771 possible binding places genome-wide EBNA1-mediated binding was also actually observed[186].

In relation to gene therapy, most progress has been made with EBV plasmid vectors, which can be combined with cationic polymers. These EBV plasmid vectors contain oriP and the *EBNA1* gene. It has been shown that EBNA1 maintains and equally partitions a plasmid that contains the viral oriP region *in cis* by tethering it to endogenous chromatin[154] (reviewed by He and Zhang[187]) (**Fig. 4B**). The mechanisms underlying the efficient transfection/expression are not yet fully understood, because EBNA1 exerts a variety of functions through sequence-specific binding to oriP. However, Kishida *et al.*[188] have shown that the efficient delivery and expression is predominantly due to the promotion of cytoplasm-to-nuclear recruitment as well as enhancement of transcription, while the episomal replication is not essentially involved. A major drawback of EBV vectors is the possibility of tumor development in human. Therefore, the possible oncogenicity of all viral vectors *in vivo* has to be thoroughly investigated[189]. For retroviruses for example, the insertion of the MuLV genome in the host gene promoter and its proviral enhancer activity underscores the potential dangers of MuLV as gene therapy vector[141]. Its weak bias for integration in genes may render ASV a preferable alternative vector [190]. As soon as the retroviral and cellular determinants of integration site selection are elucidated, safer and more effective gene therapy vectors may be developed[141]. Additionally, all the knowledge

about viral vectors, will give us in the end the opportunity to make equivalent but safer non-viral vectors.

As an alternative to the use of the whole viral vector or the viral plasmid with oriP and the *EBNA1* gene, another option is to use only the chromatin-binding motifs of the EBNA1, LANA or E2 proteins (**section 7.2**). Both the direct binding motifs of these proteins, which bind the mitotic chromosomes themselves and the indirect binding motifs, which bind Brd4 or other cellular factors on mitotic chromosomes could be useful as chromosome anchor peptides on pDNA or artificial non-viral pDNA-containing particles. Once inside the cytosol, these non-viral particles could target and attach to the chromosomes during mitosis and subsequently be enclosed in the newly formed daughter nuclei. Interestingly, the chromatin-binding part of interleukin 33 (IL-33) was shown to have striking sequence similarities with the H2A-H2B binding motif of LANA, leading to the identification of the hexapeptide MXLRSG that was determined to be crucial for docking into the H2A-H2B acidic pocket[191]. Since IL-33 is an architectural chromatin-binding nuclear factor, it has been suggested that KSHV copied the chromatin-binding motif of IL-33 to establish latent infection in human cells[191]. This suggests that incorporating the minimal chromatin-binding motif MXLRSG could serve to target pDNA to chromosomes during cell division.

Additionally, not the use of a viral protein, but rather that of the host cell protein Brd4, can be a strategy to target gene therapy particles to the host mitotic chromosomes too, as we learn from KSHV and papillomaviruses[159, 160]. Brd4 is a member of the bromodomain and extra-terminal (BET) family. Their characteristic feature is the retention on chromosomes during mitosis which possibly allows them to play a role in the transmission of epigenetic memory across the entire process of cell division[192]. Therefore, the possible consequences related to epigenetics of using proteins of this family are worthwhile studying intensively.

8.2. Targeting non-chromatin nuclear elements

Another strategy is targeting of pDNA or pDNA nanoparticles to the mitotic spindle, the NPCs, the INM or the underlying nuclear lamina. Bausinger *et al*.[193] demonstrated that PEI/pDNA complexes are transported along the microtubules of the spindle apparatus and suggest that the concentration of polyplexes at the location of the emerging daughter nuclei strongly contributes to the transfection process. This indicates that targeting the mitotic spindle could indeed be interesting to increase transfection efficiency, e.g. by the use of nucleolar and spindle associated protein (NuSAP)[194]. INM proteins which could be used for targeting to the nuclear interior are abundant. Most of them, such as Lap2β, emerin and Man1 share a common protein domain, the so-called LEM-domain[24]. Coupling this ~40 residue motif to pDNA could ensure that pDNA or pDNA-containing nanoparticles bind the INM or nuclear lamina, ensuring their presence in the interior of the forming nucleus. When the pDNA is targeted to the nuclear lamina, however, it should be taken into account that the nuclear lamins are only imported in the forming nuclei after the NE has been formed. Therefore, the pDNA should be able to pass the NPCs together with the lamins, which may be impossible to achieve. On the other hand, several studies confirmed that the permeability of the NPCs is not so strict directly after NE formation[31, 61, 84, 195], which could be in favor of pDNA nuclear import shortly after mitosis. In yeast, tethering to NPCs has been shown to promote extrachromosomal DNA partitioning during (asymmetric) cell division[196]. Whether targeting NPCs in mammalian cells could also help to increase the nuclear inclusion during or shortly after cell division is unclear. Another possible concern with the above mentioned strategies, is the presence of a large pool of endogenous proteins, which could compete for binding to the chromatin, the INM, the NPCs and the mitotic spindle. Also, it is not sure if the proteins will retain their chromatin-, INM-, NPC- or mitotic spindle-targeting properties after coupling to pDNA or pDNA-containing nanoparticles.

8.3. Cell-division responsive nanoparticles

Apart from chromatin- and/or INM-targeting, cell-division responsive pDNA-containing nanoparticles might present an interesting option to increase gene transfection efficiency. We may expect that free pDNA in the cytosol acts as a substrate for several intracellular nucleases. On the other hand, at the moment of cell division, a fraction of free pDNA seems to be able to reach the nuclei of the daughter cells. Therefore, we hypothesize that when the amount of pDNA is the highest at the onset of cell division, this should improve gene delivery efficiency by improving the at random inclusion of pDNA in the nuclei of the daughter cells. This could be achieved by cell division-responsive pDNA nanoparticles which release their pDNA only at the onset of mitosis. In this way the time between release of the pDNA and cell division is as short as possible, which presumably avoids excessive degradation of the pDNA in the cytosol before nuclear enclosure can occur. The different phases of cell division are characterized by subsequent phosphorylation reactions by CDKs. By incorporating the recognition sequence of CDK1 (S/TPXK/R)[197, 198] in pDNA-containing nanoparticles, one could obtain DNA nanoparticles which are specifically phosphorylated during cell division. The introduction of negatively-charged phosphate groups is expected to decrease the DNA-binding capacity of the nanoparticles, resulting in an enhanced release of the pDNA upon phosphorylation. This strategy has been used by Wilke *et al*.[8] who developed a pDNA carrier based on synthetic peptides. One of these peptides was derived from DNA-binding proteins and contained the repeated SPKR motif, which is a substrate for CDKs. They found that mitosis greatly improved transfection efficiency with this peptide based pDNA carrier and asssumed that phosphorylation in the early phases of mitosis strongly diminished the carriers affinity toward pDNA and thus resulted in pDNA release at the time it has the best chance to enter the daughter nuclei[199]. An additional advantage is that the pDNA is well protected against nucleases in the cytosol until it has the possibility to be enclosed in the daughter nuclei[8].

Comparable strategies have been used to develop delivery systems which are responsive to protein kinase A and to cyclic AMP-dependent protein kinase[200-203]. Also here it was demonstrated that by incorporation of the appropriate kinase recognition site, specific phosphorylation could be obtained which resulted in release and an enhanced transfection efficiency of the complexed pDNA. It should be noted that the amount of free pDNA in the cytosol probably should not rise above a certain threshold, since it has been demonstrated in cell-free systems that pDNA competes with chromatin for binding of NE membrane fragments, thereby disturbing the formation of a smooth NE[204]. Whether this can also occur in living cells, and in this way contribute to the cytotoxicity of pDNA-containing nanoparticles remains to be seen.

8.4. *Xenopus* nuclear envelope reassembly assay to study nuclear envelope dynamics

Insight in the different steps of the nuclear envelope assembly has substantially increased since the use of cell-free systems to study the reassembly of the NE *in vitro*[205, 206]. The *in vitro* assembled nuclei have a NE consisting out of two phospholipid bilayers with embedded NPCs and a peripheral nuclear lamina, just like normal eukaryotic nuclei. Furthermore, they have a functional nuclear import and export machinery and can even go through mitosis. The XNER assay, serves as a good model to study the chromatin binding and resulting inclusion in the artificial nuclei, without the interference of other extra- and intracellular barriers. In the XNER assay, membrane fraction and cytosolic extract are isolated from *Xenopus* eggs, mostly in interphase[30, 207]. It is also possible to isolate mitotic extracts, by preventing the destruction of cyclin during the extraction and maintaining its phosphorylation state. When DNA is added to a mixture of these isolated cytosolic extract and membrane fragments, the assembly of a NE occurs spontaneously as long as an energy source is provided (**Fig. 5**). In the XNER assay, mostly membrane-devoid sperm chromatin is used as a DNA template. Is has been shown, however, that the NE can even form

around protein-free DNA, after initial assembly of the DNA into nucleosomes and further organization into condensed spheres[208]. The ability of *Xenopus* eggs to form an intact, functional NE around added DNA most likely results from the large amounts of nuclear components which are stored in the eggs for subsequent cell divisions during embryo development. An additional advantage of these cell-free systems is that certain protein components can be depleted from or added to the XNER assay to assess their function in the NE assembly and disassembly processes. Furthermore, the nuclear inclusion of pDNA or pDNA-containing nanoparticles can be studied by simply adding these particles to the XNER assay. The nuclear inclusion can then easily be followed using microscopy techniques such as phase-contrast or fluorescence microscopy. It should be noted that although cell-free systems are very useful to isolate processes from the full complexity of the cellular environment, the results obtained with them should always be confirmed in living cells. Also, the XNER assay cannot be used to study targeting to H2A-H2B pockets, as the *Xenopus* sperm chromatin is devoid of them[158].

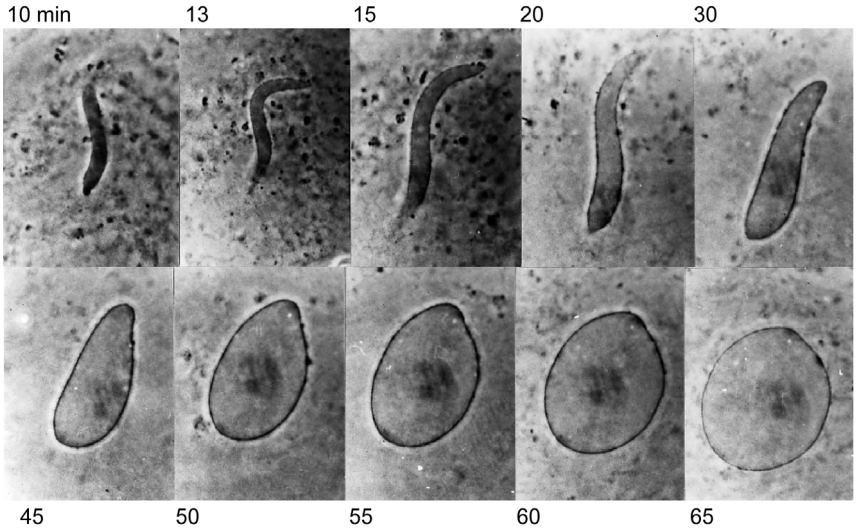

Figure 5. Different stages of the formation of an artificial nucleus around chromatin in the XNER assay. (Reproduced with permission from Journal of Cell Science [209], copyright (1997), http://jcs.biologists.org/content/110/13/1489.long)

9. MESSENGER RNA AS AN ALTERNATIVE TO PLASMID DNA

Until now, there is no non-viral carrier which could guarantee efficient delivery of pDNA to the nucleoplasm. That is the main reason why transfection efficiencies achieved by non-viral carriers are much lower than those achieved by their viral counterparts. For that reason mRNA, that exerts its biological function in the cytoplasm, was put forward as alternative to pDNA-based transfection. Contrary to the earlier belief that mRNA is too unstable to endure transfection protocols[210], it has been shown that mRNA can efficiently transfect cells[105].

As compared to pDNA delivery (**Fig. 6A**), the use of mRNA offers several advantages. Firstly, since mRNA is translated in the cytoplasm, it does not have to enter the nucleus to perform its function. As a result, high levels of proteins encoded by mRNA were detected as early as 30 minutes after transfection (**Fig. 6B**)[105]. Another consequence is that, unlike pDNA, mRNA is also effective in non-dividing cells, which is a highly desired condition for those gene therapeutic strategies which aim at slowly or non-dividing cells such as vascular endothelia, muscle cells, hepatocytes and brain cells. Secondly, the use of mRNA is safer because it cannot integrate in the genome, thus circumventing the risk of introducing insertional mutagenesis. This also implies that the expression remains transient. Transient expression is an advantage if mRNA is used for vaccination, anti-cancer or anti-infective immunotherapy but on the other hand it may be a major limitation for the treatment of inherited diseases. Thirdly, mRNA is easier to engineer into an efficient therapeutic entity because there is no need to select and incorporate an efficient promoter and terminator. Forthly, mRNA lacks unmethylated CpG motifs. These motifs, derived from bacterial or viral DNA induce strong immune responses mediated by Toll-like receptor 9 (TLR9)[211]. It should be noted, however, that mRNA transcribed *in vitro* may also cause strong immune responses mediated through other endosomal receptors (TLR3, TLR7 and TLR8)[212]. The employment of modified nucleotides has been proposed as a solution to this drawback[213, 214]. The strong immunostimulatory effect of mRNA may turn into an advantage for therapeutic vaccination strategies.

Knowing the advantages and disadvantages innate to mRNA delivery, it is still not sufficient to simply replace pDNA by mRNA in order to achieve efficient transfection. Numerous non-viral transfection agents to deliver pDNA have been propagated. Some of them have been also evaluated for their ability to complex and deliver mRNA. In this connection, cationic lipids have accomplished significantly better results than cationic polymers. The cationic lipid DOTAP (1,2-dioleoyl-3-trimethylammonium-propane) is one of the most intensively studied and effective mRNA carriers[215-217]. Similarly to pDNA, also mRNA transfection was greatly improved by mixing DOTAP with DOPE (1,2-dioleoyl-glycero-3-phosphoethanolamine) because the latter lipid is known to facilitate nucleic acids release from the complex as well as the endosomal compartment[105]. The commercially available lipid formulation Lipofectamine2000 also proved to be highly potent as an mRNA transfection agent. Moreover, mRNA release from these lipoplexes appears to be slow, leading to a prolonged protein production[105]. These encouraging results obtained with cationic lipids were not attained with cationic polymers. For example, 25 kDa PEI which is very effective for pDNA delivery, is much less efficient as an mRNA carrier. It has been shown that binding of cationic polymers to single-stranded mRNA is stronger than to pDNA which prevents its cytosolic release[215]. Our work demonstrated that galactosylated polycationic amphiphilic cyclodextrins very efficiently deliver mRNA to HepG2 cells **(chapter 4)**[104].

Also physical methods can be applied to achieve mRNA delivery. Electroporation, for example, yields a large number of transfected cells and as mRNA has to cross only the plasma membrane, less stringent electrical settings can be used than required for pDNA delivery. Therefore, electroporation in combination with mRNA is less toxic than with pDNA[218]. An advantage of electroporation is that it delivers the mRNA directly into the cytosol, thus possibly circumventing detection by the endosomal TLRs and preventing subsequent undesired immune responses.

In addition to optimizing the transfection protocol, many research groups also focused on enhancing mRNA stability. This has been achieved by improving the

mRNA cap structure, increasing the length of the polyA tail[215], the use of the 3' untranslated regions (UTRs) from stable mRNAs (i.e. β-globin) and optimizing codons[219]. For a more detailed overview the reader is referred to two recent reviews[220, 221].

The finding that mRNA can be used as a gene-therapeutic modality may broaden the range of diseases and genetic disorders to be treated by gene therapy. Depending on the specific pathologic situation, a certain protein-expression pattern will be required. The individual selection of the best delivery method and the rational choice between pDNA and mRNA, allowing to achieve that particular expression pattern may bring effective gene therapy closer to reality.

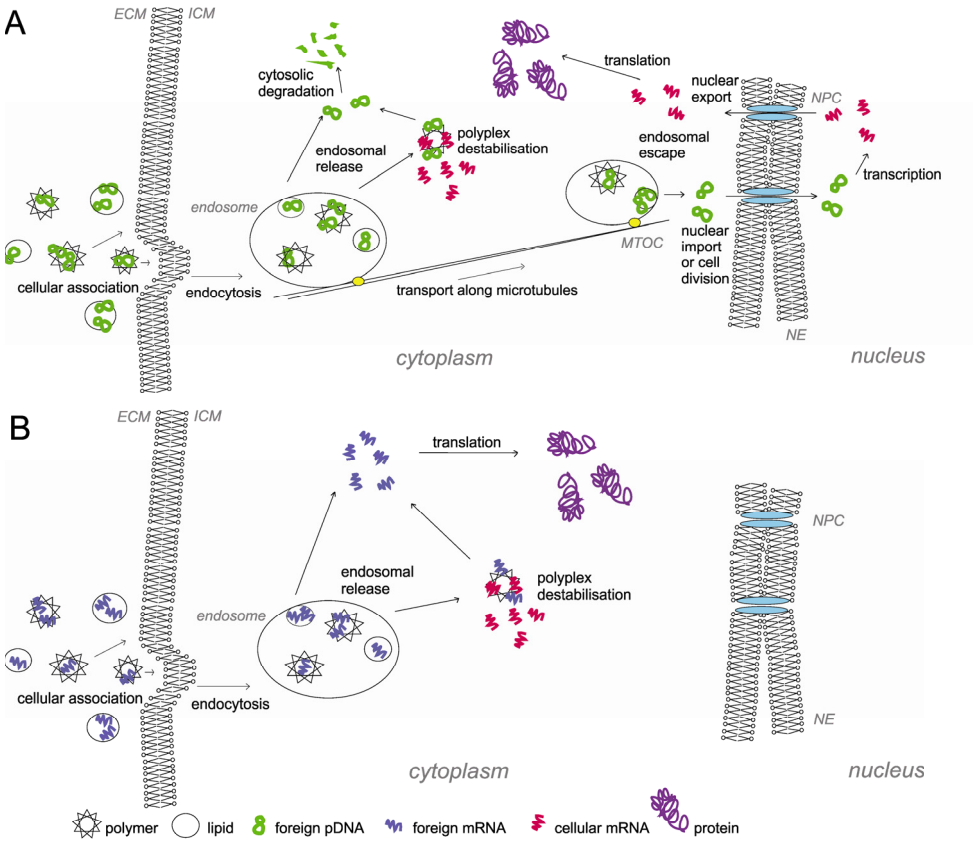

Figure 6. Nucleic acid delivery with polyplexes and lipoplexes: different transfection pathways for **(A)** pDNA and **(B)** mRNA delivery are depicted. ECM: extracellular side of the plasma membrane, ICM: intracellular side of the plasma membrane, MTOC: microtubule organizing center, NPC: nuclear pore complex, NE: nuclear envelope.

10. GENERAL CONCLUSIONS (Table 1)

In non-diving cells, all cargo that goes into and out of the cell nucleus has to pass the NPCs. In dividing cells, however, the nuclear permeability barrier temporary disappears, leading to extra opportunities for macromolecules and nanoparticles to reach the nuclear interior during or shortly after mitosis. Viruses already explored this mitotic window of opportunity, by taking advantage of cell division to strongly anchor their genome to the chromosomes of the cells. The viral genomes then integrate (retroviruses) into the host genome, or are kept as an extrachromosomal episome (latent DNA viruses) that replicates and partitions together with the host genome. However, viruses display several properties which limit their clinical utility, such as limited DNA-carrying capacity, immunogenicity and for some viral vectors, insertional mutagenesis. Therefore, the ultimate challenge is to design an artificial non-viral carrier which equals viral transfection efficiencies, but which is safe to use, non-immunogenic, non-oncogenic and relatively inexpensive and easy to produce. Unfortunately, this is difficult to achieve as it requires the integration of many different and often counteracting features in a single particle. In this review, we focused on features which could enable nuclear enclosure of pDNA-containing particles during mitosis.

The partitioning of cell organelles has been reported to be a random process. The equal distribution of key organelles located in the cytosol to the daughter cells appears to be passive or active partitioning, involving transport along microtubules. For exogenous macromolecules such as pDNA and dextrans, which cannot pass the NPCs, it has been demonstrated that NEBD is not sufficient to ensure efficient uptake into the daughter nuclei. Rather, it seems that only chromosomes and macromolecules associated with them are included in newly formed nuclei. This most likely results from the fact that a closed NE is formed around tightly compacted chromatin before nuclear expansion occurs, leaving no space for neighboring molecules, cell organelles and nanoparticles to be enclosed. Shortly after mitosis,

however, the NPCs in the newly formed NE are reported to be more permeable, thereby temporary shifting the size exclusion criteria to larger molecular weights.

The intracellular fate of small inert nanoparticles such as gold, polystyrene and iron oxide nanoparticles and quantum dots has been reported. In general, these nanoparticles are endocytosed and remain within the endosomal compartments of the cell. They are not frequently reported to be in the nucleus of the cells, although their small size (10-20 nm) most likely permits access to the nuclear interior through the NPCs. Upon cell division, in many cases a nice and uniform dilution of the endocytosed particles has been described, but this is not a general rule. Asymmetric division of stem cells, asymmetric segregation of particles in endosomes and the possible induction of autophagy are several examples of nature's way to overcome nanoparticle-induced cellular stress and which may result in a large heterogeneity of nanoparticle numbers upon continued cell proliferation.

Studies focusing on the partitioning during cell division of larger non-viral gene delivery nanoparticles (100 – 200 nm) are very rare, although insight in the cytoplasmic versus nucleoplasmic distribution of nanoparticles during subsequent cell divisions is highly relevant. Because most authors have observed increased transfection efficiencies following mitosis, the results suggest that NEBD aids the nanoparticles or pDNA in reaching the nuclear interior. However, a direct proof of this hypothesis has not been provided yet. Also we share the opinion that NEBD helps nanoparticles to deliver their pDNA to the nucleus of the cells. Furthermore, we believe that targeting of pDNA or pDNA-containing nanoparticles to chromatin could be an interesting feature to further increase transfection efficiency in dividing cells. Based upon the viral examples given, chromatin binding as such is not a guarantee for nuclear inclusion. Instead, a strong anchoring to chromatin is needed, involving multiple chromatin-binding protein recognition sites in the pDNA and the presence of multiple chromatin-tethering factors and endogenous cellular proteins in one segregation complex. To date, the chromatin-binding properties of the viral proteins EBNA1, E2 and LANA provide the most interesting features to explore chromatin

targeting. Ideally, we can incorporate some interesting viral features for chromosome binding, without the introduction of the immunogenicity, oncogenicity or insertional mutagenesis which are often associated with viral carriers. Also, development of cell-responsive particles which disintegrate at the onset of mitosis seems to be a promising concept to study. It is, however, not realistic to believe that the various options as presented by us in the foregoing, will easily lead to the ultimate goal of improving intranuclear delivery of exogenous genes. Only careful and systematic studies of the individual steps involved in the process, without ignoring the transfection process as a whole, can lead to success. The ideally designed non-viral particles will have to overcome many extra- and intracellular barriers to accomplish highly efficient pDNA expression, replication and segregation of the pDNA to the progeny cells. Furthermore, mRNA has been proved to be a promising alternative to pDNA. Since it does not require intranuclear localization to guarantee protein production, it will allow treatment of non-dividing cells.

Table 1. Intracellular partitioning and nuclear inclusion/exclusion of cell organelles, free macromolecules, inert nanoparticles, non-viral gene delivery particles and viruses upon mitosis.

		References
Cell organelles		
Endosomal vesicles	passive or active (through	[40, 41]
Golgi apparatus	interaction with the mitotic spindle	[41, 47, 49-51]
Endoplasmic reticulum /	or the chromosomes) partitioning;	[19, 37, 38, 52, 53]
Nuclear envelope	nuclear exclusion	
Free macromolecules		
Labeled dextrans	< 25 kDa: through NPCs > 25 kDa: nuclear exclusion	[31, 39, 60, 61]
plasmid DNA	labeled: nuclear exclusion unlabeled: nuclear enclosure	[60, 71-73]

Inorganic nanoparticles		
Gold particles	< 10 nm: through NPCs 10-20 nm: nuclear enclosure > 20 nm: nuclear exclusion	93, 94
Quantum dots	Symmetric or asymmetric segregation within endosomes; nuclear exclusion	83, 84
Iron oxide nanoparticles		92
Non-viral gene delivery particles		
Lipid carriers	unknown	5, 8, 13-17
Polymer carriers		5, 8, 12
Viruses	*chromatin-tethering factor*	
Murine leukemia virus (MuLV)	(p12)	139, 140
Human immunodeficiency virus (HIV)	(LEDGF/p75)	148
Avian sarcoma virus (ASV)	(IN)	138
Foamy virus (FV)	(Gag)	150, 151
Epstein Barr virus (EBV)	EBNA1	154-156
Kaposi sarcoma-associated herpesvirus (KSHV)	LANA	158, 159, 161
Bovine (BPV) and human papillomavirus (HPV)	E2	162-165

REFERENCES

1. Lam, A.P. & Dean, D.A. Progress and prospects: nuclear import of nonviral vectors. *Gene Ther.* **17**, 439-447 (2010).
2. Fackelmayer, F.O. Nuclear architecture and gene expression in the quest for novel therapeutics. *Curr. Pharm. Des.* **10**, 2851-2860 (2004).
3. Dean, D.A., Strong, D.D. & Zimmer, W.E. Nuclear entry of nonviral vectors. *Gene Ther.* **12**, 881-890 (2005).
4. Gado-Canedo, A., Santos, D.G., Chies, J.A., Kvitko, K. & Nardi, N.B. Optimization of an electroporation protocol using the K562 cell line as a model: role of cell cycle phase and cytoplasmic DNAses. *Cytotechnology* **51**, 141-148 (2006).
5. Brunner, S., Sauer, T., Carotta, S., Cotton, M., Saltik, M. & Wagner, E. Cell cycle dependence of gene transfer by lipoplex polyplex and recombinant adenovirus. *Gene Ther.* **7**, 401-407 (2000).
6. Malumbres, M. Physiological relevance of cell cycle kinases. *Physiol. Rev.* **91**, 973-1007 (2011).
7. Bollen, M., Gerlich, D.W. & Lesage, B. Mitotic phosphatases: from entry guards to exit guides. *Trends Cell Biol.* **19**, 531-541 (2009).
8. Wilke, M., Fortunati, E., Van Den Broek, M., Hoogeveen, A.T. & Scholte, B.J. Efficacy of a peptide-based gene delivery system depends on mitotic activity. *Gene Ther.* **12**, 1133-1142 (1996).
9. Labat-Moleur, F., Steffan, A.M., Brisson, C., Perron, H., Feugeas, O., Furstenberger, P., Oberling, F., Brambilla, E. & Behr, J.P. An electron microscopy study into the mechanism of gene transfer with lipopolyamines. *Gene Ther.* **3**, 1010-1017 (1996).
10. Capecchi, M.R. High efficiency transformation by direct microinjection of DNA into cultured mammalian cells. *Cell* **22**, 479-488 (1980).
11. Zabner, J., Fasbender, A.J., Moninger, T., Poellinger, K.A. & Welsh, M.J. Cellular and molecular barriers to gene transfer by a cationic lipid. *J. Biol. Chem.***270**, 18997-19007 (1995).
12. Brunner, S., Furtbauer, E., Sauer, T., Kursa, M. & Wagner, E. Overcoming the nuclear barrier: cell cycle independent nonviral gene transfer with linear PEI or electroporation. *Mol. Ther.* **5**, 80-86 (2002).
13. Mortimer, I., Tam, P., MacLachlan, I., Graham, R.W., Saravolac, E.G. & Joshi P.B. Cationic lipid-mediated transfection of cells in culture requires mitotic activity. *Gene Ther.* **6**, 403-411 (1999).
14. Tseng, W.C., Haselton, F.R. & Giorgio, T.D. Mitosis enhances transgene expression of plasmid delivered by cationic liposomes. *Biochim. Biophys. Acta* **1445**, 53-64 (1999).
15. Escriou, V., Carriere, M., Bussone, F., Wils, P. & Scherman, D. Critical assessment of the nuclear import of plasmid during cationic lipid-mediated gene transfer. *J. Gene Med.* **3**, 179-187 (2001).
16. Fasbender, A., Zabner, J., Zeiher, B.G. & Welsh, M.J. A low rate of cell proliferation and reduced DNA uptake limit cationic lipid-mediated gene

transfer to primary cultures of ciliated human airway epithelia. *Gene Ther.* **4**, 1173-1180 (1997).

17. Jiang, C., O'Connor, S.P., Fang, S.L., Wang, K.X., Marshall, J., Williams, J.L., Wilburn, B., Echelard, Y. & Cheng, S.H. Efficiency of cationic lipid-mediated transfection of polarized and differentiated airway epithelial cells in vitro and in vivo. *Hum. Gene Ther.* **9**, 1531-1542 (1998).
18. Mannisto, M., Ronkko, S., Matto, M., Honkakoski, P., Hyttinen, M., Pelkonen J. & Urtti, A. The role of cell cycle on polyplex-mediated gene transfer into a retinal pigment epithelial cell line. *J. Gene Med.* **7**, 466-476 (2005).
19. Hetzer, M.W., Walther, T.C. & Mattaj, I.W. Pushing the envelope: structure, function, and dynamics of the nuclear periphery. *Annu. Rev. Cell Dev. Biol.* **21**, 347-380 (2005).
20. Gant, T.M. & Wilson, K.L. Nuclear assembly. *Annu. Rev. Cell Dev. Biol.* **13**, 669-695 (1997).
21. van der Aa, M.A., Mastrobattista, E., Oosting, R.S., Hennink, W.E., Koning, G.A. & Crommelin, D.J. The nuclear pore complex: the gateway to successful nonviral gene delivery. *Pharm. Res.* **23**, 447-459 (2006).
22. Antonin, W., Ellenberg, J. & Dultz, E. Nuclear pore complex assembly through the cell cycle: regulation and membrane organization. *FEBS Lett.* **582**, 2004-2016 (2008).
23. Van de Vosse, D.W., Wan, Y., Wozniak, R.W. & Aitchison, J.D. Role of the nuclear envelope in genome organization and gene expression. *Wiley. Interdiscip. Rev. Syst. Biol. Med.* **3**, 147-166 (2011).
24. Margalit, A., Vlcek, S., Gruenbaum, Y. & Foisner, R. Breaking and making of the nuclear envelope. *J. Cell. Biochem.* **95**, 454-465 (2005).
25. Shimi, T., Koujin, T., Segura-Totten, M., Wilson, K.L., Haraguchi, T. & Hiraoka, Y. Dynamic interaction between BAF and emerin revealed by FRAP, FLIP, and FRET analyses in living HeLa cells. *J. Struct. Biol.* **147**, 31-41 (2004).
26. Segura-Totten, M., Kowalski, A.K., Craigie, R. & Wilson, K.L. Barrier-to-autointegration factor: major roles in chromatin decondensation and nuclear assembly. *J. Cell Biol.* **158**, 475-485 (2002).
27. Maraldi, N.M., Capanni, C., Cenni, V., Fini, M. & Lattanzi, G. Laminopathies and lamin-associated signaling pathways. *J. Cell Biochem.* **112**, 979-992 (2011).
28. Coutinho, H.D., Falcao-Silva, V.S., Goncalves, G.F. & da Nobrega, R.B. Molecular ageing in progeroid syndromes: Hutchinson-Gilford progeria syndrome as a model. *Immun. Ageing* **6**, 4 (2009).
29. Rajapakse, I. & Groudine, M. On emerging nuclear order. *J. Cell Biol.***192**, 711-721 (2011).
30. Higa, M.M., Ullman, K.S. & Prunuske, A.J. Studying nuclear disassembly in vitro using Xenopus egg extract. *Methods* **39**, 284-290 (2006).
31. Lenart, P. & Ellenberg, J. Monitoring the permeability of the nuclear envelope during the cell cycle. *Methods* **38**, 17-24 (2006).
32. de Gramont, A. & Cohen-Fix, O. The many phases of anaphase. *Trends Biochem. Sci.* **30**, 559-568 (2005).

33. Guttinger, S., Laurell, E. & Kutay, U. Orchestrating nuclear envelope disassembly and reassembly during mitosis. *Nat. Rev. Mol. Cell Biol.* **10**, 178-191 (2009).
34. Maison, C., Horstmann, H. & Georgatos, S.D. Regulated docking of nuclear membrane vesicles to vimentin filaments during mitosis. *J. Cell Biol.* **123**, 1491-1505 (1993).
35. Wilson, K.L. & Newport, J. A Trypsin-Sensitive Receptor on Membrane-Vesicles Is Required for Nuclear-Envelope Formation Invitro. *J. Cell Biol.* **107**, 57-68 (1988).
36. Chaudhary, N. & Courvalin, J.C. Stepwise reassembly of the nuclear envelope at the end of mitosis. *J. Cell Biol.* **122**, 295-306 (1993).
37. Webster, M., Witkin, K.L. & Cohen-Fix, O. Sizing up the nucleus: nuclear shape, size and nuclear-envelope assembly. *J. Cell Sci.* **122**, 1477-1486 (2009).
38. Lu, L., Ladinsky, M.S. & Kirchhausen, T. Formation of the postmitotic nuclear envelope from extended ER cisternae precedes nuclear pore assembly. *J. Cell Biol.* **194**, 425-440 (2011).
39. Swanson, J.A. & McNeil, P.L. Nuclear reassembly excludes large macromolecules. *Science* **238**, 548-550 (1987).
40. Bergeland, T., Widerberg, J., Bakke, O. & Nordeng, T.W. Mitotic partitioning of endosomes and lysosomes. *Curr. Biol.* **11**, 644-651 (2001).
41. Dunster, K., Toh, B.H. & Sentry, J.W. Early endosomes, late endosomes, and lysosomes display distinct partitioning strategies of inheritance with similarities to Golgi-derived membranes. *Eur. J. Cell Biol.* **81**, 117-124 (2002).
42. Farquhar, M.G. & Palade, G.E. The Golgi apparatus (complex)-(1954-1981)-from artifact to center stage. *J. Cell Biol.* **91**, 77s-103s (1981).
43. Pelham, H.R. Sorting and retrieval between the endoplasmic reticulum and Golgi apparatus. *Curr. Opin. Cell. Biol.* **7**, 530-535 (1995).
44. Griffiths, G. & Simons, K. The trans Golgi network: sorting at the exit site of the Golgi complex. *Science* **234**, 438-443 (1986).
45. Perroncito, A. Contribution a l'etude de la biologic cellulaire. Mitochondres, chromidies et appareil reticulaire interne dans les cellules spermatiques. Le phenomene de la dictyokinese. *Arch. Ital. Biol.* **54**, 307-345 (1910).
46. Lucocq, J.M., Pryde, J.G., Berger, E.G. & Warren, G. A mitotic form of the Golgi apparatus in HeLa cells. *J. Cell Biol.* **104**, 865-874 (1987).
47. Lucocq, J.M. & Warren, G. Fragmentation and partitioning of the Golgi apparatus during mitosis in HeLa cells. *EMBO J.* **6**, 3239-3246 (1987).
48. Lucocq, J.M., Berger, E.G. & Warren, G. Mitotic Golgi fragments in HeLa cells and their role in the reassembly pathway. *J. Cell Biol.* **109**, 463-474 (1989).
49. Birky, C.W., Jr. The partitioning of cytoplasmic organelles at cell division. *Int. Rev. Cytol. Suppl.* **15**, 49-89 (1983).
50. Shima, D.T., Haldar, K., Pepperkok, R., Watson, R. & Warren, G. Partitioning of the Golgi apparatus during mitosis in living HeLa cells. *J. Cell Biol.* **137**, 1211-1228 (1997).

51. Ho, W.C., Allan, V.J., van Meer, G., Berger, E.G. & Kreis, T.E. Reclustering of scattered Golgi elements occurs along microtubules. *Eur. J. Cell Biol.* **48**, 250-263 (1989).
52. Rabouille, C. & Jokitalo, E. Golgi apparatus partitioning during cell division. *Mol. Membr. Biol.* **20**, 117-127 (2003).
53. Zaal, K.J., Smith, C.L., Polishchuk, R.S., Altan, N., Cole, N.B., Ellenberg, J., Hirschberg, K., Presley, J.F., Roberts, T.H., Siggia, E., Phair, R.D. & Lippincott-Schwartz, J. Golgi membranes are absorbed into and reemerge from the ER during mitosis. *Cell* **99**, 589-601 (1999).
54. Shima, D.T., Cabrera-Poch, N., Pepperkok, R. & Warren, G. An ordered inheritance strategy for the Golgi apparatus: visualization of mitotic disassembly reveals a role for the mitotic spindle. *J. Cell Biol.* **141**, 955-966 (1998).
55. Luby-Phelps, K. Preparation of fluorescently labeled dextrans and ficolls. *Methods Cell Biol.* **29**, 59-73 (1989).
56. Benavente, R., Scheer, U. & Chaly, N. Nucleocytoplasmic sorting of macromolecules following mitosis: fate of nuclear constituents after inhibition of pore complex function. *Eur. J. Cell Biol.* **50**, 209-219 (1989).
57. Gautier, T., Robert-Nicoud, M., Guilly, M.N. & Hernandez-Verdun, D. Relocation of nucleolar proteins around chromosomes at mitosis. A study by confocal laser scanning microscopy. *J. Cell Sci.* **102 (Pt 4)**, 729-737 (1992).
58. Hernandez-Verdun, D. & Gautier, T. The chromosome periphery during mitosis. *Bioessays* **16**, 179-185 (1994).
59. Van Hooser, A.A., Yuh, P. & Heald, R. The perichromosomal layer. *Chromosoma* **114**, 377-388 (2005).
60. Ludtke, J.J., Sebestyen, M.G. & Wolff, J.A. The effect of cell division on the cellular dynamics of microinjected DNA and dextran. *Mol. Ther.* **5**, 579-588 (2002).
61. Miyawaki, A., Shimozono, S. & Tsutsui, H. Diffusion of Large Molecules into Assembling Nuclei Revealed Using an Optical Highlighting Technique. *Biophys. J.* **97**, 1288-1294 (2009).
62. Lukacs, G.L., Haggy, P., Seksek, O., Lechardeur, D., Freedman, N. & Verkman, A.S. Size-dependent DNA mobility in cytoplasm and nucleus. *J. Biol. Chem.* **275**, 1625-1629 (2000).
63. Lechardeur, D., Soh, K.J., Haardt, M., Joshi, P.B., Monck, M., Graham, R.W., Beatty, B., Squire, J., O'Brodovich, H. & Lukacs G.L. Metabolic instability of plasmid DNA in the cytosol: a potential barrier to gene transfer. *Gene Ther.* **6**, 482-497 (1999).
64. Escriou, V., Ciolina, C., Helbling-Leclerc, A., Wils, P. & Scherman, D. Cationic lipid-mediated gene transfer: Analysis of cellular uptake and nuclear import of plasmid DNA. *Cell Biol. Toxicol.* **14**, 95-104 (1998).
65. Pollard, H., Remy, J.S., Loussouarn, G., Demolombe, S., Behr, J.P. & Escande, D. Polyethylenimine but not cationic lipids promotes transgene delivery to the nucleus in mammalian cells. *J. Biol. Chem.* **273**, 7507-7511 (1998).

66. Subramanian, A., Ranganathan, P. & Diamond, S.L. Nuclear targeting peptide scaffolds for lipofection of nondividing mammalian cells. *Nat. Biotechnol.* **17**, 873-877 (1999).
67. Sebestyen, M.G., Ludtke, J.J., Bassik, M.C., Zhang, G., Budker, V., Lukhtanov, E.A., Hagstrom, J.E. & Wagner, E. DNA vector chemistry: the covalent attachment of signal peptides to plasmid DNA. *Nat. Biotechnol.* **16**, 80-85 (1998).
68. Dean, D.A., Dean, B.S., Muller, S. & Smith, L.C. Sequence requirements for plasmid nuclear import. *Exp. Cell Res.* **253**, 713-722 (1999).
69. Vandenbroucke, R.E., Lucas, B., Demeester, J., De Smedt, S.C. & Sanders, N.N. Nuclear accumulation of plasmid DNA can be enhanced by non-selective gating of the nuclear pore. *Nucleic acids Res.* **35**, e86 (2007).
70. Dowty, M.E., Williams, P., Zhang, G.F., Hagstrom, J.E. & Wolff, J.A. Plasmid DNA Entry into Postmitotic Nuclei of Primary Rat Myotubes. *Proc. Natl. Acad. Sci. USA* **92**, 4572-4576 (1995).
71. Remaut, K., Sanders, N.N., Fayazpour, F., Demeester, J. & De Smedt, S.C. Influence of plasmid DNA topology on the transfection properties of DOTAP/DOPE lipoplexes. *J. Control. Release* **115**, 335-343 (2006).
72. Gasiorowski, J.Z. & Dean, D.A. Postmitotic nuclear retention of episomal plasmids is altered by DNA labeling and detection methods. *Mol. Ther.* **12**, 460-467 (2005).
73. Shimizu, N., Kamezaki, F. & Shigematsu, S. Tracking of microinjected DNA in live cells reveals the intracellular behavior and elimination of extrachromosomal genetic material. *Nucleic acids Res.* **33**, 6296-6307 (2005).
74. Newmeyer, D.D., Lucocq, J.M., Burglin, T.R. & De Robertis, E.M. Assembly in vitro of nuclei active in nuclear protein transport: ATP is required for nucleoplasmin accumulation. *EMBO J.* **5**, 501-510 (1986).
75. Newport, J. Nuclear Reconstitution Invitro - Stages of Assembly around Protein-Free DNA. *Cell* **48**, 205-217 (1987).
76. Shimizu, K., Maitani, Y., Takayama, K. & Nagai, T. Formulation of liposomes with a soybean-derived sterylglucoside mixture and cholesterol for liver targeting. *Biol. Pharm. Bull.* **20**, 881-886 (1997).
77. Srinivasan, C., Lee, J., Papadimitrakopoulos, F., Silbart, L.K., Zhao, M. & Burgess, D.J. Labeling and intracellular tracking of functionally active plasmid DNA with semiconductor quantum dots. *Mol. Ther.* **14**, 192-201 (2006).
78. Kim, B.Y.S., Rutka, J.T. & Chan, W.C.W. Current Concepts: Nanomedicine. *New Engl. J. Med.* **363**, 2434-2443 (2010).
79. Derveaux, S., Stubbe, B.G., Roelant, C., Leblans, M., De Geest, B.G., Demeester J. & De Smedt, S.C. Layer-by-layer coated digitally encoded microcarriers for quantification of proteins in serum and plasma. *Anal. Chem.* **80**, 85-94 (2008).
80. Sauer, A.M., de Bruyn, K.G., Ruthardt, N., Mykhaylyk, O., Plank, C. & Brauchle, C. Dynamics of magnetic lipoplexes studied by single particle tracking in living cells. *J. Control. Release* **137**, 136-145 (2009).

81. Zhang, B.Q., Zhang, Y.J., Mallapragada, S.K. & Clapp, A.R. Sensing Polymer/DNA Polyplex Dissociation Using Quantum Dot Fluorophores. *ACS Nano* **5**, 129-138 (2011).
82. Dreaden, E.C., Mackey, M.A., Huang, X.H., Kang, B. & El-Sayed, M.A. Beating cancer in multiple ways using nanogold. *Chem. Soc. Rev.* **40**, 3391-3404 (2011).
83. Feldherr, C.M. Nucleocytoplasmic exchanges during cell division. *J. Cell Biol.* **31**, 199-203 (1966).
84. Feldherr, C.M. & Akin, D. The permeability of the nuclear envelope in dividing and nondividing cell cultures. *J. Cell Biol.* **111**, 1-8 (1990).
85. Maul, G.G., Maul, H.M., Scogna, J.E., Lieberman, M.W., Stein, G.S., Hsu, B.Y. & Borun, T.W. Time sequence of nuclear pore formation in phytohemagglutinin-stimulated lymphocytes and in HeLa cells during the cell cycle. *J. Cell Biol.* **55**, 433-447 (1972).
86. Harris, P. Electron microscope study of mitosis in sea urchin blastomeres. *J. Biophys. Biochem. Cytol.* **11**, 419-431 (1961).
87. Robbins, E. & Gonatas, N.K. The Ultrastructure of a Mammalian Cell during the Mitotic Cycle. *J. Cell Biol.* **21**, 429-463 (1964).
88. Stevens, B.J. The Fine Structure of the Nucleolus during Mitosis in the Grasshopper Neuroblast Cell. *J. Cell Biol.* **24**, 349-368 (1965).
89. Symens, N., Walczak, R., Demeester, J., Mattaj, I., De Smedt, S.C. & Remaut, K. Nuclear inclusion of nontargeted and chromatin-targeted polystyrene beads and plasmid DNA containing nanoparticles. *Mol. Pharmaceut.* **8**, 1757-1766 (2011).
90. Soenen, S.J., Hodenius, M. & De Cuyper, M. Magnetoliposomes: versatile innovative nanocolloids for use in biotechnology and biomedicine. *Nanomedicine* **4**, 177-191 (2009).
91. Liu, K.K., Wang, C.C., Cheng, C.L. & Chao, J.I. Endocytic carboxylated nanodiamond for the labeling and tracking of cell division and differentiation in cancer and stem cells. *Biomaterials* **30**, 4249-4259 (2009).
92. Walczak, P., Kedziorek, D.A., Gilad, A.A., Barnett, B.P. & Bulte, J.W. Applicability and limitations of MR tracking of neural stem cells with asymmetric cell division and rapid turnover: the case of the shiverer dysmyelinated mouse brain. *Magn. Reson. Med.* **58**, 261-269 (2007).
93. Errington, R.J., Brown, M.R., Silvestre, O.F., Njoh, K.L., Chappell, S.C., Khan, I.A., Rees, P., Wilks, S.P., Smith, P.J. & Summers, H.D. Single cell nanoparticle tracking to model cell cycle dynamics and compartmental inheritance. *Cell cycle* **9**, 121-130 (2010).
94. Summers, H.D., Rees, P., Holton, M.D., Brown, M.R., Chappell, S.C., Smith, P.J. & Errington, R.J. Statistical analysis of nanoparticle dosing in a dynamic cellular system. *Nat. Nanotechnol.* **6**, 170-174 (2011).
95. Summers, H. Can cells reduce nanoparticle toxicity? *Nano Today* **5**, 83-84 (2010).
96. Seleverstov, O., Zabirnyk, O., Zscharnack, M., Bulavina, L., Nowicki, M., Heinrich, J.M., Yezhelyev, M., Emmrich, F., O'Regan, F. & Bader, A. Quantum

dots for human mesenchymal stem cells labeling. A size-dependent autophagy activation. *Nano Lett.* **6**, 2826-2832 (2006).
97. Li, J.J., Hartono, D., Ong, C.N., Bay, B.H. & Yung, L.Y.L. Autophagy and oxidative stress associated with gold nanoparticles. *Biomaterials* **31**, 5996-6003 (2010).
98. Yuan, X., Naguib, S. & Wu, Z. Recent advances of siRNA delivery by nanoparticles. *Expert Opin. Drug Deliv.* **8**, 521-536 (2011).
99. Soenen, S.J., Brisson, A.R. & De Cuyper, M. Addressing the problem of cationic lipid-mediated toxicity: the magnetoliposome model. *Biomaterials* **30**, 3691-3701 (2009).
100. Le Bihan, O., Chevre, R., Mornet, S., Garnier, B., Pitard, B. & Lambert, O. Probing the in vitro mechanism of action of cationic lipid/DNA lipoplexes at a nanometric scale. *Nucleic acids Res.* **39**, 1595-1609 (2011).
101. Akinc, A., Thomas, M., Klibanov, A.M. & Langer, R. Exploring polyethylenimine-mediated DNA transfection and the proton sponge hypothesis. *J. Gene Med.* **7**, 657-663 (2005).
102. Braeckmans, K., Buyens, K., Bouquet, W., Vervaet, C., Joye, P., De Vos, F., Plawinski, L., Doeuvre, L., Angles-Cano, E., Sanders, N.N., Demeester, J. & De Smedt, S.C. Sizing nanomatter in biological fluids by fluorescence single particle tracking. *Nano Lett.* **10**, 4435-4442 (2010).
103. Remaut, K., Sanders, N.N., De Geest, B.G., Braeckmans, K., Demeester, J. & De Smedt, S.C. Nucleic acid delivery: Where material sciences and bio-sciences meet. *Mat. Sci. Eng. R.* **58**, 117-161 (2007).
104. Symens, N., Méndez-Ardoy, A., Díaz-Moscoso, A., Remaut, K., Demeester, J., Garcia Fernandez, J.M., De Smedt, S.C. & Rejman, J. Galactosylated cyclodextrins for transfection of hepatocytes. *Bioconjug. Chem.* **23** (6), 1276-1289 (2012).
105. Rejman, J., Tavernier, G., Bavarsad, N., Demeester, J. & De Smedt, S.C. mRNA transfection of cervical carcinoma and mesenchymal stem cells mediated by cationic carriers. *J. Control. Release* **147**, 385-391 (2010).
106. Bieber, T., Meissner, W., Kostin, S., Niemann, A. & Elsasser, H.P. Intracellular route and transcriptional competence of polyethylenimine-DNA complexes. *J. Control. Release* **82**, 441-454 (2002).
107. Zhao, N., Roesler, S. & Kissel, T. Synthesis of a new potential biodegradable disulfide containing poly(ethylene imine)-poly(ethylene glycol) copolymer cross-linked with click cluster for gene delivery. *Int. J. Pharm.* **411**, 197-205 (2011).
108. Sasaki, A. & Kinjo, M. Monitoring intracellular degradation of exogenous DNA using diffusion properties. *J. Control. Release* **143**, 104-111 (2010).
109. Keller, M., Harbottle, R.P., Perouzel, E., Colin, M., Shah, I., Rahim, A., Vaysse, L., Bergau, A., Moritz, S., Brahimi-Horn, C., Coutelle, C. & Miller, A.D. Nuclear localisation sequence templated nonviral gene delivery vectors: investigation of intracellular trafficking events of LMD and LD vector systems. *Chembiochem* **4**, 286-298 (2003).

110. Godbey, W.T., Wu, K.K. & Mikos, A.G. Tracking the intracellular path of poly(ethylenimine)/DNA complexes for gene delivery. *Proc. Natl. Acad. Sci. USA* **96**, 5177-5181 (1999).
111. Breuzard, G., Tertil, M., Goncalves, C., Cheradame, H., Geguan, P., Pichon, C. & Midoux, P. Nuclear delivery of NFkappaB-assisted DNA/polymer complexes: plasmid DNA quantitation by confocal laser scanning microscopy and evidence of nuclear polyplexes by FRET imaging. *Nucleic acids Res.* **36**, e71 (2008).
112. Bieber, T., Meissner, W., Kostin, S., Niemann, A. & Elsasser, H. Intracelullar route and transcriptional competence of polyethylenimine-DNA complexes. *J. Control. Release* **82**, 441-454 (2002).
113. Itaka, K., Harada, A., Yamasaki, Y., Nakamura, K., Kawaguchi, H. & Kataoka, K. In situ single cell observation by fluorescence resonance energy transfer reveals fast intra-cytoplasmic delivery and easy release of plasmid DNA complexed with linear polyethylenimine. *J. Gene Med.* **6**, 76-84 (2004).
114. Tseng, W.C., Purvis, N.B., Haselton, F.R. & Giorgio, T.D. Cationic liposomal delivery of plasmid to endothelial cells measured by quantitative flow cytometry. *Biotechnol. Bioeng.* **50**, 548-554 (1996).
115. Marenzi, S., Adams, R.L., Zardo, G., Lenti, L., Reale, A. & Caiafa, P. Efficiency of expression of transfected genes depends on the cell cycle. *Mol. Biol. Rep.* **26**, 261-267 (1999).
116. Liu, G., Li, D.S., Pasumarthy, M.K., Kowalczyk, T.H., Gedeon, C.R., Hyatt, S.L., Payne, J.M., Miller, T.J., Brunovskis, P., Fink, T.L., Muhammad, O., Moen, R.C., Hanson, R.W. & Cooper, M.J. Nanoparticles of compacted DNA transfect postmitotic cells. *J. Biol. Chem.* **278**, 32578-32586 (2003).
117. Greber, U.F. & Fassati, A. Nuclear import of viral DNA genomes. *Traffic* **4**, 136-143 (2003).
118. Wagner, E.K. & Hewlett, M.J. Basic Virology, Edn. second. (Blackwell publishing, Malden, Oxford, Carlton; 2004).
119. Whittaker, G.R. Virus nuclear import. *Adv. Drug Deliv. Rev.* **55**, 733-747 (2003).
120. Meehan, A.M. & Poeschla, E.M. Chromatin tethering and retroviral integration: recent discoveries and parallels with DNA viruses. *Biochim. Biophys. Acta* **1799**, 182-191 (2010).
121. Springett, G.M., Moen, R.C., Anderson, S., Blaese, R.M. & Anderson, W.F. Infection Efficiency of Lymphocytes-T with Amphotropic Retroviral Vectors Is Cell-Cycle Dependent. *J. Virol.* **63**, 3865-3869 (1989).
122. Miller, D.G., Adam, M.A. & Miller, A.D. Gene-Transfer by Retrovirus Vectors Occurs Only in Cells That Are Actively Replicating at the Time of Infection. *Mol. Cell. Biol.* **10**, 4239-4242 (1990).
123. Harel, J., Rassart, E. & Jolicoeur, P. Cell-Cycle Dependence of Synthesis of Unintegrated Viral-DNA in Mouse Cells Newly Infected with Murine Leukemia-Virus. *Virology* **110**, 202-207 (1981).
124. Roe, T.Y., Reynolds, T.C., Yu, G. & Brown, P.O. Integration of Murine Leukemia-Virus DNA Depends on Mitosis. *EMBO J.* **12**, 2099-2108 (1993).

125. Stevenson, M., Stanwick, T.L., Dempsey, M.P. & Lamonica, C.A. Hiv-1 Replication Is Controlled at the Level of T-Cell Activation and Proviral Integration. *EMBO J.* **9**, 1551-1560 (1990).
126. Zack, J.A., Arrigo, S.J., Weitsman, S.R., Go, A.S., Haislip, A. & Chen, I.S. HIV-1 entry into quiescent primary lymphocytes: molecular analysis reveals a labile, latent viral structure. *Cell* **61**, 213-222 (1990).
127. Lewis, P.F. & Emerman, M. Passage through mitosis is required for oncoretroviruses but not for the human immunodeficiency virus. *J. Virol.* **68**, 510-516 (1994).
128. Fritsch, E. & Temin, H.M. Formation and Structure of Infectious DNA of Spleen Necrosis Virus. *J. Virol.* **21**, 119-130 (1977).
129. Bader, J.P. A Change in Growth Potential of Cells after Conversion by Rous Sarcoma Virus. *J. Cell. Physiol.* **70**, 301-308 (1967).
130. Temin, H.M. Studies on Carcinogenesis by Avian Sarcoma Viruses .V. Requirement for New DNA Synthesis and for Cell Division. *J. Cell. Physiol.* **69**, 53-& (1967).
131. Weiss, R.A. Cell transformation induced by Rous sarcoma virus: analysis of density dependence. *Virology* **46**, 209-220 (1971).
132. Humphrie.Eh & Temin, H.M. Cell Cycle Dependent Activation of Rous-Sarcoma Virus-Infected Stationary Chicken Cells - Avian Leukosis Virus Group-Specific Antigens and Ribonucleic-Acid. *J. Virol* **10**, 82-87 (1972).
133. Varmus, H.E., Padgett, T., Heasley, S., Simon, G. & Bishop, J.M. Cellular Functions Are Required for Synthesis and Integration of Avian-Sarcoma Virus-Specific DNA. *Cell* **11**, 307-319 (1977).
134. Hsu, T.W. & Taylor, J.M. Effect of Aphidicolin on Avian-Sarcoma Virus-Replication. *J. Virol.* **44**, 493-498 (1982).
135. Trobridge, G. & Russell, D.W. Cell cycle requirements for transduction by foamy virus vectors compared to those of oncovirus and lentivirus vectors. *J. Virol.* **78**, 2327-2335 (2004).
136. Bieniasz, P.D., Weiss, R.A. & McClure, M.O. Cell cycle dependence of foamy retrovirus infection. *J. Virol.* **69**, 7295-7299 (1995).
137. Yamashita, M. & Emerman, M. Capsid is a dominant determinant of retrovirus infectivity in nondividing cells. *J. Virol.***78**, 5670-5678 (2004).
138. Anderson, J.L. & Hope, T.J. Intracellular trafficking of retroviral vectors: obstacles and advances. *Gene Ther.* **12**, 1667-1678 (2005).
139. Henderson, L.E., Gilden, R.V. & Oroszlan, S. Amino acid sequence homology between histone H5 and murine leukemia virus phosphoprotein p12. *Science* **203**, 1346-1348 (1979).
140. Prizan-Ravid, A., Elis, E., Laham-Karam, N., Selig, S., Ehrlich, M. & Bacharach, E. The Gag cleavage product, p12, is a functional constituent of the murine leukemia virus pre-integration complex. *PLoS Pathog.* **6**, e1001183 (2010).
141. Lewinski, M.K. & Bushman, F.D. Retroviral DNA integration--mechanism and consequences. *Adv. Genet.* **55**, 147-181 (2005).

142. Weinberg, J.B., Matthews, T.J., Cullen, B.R. & Malim, M.H. Productive Human-Immunodeficiency-Virus Type-1 (Hiv-1) Infection of Nonproliferating Human Monocytes. *J. Exp. Med.* **174**, 1477-1482 (1991).
143. Lewis, P., Hensel, M. & Emerman, M. Human-Immunodeficiency-Virus Infection of Cells Arrested in the Cell-Cycle. *EMBO J.* **11**, 3053-3058 (1992).
144. Miller, M.D., Farnet, C.M. & Bushman, F.D. Human immunodeficiency virus type 1 preintegration complexes: studies of organization and composition. *J. Virol.* **71**, 5382-5390 (1997).
145. Sherman, M.P. & Greene, W.C. Slipping through the door: HIV entry into the nucleus. *Microbes Infect.* **4**, 67-73 (2002).
146. Arhel, N. Revisiting HIV-1 uncoating. *Retrovirology* **7**, 96 (2010).
147. Fassati, A. HIV infection of non-dividing cells: a divisive problem. *Retrovirology* **3**, 74 (2006).
148. Mannioui, A., Schiffer, C., Felix, N., Nelson, E., Brussel, A., Sonigo, P., Gluckman, J.C. & Canque, B. Cell cycle regulation of human immunodeficiency virus type 1 integration in T cells: antagonistic effects of nuclear envelope breakdown and chromatin condensation. *Virology* **329**, 77-88 (2004).
149. Llano, M., Vanegas, M., Fregoso, O., Saenz, D., Chung, S., Peretz, M. & Poeschla, E.M. LEDGF/p75 determines cellular trafficking of diverse lentiviral but not murine oncoretroviral integrase proteins and is a component of functional lentiviral preintegration complexes. *J. Virol.* **78**, 9524-9537 (2004).
150. Katz, R.A., Greger, J.G., Boimel, P. & Skalka, A.M. Human immunodeficiency virus type 1 DNA nuclear import and integration are mitosis independent in cycling cells. *J. Virol.* **77**, 13412-13417 (2003).
151. Tobaly-Tapiero, J., Bittoun, P., Lehmann-Che, J., Delelis, O., Giron, M.L., de The, H. & Saib, A. Chromatin tethering of incoming foamy virus by the structural Gag protein. *Traffic* **9**, 1717-1727 (2008).
152. Mullers, E., Stirnnagel, K., Kaulfuss, S. & Lindemann, D. Prototype Foamy Virus Gag Nuclear Localization: a Novel Pathway among Retroviruses. *J. Virol.* **85**, 9276-9285 (2011).
153. Rassa, J.C. & Ross, S.R. Viruses and Toll-like receptors. *Microbes Infect.* **5**, 961-968 (2003).
154. Rosenberg, N. New transformation tricks from a barnyard retrovirus: implications for human lung cancer. *Proc. Natl. Acad. Sci. USA* **98**, 4285-4287 (2001).
155. Sears, J., Ujihara, M., Wong, S., Ott, C., Middeldorp, J. & Aiyar, A. The amino terminus of Epstein-Barr Virus (EBV) nuclear antigen 1 contains AT hooks that facilitate the replication and partitioning of latent EBV genomes by tethering them to cellular chromosomes. *J. Virol.* **78**, 11487-11505 (2004).
156. Sears, J., Kolman, J., Wahl, G.M. & Aiyar, A. Metaphase chromosome tethering is necessary for the DNA synthesis and maintenance of oriP plasmids but is insufficient for transcription activation by Epstein-Barr nuclear antigen 1. *J. Virol.* **77**, 11767-11780 (2003).

157. Nayyar, V.K., Shire, K. & Frappier, L. Mitotic chromosome interactions of Epstein-Barr nuclear antigen 1 (EBNA1) and human EBNA1-binding protein 2 (EBP2). *J. Cell Sci.* **122**, 4341-4350 (2009).
158. Kung, S.H. & Medveczky, P.G. Identification of a herpesvirus Saimiri cis-acting DNA fragment that permits stable replication of episomes in transformed T cells. *J. Virol.* **70**, 1738-1744 (1996).
159. Barbera, A.J., Chodaparambil, J.V., Kelley-Clarke, B., Joukov, V., Walter, J.C., Luger, K. & Kaye K.M. The nucleosomal surface as a docking station for Kaposi's sarcoma herpesvirus LANA. *Science* **311**, 856-861 (2006).
160. You, J., Srinivasan, V., Denis, G.V., Harrington, W.J., Jr., Ballestas, M.E., Kaye, K.M. & Howley, P.M. Kaposi's sarcoma-associated herpesvirus latency-associated nuclear antigen interacts with bromodomain protein Brd4 on host mitotic chromosomes. *J. Virol.***80**, 8909-8919 (2006).
161. You, J., Croyle, J.L., Nishimura, A., Ozato, K. & Howley, P.M. Interaction of the bovine papillomavirus E2 protein with Brd4 tethers the viral DNA to host mitotic chromosomes. *Cell* **117**, 349-360 (2004).
162. Xiao, B., Verma, S.C., Cai, Q., Kaul, R., Lu, J., Saha, A. & Robertson, E.S. Bub1 and CENP-F can contribute to Kaposi's sarcoma-associated herpesvirus genome persistence by targeting LANA to kinetochores. *J. Virol.* **84**, 9718-9732 (2010).
163. Sekhar, V., Reed, S.C. & McBride, A.A. Interaction of the betapapillomavirus E2 tethering protein with mitotic chromosomes. *J.Virol.* **84**, 543-557 (2010).
164. McBride, A.A., Oliveira, J.G. & McPhillips, M.G. Partitioning viral genomes in mitosis: same idea, different targets. *Cell cycle* **5**, 1499-1502 (2006).
165. Piirsoo, M., Ustav, E., Mandel, T., Stenlund, A. & Ustav, M. Cis and trans requirements for stable episomal maintenance of the BPV-1 replicator. *EMBO J.* **15**, 1-11 (1996).
166. Silla, T., Mannik, A. & Ustav, M. Effective formation of the segregation-competent complex determines successful partitioning of the bovine papillomavirus genome during cell division. *J. Virol.* **84**, 11175-11188 (2010).
167. McPhillips, M.G., Oliveira, J.G., Spindler, J.E., Mitra, R. & McBride, A.A. Brd4 is required for e2-mediated transcriptional activation but not genome partitioning of all papillomaviruses. *J. Virol.* **80**, 9530-9543 (2006).
168. Bastien, N. & McBride, A.A. Interaction of the papillomavirus E2 protein with mitotic chromosomes. *Virology* **270**, 124-134 (2000).
169. Mesika, A., Kiss, V., Brumfeld, V., Ghosh, G. & Reich, Z. Enhanced intracellular mobility and nuclear accumulation of DNA plasmids associated with a karyophilic protein. *Hum. Gene Ther.* **16**, 200-208 (2005).
170. Ludtke, J.J., Zhang, G., Sebestyen, M.G. & Wolff, J.A. A nuclear localization signal can enhance both the nuclear transport and expression of 1 kb DNA. *J. Cell Sci.* **112**, 2033-2041 (1999).
171. Sloots, A. & Wels, W.S. Recombinant derivatives of the human high-mobility group protein HMGB2 mediate efficient nonviral gene delivery. *FEBS J.* **272**, 4221-4236 (2005).

172. Mistry, A.R., Falciola, L., Monaco, L., Tagliabue, R., Acerbis, G., Knight, A., Harbottle, R.P., Soria, M., Bianchi, M.E., Coutell, C. & Hart, S.L. Recombinant HMG1 protein produced in Pichia pastoris: a nonviral gene delivery agent. *BioTechniques* **22**, 718-729 (1997).
173. Shen, Y., Peng, H., Deng, J., Wen, Y., Luo, X., Pan, S., Wu, C. & Feng, M. High mobility group box 1 protein enhances polyethylenimine mediated gene delivery in vitro. *Int. J. Pharm.* **375**, 140-147 (2009).
174. Wagstaff, K.M. & Jans, D.A. Nucleocytoplasmic transport of DNA: enhancing non-viral gene transfer. *Biochem. J.* **406**, 185-202 (2007).
175. Hung, S.C., Kang, M.S. & Kieff, E. Maintenance of Epstein-Barr virus (EBV) oriP-based episomes requires EBV-encoded nuclear antigen-1 chromosome-binding domains, which can be replaced by high-mobility group-I or histone H1. *Proc. Natl. Acad. Sci. USA* **98**, 1865-1870 (2001).
176. Baiker, A., Maercker, C., Piechaczek, C. Schmidt, S.D., Bode, J., Benham, C. & Lipps, H.J. Mitotic stability of an episomal vector containing a human scaffold/matrix-attached region is provided by association with nuclear matrix. *Nat. Cell Biol.* **2**, 182-184 (2000).
177. Piechaczek, C., Fetzer, C., Baiker, A., Bode, J. & Lipps, H.J. A vector based on the SV40 origin of replication and chromosomal S/MARs replicates episomally in CHO cells. *Nucleic acids Res.* **27**, 426-428 (1999).
178. Heng, H.H., Goetze, S., Ye, C.J., Liu, G., Stevens, J.B., Bremer, S.W., Wykes, S.M., Bode, J. & Krawetz, S.A. Chromatin loops are selectively anchored using scaffold/matrix-attachment regions. *J. Cell Sci.* **117**, 999-1008 (2004).
179. Alvarez, J.D., Yasui, D.H., Niida, H., Joh, T., Loh, D.Y. & Kohwi-Shigematsu, T. The MAR-binding protein SATB1 orchestrates temporal and spatial expression of multiple genes during T-cell development. *Genes Dev.* **14**, 521-535 (2000).
180. Lufino, M.M., Manservigi, R. & Wade-Martins, R. An S/MAR-based infectious episomal genomic DNA expression vector provides long-term regulated functional complementation of LDLR deficiency. *Nucleic acids Res.* **35**, e98 (2007).
181. Jenke, B.H., Fetzer, C.P., Stehle, I.M., Jonsson, F., Fackelmayer, F.O., Conradt, H., Bode, J. & Lipps, H.J. An episomally replicating vector binds to the nuclear matrix protein SAF-A in vivo. *EMBO Rep.* **3**, 349-354 (2002).
182. Tessadori, F., Zeng, K., Manders, E., Riool, M., Jackson, D. & van Driel, R. Stable S/MAR-based episomal vectors are regulated at the chromatin level. *Chromosome Res.* **18**, 757-775 (2010).
183. Van Craenenbroeck, K., Vanhoenacker, P. & Haegeman, G. Episomal vectors for gene expression in mammalian cells. *Eur. J. Biochem.* **267**, 5665-5678 (2000).
184. Schiedner, G., Morral, N., Parks, R.J., Wu, Y., Koopmans, S.C., Langston, C., Graham, F.L., Beaudet, A.L. & Kochanek, S. Genomic DNA transfer with a high-capacity adenovirus vector results in improved in vivo gene expression and decreased toxicity. *Nat. Genet.* **18**, 180-183 (1998).

185. Inoue, R., Moghaddam, K.A., Ranasinghe, M, Saeki, Y., Chiocca, E.A. & Wade-Martins, R. Infectious delivery of the 132 kb CDKN2A/CDKN2B genomic DNA region results in correctly spliced gene expression and growth suppression in glioma cells. *Gene Ther.* **11**, 1195-1204 (2004).
186. Grundhoff, A. & Ganem, D. The latency-associated nuclear antigen of Kaposi's sarcoma-associated herpesvirus permits replication of terminal repeat-containing plasmids. *J. Virol.* **77**, 2779-2783 (2003).
187. Lu, F., Wikramasinghe, P., Norseen, J., Tsai, K., Wang, P., Showe, L., Davuluri, R.V. & Lieberman, P.M. Genome-wide analysis of host-chromosome binding sites for Epstein-Barr Virus Nuclear Antigen 1 (EBNA1). *Virol. J.* **7**, 262 (2010).
188. He, J. & Zhang, Z.Q. Progress of EBNA1/oriP-based plasmid applied in gene therapy. *Sheng Wu Gong Cheng Xue Bao* **21**, 507-510 (2005).
189. Kishida, T. et al. Pleiotrophic functions of Epstein-Barr virus nuclear antigen-1 (EBNA-1) and oriP differentially contribute to the efficiency of transfection/expression of exogenous gene in mammalian cells. *J. Biotechnol.* **133**, 201-207 (2008).
190. Conese, M., Auriche, C. & Ascenzioni, F. Gene therapy progress and prospects: episomally maintained self-replicating systems. *Gene Ther.* **11**, 1735-1741 (2004).
191. Mitchell, R.S., Beitzel, B.F., Schroder, A.R., Shinn, P., Chen, H., Berry, C.C., Ecker, J.R. & Bushman, F.D. Retroviral DNA integration: ASLV, HIV, and MLV show distinct target site preferences. *PLoS Biol.* **2**, E234 (2004).
192. Roussel, L., Erard, M., Cayrol, C. & Girard, J.P. Molecular mimicry between IL-33 and KSHV for attachment to chromatin through the H2A-H2B acidic pocket. *EMBO Rep.* **9**, 1006-1012 (2008).
193. Dey, A., Chitsaz, F., Abbasi, A., Misteli, T. & Ozato, K. The double bromodomain protein Brd4 binds to acetylated chromatin during interphase and mitosis. *Proc. Natl. Acad. Sci. USA* **100**, 8758-8763 (2003).
194. Bausinger, R., von Gersdorff, K., Braeckmans, K., Ogris, M., Wagner, E., Brauchle, C. & Zumbusch, A. The transport of nanosized gene carriers unraveled by live-cell imaging. *Angew. Chem. Int. Ed. Engl.* **45**, 1568-1572 (2006).
195. Ribbeck, K., Raemaekers, T., Carmeliet, G. & Mattaj, I.W. A role for NuSAP in linking microtubules to mitotic chromosomes. *Curr. Biol.* **17**, 230-236 (2007).
196. Shimozono, S., Tsutsui, H. & Miyawaki, A. Diffusion of large molecules into assembling nuclei revealed using an optical highlighting technique. *Biophys. J.* **97**, 1288-1294 (2009).
197. Khmelinskii, A., Meurer, M., Knop, M. & Schiebel, E. Artificial tethering to nuclear pores promotes partitioning of extrachromosomal DNA during yeast asymmetric cell division. *Curr. Biol.* **21**, R17-R18 (2011).
198. Takeda, D.Y., Wohlschlegel, J.A. & Dutta, A. A bipartite substrate recognition motif for cyclin-dependent kinases. *J. Biol. Chem.* **276**, 1993-1997 (2001).
199. Endicott, J.A., Noble, M.E. & Tucker, J.A. Cyclin-dependent kinases: inhibition and substrate recognition. *Curr. Opin. Struct. Biol.* **9**, 738-744 (1999).

200. Hill, C.S., Rimmer, J.M., Green, B.N., Finch, J.T. & Thomas, J.O. Histone-DNA interactions and their modulation by phosphorylation of -Ser-Pro-X-Lys/Arg- motifs. *EMBO J.* **10**, 1939-1948 (1991).
201. Oishi, J., Ijuin, M., Sonoda, T., Kang, J.H., Kawamura, K., Mori, T., Niidome, T. & Katayama, Y. A protein kinase signal-responsive gene carrier modified RGD peptide. *Bioorg. Med. Chem. Lett.* **16**, 5740-5743 (2006).
202. Oishi, J., Kawamura, K., Kang, J.H., Kodama, K., Sonoda, T., Murata, M., Niidome, T. & Katayama, Y. An intracellular kinase signal-responsive gene carrier for disordered cell-specific gene therapy. *J. Control. Release* **110**, 431-436 (2006).
203. Katayama, Y., Fujii, K., Ito, E., Sakakihara, S., Sonoda, T., Murata, M. & Maeda, M. Intracellular signal-responsive artificial gene regulation for novel gene delivery. *Biomacromolecules.* **3**, 905-909 (2002).
204. Katayama, Y., Sonoda, T. & Maeda, M. A polymer micelle responding to the protein kinase A signal. *Macromolecules* **34**, 8569-8573 (2001).
205. Ulbert, S., Platani, M., Boue, S. & Mattaj, I.W. Direct membrane protein-DNA interactions required early in nuclear envelope assembly. *J. Cell Biol.* **173**, 469-476 (2006).
206. Burke, B. & Gerace, L. A cell free system to study reassembly of the nuclear envelope at the end of mitosis. *Cell* **44**, 639-652 (1986).
207. Newport, J.W. & Forbes, D.J. The nucleus: structure, function, and dynamics. *Annu. Rev. Biochem.* **56**, 535-565 (1987).
208. Smythe, C. & Newport, J.W. Systems for the study of nuclear assembly, DNA replication, and nuclear breakdown in Xenopus laevis egg extracts. *Methods Cell Biol.* **35**, 449-468 (1991).
209. Newport, J. Nuclear reconstitution in vitro: stages of assembly around protein-free DNA. *Cell* **48**, 205-217 (1987).
210. Wiese, C., Goldberg, M.W., Allen, T.D. & Wilson, K.L. Nuclear envelope assembly in Xenopus extracts visualized by scanning EM reveals a transport-dependent 'envelope smoothing' event. *J. Cell Sci.* **110**, 1489-1502 (1997).
211. Brennan, C.M. & Steitz, J.A. HuR and mRNA stability. *Cell. Mol. Life Sci.* **58**, 266-277 (2001).
212. Krieg, A.M. Direct immunologic activities of CpG DNA and implications for gene therapy. *J. Gene Med.* **1**, 56-63 (1999).
213. Kariko, K., Ni, H., Capodici, J., Lamphier, M. & Weissman, D. mRNA is an endogenous ligand for Toll-like receptor 3. *J. Biol. Chem.* **279**, 12542-12550 (2004).
214. Kariko, K., Buckstein, M., Ni, H. & Weissman, D. Suppression of RNA recognition by Toll-like receptors: the impact of nucleoside modification and the evolutionary origin of RNA. *Immunity* **23**, 165-175 (2005).
215. Kariko, K., Muramatsu, H., Welsh, F.A., Ludwig, J., Kato, H., Akira, S. & Weissman, D. Incorporation of pseudouridine into mRNA yields superior nonimmunogenic vector with increased translational capacity and biological stability. *Mol. Ther.* **16**, 1833-1840 (2008).

216. Bettinger, T., Carlisle, R.C., Read, M.L., Ogris, M. & Seymour, L.W. Peptide-mediated RNA delivery: a novel approach for enhanced transfection of primary and post-mitotic cells. *Nucleic acids Res.* **29**, 3882-3891 (2001).
217. Lu, D., Benjamin, R., Kim, M., Conry, R.M. & Curiel, D.T. Optimization of methods to achieve mRNA-mediated transfection of tumor cells in vitro and in vivo employing cationic liposome vectors. *Cancer Gene Ther.* **1**, 245-252 (1994).
218. Zohra, F.T., Chowdhury, E.H., Nagaoka, M. & Akaike, T. Drastic effect of nanoapatite particles on liposome-mediated mRNA delivery to mammalian cells. *Anal. Biochem.* **345**, 164-166 (2005).
219. Van Tendeloo, V.F., Ponsaerts, P., Lardon, F., Nijs, G., Lenjou, M., Van Broeckhoven, C., Van Bockstaele, D.R. & Berneman, Z.N. Highly efficient gene delivery by mRNA electroporation in human hematopoietic cells: superiority to lipofection and passive pulsing of mRNA and to electroporation of plasmid cDNA for tumor antigen loading of dendritic cells. *Blood* **98**, 49-56 (2001).
220. Marin, M. Folding at the rhythm of the rare codon beat. *Biotechnol. J.* **3**, 1047-1057 (2008).
221. Tavernier, G., Andries, O., Demeester, J., Sanders, N.N., De Smedt, S.C. & Rejman, J. mRNA as gene therapeutic: How to control protein expression. *J. Control. Release* **150**, 238-247 (2011).
222. Yamamoto, A., Kormann, M., Rosenecker, J. & Rudolph, C. Current prospects for mRNA gene delivery. *Eur. J. Pharm. Biopharm.* **71**, 484-489 (2009).

2

NUCLEAR INCLUSION OF NON-TARGETED AND CHROMATIN-TARGETED POLYSTYRENE BEADS AND PLASMID DNA-CONTAINING NANOPARTICLES

Parts of this chapter are published in:

Nathalie Symens[1], Rudolf Walczak[2], Joseph Demeester[1], Iain Mattaj[2], Stefaan C. De Smedt[1] and Katrien Remaut[1]. Nuclear inclusion of nontargeted and chromatin-targeted polystyrene beads and plasmid DNA containing nanoparticles. *Molecular Pharmaceutics* **8** (5), 1757-1766 (2011).

1. Laboratory of General Biochemistry and Physical Pharmacy, Faculty of Pharmaceutical Sciences, Ghent University, Harelbekestraat 72, 9000 Ghent, Belgium.
2. Directors' Research, Mattaj Group, European Molecular Biology Laboratory, Meyerhofstraße 1, 69117 Heidelberg, Germany.

ABSTRACT

The nuclear membrane is one of the major cellular barriers in the delivery of plasmid DNA (pDNA). Cell division has a positive influence on transfection efficiency since at the end of mitosis, pDNA or pDNA-containing complexes located near the chromatin are probably included by a random process in the nuclei of the daughter cells. Very little is known about the nuclear inclusion of nanoparticles during cell division. Using the *Xenopus* nuclear envelope reassembly (XNER) assay, we found that the nuclear enclosure of nanoparticles was dependent on their size (with 100 nm and 200 nm particles being better included than the 500 nm ones) and charge (with positively charged particles being better included than negatively charged or coated with polyethylene glycol (PEG) ones). Coupling chromatin-targeting peptides to the polystyrene beads or pDNA complexes improved their inclusion by two- to three-fold. Upon microinjection in living HeLa cells, however, nanoparticles were never observed in the nuclei of cells which divided but accumulated in a specific perinuclear region, which was identified as the lysosomal compartment. This indicates that nanoparticles can end up in the lysosomes even when they were not internalized via endocytosis. To elucidate the potential of chromatin-binding peptides, this additional barrier has to be tackled first, since it prevents free particles to be present near the chromatin at the moment of cell division.

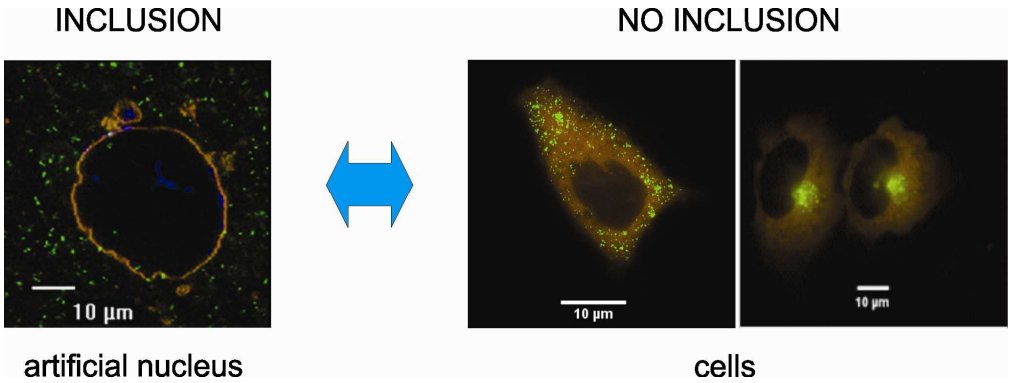

2

NUCLEAR INCLUSION OF NON-TARGETED AND CHROMATIN-TARGETED POLYSTYRENE BEADS AND PLASMID DNA-CONTAINING NANOPARTICLES

INTRODUCTION

Gene therapy shows potential in the treatment of a wide variety of genetic disorders. For gene therapy to be successful, the nucleic acids should reach their target, which is situated intracellularly. Naked nucleic acids are poorly taken up by cells. Therefore, they are administered using viral or non-viral vectors. In general, viral vectors provide high transfection efficiencies but suffer from the limited amount and size of the genetic material they can carry. In addition, they can induce severe immune responses[1, 2]. The advantage of non-viral vectors lies in the fact that they are less expensive, easier and safer to make and more suitable for long time storage. They can also deliver much larger pieces of DNA when compared to viral carriers[3]. Non-viral vectors enter the cells by endocytosis[4]. Then, they have to escape from the endosomal compartment and release their cargo into the cytosol of the cells. Subsequently, the DNA should stay intact and reach its target, which is the

nucleoplasm, in the case of plasmid DNA (pDNA). pDNA delivery and expression remain challenging despite many years of non-viral gene therapy research. Although non-viral systems have many advantages, their transfection efficiency is very low when compared to viral systems. Factors which decrease transfection efficiency include cytoplasmic sequestration (by interactions with DNA-binding proteins and cytoskeletal elements)[5, 6], enzymatic degradation[7], too strong complexation of DNA with its carrier molecules[8] and most importantly, lack of transport across the nuclear membrane, which is one of the major intracellular barriers[9, 10]. In non-dividing cells, the transfer through the nuclear pore complexes (NPCs) of intact nuclear envelopes is very inefficient. Many studies suggest that although it is not impossible, larger molecules such as pDNA do not readily cross NPCs[5, 11-14]. Several attempts to improve pDNA entry into the nucleus have been published, in which nuclear localization signal (NLS)-containing proteins or peptides were attached to the pDNA by electrostatic interactions[15] or covalent binding[16]. Also, attachment to cellular DNA-binding proteins including histones[17] and high-mobility group (HMG) proteins[18], as well as DNA containing the Simian virus 40 (SV40) promoter, enhancer and origin of replication[19], have been investigated. These attempts have met with limited success.

Interestingly, several groups have observed that the transfection efficiencies of cationic lipid-, polymer- and peptide-based transfection reagents were two- to several hundred-fold higher in dividing as compared to non-dividing cells[12, 14, 20-27]. Also, cell division had a positive influence on the nuclear inclusion of colloidal gold particles[28]. This suggests that transfection close to M phase is facilitated by nuclear envelope breakdown, since the disassembly of the nuclear envelope during cell division likely facilitates access to the nucleoplasm and chromatin. It is plausible that the naked pDNA or nanoparticles near the chromatin are included by chance in the nuclei of the daughter cells during or shortly after mitosis, as presented in **figure 1**.

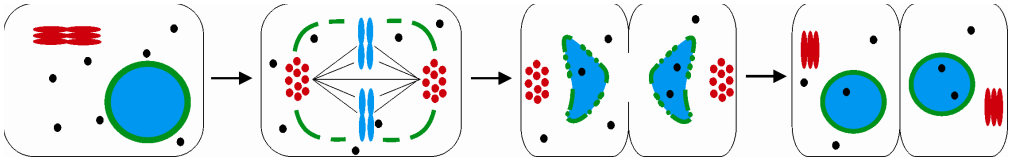

Figure 1. Nuclear inclusion during cell division. Black: nanoparticles; green: nuclear membrane; red: Golgi-apparatus and blue: chromatin.

Recently, Errington *et al.*[29] studied the fate of nanoparticles during the cell cycle. The quantum dots were asymmetrically and non-randomly diluted over daughter cells which is probably related to a survival mechanism of the cell responding to stress. Although the nuclear inclusion appears a very simple concept to study, very little is known on the nuclear entry of nanoparticles during cell division. How and to what extent can nanoparticles access the nucleoplasm during cell division? Is nuclear inclusion random or do nanoparticles need to interact with chromatin to be enclosed? Do the nanoparticles remain in the nucleoplasm during subsequent cell cycles? Many of these questions remain unanswered, although they are highly relevant for the non-viral gene delivery field. We addressed these questions by studying to which extent nanoparticles are enclosed in artificial *Xenopus laevis* nuclei and in daughter nuclei of dividing HeLa cells. The *Xenopus* nuclear envelope reassembly (XNER) assay is a model system, in which the enclosure of nanoparticles in fully functional artificial nuclei can be studied in the most ideal situation, e.g. without the presence of additional extracellular and intracellular barriers. In case of the HeLa cells, the nanoparticles were microinjected into the cytoplasm to avoid additional intracellular barriers related to the endosomal compartment. We investigated whether the size and charge of the nanoparticles had an influence on the nuclear inclusion and if the enclosure could be enhanced by modification of the nanoparticles with chromatin-binding peptides.

MATERIAL AND METHODS

Polystyrene beads

Green fluorescent carboxylated polystyrene beads (Molecular Probes, Merelbeke, Belgium) of different sizes (100, 200 and 500 nm) were used. These beads have a negative ζ-potential and were modified with Pluronic F-127 (Sigma-Aldrich, Bornem, Belgium) and dimethylamine-ethylamine (DMAEA) to obtain respectively polyethylene glycolated (PEG-ylated)[30] and positively charged beads. The latter is the result of an amide formation between the carboxylate groups on the beads and the amine group of DMAEA. The carboxylate groups were activated with an excess of EDC at pH 5. DMAEA (at pH 5) was added and the solution was shaken overnight. Microcon-YM-100 columns (Merck Millipore, Overijse, Belgium) were used to purify the positively charged beads. These beads are called 'non-targeted beads'. Additionally, the carboxylated 100 nm beads were modified via a NH_2-PEG-maleimide linker with 3 gluthatione-S-transferase (GST)-tagged peptides, namely Mel-28 (maternal effect lethal 28), mutated Mel-28 or HMGA2β (high mobility group AT hook 2 isoform β). Briefly, 10 mg/ml NH_2-PEG-maleimide (creative PEGworks, USA) was added to 500 µl 0.4% solution of the carboxylated beads and incubated overnight at 4 °C. Then, the beads were purified by centrifugation over Microcon-YM-100 columns and collected after 2 washing steps by reversed centrifugation. The modified beads were incubated overnight with 50 µg of glutathion-GST-tagged peptides to allow binding to the maleimide side of the NH_2-PEG-maleimide linker. The beads were again purified by centrifugation over Microcon-YM-100 columns and collected after 2 washing steps by reversed centrifugation. These beads are called 'targeted beads'. Mel-28, mutated Mel-28 and HMGA2β were prepared as described elsewhere[31]. Diameter and ζ-potential measurements of the non-targeted beads were determined with a Zetasizer Nano (Malvern Instruments, Hoeilaart, Belgium).

PEI/pDNA polyplexes

pDNA complexed to 7.5 kDa linear polyethyleneimine (PEI) (kindly provided to us by Olivia Merkel, Marburg University, Germany) served as a model pDNA nanoparticle. For targeting and microinjection experiments, pDNA was labeled with Cy5 (fluorescent red) using the *Label* IT Cy5 labeling kit (Mirus Bio Corporation, Eke, Belgium) and purified by columns supplied by the manufacturer. Complexes were prepared by adding a PEI-polymer solution to an equal volume of a 0.04 µg/µl pDNA solution to obtain a nitrogen to phosphate ratio of 10 (N/P ratio: the ratio of moles of the amine groups of PEI to those of the phosphate groups of the nucleic acids), followed by vortexing the dispersion for 10 seconds. The complexes were allowed to equilibrate at RT for 30 minutes prior to use. To obtain targeted PEI/pDNA nanoparticles, complexes were prepared with PEI polymers which were modified with peptides of Mel-28, mutated Mel-28 or HMGA2β through a NHS-PEG-maleimide linker. Briefly, 1 mg/ml PEI-polymer solution was incubated with 10 times excess of NHS-PEG-maleimide (Pierce, Thermo Scientific, Erembodegem-Aalst, Belgium) and purified by a Zeba Desalt spin column (Thermo scientific, Erembodegem-Aalst, Belgium) after 4 hours of incubation at RT. Then, 220 µl of the partially modified PEI polymers were incubated overnight at 4 °C with 13.5 µg of glutathion-GST-tagged peptides to allow binding to the maleimide side of the NHS-PEG-maleimide linker so that chromatin-targeted PEI polymers were obtained. Almost all glutathion-GST-tagged peptides should bind to the PEI polymers at this concentration. The PEI polymers were additionally purified by centrifugation over Microcon-YM-100 columns and collected after 2 washing steps by reversed centrifugation before use. The diameter and ζ-potential of the non-targeted and targeted PEI/pDNA polyplexes were measured with a Zetasizer Nano.

Immunostaining of GST-AT-hooks

The initial chromatin-binding properties of Mel-28, mutated Mel-28 and HMGA2β were evaluated with immunostaining against the GST-fragment of the AT-hooks.

Membrane-free extract was supplemented with GST alone or GST-AT-hooks at 1 µM final concentration, and incubated with chromatin for 10 minutes. Then, the chromatin was fixed with 4% paraformaldehyde (PFA) in phosphate buffered saline (PBS) for 10 minutes. The fixed chromatin was placed on top of 0.8 ml 30% sucrose in PBS and centrifuged onto poly-L-lysine coated cover slips. Blocking was carried out for 30 minutes in 1% bovine serum albumin (BSA) in PBS. Then, the samples were incubated with the primary anti-GST antibody in 1% BSA-PBS for 2 hours, followed by extensive washing before the fluorescein-labeled secondary antibody (in 1% BSA-PBS) was added for 1 hour. After washing, the chromatin was stained by adding 0.1 µg/ml DAPI and the samples were analysed with fluorescence microscopy.

***Xenopus* nuclear envelope reassembly (XNER) assay**

Cytosolic extract and membrane fraction needed for the XNER assay were isolated from *Xenopus laevis* eggs and sperm chromatin was prepared from *Xenopus leavis* sperm (*Xenopus laevis* testis were also kindly provided by Kris Vleminckx Lab, VIB, Ghent) as previously described by Hetzer *et al.*[32]. To study the nuclear inclusion in the XNER assay, 1 µl of polystyrene beads (green) or PEI/Cy5-pDNA nanoparticles (red) were added to a mixture of sperm chromatin (0.6 µl) and cytosolic extract (20 µl) and incubated in a water bath at 20 °C for 20 minutes. Then, 1 µl membrane fraction, 1 µl energy mix (127.5 mg/ml creatin phosphate, 2.5 mg/ml creatin kinase, 25 mM ATP and 25 mM GTP) and 1 µl glycogen (200 mg/ml) were added and this mixture was incubated in a water bath at 20 °C to allow the formation of artificial nuclei as described by Hetzer *et al.*[32]. After 90 minutes the artificial nuclei were stained with $DiIC_{18}$ (membrane staining) and DAPI (chromatin staining) and the enclosure of the nanoparticles in the nuclei was visualised with a Nikon EZC1-si (Nikon Belux, Brussels, Belgium) by fluorescence confocal laser scanning microscopy (CLSM) or fluorescence microscopy. The particles were counted by moving up and down the Z-focus to visualize the artificial nuclei in 3-D. It should be noted that in the case of 100 and 200 nm particles, because of the diffraction limit an underestimation of the amount of

particles is possible when aggregates are counted as one. However, the effect of chromatin targeting is compared to the control situation, in which the same error is expected to occur.

Microinjection of HeLa cells

HeLa cells (Human epithelial cervical cancer cells, ATCC number: CCL-2) were cultured in Dulbecco's Modified Eagle's Medium: nutrient mixture F-12 (DMEM-F12) (Gibco-Invitrogen, Merelbeke, Belgium) containing 2 mM glutamine, 10% heat-inactivated fetal bovine serum (Hyclone/Perbio, Erembodegem-Aalst, Belgium) and 100 U/ml penicillin-streptomycin liquid (Gibco-Invitrogen, Merelbeke, Belgium) at 37 °C in a humidified atmosphere containing 5% CO_2. For microinjection experiments, HeLa cells ($2.5x10^4$ cells/cm^2) were plated onto sterile glass-bottom culture dishes (MatTek Corporation, Ashland, MA, USA) and allowed to adhere for 1 day. Microinjection with polystyrene beads (green or red) or Cy5-PEI/pDNA nanoparticles (red) was performed with a Femtojet microinjector and an Injectman NI 2 micromanipulator (Eppendorf) mounted on a Nikon EZC1-si confocal laser scanning microscope. Injections were performed in the cytoplasm, using polystyrene beads or PEI/pDNA complexes in HEPES buffer. Injection solutions were supplemented with 2 mg/ml 70 kDa TRITC-dextran (Sigma-Aldrich, Bornem, Belgium) to identify the injected cells and verify whether or not they divided. After microinjection, cells were placed back in an incubator and fluorescence microscopy images were taken 30 minutes and 24 hours after injection. Labeling of the lysosomes was performed by adding 1 µl Lysosensor green (Invitrogen, Merelbeke, Belgium) to the microinjected cells. Labeling of the endosomes was performed by transfecting the cells with CellLight Early Endosomes-GFP BacMam 2.0 (Invitrogen, Merelbeke, Belgium). Colocalisation of injected fluorescent red beads with the labeled cell compartments was analyzed using Image J (http://rsbweb.nih.gov/ij/).

RESULTS

Characterisation of non-targeted and targeted nanoparticles

As non-targeted nanoparticles, we employed polystyrene beads of 100, 200 and 500 nm as this is the size range of most non-viral gene delivery complexes. Polystyrene beads of 20 and 40 nm were included in the study, as model particles which should be able to cross the NPCs. However, due to problems related to functionalization, aggregation and detection of these weakly fluorescent particles, they were not included in further studies.

The carboxylated polystyrene beads were first functionalized to obtain positively charged or PEG (polyethylene glycol)-ylated beads. In **table 1**, the mean diameter and ζ-potential of these different kinds of nanoparticles are presented. It can be seen that for each size, the negatively charged beads are always slighty larger than stated by the manufacturer. Making the beads positively charged or PEG-ylated results in a further size increase. The ζ-potential demonstrates that we succeeded in making positively charged particles. In the case of PEG-ylated particles, the ζ-potential becomes less negative due to the presence of the PEG-chains.

Table 1. Mean diameter d (nm) and ζ-potential (mV) of the negatively charged (NEG), PEG-ylated (PEG) and positively charged (POS) polystyrene beads and of PEI/pDNA complexes prepared with nonmodified PEI (NONTAR) and PEI modified with Mel-28, mutated Mel-28 (MUT) and HMGA2β. The given standard deviations are the result of repeated measurements.

	500 nm beads			200 nm beads			100 nm beads			PEI/pDNA complexes			
	NEG	PEG	POS	NEG	PEG	POS	NEG	PEG	POS	NONTAR	Mel-28	MUT	HMGA2β
d(nm)	577 ± 4	608 ± 10	589 ± 3	233 ± 1	249 ± 2	248 ± 2	116 ± 1	134 ± 1	122 ± 2	168 ± 10	131 ± 6	154 ± 7	238 ± 6
ζ(mV)	-52 ± 1	-29 ± 1	26 ± 1	-47 ± 1	-30 ± 1	26 ± 1	-45 ± 2	-23 ± 1	29 ± 1	29 ± 3	21 ± 2	2 ± 2	17 ± 2

PEI/pDNA nanoparticles were used as a model for a non-viral gene delivery system. PEI was chosen as complexation agent for pDNA since it is a well-characterized polymer for gene delivery which was reported to be able to enter the nucleus during transfection[33]. To obtain chromatin-targeted nanoparticles, both the 100 nm beads and the PEI/pDNA polyplexes were modified with chromatin-binding peptides: part of the proteins Mel-28 (maternal effect lethal 28), mutated Mel-28 or HMGA2β (high mobility group AT hook 2 isoform β). These peptides contain an AT-hook, a DNA-binding motif found in a family of proteins that binds the minor groove of the AT-rich scaffold/matrix-associated regions (S/MARs) on metaphase chromosomes[34]. Mel-28 is associated with two types of structures in the cell, one involved in nuclear envelope function and the other in chromatin organization. It is also recruited to chromatin at an early time point during nuclear assembly[35, 36]. HMGA2β is a small non-histone chromatin-associated protein that belongs to the family of the HMG proteins, which regulate the chromatin structure by specifically binding and bending the DNA and creating active and inactive chromatin regions which are essential for gene expression[37-39]. **Figure 2A** shows the sequences of the AT-hooks which were used. The specific targeting of Mel-28 (GST-AT) and HMGA2β (GST-$AT_{HMGA2\beta}$) to the chromatin can be seen after immunostaining of the GST-fragment of the chromatin-targeting peptides (**Fig. 2B**), while GST alone, or GST-tagged mutated Mel-28 (GST-AT_{MUT}) do not stain the chromatin. **Table 1** also contains the mean diameter and ζ-potential of the PEI/pDNA polyplexes before and after functionalization with the chromatin-targeting peptides. It can be seen that the charge of the functionalized polyplexes slightly decreases, while the size slightly decreases for Mel-28 and mutated Mel-28, but increases for HMGA2β.

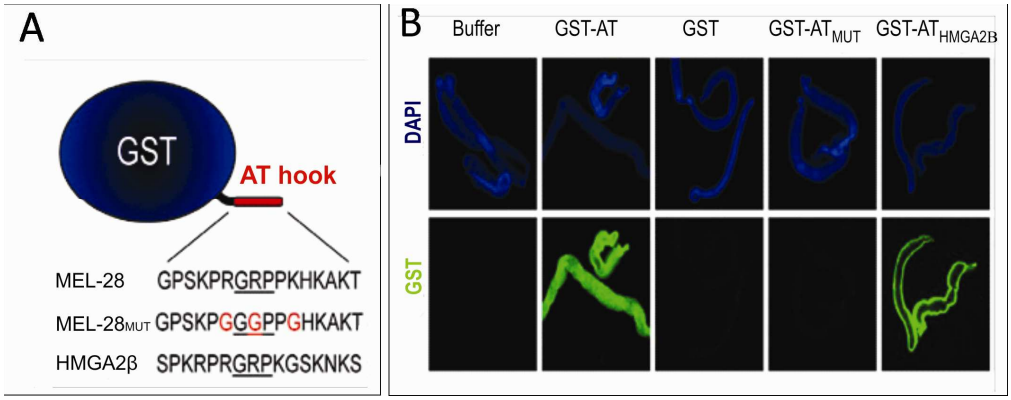

Figure 2. (A) Sequence and **(B)** *in vitro* chromatin-targeting properties of Mel-28 (GST-AT), GST alone, mutated Mel-28 (GST-AT_{MUT}) and HMGA2β (GST-$AT_{HMGA2β}$). Only Mel-28 and HMGA2β target to the chromatin (stained blue with DAPI, upper panel), as can be concluded from the green immunostaining against GST (lower panel).

Nuclear inclusion of non-targeted polystyrene beads of different size and charge in the *Xenopus* nuclear envelope reassembly nuclei

The artificial nuclei (**Fig. 3**) were obtained by performing the *Xenopus* nuclear envelope reassembly (XNER) assay. In this assay, sperm chromatin is first mixed with cytosolic extract which results in a partial decondensation of the sperm chromatin. It should be noted that *Xenopus* sperm chromatin is much more compact than normal mitotic chromatin but it is spontaneously repackaged with histones in the cytosolic extract to become normal mitotic chromatin[40-44]. Upon the addition of membrane extract and an ATP-generating buffer, the membrane fractions bind to the chromatin and eventually fuse so that nuclear membranes are formed around the chromatin material. Then, the chromatin decondenses further and nuclear proteins are imported which results in the swelling of the nuclei so that functional artificial nuclei are formed[40, 41, 43-46]. By addition of fluorescently labeled nanoparticles to the XNER assay, we could evaluate the efficiency with which different types of nanoparticles are entrapped in the formed nuclei.

Figure 3 shows representative artificial nuclei obtained with the XNER assay. Depending on where in the sample the pictures are taken, more or fewer membrane

elements or beads seem to be present, although the total number of particles and membrane elements in each situation is comparable. Only fully decondensed nuclei (> 25 µm) were counted. Between 50 and 100 functional nuclei were analyzed for each experiment with a different type of nanoparticles. The results are summarized in **figure 4** showing the percentage of nuclei containing 0, between 1 and 5, between 6 and 10, or more than 10 nanoparticles. It can be seen, in **figures 3** and **4**, that few non-targeted beads are enclosed in the artificial nuclei. The enclosure of the positively charged beads is higher than the enclosure of the negatively charged or the PEG-ylated ones (**Fig. 4**). Beads with a diameter of 100 nm and 200 nm were better enclosed than the 500 nm ones. We conclude that small (100 - 200 nm) positively charged beads have a better chance to be retained in the nucleus upon nuclear envelope reassembly.

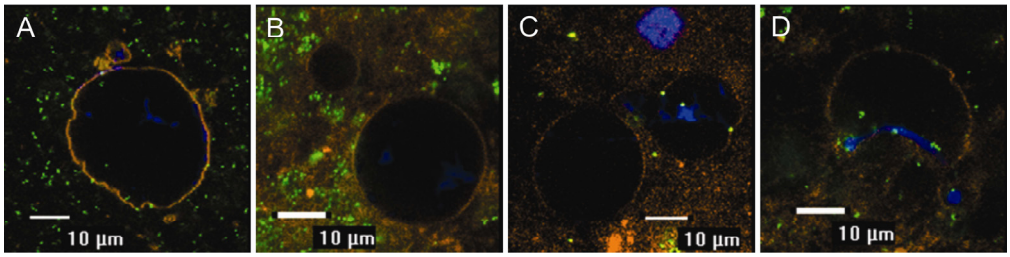

Figure 3. Representative confocal fluorescence images of the nuclear enclosure of non-targeted beads (100 nm, positively charged **(A)**; 200 nm, positively charged **(B)**; 500 nm, positively charged **(C)**) and chromatin-targeted beads (100 nm, HMGA2β **(D)**) in artificial *Xenopus* nuclei. Blue: sperm chromatin; orange: membrane fraction and green: polystyrene beads. Only fully decondensed nuclei (> 25 µm) were counted.

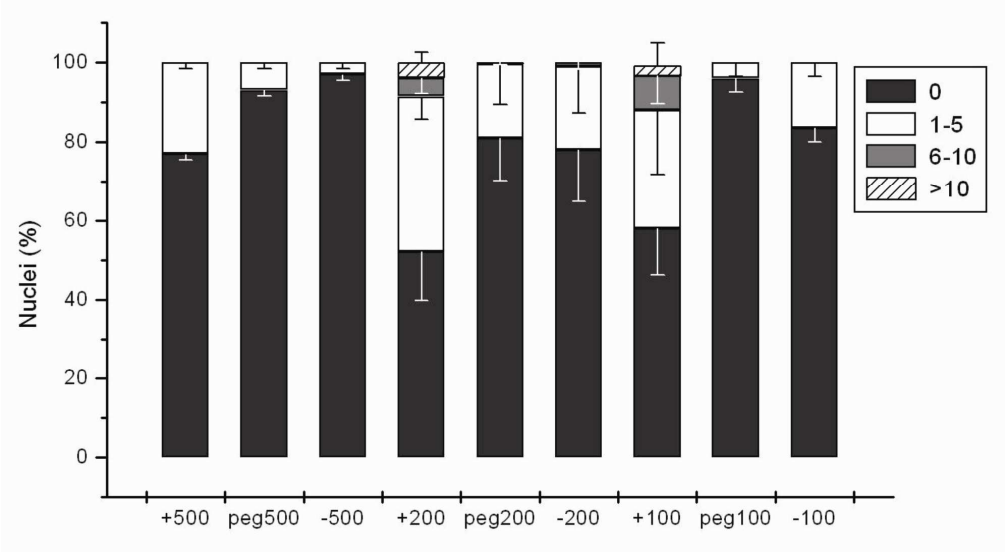

Figure 4. Nuclear enclosure of non-targeted polystyrene beads of different sizes (500, 200 or 100 nm) and ζ-potentials (positive, PEG-ylated or negative) in artificial *Xenopus* nuclei. The percentage of nuclei containing 0, 1-5, 6-10 and >10 beads is shown. Only fully decondensed nuclei (> 25 µm) were counted. At least 3 independent experiments where 50 to 100 nuclei were counted per experiment were carried out. (Mean ± SD)

Nuclear inclusion of chromatin-targeted polystyrene beads and PEI/pDNA complexes in *Xenopus* nuclear envelope reassembly nuclei

In these experiments, not only the inclusion in the artificial nuclei, but also the initial binding to chromatin before adding the membrane fraction to the XNER assay was determined. **Figure 5A** shows that the enclosure of beads modified with the chromatin-binding peptides derived from Mel-28 or HMGA2β is higher than the enclosure of the non-targeted beads (100 nm, positively charged) and the beads modified with the mutated AT-hook (Mel-28 mut), showing the potential of chromatin targeting. To verify if chromatin targeting also has an influence on pDNA complexes used in non-viral gene delivery, Cy5-labeled PEI/pDNA polyplexes were added to the XNER assay and their chromatin binding and nuclear inclusion was visualized (**Fig. 5B**). The use of chromatin-targeting AT-hooks Mel-28 and HMGA2β resulted in a two- to three-fold increase in the numbers of nanoparticles which were

included in the artificial nuclei. Thus, targeting to the chromatin can indeed enhance nuclear inclusion, although it should be noted that not all particles initially bound to the chromatin get included in the artificial nuclei (**Fig. 5**). 45%, 75%, 45% and 30% of the initially chromatin-bound particles are included in the eventually formed artificial nuclei in the case of non-targeted, HMGA2β, Mel-28 and mutated Mel-28 modified nanoparticles, respectively. These results indicate that HMGA2β-targeted particles are the most resistant to displacement assuming that one chromatin strand leads to the formation of one artificial nucleus.

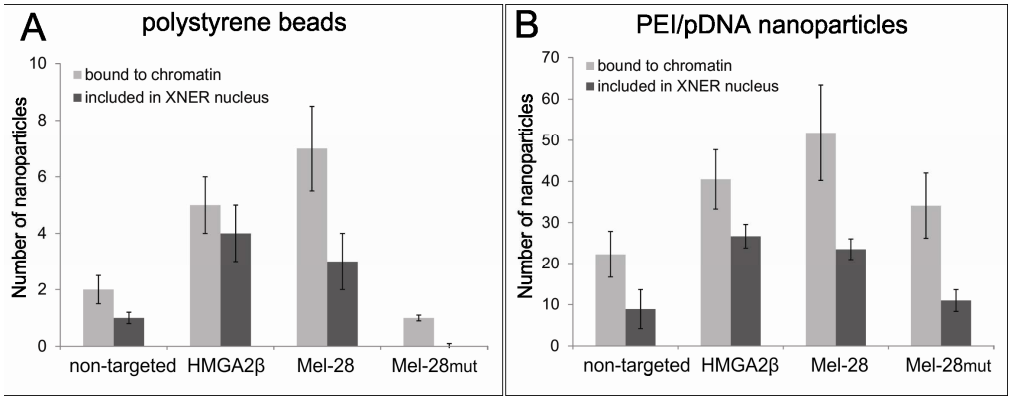

Figure 5. Binding to chromatin and nuclear enclosure of polystyrene beads and PEI/pDNA complexes. Average number of nanoparticles per chromatin strand (light grey bars) and average number of nanoparticles per artificial nucleus (dark grey bars) with non-targeted (positively charged) and targeted (HMGA2β, Mel-28 or mutated Mel-28) 100 nm polystyrene beads **(A)** or PEI/pDNA complexes **(B)**. Between 25 and 50 chromatin strands and artificial nuclei were counted. (Mean ± SD)

Nuclear inclusion of microinjected polystyrene beads and PEI/pDNA polyplexes in HeLa cells

We next verified whether polystyrene beads (100 nm) and PEI/pDNA complexes which are present in the cytosol, gain access to the nucleus during cell division. Since **figure 5A** and **B** show that even for non-targeted positively charged nanoparticles about 45% of the particles which bind to chromatin are retained in the formed nuclei, we would expect to find at least some chromatin-binding nanoparticles in the nuclei

of the daughter cells. To circumvent endocytosis and the need for endosomal escape, the non-targeted nanoparticles were directly injected into the cytoplasm of HeLa cells. Injection solutions were supplemented with TRITC-dextran to identify injected cells and verify whether or not they divided. **Figure 6** shows representative images of the intracellular distribution of 100 nm positively charged polystyrene beads (green; **Fig. 6A**) and PEI/pDNA polyplexes (red; **Fig. 6B**) before and after cell division, in injected living HeLa cells. Initially, the polystyrene beads spread through the cytoplasm, while the PEI/pDNA complexes remained closer to the place of injection (indicated by an arrow). Upon cell division, it can be seen that both the polystyrene beads and the PEI/pDNA complexes are evenly distributed over the two daughter cells, but accumulate in the perinuclear region of the daughter cells. Enclosure of nanoparticles in the nuclei of cells which had undergone division was never observed. This is in contrast to the nuclear inclusion seen in assembled nuclei in the XNER assay, where there were about 10 PEI/pDNA complexes present in the case of non-targeted complexes (**Fig. 5B**). Apart from non-targeted nanoparticles, also nanoparticles targeted with HMGA2β were microinjected (**Fig. 6C**). HMGA2β was chosen as the data in **figure 5** pointed out that in this case, the largest fraction of chromatin-bound nanoparticles is retained in the formed nuclei. Also here, however, the nanoparticles were never observed in the nuclei of divided cells, but again accumulated in the perinuclear region. Whether the nanoparticles first reach the nuclear interior and are then expelled to this perinuclear region, or accumulate in this perinuclear region already before cell division occurs remains to be determined.

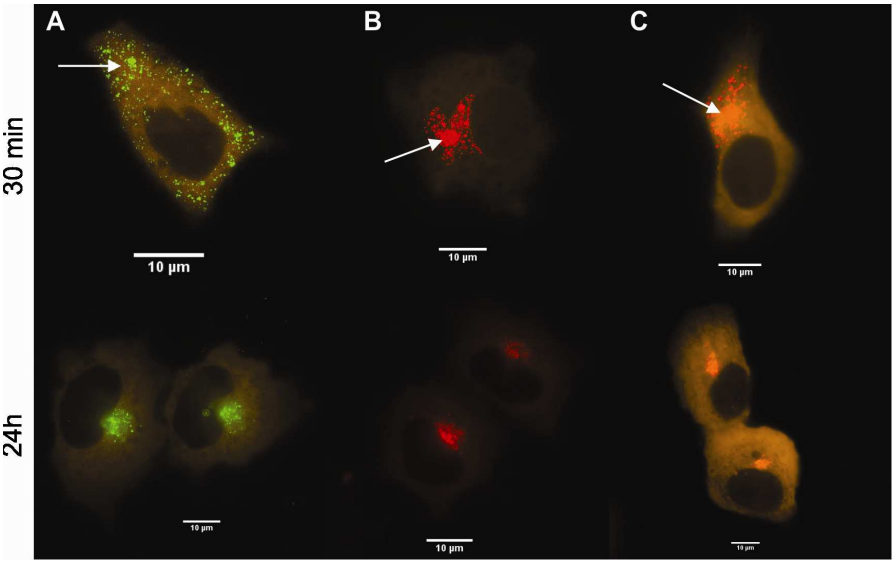

Figure 6. Intracellular distribution of nanoparticles upon cytoplasmic microinjection in HeLa cells. **(A)** Polystyrene beads (100 nm, positively charged, green), **(B)** PEI/pDNA polyplexes (± 170 nm, positively charged, red) or **(C)** PEI/pDNA-HMGA2β polyplexes (± 240 nm, positively charged, red-orange) were microinjected. 70 kDa TRITC-dextran (orange) was always injected as a marker. Pictures of the injected cells were taken 30 minutes and 24 hours after injection. The arrows indicate the initial place of injection.

Identification of the intracellular compartment where nanoparticles accumulate

We next aimed at identifying the intracellular compartment where the nanoparticles accumulate. To that end, we stained early endosomes and lysosomes. To prevent overlap between the staining colour and the injected beads, red fluorescent beads were injected instead of green ones. Colocalization of the red and the green channel was determined in Image J after a background subtract, so that colocalized pixels appear white, while non-colocalized pixels appear green or red in the overlay image. **Figure 7A** shows that there is no colocalization between the injected beads and the early endosomes. When the lysosomes were stained, no colocalization was seen 30 minutes after injection (**Fig. 7C**) while a high degree of colocalization was observed after 24 hours after injecting nanoparticles (**Fig. 7B**). This observation implies that nanoparticles can end up in the lysosomal compartment even when they are directly injected in the cytosol and not taken up by endocytosis.

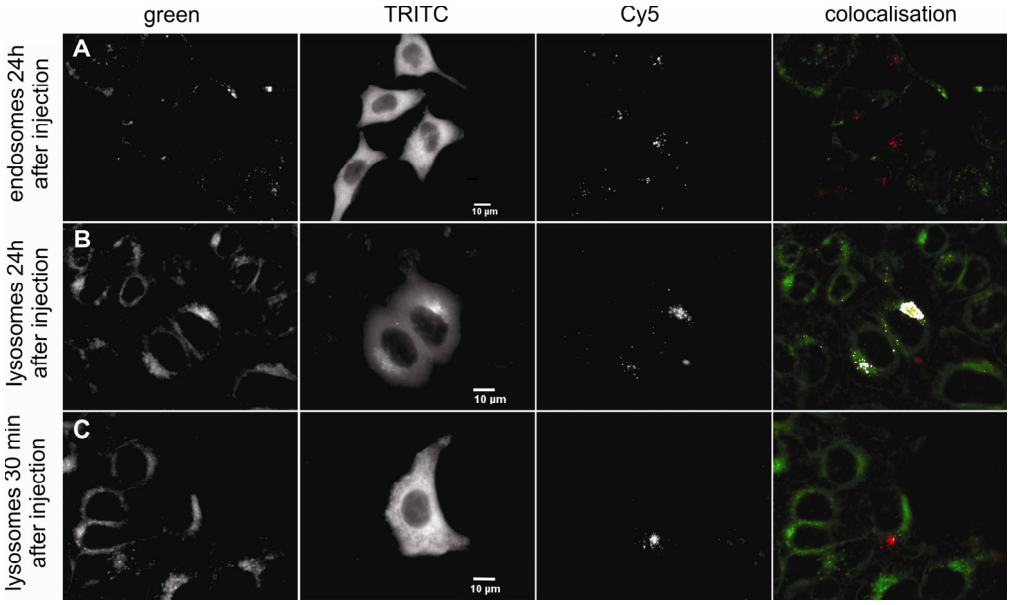

Figure 7. Identification of the intracellular compartment in which cytoplasmically microinjected red polystyrene beads accumulate in HeLa cells. 70 kDa TRITC-dextran was used as an injection marker. Pictures were taken 30 minutes **(B)** or 24 hours **(A and C)** after injection. The green panel shows the labeling of endosomes **(A)** or lysosomes **(B and C)**. The TRITC panel shows the injected cells or their daughter cells, while the Cy5 panel shows the injected red beads. Colocalization of the beads with the endosomes or lysosomes was evaluated using Image J. Colocalized pixels appear white in the colocalization panel.

DISCUSSION

What happens with nanoparticles during cell division is a highly relevant question in gene delivery, both with regard to biological activity and toxicity concerns[47]. Most studies focusing on the intracellular fate of molecules during cell division were, however, performed with macromolecules such as free pDNA or dextrans or with smaller gold particles (30-170 Å)[28]. The nuclear inclusion of larger nanoparticles, such as those used in this study, has not been systematically studied in either cell-free systems or living cells. In living-cell experiments, this can partially be explained by the difficulties to inject particles which are larger than 200 nm because of problems related to aggregation, needle clogging and long-term survival of the cells after injection. Using the cell-free XNER assay, we were able to investigate the influence of

size and charge of nanoparticles on their nuclear inclusion. We found that 100 or 200 nm particles were more efficiently included than those of 500 nm. We hypothesize that smaller particles are more efficient in penetrating the condensed chromatin. For a given size, positively charged nanoparticles were most efficiently included in the nuclei, followed by the negatively charged or PEG-ylated ones, which can be explained by aspecific interactions between positively charged beads and the negatively charged chromatin. It should be noted that for both positively and negatively charged beads, interactions of the beads with poly-ions or proteins of the cytosolic extract, before nuclear reassembly starts, could influence the overall charge and nuclear inclusion of the beads. Furthermore, we were able to demonstrate that nanoparticles or PEI/pDNA complexes which are targeted to the chromatin have about two to three times higher probability of being retained in the artificial nuclei. However, not all the particles which were first bound to the chromatin, were finally included in the nuclei. It is plausible that adding the membrane fraction results in competition for binding to the chromatin, causing the majority of chromatin-bound nanoparticles to dissociate when the nuclear membrane formation proceeds.

Based on these observations, we conclude that it should be possible to bring nanoparticles into the nuclei of dividing cells, provided that they are not too large and are able to bind to the chromatin either by their intrinsic positive charge or through the use of chromatin-binding peptides. However, unlike with the XNER assay, nuclear inclusion in dividing HeLa cells was never observed. Instead, the nanoparticles accumulated in the lysosomal compartment as evidenced by colocalization experiments. Two hypotheses could explain the lack of nuclear inclusion and the specific perinuclear localization observed in living cells: 1) the nanoparticles end up in the lysosomal compartment even before cell division occurs and are therefore not able to interact with the chromatin during cell division or 2) the nanoparticles bind to the chromatin and are included in the nuclei during cell division but are expelled from the nuclei before maturation and subsequently accumulate in the lysosomal compartment.

To examine these hypotheses, extensive, detailed real-time analysis of the intracellular distribution of the microinjected nanoparticles would be needed. Nativo *et al.*[48] also detected a large fraction of modified gold nanoparticles accumulated in the vicinity of the nucleus. Chithrani *et al.*[49] showed that nanoparticles which are about to be removed from cells are localized in late endosomes and lysosomes. In relation to recent studies which indicate that nanoparticles are potent autophagy activators, the vesicles we observe can be part of cytoplasmic secretion, exocytosis or autophagy by which the cell recycles and subsequently degrades its own components and foreign material[50].

The second hypothesis would imply that the nanoparticles can bind the chromatin, but that there is a mechanism which is able to remove the nanoparticles again so that they are not included in the maturated nuclei. Ludtke *et al.*[51] and Swanson and McNeil[52] showed that after cytoplasmic delivery by microinjection or scratch-loading, the bulk of labeled pDNA or dextran (> 25 kDa) remained outside the nucleus regardless of cell division. After nuclear injection, however, the labeled pDNA or dextran (> 25 kDa) was present in the nucleus of cells that did not divide, but mainly outside the nucleus of cells that divided[51, 52], supporting the idea that only the chromosomes themselves and macromolecules physically associated with them were included in the newly formed nuclei[52, 53]. In contrast, Gasiorowski and Dean[54] have shown that naked, unmodified pDNA microinjected directly into the nucleus was able to partition evenly to the two daughter nuclei, but that this postmitotic nuclear retention was altered by DNA labeling, resulting in nuclear exclusion of labeled pDNA, while non-modified pDNA was retained. In this study, we cannot exclude that the labeling of our pDNA has an influence on the nuclear exclusion of our PEI/pDNA polyplexes.

In summary, although nuclear inclusion was observed in the XNER assay, we hypothesize that in living cells the nanoparticles are either intracellularly 'trapped' in vesicles and are thus not free to bind to the chromatin, or the nanoparticles bind the

chromatin and enter the nuclei of dividing cells, but are then expelled and accumulate in the lysosomal compartment. The nature of the mechanism that prevents the nuclear inclusion of nanoparticles in living HeLa cells is a topic that requires further study. It is, however, an interesting observation that nanoparticles which were injected in the cytoplasm of cells end up in the lysosomal compartment, even when they are not taken up by endocytosis. We believe that nuclear inclusion should be possible when the nanoparticles are free in the cytosol at the onset of cell division. Also, as the XNER assay demonstrated, anchoring the nanoparticles to the chromatin by chromatin-targeting peptides could help to improve the nuclear inclusion. This makes it an attractive future strategy for non-viral gene delivery, provided that other intracellular barriers such as the entrapment in the lysosomal compartment are first overcome.

REFERENCES

1. Kay, M.A., Glorioso, J.C. & Naldini, L. Viral vectors for gene therapy: the art of turning infectious agents into vehicles of therapeutics. *Nat. Med.* **7**, 33-40 (2001).
2. Nayak, S. & Herzog, R.W. Progress and prospects: immune responses to viral vectors. *Gene Ther.* **17**, 295-304 (2010)
3. Mountain, A. Gene therapy: the first decade. *Trends Biotechnol.* **18**, 119-128 (2000).
4. Wattiaux, R., Laurent, N., Wattiaux-De Coninck, S. & Jadot, M. Endosomes, lysosomes: their implication in gene transfer. *Adv. Drug Deliv. Rev.* **41**, 201-208 (2000).
5. Dowty, M.E., Williams, P., Zhang, G.F., Hagstrom, J.E. & Wolff, J.A. Plasmid DNA Entry into Postmitotic Nuclei of Primary Rat Myotubes. *Proc. Natl. Acad. Sci. USA* **92**, 4572-4576 (1995).
6. Capecchi, M.R. High efficiency transformation by direct microinjection of DNA into cultured mammalian cells. *Cell* **22**, 479-488 (1980).
7. Lechardeur, D., Sohn, K.J., Haardt, M., Joshi, P.B., Monck, M., Graham, R.W., Beatty, B., Squire, J., O'Brodovich, H. & Lukacs, G.L. Metabolic instability of plasmid DNA in the cytosol: a potential barrier to gene transfer. *Gene Ther.* **6**, 482-497 (1999).
8. Xu, Y. & Szoka, F.C., Jr. Mechanism of DNA release from cationic liposome/DNA complexes used in cell transfection. *Biochem.* **35**, 5616-5623 (1996).
9. Lechardeur, D. & Lukacs, G.L. Nucleocytoplasmic transport of plasmid DNA: A perilous journey from the cytoplasm to the nucleus. *Hum. Gene Ther.* **17**, 882-889 (2006).
10. Mirzayans, R., Aubin, R.A. & Paterson, M.C. Differential expression and stability of foreign genes introduced into human fibroblasts by nuclear versus cytoplasmic microinjection. *Mutat. Res.* **281**, 115-122 (1992).
11. Mannisto, M., Ronkko, S., Matto, M., Honkakoski, P., Hyttinen, M., Pelkonen, J. & Urtti, A. The role of cell cycle on polyplex-mediated gene transfer into a retinal pigment epithelial cell line. *J. Gene Med.* **7**, 466-476 (2005).
12. Escriou, V., Carriere, M., Bussone, F., Wils, P. & Scherman, D. Critical assessment of the nuclear import of plasmid during cationic lipid-mediated gene transfer. *J. Gene Med.* **3**, 179-187 (2001).
13. Matsui, H., Johnson, L.G., Randell, S.H. & Boucher, R.C. Loss of binding and entry of liposome-DNA complexes decreases transfection efficiency in differentiated airway epithelial cells. *J. Biol. Chem.* **272**, 1117-1126 (1997).
14. Fasbender, A., Zabner, J., Zeiher, B.G. & Welsh, M.J. A low rate of cell proliferation and reduced DNA uptake limit cationic lipid-mediated gene transfer to primary cultures of ciliated human airway epithelia. *Gene Ther.* **4**, 1173-1180 (1997).

15. Collas, P., Husebye, H. & Alestrom, P. The nuclear localization sequence of the SV40 T antigen promotes transgene uptake and expression in zebrafish embryo nuclei. *Transgenic Res.* **5**, 451-458 (1996).
16. Sebestyen, M.G. et al. DNA vector chemistry: the covalent attachment of signal peptides to plasmid DNA. *Nat. Biotechnol.* **16**, 80-85 (1998).
17. Chen, J., Stickles, R.J. & Daichendt, K.A. Galactosylated histone-mediated gene transfer and expression. *Hum. Gene Ther.* **5**, 429-435 (1994).
18. Mistry, A.R., Falciola, L., Monaco, L., Tagliabue, R., Acerbis, G., Knight, A., Harbottle, R.P., Soria, M., Bianchi, M.E., Coutelle, C. & Hart, S.L. Recombinant HMG1 protein produced in Pichia pastoris: a nonviral gene delivery agent. *BioTechniques* **22**, 718-729 (1997).
19. Dean, D.A. Import of plasmid DNA into the nucleus is sequence specific. *Exp. Cell Res.* **230**, 293-302 (1997).
20. Mortimer, I., Tam, P., MacLachlan, I., Graham, R.W., Saravolac, E.G. & Joshi, P.B. Cationic lipid-mediated transfection of cells in culture requires mitotic activity. *Gene Ther.* **6**, 403-411 (1999).
21. Wilke, M., Fortunati, E., vandenBroek, M., Hoogeveen, A.T. & Scholte, B.J. Efficacy of a peptide-based gene delivery system depends on mitotic activity. *Gene Ther.* **3**, 1133-1142 (1996).
22. Brunner, S., Sauer, T., Carotta, S., Cotton, M., Saltik, M. & Wagner, E. Cell cycle dependence of gene transfer by lipoplex polyplex and recombinant adenovirus. *Gene Ther.* **7**, 401-407 (2000).
23. Jiang, C., O'Connor, S.P., Fang, S.L., Wang, K.X., Marshall, J., Williams, J.L., Wilburn, B., Echelard, Y. & Cheng, S.H. Efficiency of cationic lipid-mediated transfection of polarized and differentiated airway epithelial cells in vitro and in vivo. *Hum. Gene Ther.* **9**, 1531-1542 (1998).
24. Tseng, W.C., Haselton, F.R. & Giorgio, T.D. Mitosis enhances transgene expression of plasmid delivered by cationic liposomes. *Biochim. Biophys. Acta* **1445**, 53-64 (1999).
25. Mannisto, M., Reinisalo, M., Ruponen, M., Honkakoski, P., Tammi, M. & Urtti, A. Polyplex-mediated gene transfer and cell cycle: effect of carrier on cellular uptake and intracellular kinetics, and significance of glycosaminoglycans. *J. Gene Med.* **9**, 479-487 (2007).
26. Nicolau, C. & Sene, C. Liposome-Mediated DNA Transfer in Eukaryotic Cells - Dependence of the Transfer Efficiency Upon the Type of Liposomes Used and the Host-Cell Cycle Stage. *Biochim. Biophys. Acta* **721**, 185-190 (1982).
27. Oudrhiri, N., Vigneron, J.P., Peuchmaur, M., Leclerc, T., Lehn, J.M. & Lehn, P. Gene transfer by guanidinium-cholesterol cationic lipids into airway epithelial cells in vitro and in vivo. *Proc. Natl. Acad. Sci. USA* **94**, 1651-1656 (1997).
28. Feldherr, C.M. Nucleocytoplasmic exchanges during cell division. *J. Cell Biol.* **31**, 199-203 (1966).
29. Errington, R.J., Brown, M.R., Silvestr, O.F., Njoh, K.L., Chappell, S.C., Khan, I.A., Rees, P., Wilks, S.P., Smith, P.J. & Summers, H.D. Single cell nanoparticle

tracking to model cell cycle dynamics and compartmental inheritance. *Cell cycle* **9**, 121-130 (2010).
30. Peeters, L., Sanders, N.N., Braeckmans, K., Boussery, K., Van de Voorde, J., De Smedt, S.C. & Demeester, J. Vitreous: a barrier to nonviral ocular gene therapy. *Invest. Ophthalmol. Vis. Sci.* **46**, 3553-3561 (2005).
31. Franz, C., Walczak, R., Yavus, S., Santarella, R., Gentzel, M., Askjaer, P., Galy, V., Hetzer, M., Mattaj, I.W. & Antonin, W. MEL-28/ELYS is required for the recruitment of nucleoporins to chromatin and postmitotic nuclear pore complex assembly. *EMBO Rep.* **8**, 165-172 (2007).
32. Hetzer, M., Bilbao-Cortes, D., Walther, T.C., Gruss, O.J. & Mattaj, I.W. GTP hydrolysis by Ran is required for nuclear envelope assembly. *Mol. Cell* **5**, 1013-1024 (2000).
33. Breuzard, G., Tertil, M., Goncalves, C., Cheradame, H., Geguan, P., Pichon, C. & Midoux, P. Nuclear delivery of NFkappaB-assisted DNA/polymer complexes: plasmid DNA quantitation by confocal laser scanning microscopy and evidence of nuclear polyplexes by FRET imaging. *Nucleic acids Res.* **36**, e71 (2008).
34. Aravind, L. & Landsman, D. AT-hook motifs identified in a wide variety of DNA-binding proteins. *Nucleic acids Res.* **26**, 4413-4421 (1998).
35. Gunsalus, K.C., Ge, H., Schetter, A.J., Goldberg, D.S., Han, J.D., Hao, T., Berriz, G.F., Bertin, N., Huang, J., Li, N., Mani, R., Hyman, A.A., Sonnichsen, B., Echeverri, C.J., Roth, F.P., Vidal, M. & Piano, F. Predictive models of molecular machines involved in Caenorhabditis elegans early embryogenesis. *Nature* **436**, 861-865 (2005).
36. Fernandez, A.G. & Piano, F. MEL-28 is downstream of the Ran cycle and is required for nuclear-envelope function and chromatin maintenance. *Curr. Biol.* **16**, 1757-1763 (2006).
37. Zhou, X., Benson, K.F., Przybysz, K., Liu, J., Hou, Y., Cherath, L. & Chada, K. Genomic structure and expression of the murine Hmgi-c gene. *Nucleic acids Res.* **24**, 4071-4077 (1996).
38. Catez, F., Yang, H., Tracey, K.J., Reeves, R., Misteli, T. & Bustin, M. Network of dynamic interactions between histone H1 and high-mobility-group proteins in chromatin. *Mol. Cell Biol.* **24**, 4321-4328 (2004).
39. Bianchi, M.E. & Agresti, A. HMG proteins: dynamic players in gene regulation and differentiation. *Curr. Opin. Genet. Dev.* **15**, 496-506 (2005).
40. Lohka, M.J. & Masui, Y. Roles of Cytosol and Cytoplasmic Particles in Nuclear-Envelope Assembly and Sperm Pronuclear Formation in Cell-Free Preparations from Amphibian Eggs. *J. Cell Biol.* **98**, 1222-1230 (1984).
41. Lohka, M.J. & Masui, Y. Formation in vitro of sperm pronuclei and mitotic chromosomes induced by amphibian ooplasmic components. *Science* **220**, 719-721 (1983).
42. Laskey, R.A., Mills, A.D., Philpott, A., Leno, G.H., Dilworth, S.M. & Dingwall, C. The role of nucleoplasmin in chromatin assembly and disassembly. *Philos. Tran. R. Soc. Lond. B. Biol. Sci.* **339**, 263-269; discussion 268-269 (1993).

43. Philpott, A. & Leno, G.H. Nucleoplasmin remodels sperm chromatin in Xenopus egg extracts. *Cell* **69**, 759-767 (1992).
44. Philpott, A., Leno, G.H. & Laskey, R.A. Sperm Decondensation in Xenopus Egg Cytoplasm Is Mediated by Nucleoplasmin. *Cell* **65**, 569-578 (1991).
45. Newport, J. & Dunphy, W. Characterization of the Membrane-Binding and Fusion Events during Nuclear-Envelope Assembly Using Purified Components. *J. Cell Biol.* **116**, 295-306 (1992).
46. Gant, T.M. & Wilson, K.L. Nuclear assembly. *Annu Rev. Cell Dev. Biol.* **13**, 669-695 (1997).
47. Summers, H. Can cells reduce nanoparticle toxicity? *Nano Today* **5**, 83-84 (2010).
48. Nativo, P., Prior, I.A. & Brust, M. Uptake and intracellular fate of surface-modified gold nanoparticles. *ACS Nano* **2**, 1639-1644 (2008).
49. Chithrani, B.D. & Chan, W.C. Elucidating the mechanism of cellular uptake and removal of protein-coated gold nanoparticles of different sizes and shapes. *Nano Lett.* **7**, 1542-1550 (2007).
50. Seleverstov, O., Phang, J.M. & Zabirnyk, O. Semiconductor nanocrystals in autophagy research: methodology improvement at nanosized scale. *Methods Enzymol.* **452**, 277-296 (2009).
51. Ludtke, J.J., Sebestyen, M.G. & Wolff, J.A. The effect of cell division on the cellular dynamics of microinjected DNA and dextran. *Mol. Ther.* **5**, 579-588 (2002).
52. Swanson, J.A. & McNeil, P.L. Nuclear reassembly excludes large macromolecules. *Science* **238**, 548-550 (1987).
53. Benavente, R., Scheer, U. & Chaly, N. Nucleocytoplasmic sorting of macromolecules following mitosis: fate of nuclear constituents after inhibition of pore complex function. *Eur. J. Cell Biol.* **50**, 209-219 (1989).
54. Gasiorowski, J.Z. & Dean, D.A. Postmitotic nuclear retention of episomal plasmids is altered by DNA labeling and detection methods. *Mol. Ther.* **12**, 460-467 (2005).

3

HOW DOES NON-CODING DNA INFLUENCE LIPOFECTION EFFICIENCY OF HELA CELLS?

Parts of this chapter are submitted for publication:

Nathalie Symens, Joanna Rejman, Bart Lucas, Joseph Demeester, Stefaan C. De Smedt and Katrien Remaut. How does non-coding DNA influence lipofection efficiency of HeLa cells? *(submitted manuscript)*

Laboratory of General Biochemistry and Physical Pharmacy, Ghent University, Harelbekestraat 72, 9000 Ghent, Belgium

ABSTRACT

In cationic carrier-mediated gene delivery, the disproportional relationship between the quantity of delivered DNA and the amount of encoded protein produced is a well-known phenomenon. The numerous intracellular barriers which need to be overcome by pDNA to reach the nucleoplasm play a major role in it. In contrast to what one would expect, a partial replacement of coding pDNA by non-coding DNA does not lead to a decrease in transfection efficiency. The mechanism underlying this observation is still unclear. Therefore, we investigated which constituents of the transfection process might contribute to this phenomenon. Our data reveal that the topology of the non-coding plasmid DNA plays a major role. Non-coding pDNA can be used only in a supercoiled form to replace coding pDNA in lipoplexes, without a loss in transfection levels. When non-coding pDNA is linearized or partly digested, it diminishes the transfection potential of coding pDNA, as does non-coding salmon DNA. The difference in transfection efficiencies could not be attributed to diverse physicochemical characteristics of the lipoplexes containing different types of non-coding DNA or to the extent of their internalization. At the level of endosomal release, however, nucleic acid release from the endosomal compartment proceeds faster when lipoplexes contain non-coding salmon DNA. Since the half-life of pDNA in the cytosol hardly exceeds 90 minutes, it is conceivable that prolonged release of coding pDNA from complexes carrying supercoiled non-coding pDNA may explain its positive effect on transfection, while this depot effect does not exist when non-coding salmon DNA is used.

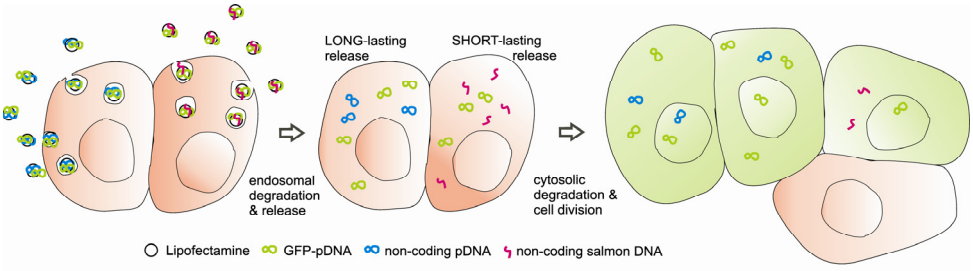

3

HOW DOES NON-CODING DNA INFLUENCE LIPOFECTION EFFICIENCY OF HELA CELLS?

INTRODUCTION

In order to ensure acceptable transgene expression efficiencies relatively high amounts of DNA have to be applied to cells. For example, 1-2 µg pDNA is normally used to transfect 150.000 HeLa cells. This corresponds to roughly 5-15 pg per cell. For comparison, the total DNA content of a human cell is 7.1 pg[1]. Such quantities of delivered DNA do not correspond to the amount of protein produced. Only a relative low fraction of the treated cells produces the encoded protein. This disproportional relationship has been studied by several groups which observed that part of the coding pDNA can be replaced by non-coding DNA without a serious drop in expression efficiency[2-7]. A profound understanding of this phenomenon is still lacking however. It is conceivable that several of the known hurdles in the transfection pathway play a role in it (**Fig. 1**). Interaction of naked DNA with the plasma

membrane is very weak due to the relatively high negative-charge density of both the DNA and the cell surface. Complexing the DNA to polycations has been shown to substantially increase the cellular binding and internalization of DNA by neutralization of its negative charge. It has been demonstrated that the extent of interaction of the polycation/DNA complex with the plasma membrane depends on the charge ratio between the polycationic agent and the DNA[8]. Numerous studies have shown that such cationic non-viral vector/DNA complexes enter cells via endocytosis (**Fig. 1, step 1**)[9]. It has been suggested that not all of the known endocytic pathways, each with their specific characteristics, are equally transfection-productive[10]. If DNA is not timely released from the endosomal compartment, it is likely to be degraded in the lysosomal compartment where most endocytic mechanisms eventually end[11]. Once released from the endosomal compartment (**Fig. 2, step 2**), pDNA stills needs to traverse the crowded cytoplasm to reach the nucleoplasm. This passage is not easy since the cytosol is very viscous due to the high concentration of proteins and other molecules. Moreover, it is packed with numerous organelles suspended in the intricate network of the cytoskeleton[12]. Another factor endangering the efficiency of the transfection process is that pDNA, once deprived of its cationic carrier, is exposed to degradation by cytosolic nucleases (**Fig. 1, step 3**). The estimated half-life of free DNA in the cytosol is around 50-90 minutes[13]. Therefore, it would be advantageous if pDNA could be transported, while still in the endosomes, along microtubules or the actin network toward the perinuclear region where it could be released[14, 15]. Another major barrier yet to overcome is the nuclear membrane (**Fig. 1, step 4**)[16-18]. All transnuclear traffic of macromolecules, including proteins and RNAs, is regulated through the nuclear pore complexes (NPCs) by passive or active nucleocytoplasmic transport[19]. The size of the nuclear pores inhibits direct entry of pDNA into the nucleus[20-24]. Since the many attempts to improve transport through NPCs were not particularly successful, it appears that pDNA requires mitosis to gain entry into the newly formed daughter nuclei[25]. Nonetheless, even the ultimate delivery in the nucleoplasm does not guarantee expression of the foreign DNA[6]. To ensure maximal

transfection, the proper intranuclear compartment must be reached[26-28]. Transcription-active genes are localized at the NPCs[29] or in the center of the nucleus (euchromatin)[30], while positioning of genes to (centromeric) heterochromatin at the nuclear periphery causes silencing[31]. Furthermore, methylation by interference with binding of transcription factors or histone deacetylation by tightly packing the DNA into heterochromatin, renders the transgene incompatible with transcription[32]. Other problems potentially interfering with effective transfection are the cytotoxicity of the transfection agents[33, 34], the immune responses induced by the gene product[33] and the unmethylated CpG motifs present in the prokaryotic pDNA that is usually used to pack the gene in[35].

The aim of this study was to define factors that are instrumental to the positive effect of non-coding pDNA on transfection efficiency mediated by complexes made of pDNA with Lipofectamine. Moreover, we tried to identify which steps along the transfection pathway could explain this phenomenon.

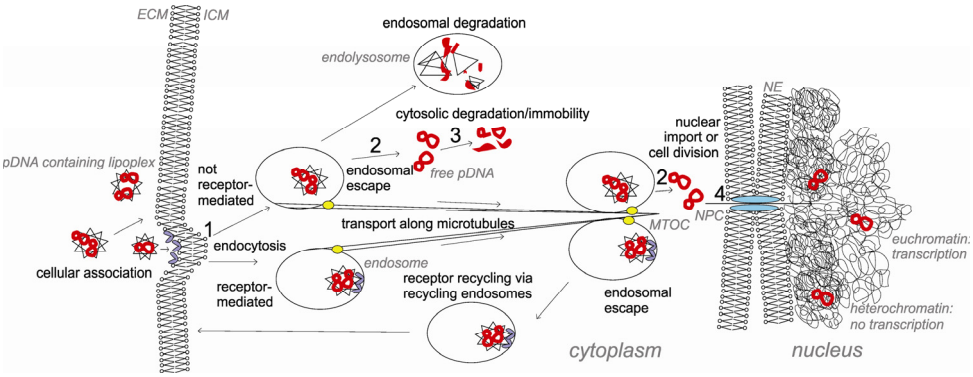

Figure 1. Intracellular barriers interfering with efficient transfection mediated by non-viral lipid carriers: from interaction with the plasma membrane to entry to the nucleus. ECM: extracellular side of the plasma membrane, ICM: intracellular side of the plasma membrane, MTOC: microtubule organizing center, NPC: nuclear pore complex and NE: nuclear envelope. Important steps during the transfection pathway of lipoplexes were investigated including **(1)** internalization of lipoplexes, **(2)**

endosomal release of pDNA, **(3)** cytosolic degradation of pDNA and **(4)** nuclear delivery of pDNA.

MATERIAL AND METHODS

Cell culture conditions

HeLa cells (human epithelial cervical carcinoma cells, ATCC CCL-2, France) were cultured in Dulbecco's Modified Eagle's Medium containing the growth factor F12 and phenol red (DMEM-F12) (Gibco-Invitrogen, Merelbeke, Belgium) containing 2 mM glutamine, 10% heat-inactivated fetal bovine serum (FBS) (Hyclone/Perbio, Thermo Fisher Scientific, Erembodegem-Aalst, Belgium) and 100 U/ml penicillin-streptomycin (Invitrogen-Gibco, Merelbeke, Belgium) at 37 °C in a humidified atmosphere containing 5% CO_2. For the experiments, HeLa cells were seeded in 24-well plates ($7.5x10^4$ cells/well) the day before transfection.

Plasmid and salmon DNA

Heat-competent *E. coli* transformed with the gWIZ-GFP plasmid encoding GFP (GeneTherapy Systems, San Diego, California; further named coding pDNA) or the pGL-3 plasmid encoding luciferase (Promega, Leiden, The Netherlands; coding pDNA used as control for the uptake experiments) or the pGEM4Z-EGFP-A64 plasmid (previously described by Rejman *et al.*[36] and further named non-coding pDNA) or the ΔCpG plasmid encoding luciferase (InvivoGen, Toulouse, France; further named non-coding ΔCpG pDNA) or the pBlue-Luc-A50 plasmid (previously described by Rejman *et al.*[36]; this plasmid was used to produce mRNA encoding luciferase) were grown in LB medium with appropriate antibiotics at 37 °C for 20 h. pDNA was isolated and purified with the Qiafilter Plasmid Giga Kit (Qiagen, Venlo, The Netherlands) according to the manufacturer's instructions.

UltraPure salmon sperm DNA was purchased from Invitrogen (Merelbeke, Belgium). The average size is ≤ 2000 bp.

mRNA production

To produce mRNA by *in vitro* transcription, the pBlue-Luc-A50 plasmid was first purified using a QIAquick PCR purification kit (Qiagen, Venlo, The Netherlands). The plasmid was linearized using the DraI restriction enzyme and then used as template for the *in vitro* transcription reaction using a T7 mMessage mMachine kit (Ambion, Merelbeke, Belgium) according to the manufacturer's instructions. mRNA was purified by DNase I digestion, which was followed by LiCl precipitation and 70% ethanol wash. The produced mLuc (further named mRNA encoding luciferase) was both capped and polyadenylated. mRNA was stored in small aliquots at -80 °C.

Open circular, linear and fragmented pDNA

pDNA was incubated for 2 h on a heating block at 65 °C to make it open circular (OC). The non-coding pGEM4Z-EGFP-A64 pDNA was linearized (LIN) overnight (at 37 °C) with the SpeI restriction enzyme. To obtain partly digested non-coding pDNA (DIG), the pGEM4Z-EGFP-A64 plasmid was digested with two sets of restriction enzymes: (EcoRI, PstI, BglII, ApaLI, XmnI, AclI, SpeI and HindIII) or (EcoRI, XmnI, SpeI and HindIII). The two digestion solutions were then pooled. The coding gWIZ-GFP pDNA was linearized with XhoI (4 h at 37 °C). After digestions, pDNAs were purified with the QIAquick PCR purification kit (Qiagen, Venlo, The Netherlands).

pDNA labeling

For the uptake experiments, pGL-3 pDNA was labeled with YOYO-1 (Molecular Probes-Invitrogen, Merelbeke, Belgium) according to the manufacturer's instructions. Briefly, for a 10:1 base pair to dye ratio, 150 µl of 10 µM of YOYO-1 was mixed with 50 µl of 0.2 µg/µl pDNA. The mixture was incubated in the dark for 1 h at RT. The labeled pDNA was then purified by salt/ethanol precipitation.

Lipoplexes and transfection

The ratio of cationic carrier/DNA was optimized based on the manufacturer's instructions. Briefly, 4 µl of Lipofectamine2000 (Invitrogen, Merelbeke, Belgium) were complexed with a total amount of 2 µg DNA (coding pDNA only or mixtures of coding pDNA and non-coding DNA) or with 0.25 µg mRNA + 1.75 µg non-coding DNA. For some experiments, also lipoplexes containing only coding pDNA (0.25, 0.5, 1 or 2 µg) were prepared. A 50 µl DNA or mRNA solution in OPTIMEM (Gibco-Invitrogen, Merelbeke, Belgium) was added to a 50 µl Lipofectamine 2000 solution in OPTIMEM. After 10 min of incubation, 400 µl OPTIMEM (Gibco-Invitrogen, Merelbeke, Belgium) were added and the mixture was added to HeLa cells. After 4 h for DNA transfection and after 2 h for mRNA transfection, the transfection medium was replaced by fresh culture medium.

Diameter of lipoplexes

The diameter of the lipoplexes was measured with a Zetasizer Nano (Malvern Instruments, Hoeilaart, Belgium). The lipoplexes were prepared as described earlier in DMEM (Gibco-Invitrogen, Merelbeke, Belgium).

Flow cytometry

A BD FACSCalibur (BD, Erembodegem, Belgium) flow cytometer was used to determine the percentage of GFP- and YOYO-1 positive cells. For uptake experiments, the fraction of cells containing YOYO-1 labeled lipoplexes was assessed and mean fluorescence intensities per cell were quantified 4 h after transfection. Fluorescence of lipoplexes bound to the plasma membrane was quenched with trypan blue. To evaluate transfection efficiency, numbers of cells expressing GFP and mean fluorescence intensities per cell were quantified. The measurements were carried out 24 h after transfection.

Fluorescence of YOYO-1 labeled reporter pDNA

The fluorescence of YOYO-1 (λ_{ex} 491 nm, λ_{em} 509 nm) labeled coding pDNA was measured with an Envision plate reader (Perkin Elmer, Zaventem, Belgium) and compared with the fluorescence of lipoplexes containing YOYO-1 labeled coding pDNA and lipoplexes containing both YOYO-1 labeled coding pDNA and non-labeled non-coding DNA.

Mimicking endosomal release

The ability of the lipoplexes to escape out of the early endosomes was investigated as previously described by Xu and Szoka[37]. Lipoplexes (coding pDNA with or without non-coding pDNA or non-coding salmon DNA) were prepared as described earlier. Then, negatively charged liposomes with the same lipid composition as early endosomal membranes namely phosphatidylcholine (PC) : phosphatidylethanolamine (PE) : phosphatidylserine (PS) in a molar ratio 6:3:1 (Avanti Polar Lipids, Delfzijl, The Netherlands) were added. Free DNA was labeled with PicoGreen (λ_{ex} 502 nm, λ_{em} 520 nm) (Molecular Probes, Merelbeke, Belgium) added to the solution. The changes in fluorescence, indicating an increase in the amount of free pDNA were measured over time with a spectrometer (SLM-Aminco Bowman Series 2, Thermo Fisher Scientific, Erembodegem-Aalst, Belgium).

Luciferase assay

The culture medium was removed and the cells were washed twice with PBS (Gibco-Invitrogen, Merelbeke, Belgium). This was followed by adding 100 µL of Cell Culture Lysis Reagent (Promega, Leiden, The Netherlands). After 30 min the samples were centrifuged (12000 rpm at 4 °C for 5 min). 40 µl of the supernatants were transferred to a 96-well plate. Luciferase activity of each sample was assayed in a GloMax 96 Luminometer (Promega, Leiden, The Netherlands) by adding 100 µl of the substrate solution to each well. The emitted light was measured over a 10 s-period. The protein content of each sample was determined by a standard Bradford assay (Biorad,

Nazareth Eke, Belgium). The results are expressed as relative light units per µg of protein (RLU/µg).

Digestion with DNase I

0.25 µg coding pDNA, 0.25 µg coding pDNA mixed with 1.75 µg non-coding pDNA or 0.25 µg coding pDNA mixed with 1.75 µg non-coding salmon DNA were digested with DNase I (Ambion-Invitrogen, Merelbeke, Belgium). The non-coding pDNA was in a supercoiled or linear form. $5x10^{-4}$ units of DNase I was added. The incubations with the enzyme were performed in the supplied buffer on a heating block at 37 °C for 20 minutes. Samples derived from the solutions with digested DNA were loaded together with 5 µl of a loading buffer containing EDTA on a 1.5 % agarose gel and run for 2 h at 100 V. The DNA was stained with ethidium bromide.

HeLa cell synchronization

For the experiments on synchronized HeLa cells, two sets of 12-well plates were prepared. The cells were seeded at 50 000 cells per well. For the synchronization of HeLa cells, the culture medium was replaced one day after seeding with culture medium containing 2 mM thymidine (Sigma-Aldrich, Bornem, Belgium). After 19 h, the culture medium was replaced again by fresh medium without thymidine. The medium was replaced by medium containing 2 mM thymidine 9 h later. After another 17 h of incubation, a synchronized HeLa cell culture was obtained. Non-synchronized cells were left to grow until the moment of transfection. Transfections were performed under the same conditions and with the same quantities of pDNA as for the other experiments.

RESULTS

Effect of non-coding supercoiled pDNA

The data presented in **figure 2** demonstrate the transfection levels obtained with different concentrations of coding pDNA alone and after supplementing coding pDNA with a certain amount of non-coding pDNA in Lipofectamine lipoplexes. As shown in **figure 2A**, mixing 0.5 µg of coding pDNA with 1.5 µg of non-coding pDNA results in a substantial increase in the number of transfected cells, reaching the same number of transfected cells as in case of lipoplexes carrying 2 µg of coding pDNA. Also for the lower ratio (0.25 µg + 1.75 µg), a significant increase in the number of GFP-positive cells was observed upon addition of non-coding pDNA. These results confirm earlier observations obtained with linear PEI[5], Lipofectamine[2, 3], envelope type nano-devices (pDNA/poly-L-lysine complexes coated with DOPE)[3] and microinjection[38]. Nonetheless, the mechanism underlying these observations remained to be elucidated. Therefore, we aimed at defining factors involved in this phenomenon. To that end we first tested whether different types of DNA would effectuate the same transfection efficiencies.

Unmethylated CpG sequences in pDNA molecules are recognized by Toll-Like Receptor 9 (TLR 9) in the endosomal compartment. TLR 9 induces antibacterial and antiviral immune responses. Even though it is predominantly expressed by cells of the immune system, it has also been detected in several tumor cell lines including HeLa cells[39]. Importantly, the immune stimulatory effects caused by these sequences are shown to inhibit gene expression[40, 41]. Therefore, in the next set of experiments we used a plasmid without unmethylated CpG motives (ΔCpG) as a source of non-coding pDNA. The data presented in **figure 2** demonstrate that including this plasmid in lipoplexes had the same positive effect on the transfection efficiency as the non-coding pDNA tested in the previous experiments. It should be noted, however, that the relative fluorescence intensities of the GFP-positive cells (**Fig. 2B**) after transfection with lipoplexes carrying the non-coding ΔCpG pDNA were always higher than in cells transfected with lipoplexes carrying the previous described non-coding

pDNA. Thus, non-coding pDNA that does not stimulate the immune system resulted indeed in higher levels of gene expression. This can indicate that the number of coding pDNA copies successfully delivered to the nucleus was larger for the lipoplexes containing non-coding ΔCpG plasmids. It is possible that the co-delivery of non-coding ΔCpG plasmids lowers the immune response, making both the coding and non-coding pDNA less fast recognized as foreign, resulting in a delay of their removal and/or a better transcription.

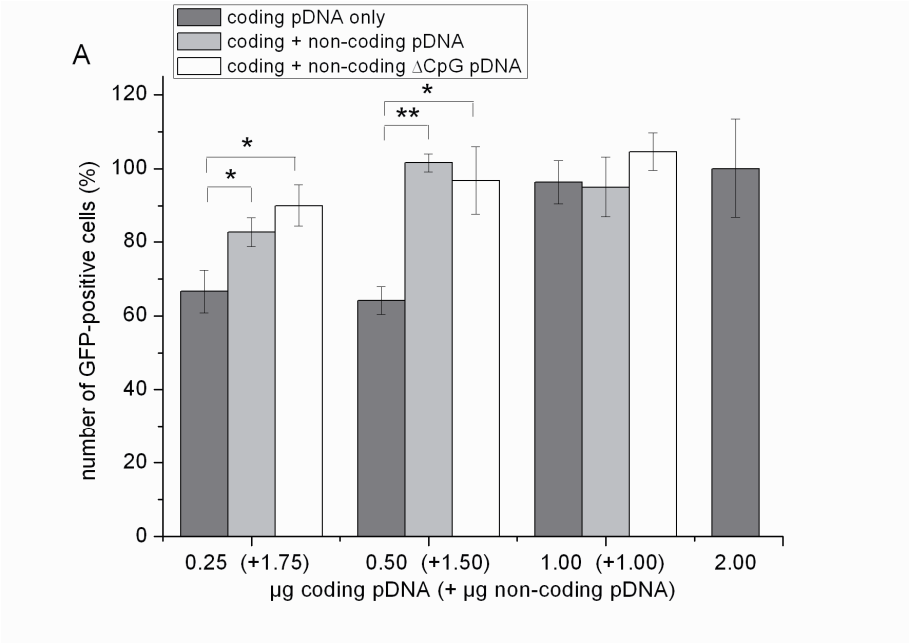

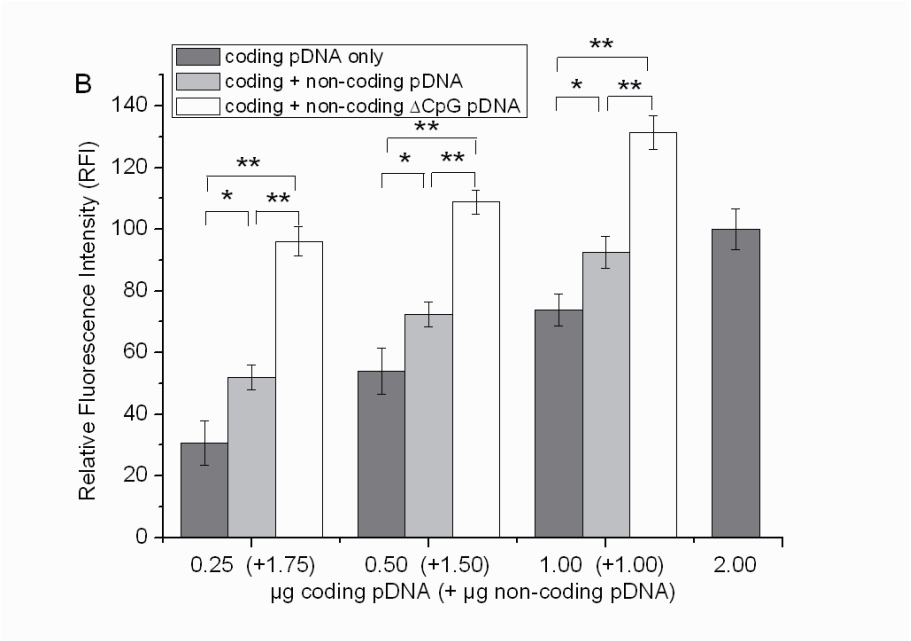

Figure 2. GFP expression in HeLa cells transfected with Lipofectamine lipoplexes in the absence or presence of non-coding pDNA. **(A)** The number (%) and **(B)** the relative fluorescence intensities (RFI) of GFP-positive cells are referred to the condition where lipoplexes contained 2 μg of coding pDNA only. The dark grey bars represent the number or relative fluorescence intensities of GFP-positive cells after transfection with lipoplexes containing only coding pDNA: 0.25 μg, 0.5 μg, 1 μg and 2 μg. The light grey bars represent the number or relative fluorescence intensities of GFP-positive cells after transfection with lipoplexes containing both coding pDNA and non-coding pDNA. The white bars represent the number or relative fluorescence intensities of GFP-positive cells after transfection with lipoplexes containing both coding pDNA and non-coding ΔCpG pDNA. The total pDNA amount was always 2 μg (and thus the quantity of Lipofectamine2000 was always the same): 0.25 μg coding + 1.75 μg non-coding, 0.5 μg coding + 1.5 μg non-coding and 1 μg coding + 1 μg non-coding pDNA. The results were analyzed for the statistical significance: * $p < 0.05$ and ** $p < 0.001$. (Mean ± SD)

Effect of non-coding salmon DNA and non-coding linearized pDNA

In a following set of experiments we studied the effect of non-coding salmon DNA on the transfection efficiency of lipoplexes. As shown in **figure 3**, addition of non-coding salmon DNA has an antagonistic effect on both the percentage (**Fig. 3A**) and the relative fluorescence intensities (**Fig. 3B**) of the GFP-positive cells. This is in

contradiction with earlier work with PEI polyplexes. For linear PEI, it was shown that non-coding salmon DNA can be used to partially replace coding pDNA. Kichler *et al.*[4] demonstrated that more than half of the coding pDNA can be replaced by non-coding salmon DNA or even polyglutamic acid without substantially decreasing the luciferase activity after transfection with linear PEI both in cultured cells and after systemic administration in mice. Also Carpentier *et al*.[6] used non-coding salmon DNA to dilute coding pDNA and keep total DNA and linear PEI concentrations constant. They showed that 50% of relative GFP expression could be obtained with only 10% of coding pDNA. Unfortunately, the authors did not compare these transfection data with the results obtained in the absence of non-coding salmon DNA. Very recently, also Rajendra *et al*.[7] showed that replacement of 67% of coding pDNA by herring sperm DNA in PEI polyplexes only had a 25% decrease of transfection efficiency. Similar experiments with Lipofectamine instead of PEI were lacking. We report for the first time the inhibitory effect of non-coding salmon DNA. These discrepancies with our data could be attributed to the different mechanisms of endosomal escape proposed for lipo- and polyplexes, as pointed out in the discussion section.

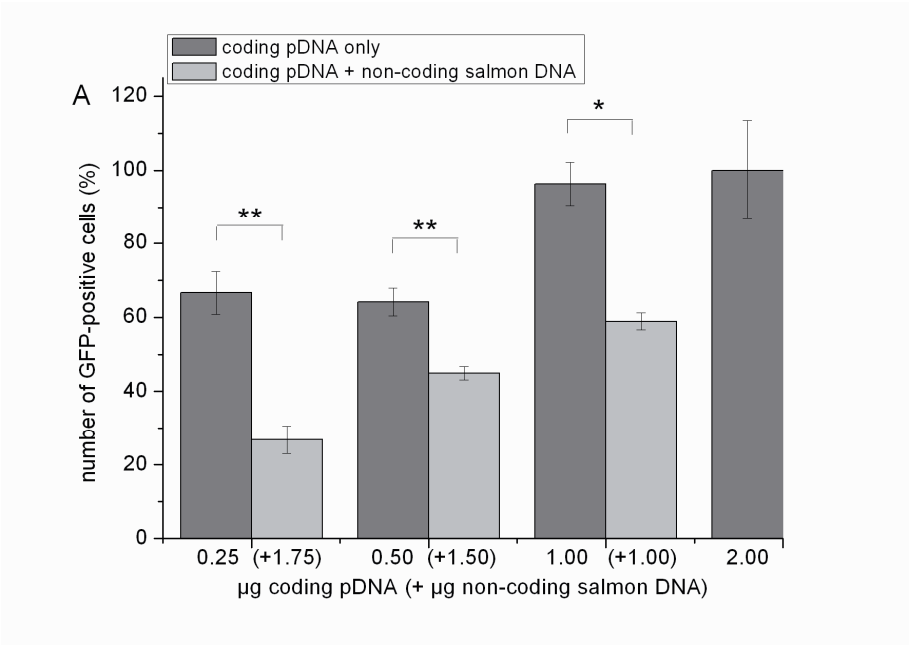

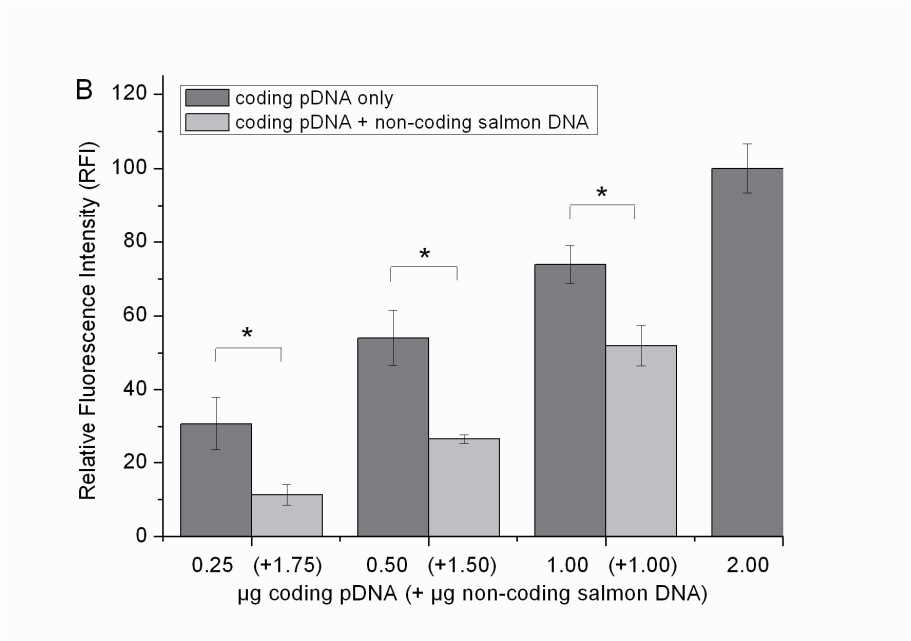

Figure 3. GFP expression in HeLa cells transfected with Lipofectamine lipoplexes containing coding pDNA and non-coding salmon DNA. **(A)** The number (%) and **(B)** the relative fluorescence intensities (RFI) of GFP-positive cells are referred to the condition where lipoplexes contained 2 µg of coding pDNA only (100%). The dark grey bars represent the number or relative fluorescence intensities of GFP-positive cells after transfection with lipoplexes containing only coding pDNA: 0.25 µg, 0.5 µg, 1 µg and 2 µg. The light grey bars represent the number or relative fluorescence intensities of GFP-positive cells after transfection with lipoplexes containing both coding pDNA and non-coding salmon DNA. The total pDNA amount was always 2 µg (and thus the quantity of Lipofectamine2000 was always the same): 0.25 µg coding + 1.75 µg non-coding, 0.5 µg coding + 1.5 µg non-coding and 1 µg coding + 1 µg non-coding salmon DNA. The results were analyzed for the statistical significance: * $p < 0.05$ and ** $p < 0.001$. (Mean ± SD)

We further addressed the question to what extent the structure and size of non-coding DNA influence its potential to increase transfection efficiency of coding pDNA. To that end, non-coding pDNA was linearized or partly digested with a set of restriction enzymes. In this set of experiments, we focused on the condition in which 0.25 µg of coding pDNA was mixed with 1.75 µg non-coding DNA. **Figure 4** presents fractions of GFP-positive cells after transfection with lipoplexes containing coding

pDNA only or coding pDNA mixed with either supercoiled non-coding pDNA (SC), linear non-coding pDNA (LIN) or partly digested non-coding pDNA (DIG). For comparison we also included the data obtained in the presence of non-coding salmon DNA. The results clearly demonstrate that only the presence of supercoiled non-coding pDNA leads to increased numbers of GFP-positive cells. Linearization or fragmentation of non-coding pDNA decreased transfection efficiency of coding pDNA. In other words, linear or partly digested non-coding pDNA has, like non-coding salmon DNA, an antagonistic effect on transfection efficiency, yet it is less pronounced.

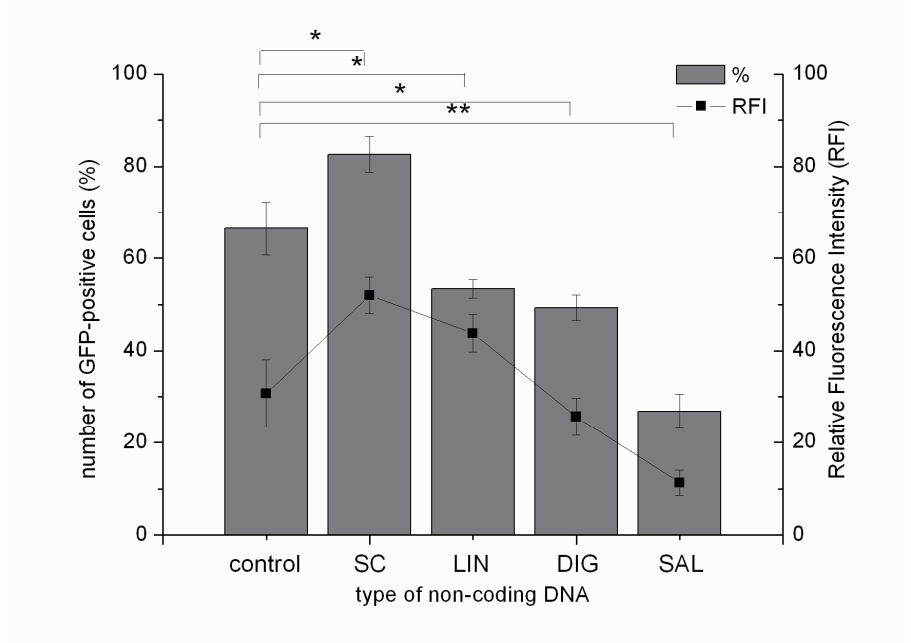

Figure 4. GFP expression in HeLa cells transfected with Lipofectamine lipoplexes containing coding pDNA and non-coding supercoiled, linear or partly digested pDNA. The number (bars) and the relative fluorescence intensities (symbols) of the GFP-positive cells are calculated relative to the condition where lipoplexes contained 2 µg of coding pDNA only (100%). Transfections with lipoplexes containing 0.25 µg coding pDNA only (control), 0.25 µg coding pDNA and 1.75 µg of supercoiled non-coding pDNA (SC), 0.25 µg coding pDNA and 1.75 µg of linear non-coding pDNA (LIN), 0.25 µg coding pDNA and 1.75 µg of partly digested non-coding pDNA (DIG) or 0.25 µg coding pDNA and 1.75 µg of salmon DNA (SAL) are compared. The results were analyzed for the statistical significance: * $p < 0.05$ and ** $p < 0.001$. (Mean ± SD)

Physicochemical characterization

Differences in the physicochemical characteristics of lipoplexes containing coding pDNA alone and lipoplexes carrying different types of non-coding DNA could explain the differences in their transfection efficiencies. Therefore, the diameter of selected lipoplexes was measured. We focused on the condition in which 0.25 µg of coding pDNA was mixed with 1.75 µg non-coding supercoiled pDNA or non-coding salmon DNA. As shown in **figure 5**, the diversely composed lipoplexes do not show significant differences in size. They all have an average diameter of 250 nm. These data demonstrate that the differences in transfection efficiencies cannot be attributed to the physicochemical characteristics.

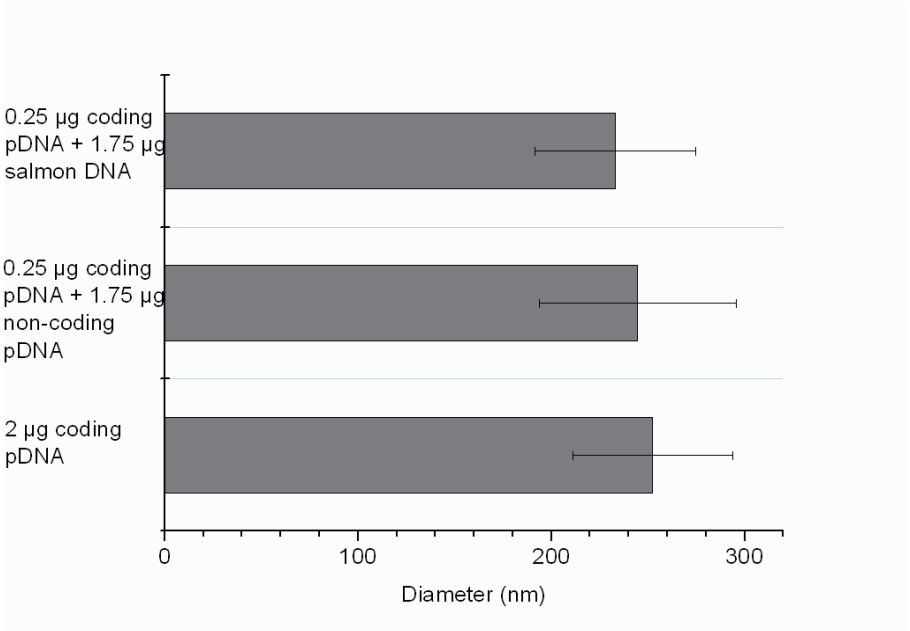

Figure 5. Diameter (nm) of lipoplexes. The diameters of Lipofectamine2000 lipoplexes containing coding pDNA alone (2 µg) and lipoplexes containing 0.25 µg coding pDNA and 1.75 µg non-coding DNA (non-coding supercoiled pDNA or non-coding salmon DNA) are presented. (Mean ± SD)

Cellular internalization of lipoplexes

The results presented in **figures 2** and **3** clearly indicate that lipoplexes containing non-coding supercoiled pDNA were far more efficient in transfecting cells than those carrying non-coding salmon DNA. Therefore, we tested whether these complexes are differently processed by the cells. In this set of experiments, we also focused on the condition in which 0.25 µg of coding pDNA was mixed with 1.75 µg non-coding supercoiled pDNA or non-coding salmon DNA.

The transfection of cells begins when the cationic particles interact with the plasma membrane and are taken up by endocytosis (**Fig. 1, step 1**). To study if there is a difference in the uptake of lipoplexes carrying coding pDNA, coding pDNA mixed with non-coding supercoiled pDNA and coding pDNA mixed with non-coding salmon DNA, HeLa cells were incubated for 4 h with the three types of particles. The coding pDNA was labeled with YOYO-1. To verify that the fluorescence intensities remain the same after complexing YOYO-1 labeled coding pDNA with Lipofectamine in the presence or absence of non-coding DNA, the relative fluorescence intensities were measured with a fluorometer (**Fig. 6A**). **Figure 6B** shows that the fluorescent coding pDNA in the three types of lipoplexes was taken up to the same extent by the same number of HeLa cells. Therefore, the different transfection efficiencies presented in **figures 2** and **3** cannot be explained by a difference in the amount of coding pDNA that was internalized. These data confirm the hypothesis of van Gaal *et al*.[5] proposed for linear PEI complexes and the results of Moriguchi *et al*.[2, 3] that there is no preferential uptake of particles which are physicochemically equivalent.

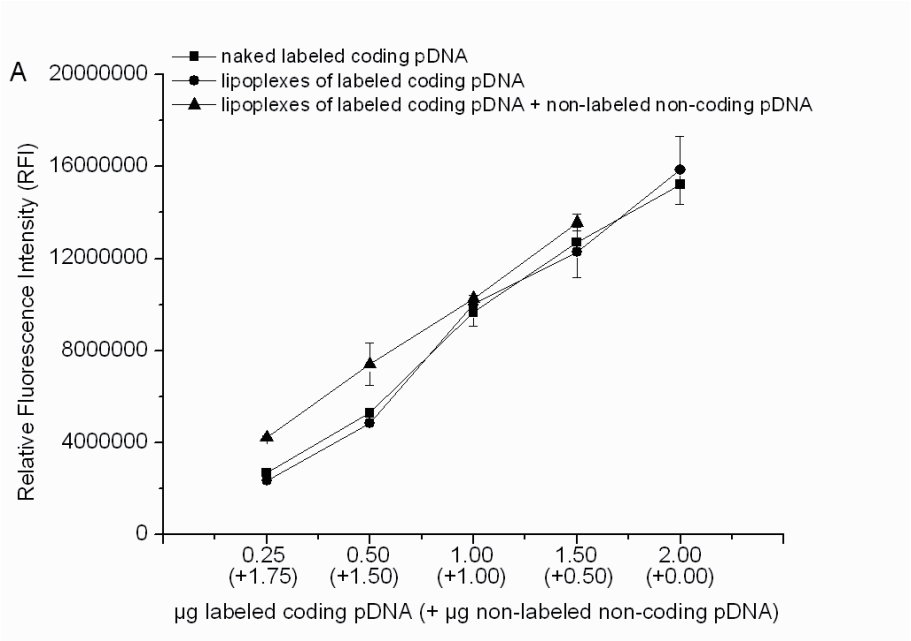

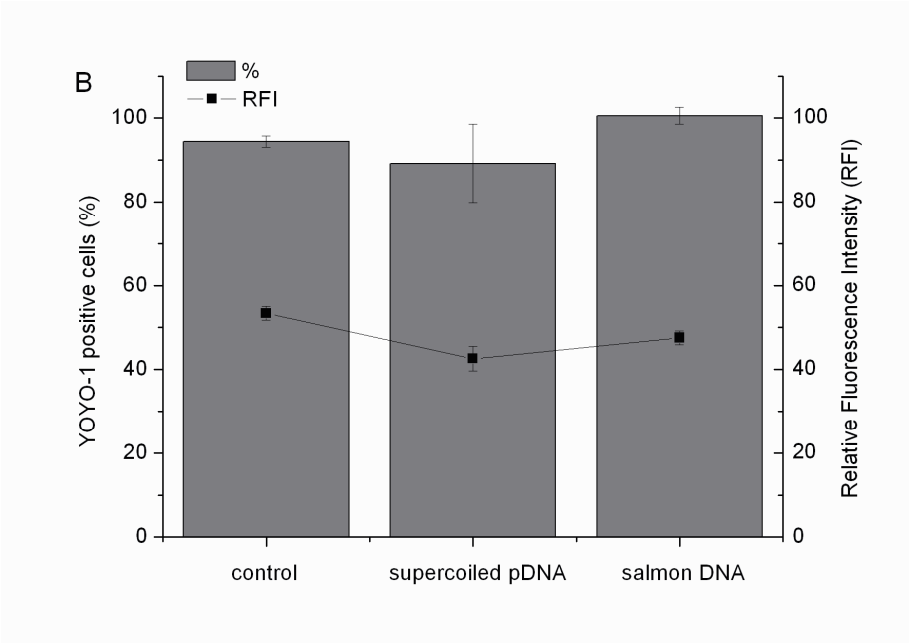

Figure 6. The uptake of Lipofectamine lipoplexes containing YOYO-1 labeled coding pDNA. **(A)** Relative fluorescence intensities (RFI) of coding pDNA labeled with YOYO-1 (squares), lipoplexes containing coding pDNA labeled with YOYO-1 (circles) and lipoplexes containing coding pDNA labeled with YOYO-1 and non-labeled non-coding

pDNA (triangles). **(B)** The number (bars) and the relative fluorescence intensities (symbols) of the YOYO-1 positive HeLa cells are shown. All are calculated relative to the condition where lipoplexes contained 2 µg of YOYO-1 labeled coding pDNA only (100%). The results after transfection with lipoplexes containing 0.25 µg YOYO-1 labeled coding pDNA (control), 0.25 µg YOYO-1 labeled coding pDNA + 1.75 µg non-labeled non-coding supercoiled pDNA (supercoiled pDNA) and 0.25 µg YOYO-1 labeled coding + 1.75 µg non-labeled non-coding salmon DNA (salmon DNA) are presented. (Mean ± SD)

Release from the endosomal compartment

To ensure transfection, the internalized lipoplexes need to timely escape from the endosomal compartment (**Fig. 1, step 2**). According to the model proposed by Xu and Szoka[37] negatively charged phospholipids present in the endosomal membrane form neutral charge pairs with cationic lipids present in the lipoplexes allowing DNA to be released from the complexes and, simultaneously, from the endosomal compartment. In this set of experiments, we hypothesized that different release kinetics may translate into different transfection efficiencies. To mimic the endosomal release of DNA, lipoplexes containing only coding pDNA, coding pDNA mixed with non-coding supercoiled pDNA or coding pDNA mixed with non-coding salmon DNA were allowed to interact under physiological conditions with liposomes composed of phosphatidylcholine (PC), phosphatidylethanolamine (PE) and phosphatidylserine (PS) (6:3:1). These negatively charged liposomes mimic the composition of the early endosomal membranes. The changes in the amount of free DNA accessible to PicoGreen, a fluorescent dye that binds to free DNA, were then recorded with a fluorometer. As shown in **figure 7**, the addition of anionic vesicles to lipoplexes containing only coding pDNA or coding pDNA mixed with non-coding supercoiled pDNA resulted in a slow release of pDNA from the complexes. The release of DNA from complexes containing coding pDNA mixed with non-coding salmon DNA, however, advanced at a higher rate. These results may provide some insight into the mechanism responsible for the better performance of lipoplexes containing only supercoiled pDNA as compared to those carrying additional non-coding salmon DNA.

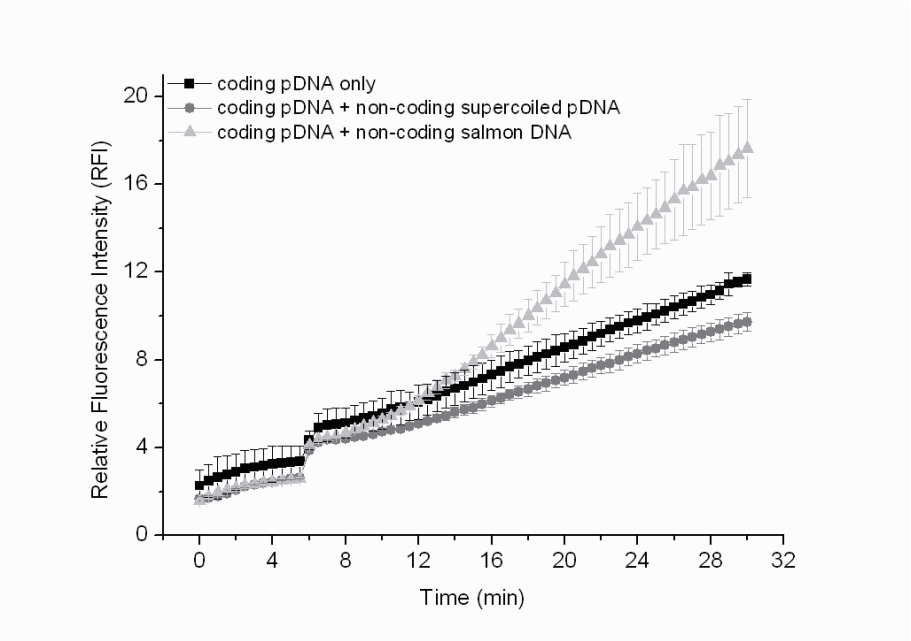

Figure 7. Accessibility of DNA towards PicoGreen, mimicking endosomal release of DNA from lipoplexes. Lipofectamine lipoplexes containing 2 µg of coding pDNA (black squares), 0.25 µg of coding pDNA and 1.75 µg of non-coding supercoiled pDNA (dark grey circles) or 0.25 µg of coding pDNA and 1.75 µg of non-coding salmon DNA (light grey triangles) were added to a PicoGreen solution. Six minutes later anionic vesicles composed of phosphatidylcholine (PC), phosphatidylethanolamine (PE) and phosphatidylserine (PS) (6:3:1) were added. The changes in fluorescence, which correlate with the amount of accessible DNA, were recorded over time with a fluorometer. (Mean ± SD)

To confirm that DNA is released faster into the cytosol from lipoplexes containing non-coding salmon DNA than from lipoplexes containing non-coding pDNA, we performed an experiment in which coding pDNA was replaced by mRNA encoding luciferase. Since mRNA is translated in the cytosol, kinetics of protein production provides a measure of the rate of endosomal release. **Figure 8** presents the levels of luciferase activity after transfection with mRNA in the presence of non-coding supercoiled pDNA or non-coding salmon DNA. In the first 2 h after transfection, the luciferase activity increases over time for the both types of lipoplexes. After 1 h, it was significantly higher in the cells transfected with lipoplexes containing non-coding

salmon DNA, showing that more mRNA has already reached the cytosol in this time frame. Onwards from 6 h post transfection, however, luciferase expression dropped considerably in cells transfected with lipoplexes with non-coding salmon DNA, but remained constant in cells transfected with lipoplexes containing non-coding supercoiled pDNA. These results point out that there is indeed a substantial difference in the nucleic acid release kinetics over time. While lipoplexes containing non-coding salmon DNA release mRNA rapidly and over a short period of time, lipoplexes carrying non-coding supercoiled pDNA ensure a slow release of nucleic acids over a prolonged period of time.

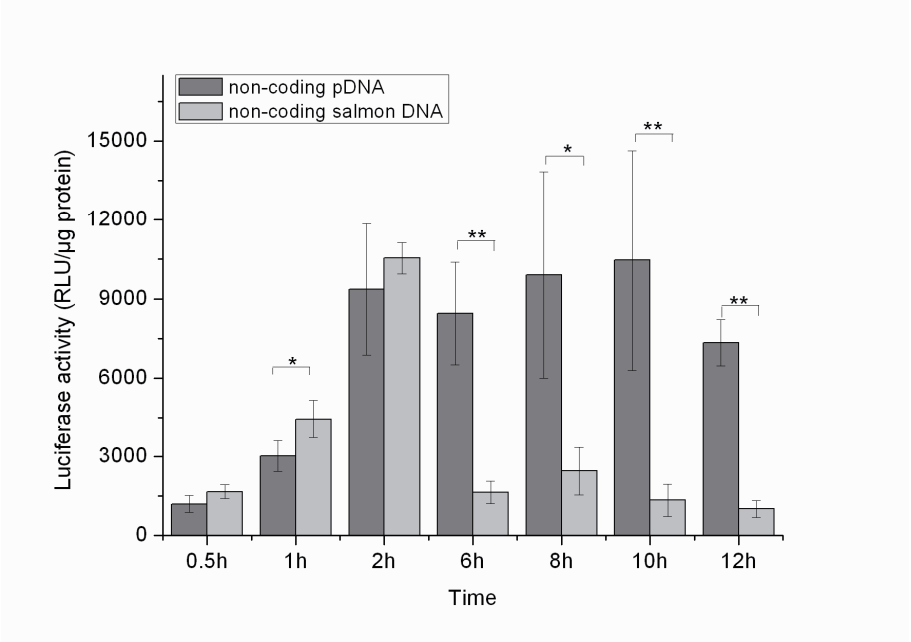

Figure 8. Luciferase activity (RLU/µg protein) in HeLa cells transfected with Lipofectamine lipoplexes containing mRNA encoding luciferase and non-coding supercoiled pDNA or non-coding salmon DNA. The dark grey bars represent levels of luciferase activity after transfection with lipoplexes containing 0.25 µg of coding mRNA and 1.75 µg of non-coding supercoiled pDNA. The light grey bars represent levels of luciferase activity after transfection with lipoplexes containing 0.25 µg of coding mRNA and 1.75 µg of non-coding salmon DNA. The results were analyzed for the statistical significance: * $p < 0.05$ and ** $p < 0.001$. (Mean ± SD)

Cytosolic degradation of DNA

pDNA that has been released from the endosomal compartment, but that is no longer protected by cationic lipids, is exposed to degradation by DNases (**Fig. 1, step 3**)[42]. Degradation by nucleases presents a potential hazard to the intranuclear delivery of an intact gene[13]. Therefore, we tested whether non-coding DNA can protect coding DNA from degradation. To that end, we digested coding pDNA (0.25 µg) mixed with non-coding pDNA or non-coding salmon DNA (1.75 µg) with DNase I. The samples were analyzed by gel electrophoresis. The results of the DNase I digestion are presented in **figures 9A** and **B**. Since supercoiled coding pDNA (framed in **Fig. 9**) is by far the most transcriptionally active topoisomer[43-45], we first identified three forms of plasmid DNA. The bands of the supercoiled, open circular or linear form of coding pDNA are presented in lanes 1-3. As shown in **figure 9A** (lane 6), the band of the supercoiled form of coding pDNA, almost totally disappeared after digestion in the absence of non-coding pDNA, demonstrating its degradation. When coding pDNA was mixed with supercoiled (lane 7) or linearized non-coding pDNA (lane 8), the band of the supercoiled form of coding pDNA clearly remained detectable. As shown in **figure 9B** also non-coding salmon DNA protected coding pDNA against digestion. It can be seen that in the absence of salmon DNA, the band of supercoiled pDNA completely disappeared (lane 5). In the presence of salmon DNA, part of the supercoiled pDNA was still detected (lane 6). We conclude that the presence of both non-coding (supercoiled and linear) pDNA and non-coding salmon DNA protects coding pDNA against DNase I activity.

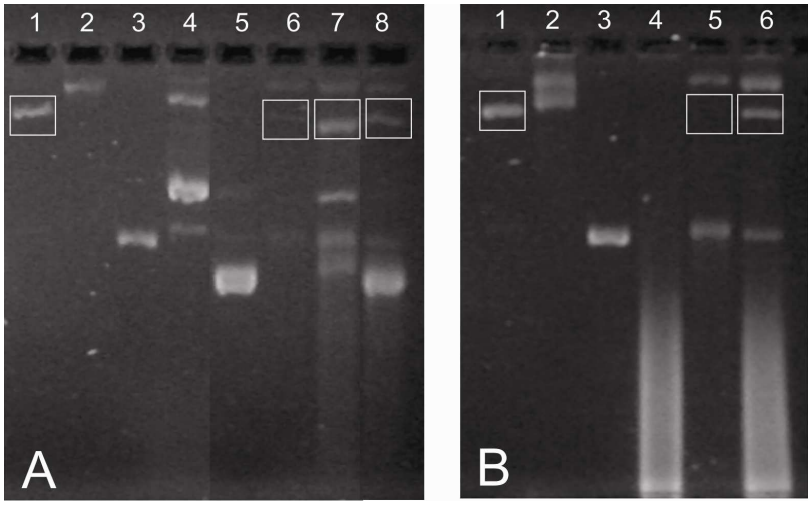

Figure 9. Digestion of coding pDNA in the absence or presence of non-coding DNA. **(A)** Agarose gel of digested coding pDNA in the absence or presence of non-coding pDNA. Lane 1 – supercoiled coding pDNA, lane 2 – open circular coding pDNA, lane 3 – linear coding pDNA, lane 4 – supercoiled non-coding pDNA, lane 5 – linear non-coding pDNA, lane 6 – coding pDNA digested with DNase I, lane 7 – (coding pDNA + supercoiled non-coding pDNA) digested with DNase I and lane 8 – (coding pDNA + linear non-coding pDNA) digested with DNase I. **(B)** Agarose gel of digested coding pDNA in the absence or presence of non-coding salmon DNA. Lane 1 – supercoiled coding pDNA, lane 2 – open circular coding pDNA, lane 3 – linear coding pDNA, lane 4 – non-coding salmon DNA, lane 5 - coding pDNA digested with DNase I, lane 6 – (coding pDNA + non-coding salmon DNA) digested with DNase I. The frames highlight the position of supercoiled coding pDNA.

Effect of synchronized cell division on transfection efficiency

To elucidate the effect of synchronized cell division (**Fig. 1, step 4**) on levels of transfection efficiency, lipoplexes containing different concentrations of coding pDNA alone, or coding pDNA supplemented with non-coding supercoiled pDNA were applied to a cell population which was either dividing asynchronously or synchronously. In **figure 10,** the number and relative fluorescence intensities of the GFP-positive cells for each type of lipoplex in asynchronously dividing cells is compared with the corresponding transfection efficiency in a synchronized cell population. For the lowest concentration of coding pDNA alone (0.25), the number of GFP-positive cells is almost half of what is obtained in synchronously dividing cells.

For the higher pDNA concentrations, however, the level of transfection in asynchronously dividing cells is almost 90% of what is obtained when compared to their synchronized counterparts. Therefore, it appears that synchronization only has benefit for lower pDNA concentrations. Interestingly, the need for synchronization could be overcome when supplementing the lowest concentration of coding pDNA with non-coding supercoiled pDNA (0.25 + 1.75). The number of transfected cells in an asynchronously dividing cell population increases to almost the same levels obtained for synchronized cells. It should be noted that the relative fluorescence intensities per cell are rather similar for asynchronously dividing and synchronously dividing cells, both in the absence or presence of non-coding supercoiled pDNA. This indicates that if the pDNA reaches the nucleoplasm of both asynchronously and synchronously dividing cells, the same amount of protein per cell is produced.

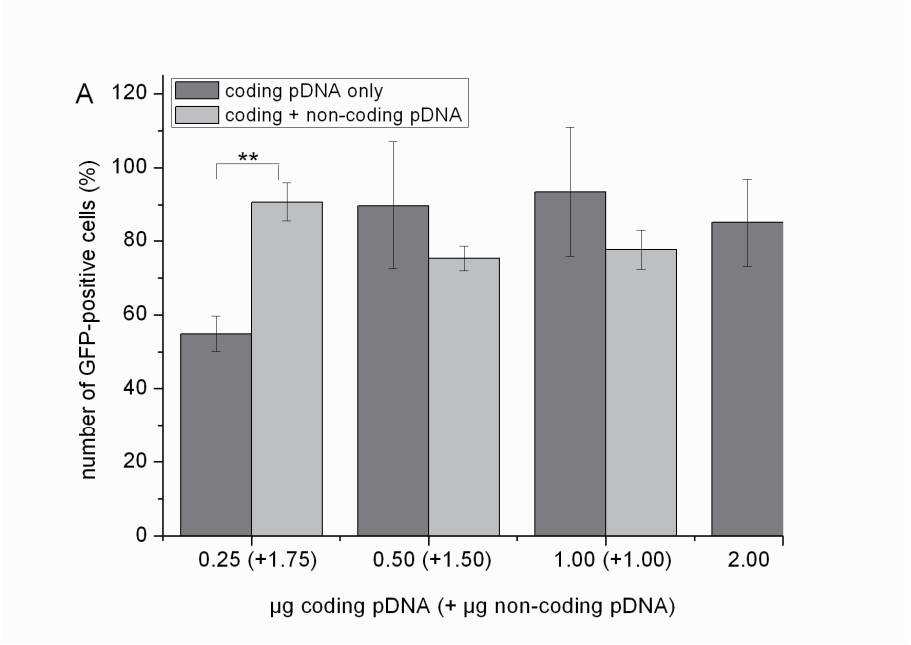

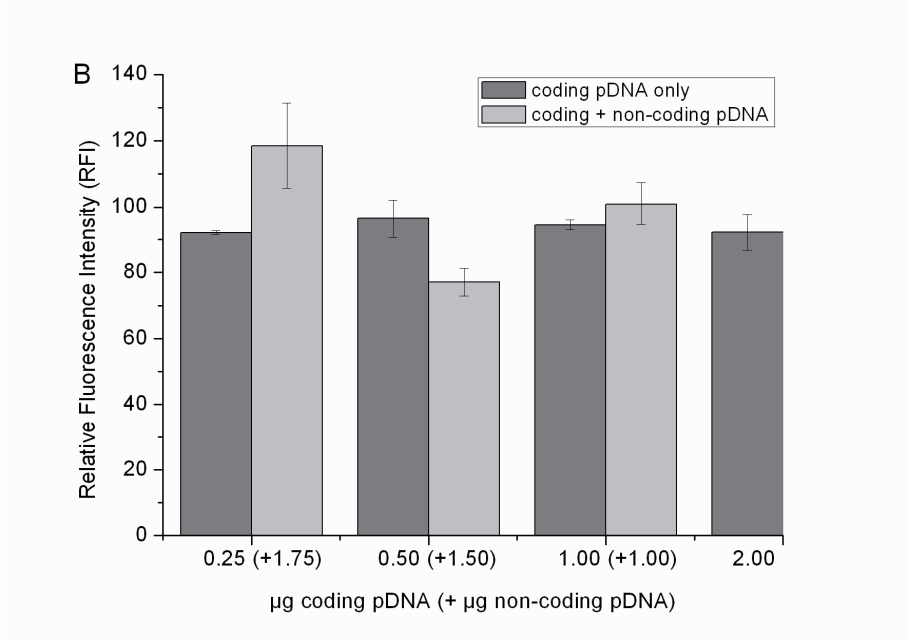

Figure 10. Effect of synchronized cell division on transfection efficiency in the absence or presence of non-coding supercoiled pDNA. **(A)** The number (%) and **(B)** the relative fluorescence intensities (RFI) of GFP-positive cells in an asynchronously dividing cell population, relative to the number and relative fluorescence intensities of GFP-positive cells obtained with the same formulation applied to synchronously dividing cells (100%). The dark grey bars represent the results obtained after transfection with lipoplexes containing only coding pDNA: 0.25 µg, 0.5 µg, 1 µg and 2 µg. The light grey bars represent the results obtained after transfection with lipoplexes containing both coding pDNA and non-coding supercoiled pDNA. The total pDNA amount was always 2 µg (and thus the quantity of Lipofectamine2000 was always the same): 0.25 µg coding + 1.75 µg non-coding, 0.5 µg coding + 1.5 µg non-coding and 1 µg coding + 1 µg non-coding supercoiled pDNA. The results were analyzed for the statistical significance: * $p < 0.05$ and ** $p < 0.001$. (Mean ± SD)

DISCUSSION

The delivery of pDNA is an interesting strategy to produce proteins intracellularly. We (**Fig. 2**) and others, have observed that coding pDNA can be partially replaced with non-coding pDNA without significant decrease in transfection efficiency[2, 3, 5, 38]. Importantly, we found that this is only true for non-coding pDNA in the supercoiled conformation. When linearized or partially digested non-coding pDNA or non-coding salmon DNA was used to supplement coding pDNA in lipoplexes, the transfection efficiency significantly decreased (**Fig.3** and **Fig. 4**). This is in contradiction with earlier results with PEI polyplexes demonstrating that coding pDNA can be partially substituted with non-coding salmon DNA, without diminishing transfection efficiency[4, 6, 7]. The difference may be explained by the different mechanisms proposed for the endosomal release of lipo- and polyplexes. The model proposed by Xu and Szoka[37] for lipid-mediated endosomal release implies that nucleic acids are released from the endosomal compartment in a free form, i.e. without their cationic lipid carrier. In contrast, the proton sponge hypothesis formulated by Boussif *et al*.[46] implies that the dissociation of the PEI carrier from DNA occurs only in the cytosol. Indeed, Huth *et al*.[47] demonstrated that RNAs present in the cytosol induce dissociation of PEI from pDNA. As the endosomal escape of PEI polyplexes is mainly determined by the buffering capacity of the polyplexes, it is logical that non-coding salmon DNA will not influence their endosomal release properties. Instead, as shown by Kichler *et al.*[4] the amount of PEI polymer used determines transfection efficiency, independent of whether they carry coding pDNA alone or a mixture of coding and non-coding DNA.

Our results clearly demonstrated that lipoplexes containing non-coding supercoiled pDNA were far more efficient in transfecting cells than those carrying non-coding salmon DNA. Therefore, we tested whether these two types of lipoplexes were differently processed by the cells. The transfection process starts when lipoplexes interact with the plasma membrane and are taken up by endocytosis (**Fig. 1 and 11, step 1**). It could be reasoned that mixing non-coding DNA with coding pDNA changes

the physicochemical properties of lipoplexes, so that their interaction with the plasma membrane is altered. In consequence, the uptake and accordingly the dose of intracellularly delivered coding pDNA could be affected. Our data showed that the physicochemical characteristics and the uptake of coding pDNA from lipoplexes in the presence or absence of different types of non-coding DNA were the same. Both the number of cells that internalized coding pDNA, as well as the amount of coding pDNA delivered per cell were equal (**Fig. 6**).

After being taken up, lipoplexes are present in the endosomal compartment. Our results revealed that DNA release (**Fig. 1 and 11, step 2**) from lipoplexes containing only supercoiled pDNA (coding alone or coding mixed with non-coding) and lipoplexes containing coding pDNA mixed with non-coding salmon DNA proceeded differently. As shown in **figure 7,** DNA release from lipoplexes containing both coding pDNA and non-coding salmon DNA advances faster, which results in higher concentrations of coding pDNA in the cytosol during a relatively short time window. These results were confirmed by transfections employing mRNA encoding luciferase. Since mRNA is translated as soon as it is released into the cytosol, the luciferase production offers a measure of the rate of endosomal release[36]. **Figure 8** demonstrates that luciferase production within the first hour after adding the lipoplexes to the cells is indeed significantly higher for the lipoplexes containing coding mRNA and non-coding salmon DNA when compared to coding mRNA and non-coding supercoiled pDNA. In contrast, from 6 hours post transfection onward luciferase expression dropped considerably in cells transfected with lipoplexes carrying non-coding salmon DNA, but it remained constant in cells transfected with lipoplexes containing non-coding supercoiled pDNA.

After endosomal release, free DNA present in the cytosol is subject to degradation by DNases (**Fig. 1 and 11, step 3**). Our data demonstrated that coding pDNA gets degraded to lesser extents in the presence of non-coding supercoiled or linearized pDNA as well as non-coding salmon DNA. Therefore, we conclude that partial protection against degradation by non-coding pDNA cannot be the sole reason for

the increased transfection efficiency. This is in agreement with the findings of Kichler *et al.*[4] and the hypothesis of van Gaal *et al.*[5], that reduced degradation of coding pDNA in the presence of non-coding DNA, cannot be the key reason of higher expression efficiencies in the presence of non-coding DNA. Moreover, Kichler *et al.*[4] showed that non-coding DNA could be replaced to some extent with polyglutamic acid which is insensitive to DNases.

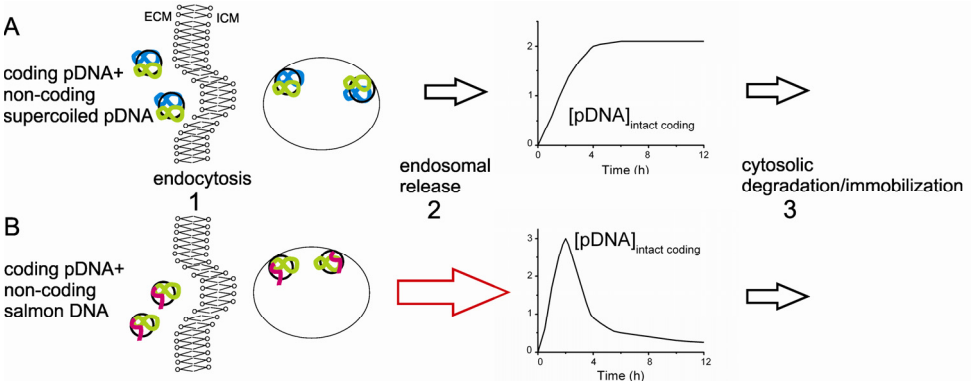

Figure 11. Transfection pathways of lipoplexes carrying coding pDNA mixed with non-coding supercoiled pDNA **(A)** and lipoplexes carrying coding pDNA mixed with non-coding salmon DNA **(B)**. The internalization **(1)** of both types of lipoplexes is equal. Release of DNA from the endosomal compartment **(2)** into the cytosol is faster for lipoplexes containing non-coding salmon DNA than for the ones carrying non-coding pDNA. Both types of non-coding DNA protect coding pDNA against enzymatic degradation to the same extent **(3)**. The effective amount of intact coding pDNA in the cytosol (**graphs**) is determined by a ratio between the amount of coding pDNA released from the endosomal compartment **(2)** and the amount of coding pDNA being degraded in the cytosol and/or immobilized in the cytoplasm **(3)**. ECM: extracellular side of the plasma membrane; ICM: intracellular side of the plasma membrane.

We hypothesize that if coding pDNA is released from the endosomal compartment within a relatively short time window, the chance that cell division, needed for coding pDNA to enter the nucleus, concurs is very small (**Fig. 1, step 4**). In consequence, only a small fraction of the cells gets transfected. If coding pDNA is released to the cytosol over a longer period of time, the likelihood that it coincides with mitosis increases.

This results in transfection of a larger fraction of the cell population. This hypothesis was supported by comparing transfections in asynchronously and synchronously dividing cell populations (**Fig. 10**).

In conclusion, our data demonstrate that a higher dose of administered pDNA may be advantageous in a sense that the endosomes may act as depot organelles for the delivery of intact pDNA. The conformation of pDNA plays, however, a major role, as this depot effect only occurs when supercoiled non-coding pDNA is employed. In the presence of non-coding salmon DNA, the endosomal release rate is relatively fast and therefore endosomes no longer act as a depot organelles. Instead, the burst release of coding pDNA from the endosomal compartment, shortens the time frame during which intact coding pDNA is present in the cytosol, as most of the coding pDNA will be degraded before cell division occurs.

We cannot exclude, however, that later steps in the transfection process are also of importance. One should keep in mind that once in the nucleus, pDNA must be able to arrive at the transcriptionally active regions. It is conceivable that some pDNA is bound and inactivated by histones and thereby ends up as heterochromatin. The fraction of histones, which has to be involved in this binding increases with numbers of pDNA copies delivered to the nucleus. This clearly increases the chances of some pDNA to remain active and ensures increased transfection efficiencies when a higher starting dose of pDNA is used for transfections. Other important steps in the transfection pathway such as cytosolic trafficking toward the nucleus, transcription and translation may also contribute, but current technology does not yet allow thorough evaluation of the role of these processes in this connection.

REFERENCES

1. Ausubel, F.M., Brent, R., Kingstion, R.E., Moore, D.D., Seidman, J.D. & Struhl, K. Current protocols in Molecular Biology. (John Wiley & Sons Inc., New York; 1990).
2. Moriguchi, R., Kogure, K. & Harashima, H. Non-linear pharmacodynamics in the transfection efficiency of a non-viral gene delivery system. *Int. J. Pharm.* **363**, 192-198 (2008).
3. Moriguchi, R., Kogure, K., Iwasa, A., Akita, H. & Harashima, H. Non-linear pharmacodynamics in a non-viral gene delivery system: positive non-linear relationship between dose and transfection efficiency. *J. Control. Release* **110**, 605-609 (2006).
4. Kichler, A., Leborgne, C. & Danos, O. Dilution of reporter gene with stuffer DNA does not alter the transfection efficiency of polyethylenimines. *J. Gene Med.* **7**, 1459-1467 (2005).
5. van Gaal, E.V., Oosting, R.S., Hennink, W.E., Crommelin, D.J. & Mastrobattista, E. Junk DNA enhances pEI-based non-viral gene delivery. *Int. J. Pharm.* **390**, 76-83 (2010).
6. Carpentier, E., Paris, S., Kamen, A.A. & Durocher, Y. Limiting factors governing protein expression following polyethylenimine-mediated gene transfer in HEK293-EBNA1 cells. *J. Biotechnol.* **128**, 268-280 (2007).
7. Rajendra, Y., Kiseljak, D., Manoli, S., Baldi, L., Hacker, D.L. & Wurm, F.L. Role of non-specific DNA in reducing coding DNA requirement for transient gene expression with CHO and HEK-293E cells. *Biotechnol. Bioeng.* (2012).
8. Wiethoff, C.M. & Middaugh, C.R. Barriers to nonviral gene delivery. *J. Pharm. Sci.* **92**, 203-217 (2003).
9. Wattiaux, R., Laurent, N., Wattiaux-De Coninck, S. & Jadot, M. Endosomes, lysosomes: their implication in gene transfer. *Adv. Drug Deliv. Rev.* **41**, 201-208 (2000).
10. Rejman, J., Bragonzi, A. & Conese, M. Role of clathrin- and caveolae-mediated endocytosis in gene transfer mediated by lipo- and polyplexes. *Mol. Ther.* **12**, 468-474 (2005).
11. Nishikawa, M. & Huang, L. Nonviral vectors in the new millennium: delivery barriers in gene transfer. *Hum. Gene Ther.* **12**, 861-870 (2001).
12. Lechardeur, D., Sohn, K.J., Haardt, M., Joshi, P.B., Monck, M., Graham, R.W., Beatty, B., Squire, J., O'Brodovich, H. & Lukacs, G.L. Metabolic instability of plasmid DNA in the cytosol: a potential barrier to gene transfer. *Gene Ther.* **6**, 482-497 (1999).
13. Sodeik, B., Ebersold, M.W. & Helenius, A. Microtubule-mediated transport of incoming herpes simplex virus 1 capsids to the nucleus. *J. Cell Biol.* **136**, 1007-1021 (1997).
14. van Loo, N.D., Fortunati, E., Ehlert, E., Rabelink, M., Grosveld, V. & Scholte, B.J. Baculovirus infection of nondividing mammalian cells: mechanisms of entry and nuclear transport of capsids. *J. Virol.* **75**, 961-970 (2001).

15. Lechardeur, D. & Lukacs, G.L. Nucleocytoplasmic transport of plasmid DNA: A perilous journey from the cytoplasm to the nucleus. *Hum. Gene Ther.* **17**, 882-889 (2006).
16. Mirzayans, R., Aubin, R.A. & Paterson, M.C. Differential expression and stability of foreign genes introduced into human fibroblasts by nuclear versus cytoplasmic microinjection. *Mutat. Res.* **281**, 115-122 (1992).
17. Capecchi, M.R. High efficiency transformation by direct microinjection of DNA into cultured mammalian cells. *Cell* **22**, 479-488 (1980).
18. Gorlich, D. & Mattaj, I.W. Nucleocytoplasmic transport. *Science* **271**, 1513-1518 (1996).
19. Dowty, M.E., Williams, P., Zhang, G.F., Hagstrom, J.E. & Wolff, J.A. Plasmid DNA Entry into Postmitotic Nuclei of Primary Rat Myotubes. *Proc. Natl. Acad. Sci. USA* **92**, 4572-4576 (1995).
20. Mannisto, M., Ronkko, S., Matto, M., Honkakoski, P., Hyttinen, M., Pelkonen, J. & Urtti, A. The role of cell cycle on polyplex-mediated gene transfer into a retinal pigment epithelial cell line. *J. Gene Med.* **7**, 466-476 (2005).
21. Escriou, V., Carriere, M., Bussone, F., Wils, P. & Scherman, D. Critical assessment of the nuclear import of plasmid during cationic lipid-mediated gene transfer. *J. Gene Med.* **3**, 179-187 (2001).
22. Matsui, H., Johnson, L.G., Randell, S.H. & Boucher, R.C. Loss of binding and entry of liposome-DNA complexes decreases transfection efficiency in differentiated airway epithelial cells. *J. Biol. Chem.* **272**, 1117-1126 (1997).
23. Fasbender, A., Zabner, J., Zeiher, B.G. & Welsh, M.J. A low rate of cell proliferation and reduced DNA uptake limit cationic lipid-mediated gene transfer to primary cultures of ciliated human airway epithelia. *Gene Ther.* **4**, 1173-1180 (1997).
24. Symens, N., Soenen, S.J., Rejman, J., Braeckmans, K., De Smedt, S.C. & Remaut, K. Intracellular partitioning of cell organelles and extraneous nanoparticles during mitosis. *Adv. Drug Deliv. Rev.* **64**, 78-94 (2012).
25. Lam, A.P. & Dean, D.A. Progress and prospects: nuclear import of nonviral vectors. *Gene Ther.* **17**, 439-447 (2010).
26. Dean, D.A., Strong, D.D. & Zimmer, W.E. Nuclear entry of nonviral vectors. *Gene Ther.* **12**, 881-890 (2005).
27. Fackelmayer, F.O. Nuclear architecture and gene expression in the quest for novel therapeutics. *Curr. Pharm. Des.* **10**, 2851-2860 (2004).
28. Van de Vosse, D.W., Wan, Y., Wozniak, R.W. & Aitchison, J.D. Role of the nuclear envelope in genome organization and gene expression. *Wiley. Interdiscip. Rev. Syst. Biol. Med.* **3**, 147-166 (2011).
29. Tanabe, H., Habermann, F.A., Solovei, I., Cremer, M. & Cremer, T. Non-random radial arrangements of interphase chromosome territories: evolutionary considerations and functional implications. *Mut. Res.* **504**, 37-45 (2002).

30. Brown, K.E., Guest, S.S., Smale, S.T., Hahm, K., Merkenschlager, M. & Fisher, A.G. Association of transcriptionally silent genes with Ikaros complexes at centromeric heterochromatin. *Cell* **91**, 845-854 (1997).
31. Jones, P.A. The DNA methylation paradox. *Trends Genet.* **15**, 34-37 (1999).
32. Tousignant, J.D., Gates, A.L., Ingram, L.A., Johnson, C.L., Nietupski, J.B., Cheng, S.H., Eastman, S.J. & Scheule, R.K. Comprehensive analysis of the acute toxicities induced by systemic administration of cationic lipid:plasmid DNA complexes in mice. *Hum. Gene Ther.* **11**, 2493-2513 (2000).
33. Brazeau, G.A., Attia, S., Poxon, S. & Hughes, J.A. In vitro myotoxicity of selected cationic macromolecules used in non-viral gene delivery. *Pharm. Res.* **15**, 680-684 (1998).
34. Krieg, A.M. Direct immunologic activities of CpG DNA and implications for gene therapy. *J. Gene Med.* **1**, 56-63 (1999).
35. Rejman, J., Tavernier, G., Bavarsad, N., Demeester, J. & De Smedt, S.C. mRNA transfection of cervical carcinoma and mesenchymal stem cells mediated by cationic carriers. *J. Control. Release* **147**, 385-391 (2010).
36. Xu, Y. & Szoka, F.C., Jr. Mechanism of DNA release from cationic liposome/DNA complexes used in cell transfection. *Biochem.* **35**, 5616-5623 (1996).
37. Ludtke, J.J., Sebestyen, M.G. & Wolff, J.A. The effect of cell division on the cellular dynamics of microinjected DNA and dextran. *Mol. Ther.* **5**, 579-588 (2002).
38. Nishimura, M. & Naito, S. Tissue-specific mRNA expression profiles of human toll-like receptors and related genes. *Biol. Pharm. Bull.* **28**, 886-892 (2005).
39. Tan, Y., Li, S., Pitt, B.R. & Huang, L. The inhibitory role of CpG immunostimulatory motifs in cationic lipid vector-mediated transgene expression in vivo. *Hum. Gene Ther.* **10**, 2153-2161 (1999).
40. Qin, L., Ding, Y., Pahud, D.R., Chang, E., Imperiale, M.J. & Bromberg, J.S. Promoter attenuation in gene therapy: interferon-gamma and tumor necrosis factor-alpha inhibit transgene expression. *Hum. Gene Ther.* **8**, 2019-2029 (1997).
41. Howell, D.P., Krieser, R.J., Eastman, A. & Barry, M.A. Deoxyribonuclease II is a lysosomal barrier to transfection. *Mol. Ther.* **8**, 957-963 (2003).
42. Sekiguchi, J.M., Swank, R.A. & Kmiec, E.B. Changes in DNA topology can modulate in vitro transcription of certain RNA polymerase III genes. *Mol. Cell. Biochem.* **85**, 123-133 (1989).
43. Handa, H., Watanabe, H., Suzuki, Y. & Hirose, S. Effect of DNA supercoiling on in vitro transcription from the adenovirus early region 4. *FEBS Letters* **249**, 17-20 (1989).
44. Remaut, K., Sanders, N.N., Fayazpour, F., Demeester, J. & De Smedt, S.C. Influence of plasmid DNA topology on the transfection properties of DOTAP/DOPE lipoplexes. *J. Control. Release* **115**, 335-343 (2006).
45. Boussif, O., Lezoualc'h, F., Zanta, M.A., Mergny, M.D., Scherman, D., Demeneix, B. & Behr, J.P. A versatile vector for gene and oligonucleotide

transfer into cells in culture and in vivo: polyethylenimine. *Proc. Natl. Acad. Sci. USA* **92**, 7297-7301 (1995).

46. Huth, S., Hoffmann, F., von Gersdorff, K., Laner, A., Reinhardt, D., Rosenecker, J. & Rudolph, C. Interaction of polyamine gene vectors with RNA leads to the dissociation of plasmid DNA-carrier complexes. *J. Gene Med.* **8**, 1416-1424 (2006).

4

EFFICIENT TRANSFECTION OF HEPATOCYTES MEDIATED BY mRNA COMPLEXED TO GALACTOSYLATED CYCLODEXTRINS

Parts of this chapter are published in:

Nathalie Symens[†], Alejandro Méndez-Ardoy[‡], Alejandro Díaz-Moscoso[§], Elena Sánchez-Fernández[§], Katrien Remaut[†], Joseph Demeester[†], José M. García Fernández[§], Stefaan C. De Smedt[†] and Joanna Rejman[†]. Efficient transfection of hepatocytes mediated by mRNA complexed to galactosylated cyclodextrins. *Bioconjugate Chemistry*, **23** (6), 1276-1289 (2012).

† Laboratory of General Biochemistry and Physical Pharmacy, Ghent University, Harelbekestraat 72, 9000 Ghent, Belgium

‡ Departamento de Química Organica, Universidad de Sevilla, c/ Professor Garcia Gonzalez 1, 41012 Sevilla, Spain

§ Instituto de Investigaciones Químicas (IIQ) (CSIC-Universidad de Sevilla), Américo 49, Isla de Cartuja, 41092 Sevilla, Spain

ABSTRACT

In this study we aimed at specific targeting of polycationic amphiphilic cyclodextrins (paCDs) to HepG2 cells via the asialoglycoprotein receptor (ASGPr). The transfection efficiencies of paCDs modified with galactose-moieties were evaluated. In preliminary experiments, attempts to transfect HepG2 cells with pDNA complexed with different modified paCDs resulted in very low transfection levels. In additional series of experiments we found out that cyclodextrin/nucleic acid complexes (CDplexes) were efficiently taken up by the cells and that photochemical internalization, which facilitates release from endosomes, did not improve transfection. Further experiments showed that pDNA can be readily released from the CDplexes when exposed to negatively charged vesicles. These observations imply that the lack of transfection cannot be attributed to a lack of internalization, release of CDplexes from the endosomal compartment or release of free pDNA from the CDplexes. This in turn suggests that the nuclear entry of the pDNA represents the main limiting factor in the transfection process. To verify that, HepG2 cells were transfected with targeted CDplexes containing mRNA, that does not require entry into the nucleus for being translated. With mRNA encoding the green fluorescent protein (GFP), fractions of GFP-positive cells up to 31% were obtained. The results confirmed that the galactosylated complexes were specifically internalized via the ASGPrs.

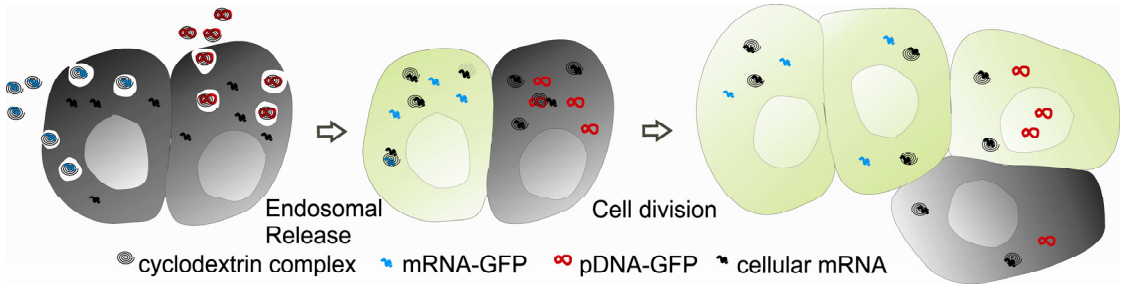

4

EFFICIENT TRANSFECTION OF HEPATOCYTES MEDIATED BY mRNA COMPLEXED TO GALACTOSYLATED CYCLODEXTRINS

INTRODUCTION

Although the liver has unique features which make it attractive for *in vivo* and *ex vivo* gene delivery, no effective treatment of any liver-associated genetic disease has been obtained thus far despite many years of research on viral and non-viral vectors[1, 2]. Several problems still have to be overcome before gene-therapeutic treatment of liver disease may become reality. The formation of aggregates of vectors and blood components, which may occur upon systemic administration, should be prevented[3]. The induction of host immune responses against the transgene product and/or the vector[4] is another major hurdle which needs to be overcome, possibly by the use of liver-specific promoters[5, 6], hepatocyte-specific targeting[7] and/or the use of polyethylene glycol (PEG)-moieties[8]. Gene delivery by means of non-viral vectors meets with additional obstacles at the intracellular level which mostly do not present

a problem for viral vectors[9-11]. The major ones are the escape of the delivered genetic material from the endosomal compartment and its translocation into the nucleus[12].

Recently, a new family of polycationic amphiphilic cyclodextrins (paCDs) has been developed. These paCDs are equipped with thiourea segments, polycationic clusters and lipophilic tails (**Fig. 1**). They were shown to efficiently complex polyanionic nucleic acids[13-16]. The resulting positively charged cyclodextrin/nucleic acid complexes (CDplexes) (**Fig. 2**) can interact with the negatively charged proteoglycans at the cell surface and be taken up by endocytosis[17-19]. Involvement of the lipophilic tails in the internalization and endosomal release process is probably of minor importance because it is conceivable that the hydrocarbon chains are oriented toward the inner core of the CDplex, which will limit their interaction with plasma and endosomal membrane lipids[15].

The general scheme for the synthesis of paCDs allows the introduction of additional functional elements allowing visualization or targeting[15, 20]. We hypothesized that this could be exploited to design paCD systems for hepatocyte-specific cell uptake by the incorporation of multivalent D-galactose ligands which could interact with the asialoglycoprotein receptor (ASGPr)[21]. The ASGPr is predominantly expressed on the basolateral surface of mammalian hepatocytes and is responsible for the clearance of glyco- and lipoproteins[22]. The extracellular domain of the receptor specifically recognizes and binds ligands with terminal galactose (Gal) or N-acetylgalactosamine (Gal*N*Ac) residues upon which clathrin-mediated internalization of the receptor-ligand complex occurs, which provides a unique means for the development of liver-specific carriers for drug and gene delivery to the hepatic parenchymal cells[23]. ASGPr-ligand containing endosomes are captured by microtubules just below the actin layer at the cell periphery and they are actively transported to the center of the cell along microtubules by cytoplasmic dynein[24]. The early endosomes interact then with vesicles in which the uncoupling of receptors and ligands occurs[25]. It is generally believed that the acidification within this compartment leads to dissociation of the

ligand from the receptor, while receptor molecules are recycled back to the plasma membrane[26]. However, several groups have reported that the efficient dissociation of intracellular ASGPr-ligand complexes is independent of pH changes[27] and may require inactivation of the receptors[28]. There is also strong evidence that a large fraction of the receptor recycles back to the cell surface still associated with its ligand[29]. Ligand-ASGPr interaction is based on the sugar preference (N-acetylgalactosamine >> galactose[30]), the antennary structure (tetra- > tri- >> di- >> mono-antennary[31]) and sugar spacing (20 >> 10 >> 4 Å)[32, 33].

In our present study, we aimed at specific targeting of HepG2 cells via the ASGPr. HepG2 cells derive from human hepatoblastoma. They are able to form bile canalicular structures (apical) between two neighboring cells which means they can exhibit a certain degree of polarity. The basolateral membrane domains of hepatocytes in the intact liver face the sinusoidal blood and adjacent cells. Apical and basolateral membrane domains are separated by tight junctions which prevent intermixing of membrane components between both domains[34]. These properties make us believe that HepG2 cells bear sufficient resemblance to the human hepatocyte *in vivo* and present a useful model to study the uptake and transfection potential of modified paCDs in human liver cells[35].

In the present work, a paCD derivative bearing 14 hexanoyl chains at the secondary hydroxyl face and 21 protonable amino groups at the primary face (**Fig. 1**, **Hex-CD-N_{21}**) was used as a reference compound. To evaluate the possibility to specifically target HepG2 cells, the transfection efficiencies of reference CDs modified with galactose-moieties were investigated in a series of preliminary experiments. Attempts to transfect HepG2 cells with pDNA complexed with different modified CDs resulted in hardly any transfection. To determine the cause of this failure, we performed a set of additional experiments. These strongly pointed to the nuclear envelope as the major barrier toward successful transfection of HepG2 cells with the pDNA-CDplexes. To verify this hypothesis, we transfected HepG2 cells with mRNA

instead of pDNA. We were able to show remarkable transfection efficiencies with mRNA-CDplexes. With mRNA encoding the green fluorescent protein (GFP), fractions of GFP-positive cells up to 31% were obtained. Furthermore, the galactosylated mRNA-CDplexes were shown to be specifically taken up via the ASGPrs. These results lead us to believe that properly modified paCDs complexed with mRNA may represent a promising system to transfect hepatocytes *in vivo.*

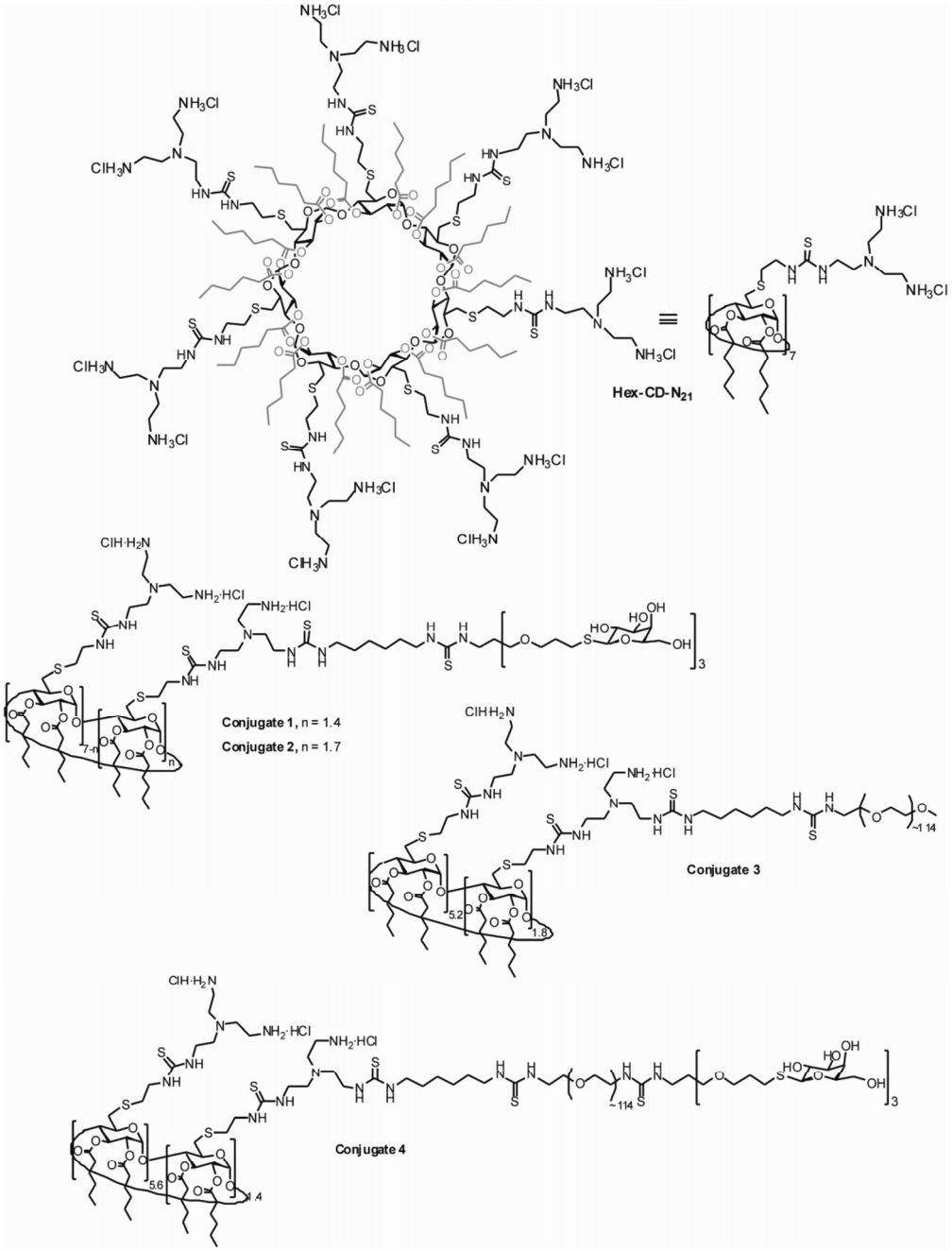

Figure 1. Chemical structures of modified polycationic amphiphilic cyclodextrins: reference hexanoylated CD with 21 potentially protonable nitrogens (**Hex-CD-N_{21}**; only the primary amino groups are represented as the corresponding hydrochlorides according to the microanalytical data of the synthesized compound), 10% tri-

antennary-galactose-bearing reference CD (**conjugate 1**; Gal10CDs), 12% tri-antennary-galactose-bearing reference CD (**conjugate 2**; Gal12CDs), 13% thio-PEG_{5000}-bearing reference CD (**conjugate 3**; PEGCDs) and 10% thio-PEG_{5000}-tri-antennary-galactose-bearing reference CD (**conjugate 4**; GalPEGCDs). These abbreviations are used throughout the text.

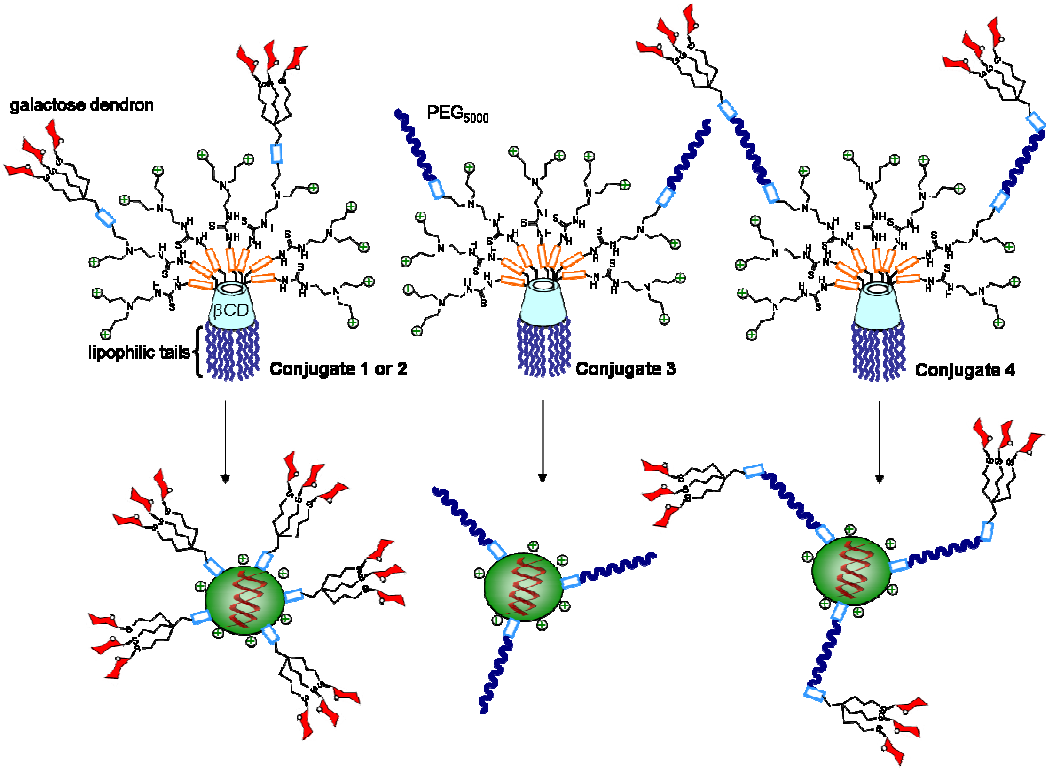

Figure 2. Schematic representation of the polycationic amphiphilic cyclodextrin derivatives prepared in this work (top) and of the different CDplexes which are generated after complexation with nucleic acids (down). The positive charges represent protonated amino groups.

EXPERIMENTAL PROCEDURES

Cyclodextrin synthesis and conjugation

The chemical structures of the five different paCDs (abbreviations between brackets): reference CDs (**Hex-CD-N_{21}**), 10% tri-antennary-galactose-bearing reference CDs (Gal10CDs; **conjugate 1**), 12% tri-antennary-galactose-bearing reference CDs (Gal12CDs; **conjugate 2**), 13% thio-PEG_{5000}-bearing reference CDs (PEGCDs; **conjugate 3**) and 10% thio-PEG_{5000}-tri-antennary-galactose-bearing reference CDs (GalPEGCDs, **conjugate 4**) are shown in **figure 1**. Their schematic representations before and after complexation with nucleic acids are represented in **figure 2** and their synthesis schemes are shown in **schemes 1** to **3**.

Common reagents and materials were purchased from commercial sources. Optical rotations were measured at RT in 1-dm tubes on a Perkin-Elmer 141 MC polarimeter. Infrared (IR) spectra were recorded on a Bomen Michelson MB-120 FTIR spectrophotometer. ^{1}H (and ^{13}C NMR) spectra were recorded at 300 (75.5 for ^{13}C) and 500 (125.7 for ^{13}C) MHz with Bruker 300 and 500 DRX instruments. 1D ^{1}H TOCSY (total correlation spectroscopy), 2D ^{1}H TOCSY, COSY (correlation spectroscopy), ^{1}H-^{13}C HMQC (heteronuclear multiple quantum correlation) and HSQC (heteronuclear single quantum correlation) experiments were used to assist NMR (nuclear magnetic resonance) assignments. Thin-layer chromatography (TLC) was carried out on aluminium sheets coated with Kieselgel 60 F254 (Merck), with visualization by UV light and by charring with 10% H_2SO_4 or 0.2% ninhydrin. Column chromatography was carried out on Silica Gel 60 (Merck, 230-400 mesh). Gel permeation chromatography (GPC) of the fully unprotected βCD adducts was carried out on a Sephadex G-25 (eluent H_2O) column (Pharmacia Amersham) attached to a Gradifrac system using a UV detector set at 248 nm. Electrospray mass spectra (ESIMS) were obtained with a Bruker Esquire6000 instrument. Heptakis [6-(2-(*N'*-(2-(*N,N*-bis-(2-aminoethyl)amino)ethyl)thioureido)ethylthio)-2,3-di-*O*-hexanoyl]cyclomaltoheptose (**Hex-CD-N_{21}**) was synthesized following the procedure previously reported [15]. 2,3,4,6-Tetra-*O*-acetyl-1-thio-α-D-galactopyranose (**6**) was prepared from D-galactose

pentaacetate in three steps by transformation into the corresponding glycosyl bromide, reaction with thiourea and subsequent hydrolysis of the resulting isothiouronium salt with potassium metabisulfite ($K_2S_2O_5$) [36]. Elemental analyses were performed at the Instituto de Investigaciones Químicas (Sevilla, Spain). Triphenylphosphine, trifluoromethanesulfonic anhydride and *N,N*-dimethylformamide are indicated by the acronyms TPP, Tf_2O and DMF, respectively **(Scheme 1)**.

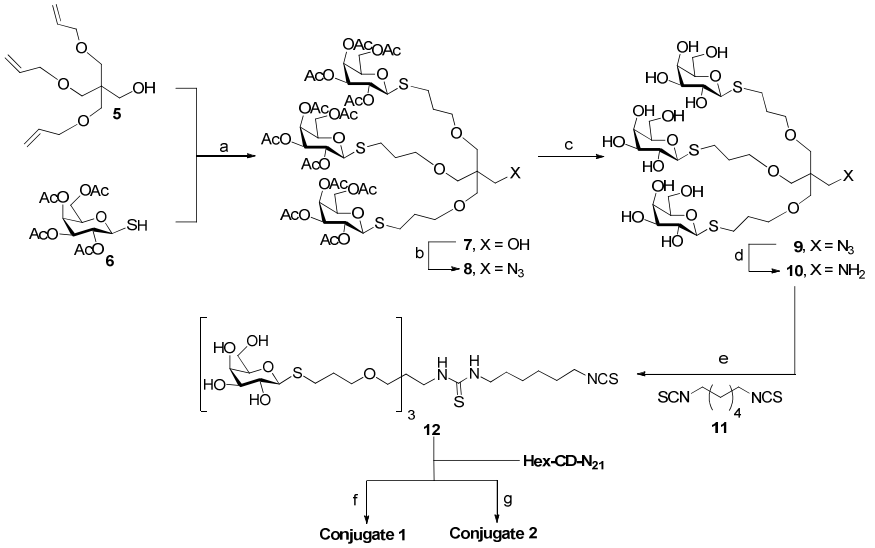

Scheme 1. Reaction scheme of 10% tri-antennary-galactose-bearing reference CDs (conjugate 1; Gal10CDs) or 12% tri-antennary-galactose-bearing reference CDs (conjugate 2; Gal12CDs). Reagents and conditions: (a) AIBN, dioxane, 75 °C, 9 h, 64%. (b) i. Tf_2O, DCM, py, -25 °C, 30 min. ii. NaN_3, DMF, RT, 17 h, 87%. (c) NaOMe, MeOH, RT, 3h, Amberlite 120 (H^+), 99%. (d) TPP, 1:3 water-dioxane; then NH_4OH, RT, 24 h, 99%. (e) acetone-water, $NaHCO_3$, RT, 20 h, 99%. (f) DMF, Et_3N, RT, 4 days, 75%. (g) DMF, Et_3N, RT, 4 days, 78%.

2,2,2-Tris[5-(2,3,4,6-tetra-O-acetyl-β-D-galactopyranosylthio)-2-oxapentyl]ethanol (7). A solution of the tri-*O*-allylated pentaerythritol derivative **5**[37] (745 mg, 2.91 mmol), 2,3,4,6-tetra-*O*-acetyl-1-thio-β-D-galactopyranose[36] (**6**, 3.18 g, 8.74 mmol) and azobisisobutyronitrile (AIBN) (477 mg, 2.91 mmol) in dry and degassed dioxane (21 ml), was stirred at 75 °C under Ar atmosphere for 3 h. Then, a solution of **6** (3.18 g) and AIBN (477 mg) in dioxane (21 ml) was added and the reaction mixture was stirred at 75 °C for 6 h (TLC monitoring). The solvent was removed under reduced pressure and the residue was purified by column chromatography (1:1 EtOAc-petroleum ether). Yield: 2.48 g (64%); R_f = 0.22 (2:1 EtOAc-petroleum ether); $[\alpha]_D$ = -8.5 (c 1.0 in $CHCl_3$); ^{1}H NMR (500 MHz, $CDCl_3$) δ 5.44 (d, 3 H, $J_{3,4}$ = 3.0 Hz, H-4), 5.23 (t, 3 H, $J_{1,2} = J_{2,3}$ = 10.0 Hz, H-2), 5.07 (dd, 3 H, H-3), 4.51 (d, 3 H, H-1), 4.17 (dd, 3 H, $J_{6a,6b}$ = 11.3 Hz, $J_{5,6a}$ = 6.6 Hz, H-6a), 4.11 (dd, 3 H, $J_{5,6b}$ = 6.9 Hz, H-6b), 3.96 (t, 3 H, H-5), 3.67 (bs, 2 H, CH_2OH), 3.49 (t, 6 H, $^3J_{H,H}$ = 6.1 Hz, H-3_{Pent}), 3.43 (s, 6 H, H-1_{Pent}), 2.81, 2.74 (2 dt, 6 H, $^2J_{H,H}$ = 13.0 Hz, $^3J_{H,H}$ = 7.2 Hz, H-5_{Pent}), 2.17-1.99 (4 s, 36 H, *Me*CO), 1.93-1.85 (m, 6 H, H-4_{Pent}); ^{13}C NMR (125.7 MHz, $CDCl_3$) δ 170.4-169.6 (Me*CO*), 84.4 (C-1), 74.4 (C-5), 71.9 (C-3), 71.2 (C-1_{Pent}), 69.7 (C-3_{Pent}), 67.2 (C-2, C-4), 65.4 (*C*H_2OH), 61.4 (C-6), 45.0 (Cq), 29.9 (C-4_{Pent}), 27.2 (C-5_{Pent}), 21.0-20.6 (*Me*CO). ESIMS: *m/z* 1371.2 [M + Na]$^+$. Anal. Calcd for $C_{56}H_{84}O_{31}S_3$: C 49.84, H 6.27, S 7.13. Found: C 49.89, H 6.12, S 6.89 (**Scheme 1**)(**Fig. 3_1**).

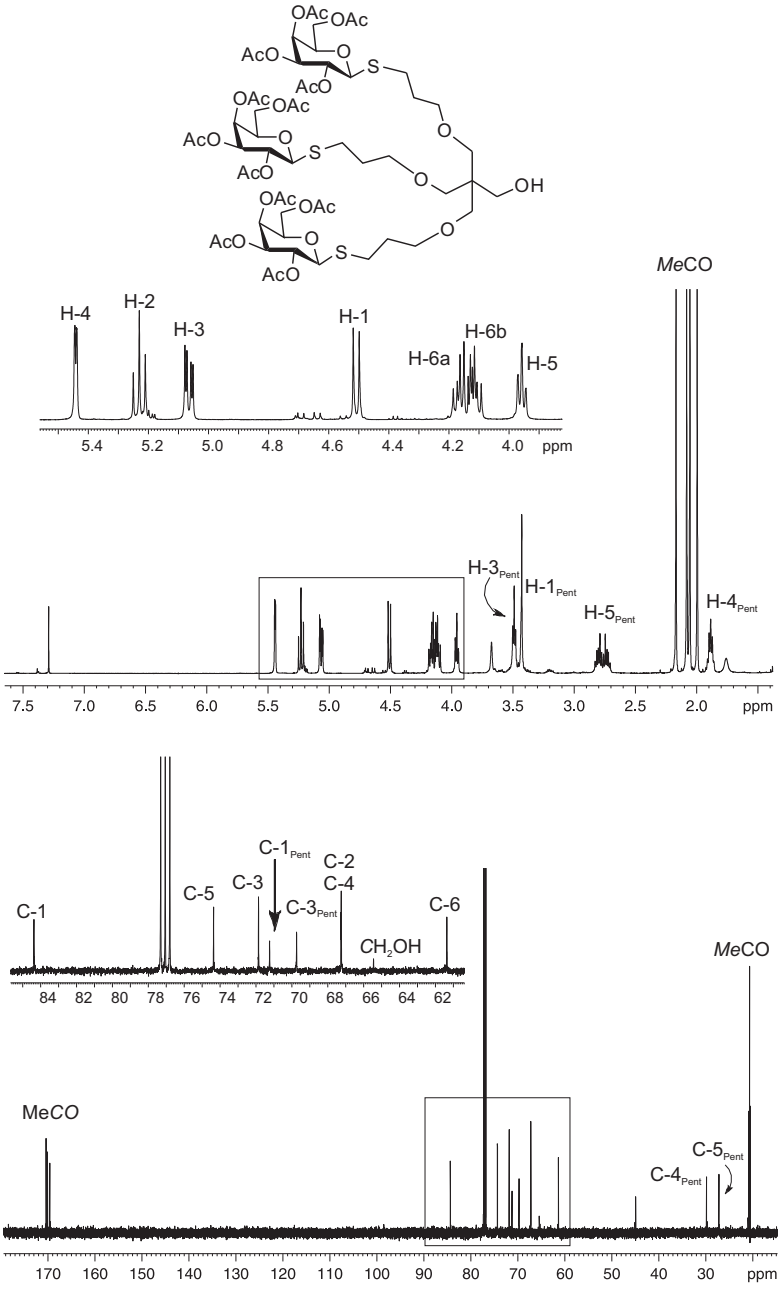

Figure 3_1. ^{1}H and ^{13}C NMR spectra (500 MHz and 125.7 MHz, $CDCl_3$) of **7.**

2,2,2-Tris[5-(2,3,4,6-tetra-O-acetyl-β-D-galactopyranosylthio)-2-oxapentyl]ethyl azide (8). To a solution of **7** (204 mg, 0.15 mmol) in dry dichloromethane (DCM) (1 ml), pyridine (60 µl) and Tf_2O (30 µl, 0.19 mmol) were added at -25 °C under Ar atmosphere. The solution was stirred for 15 min at -25 °C (TLC monitoring), diluted with CH_2Cl_2, washed with cold aq saturated $NaHCO_3$, dried (Na_2SO_4) and concentrated. The residue was dissolved in DMF (1 ml) and NaN_3 (30 mg, 0.45 mmol) was added. The mixture was stirred at RT for 17 h and concentrated. The resulting residue was dissolved in DCM, washed with water, dried (Na_2SO_4), concentrated and purified by column chromatography (3:2 EtOAc-petroleum ether). Yield: 179 mg (87%); R_f = 0.54 (2:1 EtOAc-petroleum ether); $[\alpha]_D$ = -12.4 (c 1.6 in $CHCl_3$); ^{1}H NMR (500 MHz, $CDCl_3$) δ 5.41 (d, 3 H, $J_{3,4}$ = 3.0 Hz, H-4), 5.19 (t, 3 H, $J_{1,2} = J_{2,3}$ = 10.0 Hz, H-2), 5.03 (dd, 3 H, H-3), 4.48 (d, 3 H, H-1), 4.06-4.17 (m, 6 H, H-6), 3.92 (t, 3 H, $J_{5,6}$ = 6.5 Hz, H-5), 3.44 (t, 6 H, $^3J_{H,H}$ = 6.0 Hz, H-3_{Pent}), 3.31 (s, 2 H, CH_2N_3), 3.30 (s, 6 H, H-1_{Pent}), 2.77, 2.70 (2 dt, 6 H, $^2J_{H,H}$ = 12.5 Hz, $^3J_{H,H}$ = 5.5 Hz, H-5_{Pent}), 2.13-1.96 (4 s, 36 H, *Me*CO), 1.90-1.80 (m, 6 H, H-4_{Pent}); ^{13}C NMR (125.7 MHz, $CDCl_3$) δ 170.3-169.5 (Me*CO*), 84.4 (C-1), 74.3 (C-5), 71.8 (C-3), 69.6 (C-1_{Pent}, C-3_{Pent}), 67.5 (C-2), 67.2 (C-4), 61.3 (C-6), 52.0 (*C*H_2N_3), 45.4 (Cq), 29.9 (C-4_{Pent}), 27.3 (C-5_{Pent}), 21.0-20.5 (*Me*CO). ESIMS: *m/z* 1396.4 $[M + Na]^+$. Anal. Calcd for $C_{56}H_{83}O_{30}S_3N_3$: C 48.94, H 6.09, N 3.06, S 7.00. Found: C 48.85, H 5.92, N 2.86, S 6.81 (**Scheme 1**)(**Fig. 3_2**).

CAUTION! Sodium azide (NaN_3) is extremely toxic and potentially explosive under certain conditions. The use of dichloromethane as reaction medium may result in the formation of highly explosive unstable diazidomethane. Even though the risk is mitigated in the presence of water, dichloromethane should be replaced for the liquid-liquid extraction by a non-chlorinated solvent such as ethyl acetate (EtOAc) if the synthesis is scaled-up over 1 g.

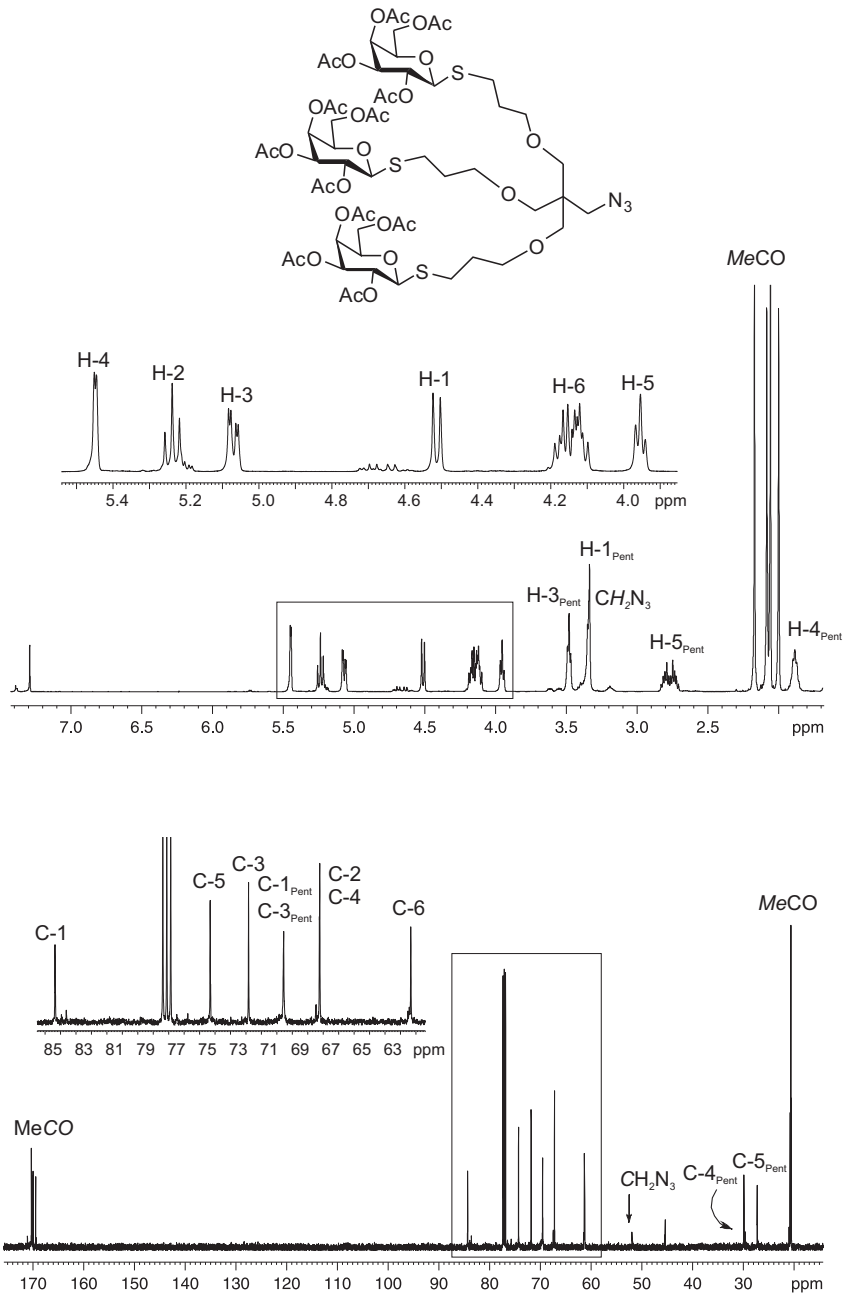

Figure 3_2. ^{1}H and ^{13}C NMR spectra (500 MHz and 125.7 MHz, $CDCl_3$) of **8.**

Tris[5-β-D-galactopyranosylthio)-2-oxapentyl]-ethylazide (9). A solution of **8** (50 mg, 36.4 µmol) in MeOH (5 ml) was treated with MeONa (2.4 mg, 43.7 µmol, 0.1 equiv) at RT for 3 h. Then, the mixture was neutralized with acid resin (Amberlite IR-120 H^+), filtered and concentrated. Yield: 31.4 mg (99%). R_f = 0.7 (MeOH). $[\alpha]_D$ = -24.8 (c 0.99, MeOH), IR (NaCl): υ_{max} = 2106 cm^{-1}; ^{1}H NMR (500 MHz, CD_3OD, 313 K): δ 4.34 (d, 3 H, $J_{1,2}$ = 9.6 Hz, H-1), 3.92 (d, 3 H, $J_{3,4}$ = 3.0 Hz, H-4), 3.77 (dd, 3 H, $J_{5,6a}$ = 6.7 Hz, $J_{6a,6b}$ = 11.4 Hz, H-6a), 3.72 (dd, 3 H, $J_{5,6b}$ = 5.5 Hz, H-6b), 3.58 (t, 3 H, $J_{2,3}$ = 9.6 Hz, H-2), 3.56 (m, 9 H, H-5, H-3_{Pent}), 3.50 (dd, 3 H, H-3), 3.39 (m, 8 H, CH_2N_3, H-1_{Pent}), 2.85, 2.79 (2 dt, 6 H, $^2J_{H,H}$ = 13.0 Hz, $^3J_{H,H}$ = 7.3 Hz, H-5_{Pent}), 1.92 (m, 6 H, $^3J_{H,H}$ = 6.6 Hz, H-4_{Pent}); ^{13}C NMR (125.7 MHz, CD_3OD, 313 K): δ 87.9 (C-1), 80.6 (C-2), 76.3 (C-3), 71.6 (C-3_{Pent}), 71.0 (C-5), 70.7 (C-1_{Pent}), 70.6 (C-4), 62.7 (C-6), 53.3 (CH_2N_3), 46.7 (Cq), 31.4 (C-4_{Pent}), 28.0 (C-5_{Pent}). ESIMS: *m/z* 891.8 $[M + Na]^+$, 867.7 $[M - H]^-$, 903.6 $[M + Cl]^-$. Anal. Calcd for $C_{32}H_{59}N_3O_{18}S_3$: C, 44.18; H, 6.84; N, 4.83; S, 11.06. Found: C, 43.81; H, 6.69; N, 4.60; S, 10.83 (**Scheme 1**)(**Fig. 3_3**).

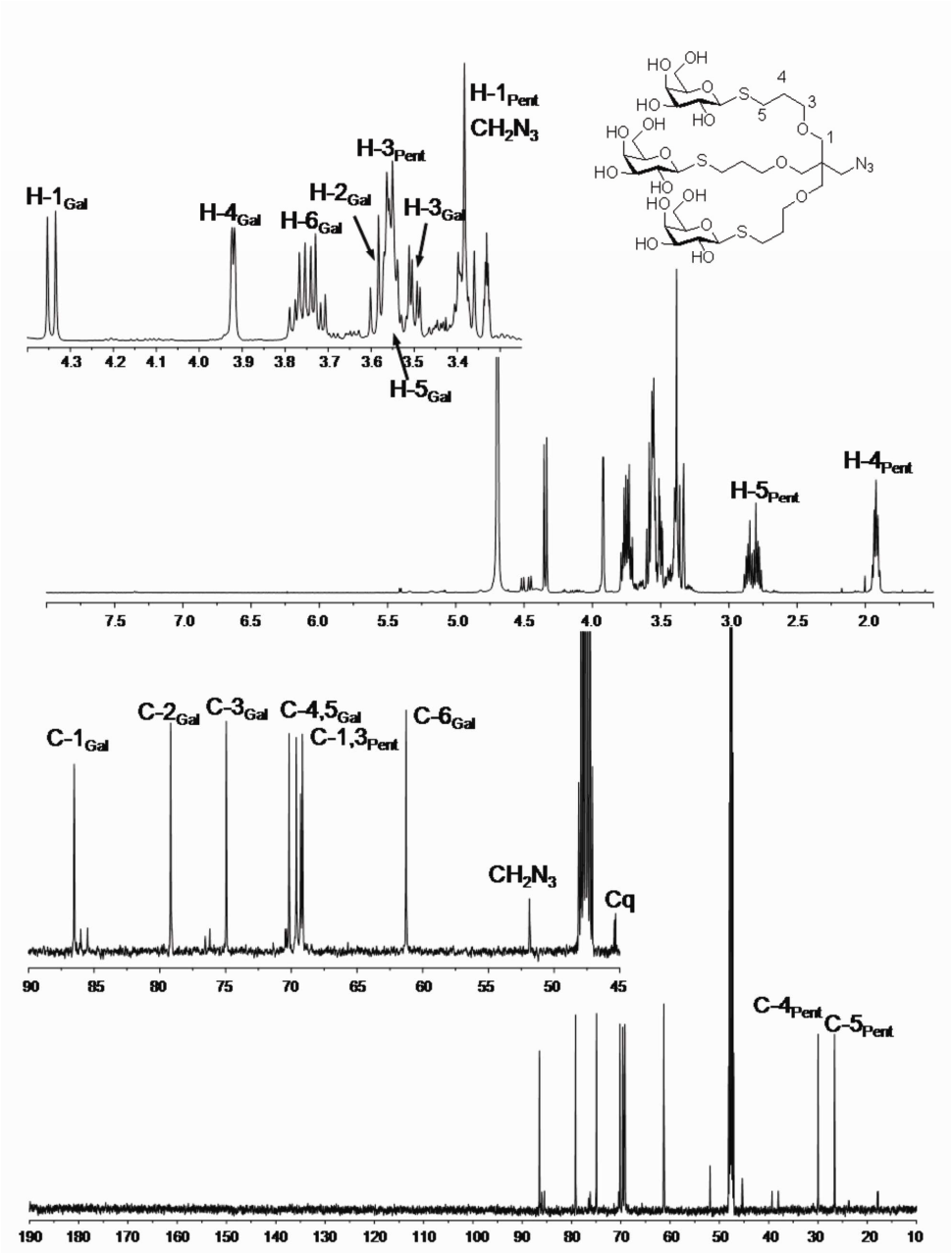

Figure 3_3. ^{1}H and ^{13}C NMR spectra (500 MHz and 125.7 MHz, CD_3OD, 313K) of **9.**

Tris[5-β-D-galactopyranosylthio)-2-oxapentyl]ethylamine (10). To a solution of **9** (60 mg, 69 µmol) and TPP (63 mg, 0.24 mmol, 3.5 eq.) in a 1:3 mixture of water:dioxane (4 ml) was added a solution of 25% NH_4OH in water (1 ml) and the mixture was stirred at RT for 24 h. Solvents were removed under reduced pressure and the residue was washed with DCM (10 ml) and water (10 ml). The aqueous layer was washed twice with DCM (10 ml) and once with AcOEt (10 ml) and finally freeze dried. Yield: 58.1 mg (99%). R_f = 0.1 (MeOH). $[\alpha]_D$ = -15.2 (c 1.05, H_2O); ^{1}H NMR (500 MHz, D_2O, 313 K): δ 4.58 (d, 3 H, $J_{1,2}$ = 9.7 Hz, H-1), 4.11 (d, 3 H, $J_{3,4}$ = 2.7 Hz, H-4), 3.85 (m, 12 H, H-6a, H-6b, H-1_{Pent}), 3.77 (dd, 3 H, $J_{2,3}$ = 8.7 Hz, H-3), 3.70 (m, 12 H, H-2, H-5, H-3_{Pent}), 3.58 (s, 2 H, C$H_2$$NH_2$), 2.95 (m, 6 H, H-$5_{Pent}$), 2.06 (m, 6 H, $^3J_{H,H}$ = 6.6 Hz, H-4_{Pent}); ^{13}C NMR (125.7 MHz, D_2O, 313 K): δ 86.2 (C-1), 79.1 (C-2), 74.2 (C-3), 70.5, 70.3 (C-$1,3_{Pent}$), 69.9 (C-5), 69.1 (C-4), 61.3 (C-6), 43.9 (CH_2NH_2), 42.4 (Cq), 29.4 (C-4_{Pent}), 27.0 (C-5_{Pent}). ESIMS: *m/z* 843.9 $[M + H]^+$, 865.8 $[M + Na]^+$, 841.7 $[M - H]^-$, 877.6 $[M + Cl]^-$. Anal. Calcd for $C_{32}H_{61}NO_{18}S_3$: C, 45.54; H, 7.28; N, 1.66. Found: C, 45.15; H, 6.978; N, 1.31 (**Scheme 1**)(**Fig. 3_4**).

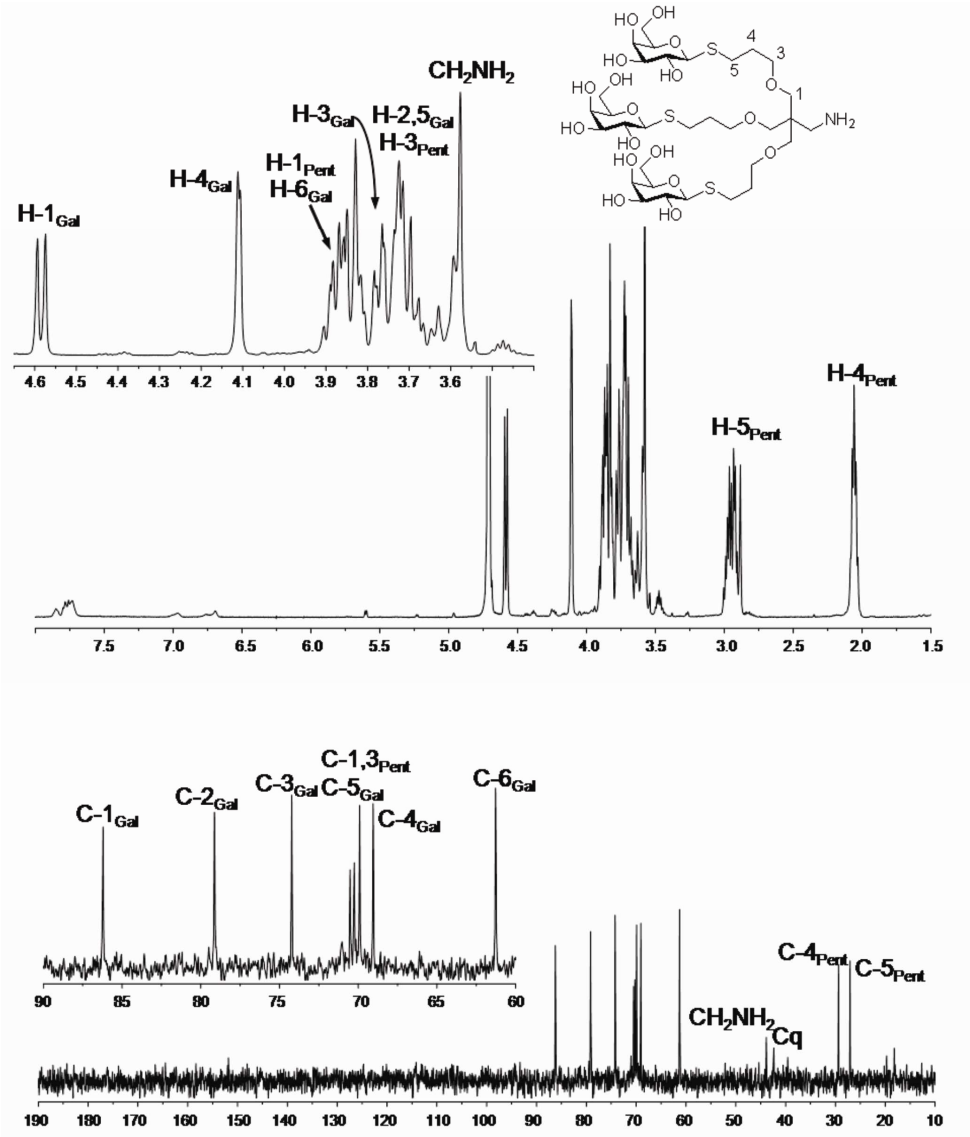

Figure 3_4. ^{1}H and ^{13}C NMR spectra (500 MHz and 125.7 MHz, D_2O, 313K) of **10.**

N-(6-isothiocyanate)hexyl-N'-2,2,2-tris[5-β-D-galactopyranosylthio-2-oxapentyl]ethylthiourea (12). To a solution of 1,6-hexamethylenediisothiocyanate[38] (**11**, 36 mg, 178 μmol, 5 equiv) in acetone (3 ml), a solution of **10** (30 mg, 35 μmol) and saturated aqueous $NaHCO_3$ (35 μl) in water (2 ml) was added dropwise under vigorously stirring. The mixture was stirred at RT during 20 h. Then, solvents were eliminated under vacuum and the residue was purified by column chromatography (5:1 MeCN-H_2O). Yield: 37 mg (99%). R_f = 0.81 (MeCN-H_2O 3:1). $[\alpha]_D$ = -12.8 (c 0.78, MeOH); IR (NaCl): υ_{max} = 2110 cm^{-1}, ^1H NMR (500 MHz, D_2O, 298 K): δ 4.58 (d, 3 H, $J_{1,2}$ = 9.5 Hz, H-1), 4.10 (d, 3 H, $J_{3,4}$ = 3.2 Hz, H-4), 3.84 (m, 12 H, H-6a, H-6b, H-1_{Pent}), 3.77 (dd, 3 H, $J_{2,3}$ = 9.5 Hz, H-3), 3.74 (t, 2 H, $^3J_{H,H}$ = 6.8 Hz, CH_2NCS), 3.71 (m, 9 H, H-5, H-3_{Pent}), 3.69 (t, 3 H, H-2), 3.59 (m, 4 H, CH_2NH), 2.96 (2 dt, 6 H, $^2J_{H,H}$ = 13.7 Hz, $^3J_{H,H}$ = 7.0 Hz, H-5_{Pent}), 2.06 (m, 6 H, $^3J_{H,H}$ = 6.5 Hz, H-4_{Pent}), 1.86, 1.75, 1.59, 1.53 (4m, 8 H, $^3J_{H,H}$ = 6.8 Hz, $CH_2CH_2CH_2$); ^{13}C NMR (125.7 MHz, D_2O, 298 K): δ 181.3 (CS), 127.4 (NCS), 86.3 (C-1), 79.0 (C-2), 74.2 (C-3), 70.4, 70.0 (C-$1,3_{Pent}$, C-5), 69.0 (C-4), 61.2 (C-6), 45.1 (CH_2NCS), 44.3 (Cq, CH_2NH), 29.6 (C-4_{Pent}), 27.2 (C-5_{Pent}), 29.1, 28.4, 28.8, 27.5 ($CH_2CH_2CH_2$). ESIMS: *m/z* 1065.8 $[M + Na]^+$, 1082.8 $[M + K]^+$, 1041.7 $[M - H]^-$, 1077.6 $[M + Cl]^-$. Anal. Calcd for $C_{40}H_{73}N_3O_{18}S_5$: C, 46.00; H, 7.05; N, 4.02; S, 15.02. Found: C, 45.87; H, 6.804; N, 3.93; S, 15.02 (**Scheme 1**)(**Fig. 3_5**).

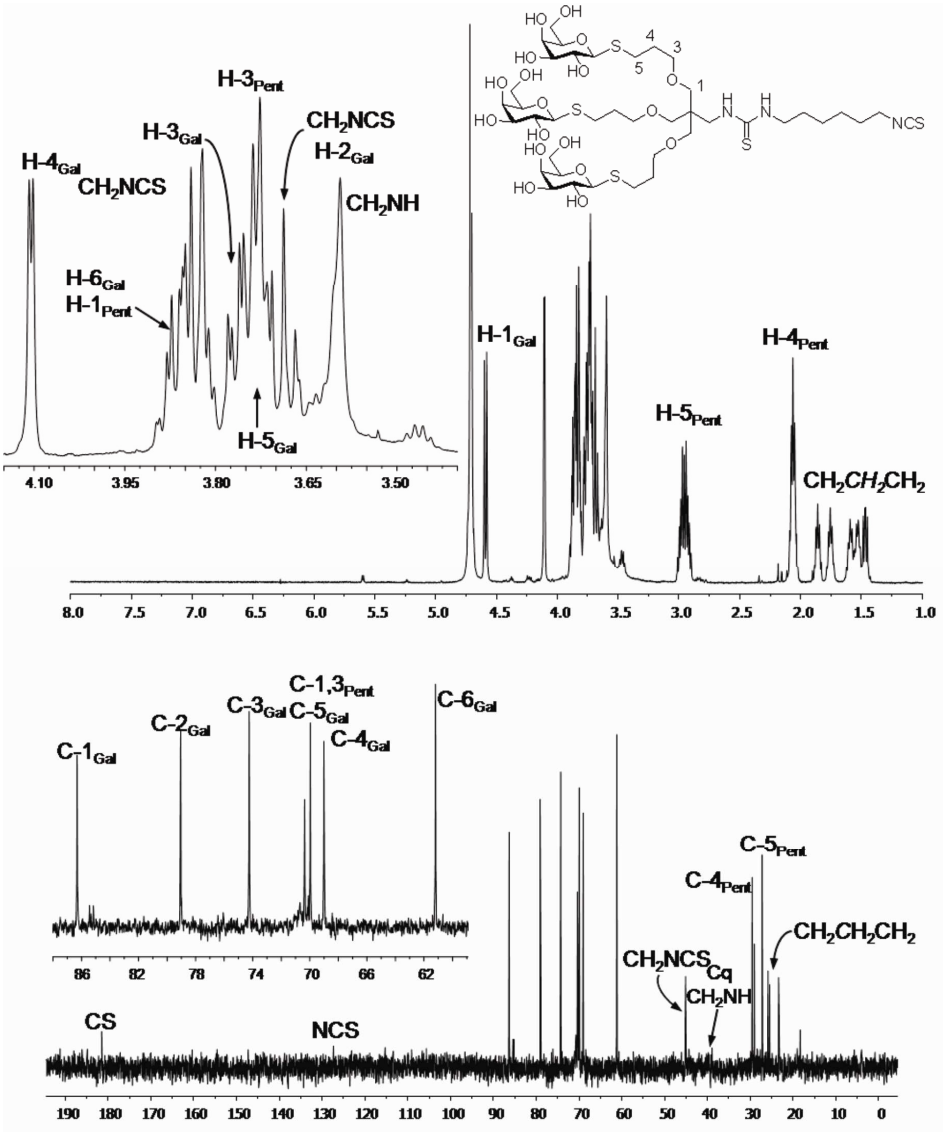

Figure 3_5. ^{1}H and ^{13}C NMR spectra (500 MHz and 125.7 MHz, D_2O) of **12.**

O-Methyl-O'-[3-(6-isothiocyanatohexyl)thioureidoethyl]polyethylene glycol 5000 (14). To a solution of *O*-methyl-*O*'-(2-aminoethyl) polyethylene glycol 5000 hydrochloride (**13,** 50 mg, 10 µmol) in freshly distilled DCM (2.5 ml), Et_3N (5 µl, 40 µmol, 4 equiv) was added. Then, a solution of 1,6-hexamethylenediisothiocyanate (**11**, 40 mg, 0.2 mmol, 20 equiv) in DCM (2.5 ml) was added and the reaction mixture was stirred for 16 h at RT. The solvent was evaporated down to 1 ml, and the crude was precipitated by addition of Et_2O (20 ml). The solid was filtered and washed with Et_2O until complete removal of unreacted 1,6-diisothiocyanatohexane (TLC). Yield: 42 mg (84%). R_f = 0.60 (5:1 DCM-MeOH). IR (ATR): υ_{max} = 2881, 1341, 1103, 960, 842 cm^{-1}; UV (CH_2Cl_2): 248 nm (ε_{mM}3.7). ^1H NMR (500 MHz, $CDCl_3$): δ 3.76-3.45 (m, 506 H, CH_2OCH_2, S=CNHCH_2, CH_2NCS, CH_2OCH_3), 3.35 (s, 3 H, OCH_3), 1.68 (m, 1 H, $^3J_{H,H}$ = 6.6 Hz, CH_2), 1.58 (m, 1 H, $^3J_{H,H}$ = 7.5 Hz, CH_2), 1.45, 1.36 (m, 2 H, 2 x CH_2). ESIMS: *m/z* 2693.1 ± 22 $[M \pm 44\ n + 2\ Na]^{2+}$ (**Scheme 2**)(**Fig. 3_6**).

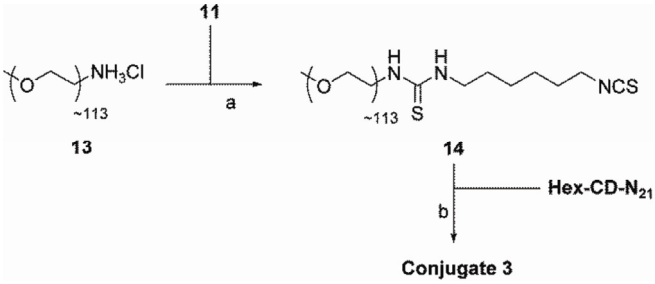

Scheme 2. Reaction scheme of 13% thio-PEG_{5000}-bearing reference CDs (conjugate 3; PEGCDs). Reagents and conditions: (a) DCM, Et_3N, RT, 16h, 84%. (b) DMF, Et_3N, RT, 6 days, 86%.

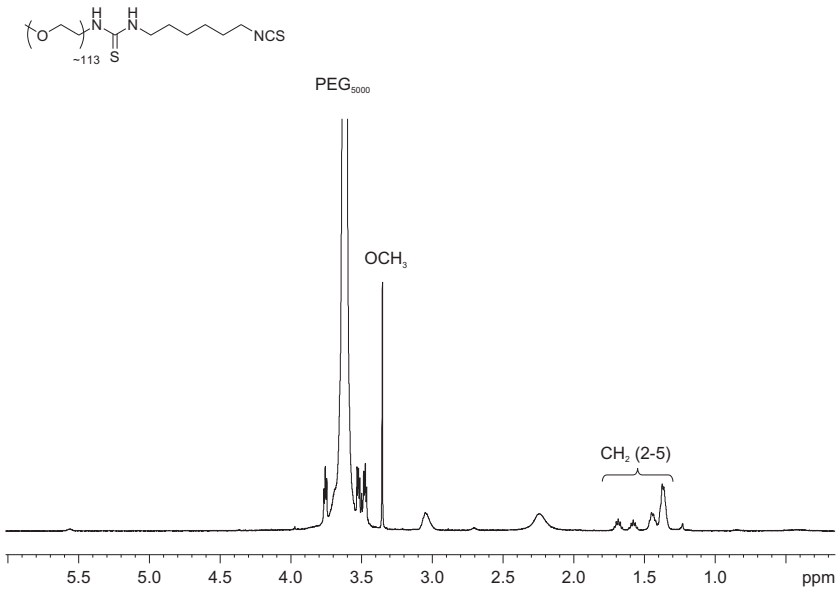

Figure 3_6. ^{1}H NMR spectra (500 MHz, $CDCl_3$) of **14**.

2,2,2-Tris[5-(2,3,4,6-tetra-O-acetyl-β-D-galactopyranosylthio)-2-oxapentyl]ethyl isothiocyanate (15). To a solution of the corresponding azide derivative **8** (892 mg, 0.65 mmol) in dioxane (30 ml), TPP (190 mg, 0.71 mmol) and CS_2 (0.4 ml, 6.5 mmol) were added. The reaction mixture was stirred at RT for 16 h under Ar atmosphere, then concentrated and the residue was purified by column chromatography using 1:1 EtOAc-petroleum ether as an eluent. Yield: 618 mg (68%); R_f = 0.54 (2:1 EtOAc-petroleum ether); $[\alpha]_D$ = -10.7 (c 1.0 in $CHCl_3$); ^{1}H NMR (400 MHz, $CDCl_3$) δ 5.43 (d, 3 H, $J_{3,4}$ = 3.0 Hz, H-4), 5.21 (t, 3 H, $J_{1,2} = J_{2,3}$ = 10.0 Hz, H-2), 5.05 (dd, 3 H, H-3), 4.50 (d, 3 H, H-1), 4.15 (dd, 3 H, $J_{6a,6b}$ = 12.0 Hz, $J_{5,6a}$ = 6.8 Hz, H-6a), 4.09 (dd, 3 H, $J_{5,6b}$ = 6.8 Hz, H-6b), 3.94 (t, 3 H, H-5), 3.57 (s, 2 H, CH_2NCS), 3.47 (t, 6 H, $^{3}J_{H,H}$ = 6.0 Hz, H-3_{Pent}), 3.35 (bs, 6 H, H-1_{Pent}), 2.79, 2.71 (2 dt, 6 H, $^{2}J_{H,H}$ = 12.8 Hz, $^{3}J_{H,H}$ = 7.2 Hz, H-5_{Pent}), 2.15-1.98 (4 s, 36 H, *Me*CO), 1.91-1.83 (6 H, m, H-4_{Pent}); ^{13}C NMR (125.7 MHz, $CDCl_3$) δ 170.3-169.5 (Me*CO*), 84.4 (C-1), 74.3 (C-5), 71.8 (C-3), 69.7 (C-3_{Pent}), 69.5 (C-1_{Pent}), 67.2 (C-2, C-4), 61.3 (C-6), 45.9 (CH_2NCS), 45.6 (Cq), 29.8 (C-4_{Pent}), 27.3 (C-5_{Pent}), 21.0-

20.6 (*Me*CO). ESIMS: *m/z* 1412.3 $[M + Na]^+$. Anal. Calcd for $C_{57}H_{83}O_{30}S_4N$: C 49.23, H 6.02, N 1.01, S 9.22. Found: C 49.24, H 6.03, N 1.15, S 9.22 (**Scheme 3**)(**Fig. 3_7**).

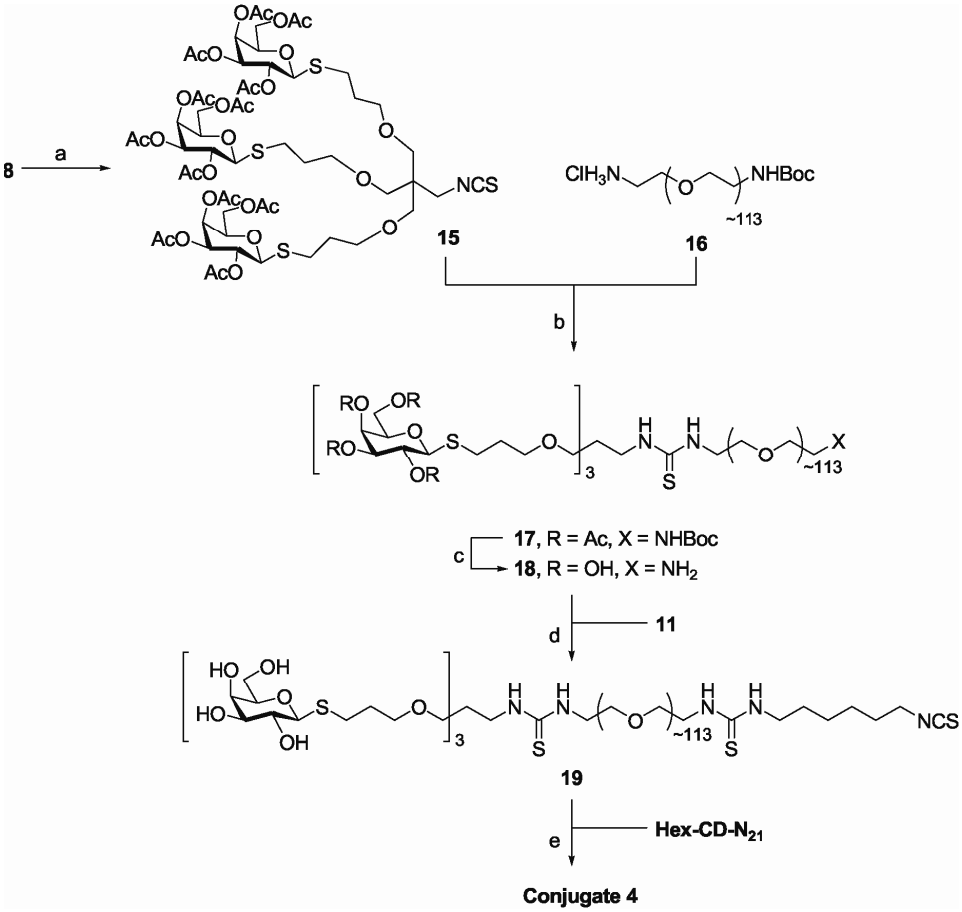

Scheme 3. Reaction scheme of 10% thio-PEG_{5000}-tri-antennary-galactose-bearing reference CDs (conjugate 4; GalPEGCDs). Reagents and conditions: (a) CS_2, TPP, dioxane, RT, 16 h, 68%. (b) $NaHCO_3$, acetone-water, RT, overnight, 63%. (c) i. MeONa, MeOH, RT, 3h. ii. H_2O:TFA, RT, 1 h, 99%. (d) $NaHCO_3$, water-acetone, RT, 16 h, 90%. (e) DMF, Et_3N, 40 °C, 2 days, 70%.

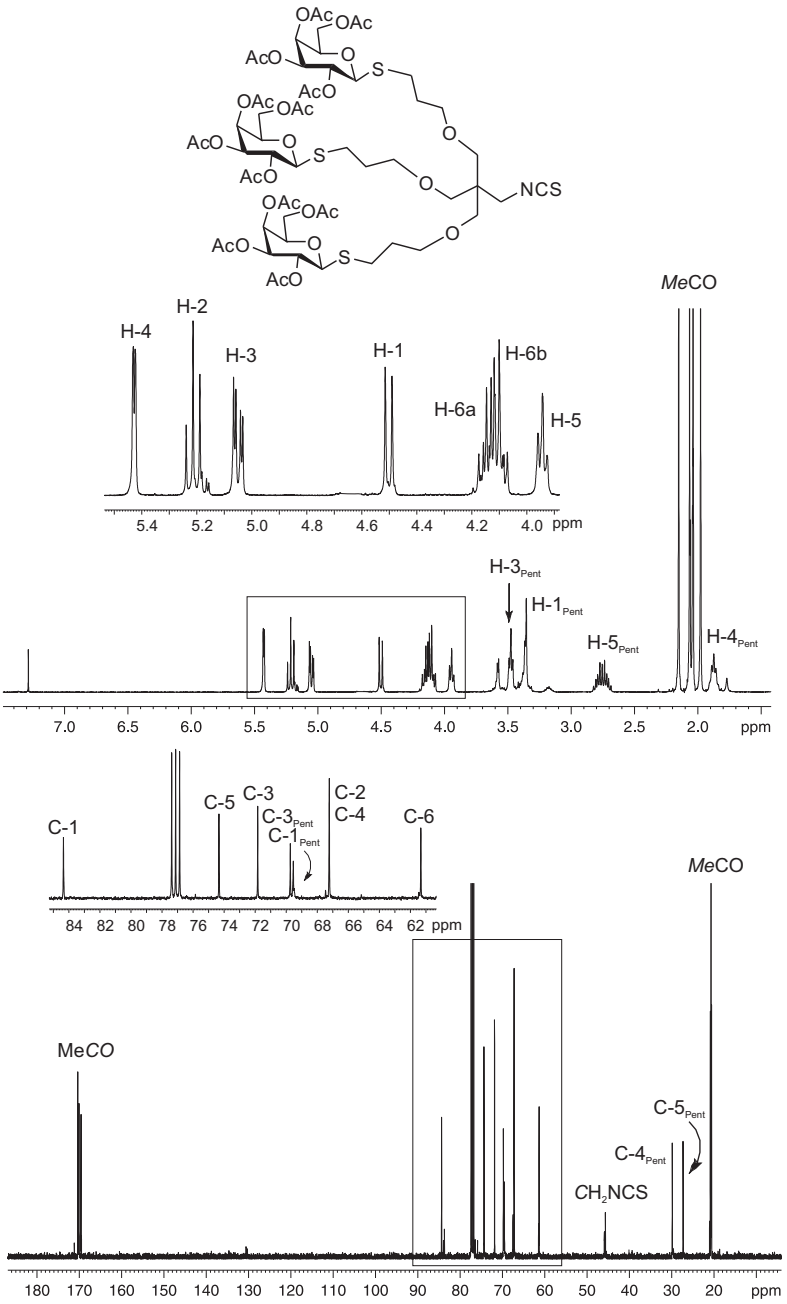

Figure 3_7. ^{1}H and ^{13}C NMR spectra (400 MHz and 125.7 MHz, $CDCl_3$) of **15.**

O-[2-(2-(Tris(5-(2,3,4,6-tetra-O-acetyl-β-D-galactopyranosylthio))-2-oxapentyl)ethylthioureido)ethyl]-O'-2-[(N-(tert-butoxycarbonyl)amino)ethyl] polyethylene glycol 5000 (17). To a solution of *O*-(2-aminoethyl)-*O*'-[2-(Boc-amino)ethyl] PEG_{5000} hydrochloride (**16**, 30 mg, 6 µmol) and $NaHCO_3$ (1 mg, 12 µmol, 2 equiv) in water (80 µl), a solution of **15** (41 mg, 30 µmol, 5 equiv) in acetone (5 ml) was added. The reaction mixture was stirred overnight at RT. The acetone was evaporated and the solution was diluted with water (1 ml) and extracted with CH_2Cl_2 (6 x 5 ml). The organic layer was dried, filtered and concentrated up to 1 ml. Then the crude was precipitated by addition of Et_2O (15 ml). The solid was filtered and washed with Et_2O until removal of unreacted **15** (TLC). Yield: 24.1 mg (63%). R_f = 0.65 (5:1 DCM-MeOH). $[\alpha]_D$ = -1.6 (c 0.82, DCM). IR (ATR): υ_{max} = 2882, 1712, 1343, 1240, 1109 cm^{-1}. UV (CH_2Cl_2): 246 nm (ε_{mM}7.8); ^{1}H NMR (500 MHz, CD_3OD): δ 5.46 (bs, 1 H, H-4), 5.18 (m, 1 H, H-2), 4.95 (t, 1 H, $J_{2,3} = J_{3,4}$ = 10.0 Hz, H-3), 4.78 (d, 1 H, $J_{1,2}$ = 9.8 Hz, H-1), 4.30 (dd, 1 H, $J_{6a,6b}$ = 11.5 Hz, $J_{5,6a}$ = 7.5 Hz, H-6a), 4.19 (dd, 1 H, $J_{5,6a}$ = 4.6 Hz, H-6b), 3.80-3.50 (m, 554 H, C*H*$_2$NHC=S, C*H*$_2$OC*H*$_2$, H-5, H-3$_{Pent}$, H-5$_{Pent}$), 3.45 (s, 2 H, H-1$_{Pent}$), 3.24 (t, 2 H, $^3J_{H,H}$ = 5.3 Hz, C*H*$_2$NHBoc), 2.84 (2 m, 2 H, H-5$_{Pent}$), 2.18, 2 x 2.09, 1.98 (4 s, 12 H, MeCO), 1.93 (m, 2 H, H-4$_{Pent}$), 1.48 (s, 9 H, CMe_3). ESIMS: *m/z* 3197.5 ± 22 [M ± 44 x n + 2 K]$^{2+}$ (**Scheme 3**)(**Fig. 3_8**).

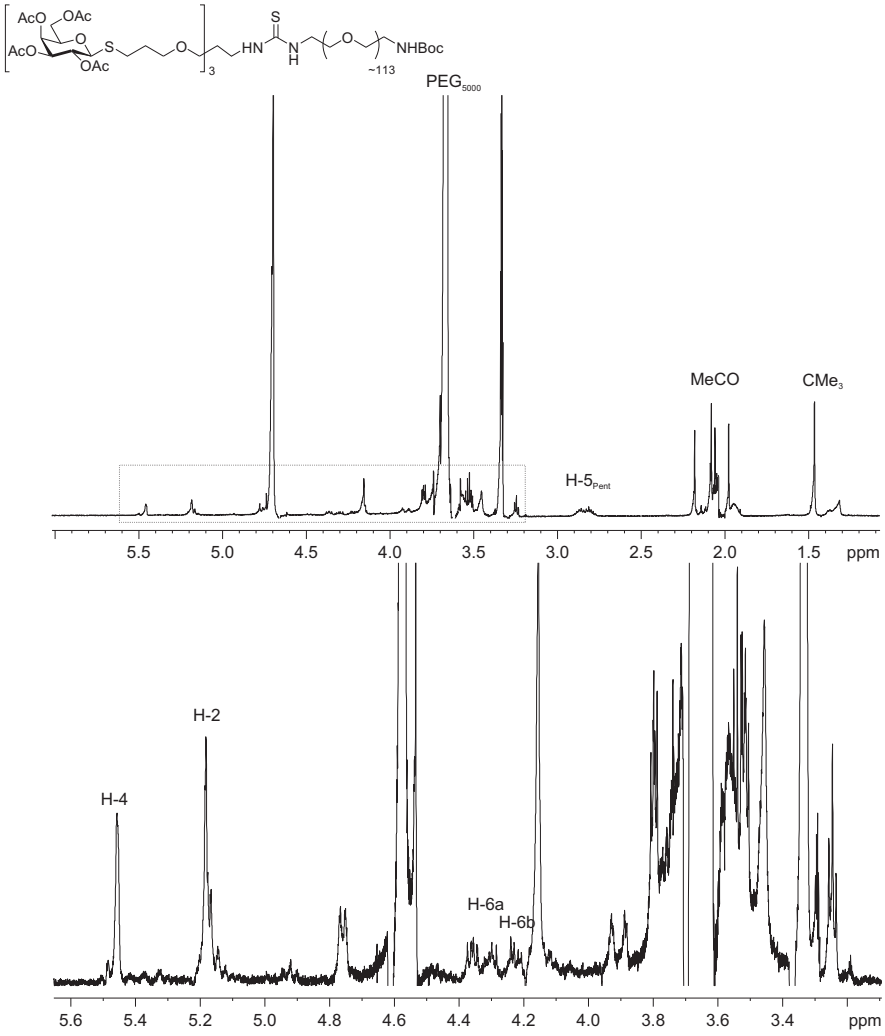

Figure 3_8. ^{1}H NMR spectra (500 MHz, CD_3OD) of **17**.

O-[2-(2-(Tris(5-β-D-galactopyranosylthio)-2-oxapentyl)ethylthioureido) ethyl]-O'-2-(aminoethyl)polyethylene glycol 5000 (18). To a solution of **17** (12.3 mg, 2 µmol) in MeOH (1 ml), MeONa 1 M (2.3 µl) was added and the reaction mixture was stirred for 3 h at RT. The solution was neutralized (Amberlite IRA-120), filtered and concentrated. The residue was treated with TFA-H_2O (1:1, 0.4 ml) for 1 h, the solvent was coevaporated several times with water. Yield: 12 mg (99%). R_f = 0.59 (5:1 DCM-MeOH). $[\alpha]_D$ = -1.3 (c 0.66, MeOH). IR (ATR): υ_{max} = 3373, 2881, 1465, 1342, 1104 cm^{-1}. UV (CH_2Cl_2): 244 nm (ε_{mM}7.6). ^1H NMR (500 MHz, CD_3OD): δ 4.36 (d, 2 H, $J_{1,2}$ = 8.7 Hz, H-1), 3.92 (d, 2 H, $J_{3,4}$ = 8.6 Hz, H-4), 3.80-3.40 (m, 628 H, $CH_2CH_2NH_2$, CH_2OCH_2, S=CNHCH_2, H-5, H-6a, H-6b, H-1_{Pent}, H-3_{Pent}), 3.58 (t, 2 H, $J_{2,3}$ = 9.7 Hz, H-2), 3.50 (dd, 2 H, H-3), 3.23 (t, 2 H, $^3J_{H,H}$ = 4.5 Hz, CH_2NH_2), 2.84 (m, 4 H, H-5_{Pent}), 1.93 (m, 4 H, $^3J_{H,H}$ = 6.3 Hz, H-4_{Pent}). ESIMS: *m/z* 2759.4 ± 22 $[M \pm 44 \times n + Na + K]^{2+}$ (**Scheme 3**)(**Fig. 3_9**).

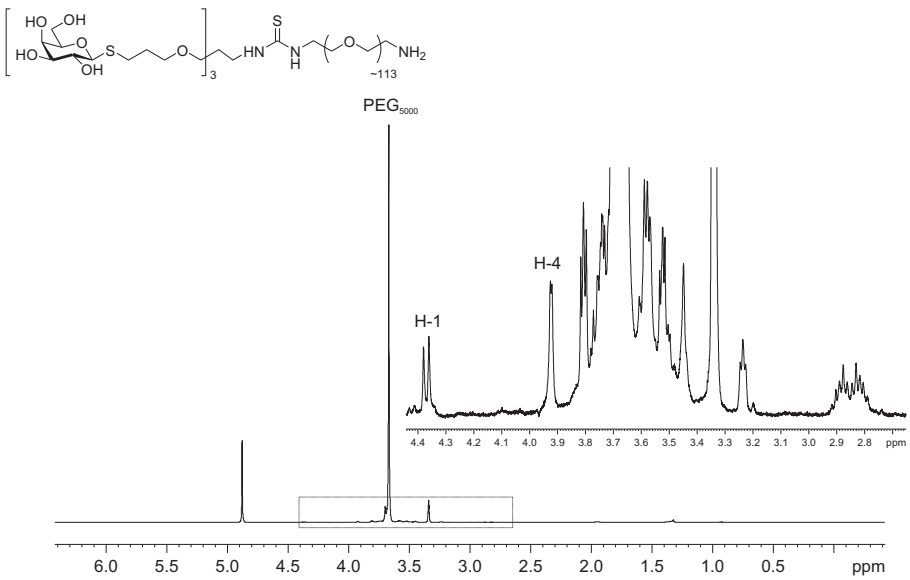

Figure 3_9. ^1H NMR spectra (500 MHz, CD_3CD) of **18**.

O-[2-(Tris(5-ß-D-galactopyranosylthio)-2-oxapentyl)ethylthioureido]ethyl]-O'-2-(3-(6-isothiocyanatohexyl)thioureidoethyl)polyethylene glycol 5000 (19). To a solution of **18** (39.5 mg, 7 µmol) and $NaHCO_3$ (1 mg, 13 µmol, 2 equiv) in water (500 µl), a solution of 1,6-hexamethylenediisothiocyanate (**11**, 12 mg, 34 µmol, 5 eq) in acetone (1 ml) was added and the reaction mixture was stirred overnight at RT. The acetone was evaporated and the solution was diluted in water (1 ml) and extracted with DCM (6 x 5 ml). The solvent was evaporated to 1 ml and the crude was precipitated by addition of Et_2O (30 ml). The solid was filtered and washed with Et_2O until removal of unreacted 1,6-hexamethylenediisothiocyanate (TLC). Yield: 35 mg (90%). R_f = 0.59 (5:1 DCM-MeOH). $[\alpha]_D$ = -0.4 (c 0.8, DMSO). IR (ATR): υ_{max} = 3333, 2881, 1467, 1342, 1101, 961, 842 cm^{-1}. ^1H NMR (500 MHz, 5:1 $CDCl_3$-CD_3OD): δ 4.18 (d, 3 H, $J_{1,2}$ = 10.0 Hz, H-1), 3.82 (d, 3 H, $J_{3,4}$ = 5.3 Hz, H-4), 3.70-3.00 (m, 568 H, H-1_{Pent}, CH_2OCH_2, H-5, H-6a, H-6b, H-3_{Pent}, H-2, H-3, 4 x S=CNHCH_2, CH_2NCS), 2.67 (m, 6 H, H-5_{Pent}), 1.77 (m, 6 H, $^3J_{H,H}$ = 5.1 Hz, H-4_{Pent}), 1.59 (m, 2 H, $^3J_{H,H}$ = 5.1 Hz, CH_2), 1.50 (m, 2 H, $^3J_{H,H}$ = 7.6 Hz, CH_2), 1.33 (m, 4 H, 2 x CH_2) (**Scheme 3**)(**Fig. 3_10**).

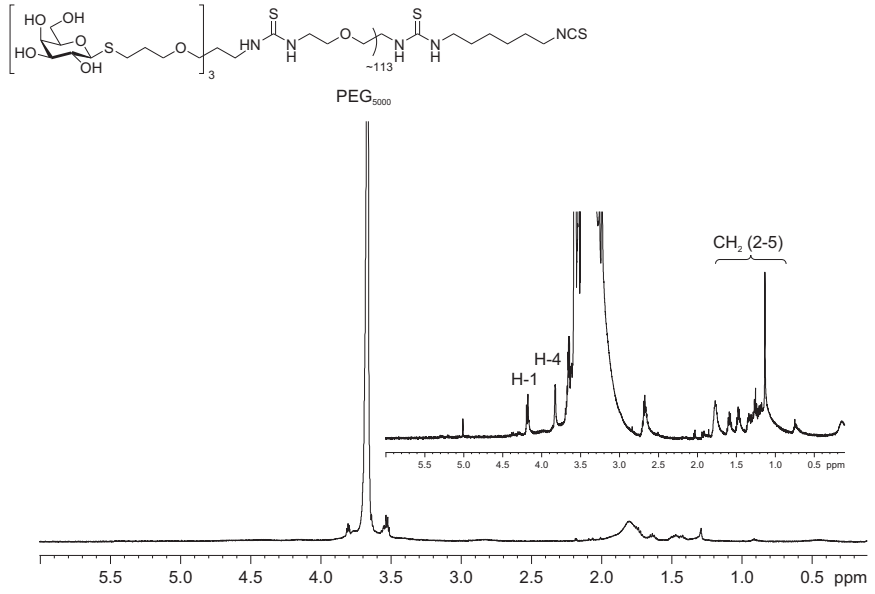

Figure 3_10. ^1H NMR spectra (500 MHz, CD_3CD) of **19**.

Conjugates 1 and 2 (Gal10CDs and Gal12CDs). To a solution of **Hex-CD-N_{21}** (25 mg, 5.25 µmol) and Et_3N (20 µl, 0.147 mmol, 2 equiv) in DMF (1 ml), a solution of **12** (11.5 or 23 mg, 11 or 22 µmol, 0.15 or 0.3 eq.) in DMF (2 ml) was dropwise added. The mixture was stirred at RT for 4 days. The solvent was removed under reduced pressure and the residue was purified by gel exclusion chromatography (Sephadex G-25, H_2O) and freeze dried from diluted HCl. Yield: 24 and 26 mg, respectively (75% and 78%). ^{1}H NMR (500 MHz, CD_3OD, 313 K): δ 5.36 (bt, 7 H, H-3), 5.18 (bd, 7 H, H-1), 4.84 (m, 7 H, H-2), 4.38 (m, 4.2 or 5.1, H-1_{Gal}), 4.21 (m, 11.2 or 12.1 H, H-5, H-4_{Gal}), 3.96 (7 H, H-4), 3.80-3.40 (m, 43 H, C*H*$_2$NHCS, H-2_{Gal}, H-3_{Gal},H-5_{Gal}, H-1_{Pent}, H-3_{Pent}, H-$6a_{Gal}$, H-$6b_{Gal,}$ C*H*$_2$CH$_2$S$_{cyst}$) 3.03 (m, 28 H, C*H*$_2$NH$_2$), 2.79 (m, 45 H, CH_2N, H-6a, H-6b, H-5_{Pent}), 2.46 (m, 17.6 H, $CH_2S_{Cyst,}$), 2.37, 2.29 (2 m, 28 H, CH_2CO) 1.90 (m, 8.4 or 10.2 H, H-4_{Pent}), 1.66, 1.42-1.31 (2 m, 89 H, C*H*$_2$CH$_2$CH$_3$, C*H*$_2$CH$_3$), 0.86 (m, 42 H, CH_3) (**Scheme 1**)(**Fig. 3_11**).

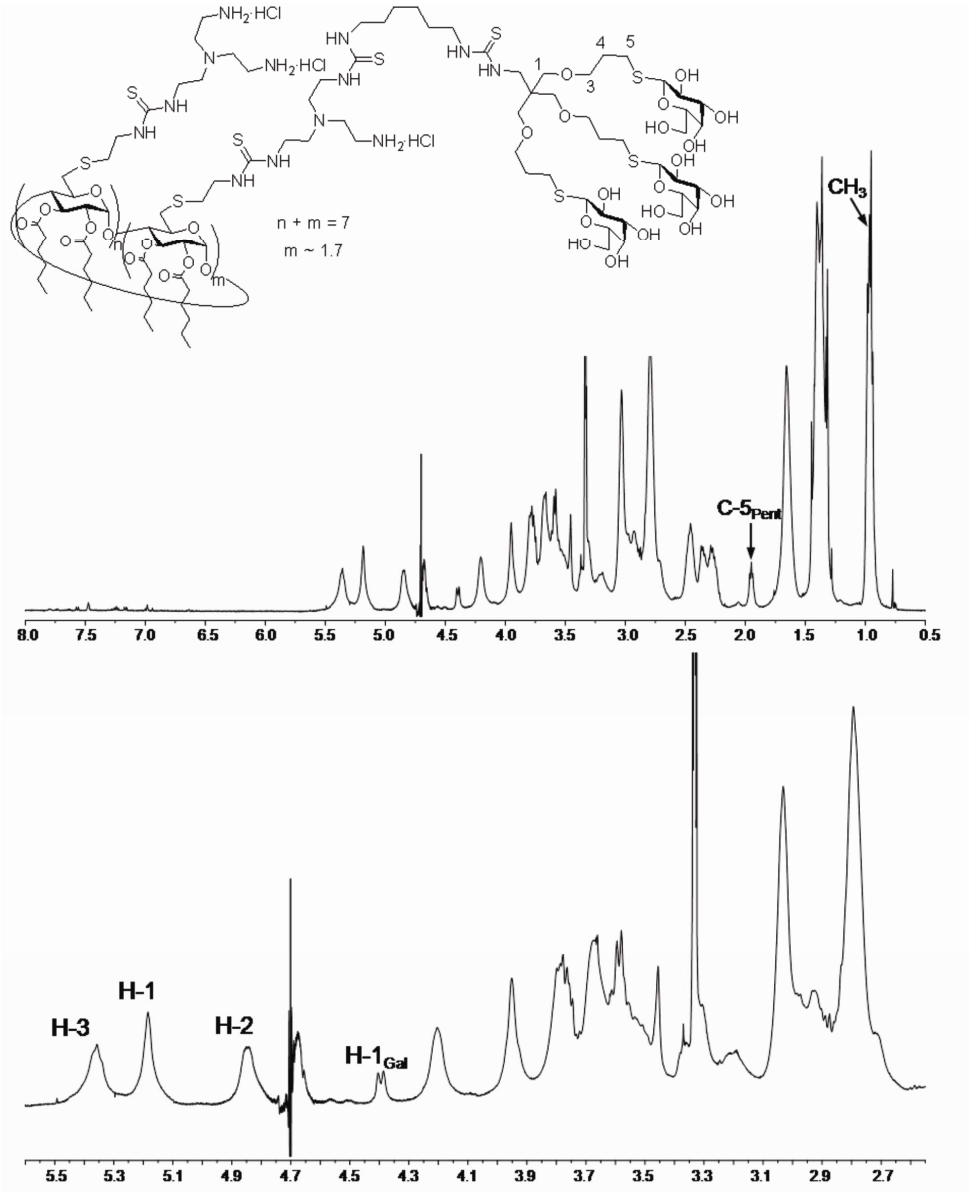

Figure 3_11. ^{1}H NMR spectra (500 MHz, CD_3OD) of **conjugate 2 (Gal12CDs)**.

Conjugate 3 (PEGCDs). To a solution of **Hex-CD-N_{21}** (14,7 mg, 3 µmol) and Et_3N (22 µl, 80 µmol, 4 equiv) in dry DMF (1 ml) under Ar atmosphere, a solution of **14** (22,6 mg, 4.3 µmol, 1.4 equiv) in DMF (1 ml) was added, and the reaction mixture was stirred for 6 days at RT. The solvents were removed under reduced pressure and the residue was diluted with water (60 ml) and dialyzed against a 3 kDa membrane. The solution was acidified with HCl 1 M and freeze-dried to give a white powder. Yield 32 mg (86%). $[\alpha]_D$ = +17.6 (c 1.1, MeOH). IR υ_{max} = 2883, 1749, 1341, 1101, 961, 841 cm^{-1}. UV (DCM): α_{max} 246 nm (ε_{mM} 86). ^1H NMR (500 MHz, CD_3OD): δ 5.39 (bs, 7 H, H-3), 5.19 (bs, 7 H, H-1), 4.85 (m, 7 H, H-2), 4.20 (bs, 7 H, H-5), 3.97 (bs, 7 H, H-4), 3.85-3.40 (m, 898 H, OCH_2CH_2, 4 x S=CNHCH_2, $NHCH_2CH_2O$, $CH_2CH_2S_{Cyst}$), 3.37 (s, 7.2 H, OCH_3), 3.24 (m, 70 H, $CH_2CH_2NH_2$, H-6a, H-6b), 2.89 (m, 28 H, CH_2CH_2NHCS, $CH_2CH_2S_{Cyst}$), 2.50-2.20 (m, 28 H, CH_2CO), 1.65 (m, 28 H, CH_2CH_2CO), 1.60-1.40 (m, 8 H, 4 x CH_2), 1.37 (m, 56 H, CH_3CH_2, $CH_3CH_2CH_2$), 0.95, 0.94 (2 t, 42 H, $^3J_{H,H}$ = 7.0 Hz, CH_3) (**Scheme 2**)(**Fig. 3_12**).

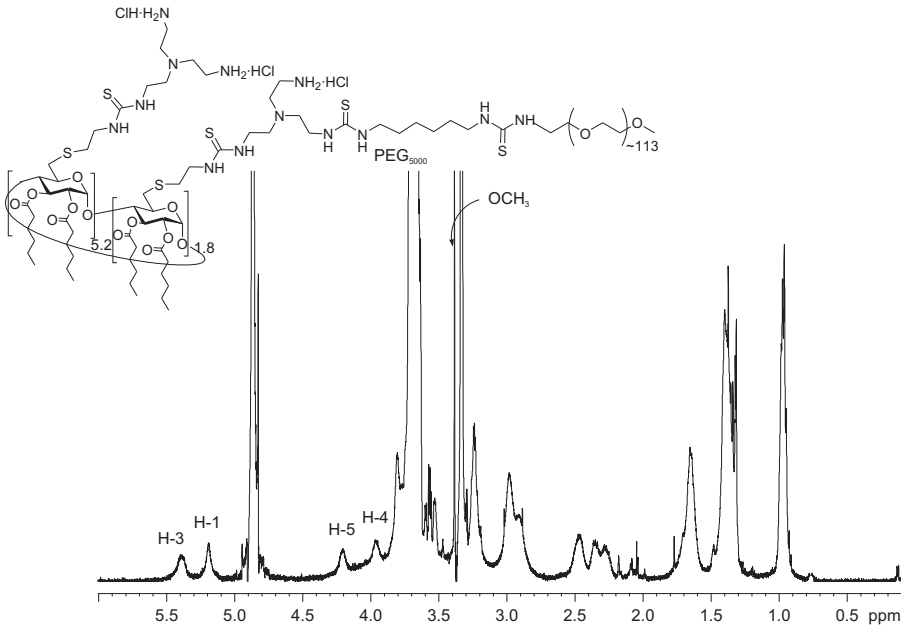

Figure 3_12. ^1H NMR spectra (500 MHz, CD_3OD) of **conjugate 3 (PEGCDs)**.

Conjugate 4 (GalPEGCDs). A solution of **Hex-CD-N_{21}** (10.7 mg, 2.2 µmol), **19** (19.4 mg, 3.1 µmol, 1.4 equiv) and Et_3N (8 µl, 61 µmol, 2 equiv) in dry DMF (1 ml) was stirred at RT overnight and at 40 °C for 24 h. The solvent was evaporated under reduced pressure and the residue was diluted with water (60 ml) and dialyzed using a 3 kDa membrane. The solution was acidified with 1 M HCl and freeze-dried. Yield 21 mg (70%). $[\alpha]_D$ = +17.3 (c 0.3, MeOH). IR υ_{max} = 2881, 1750, 1342, 1105, 962, 841 cm^{-1}. UV (MeOH): α_{max} 242 nm (ε_{mM} 56). ^1H NMR (500 MHz, CD_3OD): δ 5.37 (bs, 7 H, H-3), 5.19 (bs, 7 H, H-1), 4.85 (m, 7 H, H-2), 4.36 (d, 3.4 H, $J_{1,2}$ = 9.4 Hz, H-1_{Gal}), 4.20 (bs, 7 H, H-5), 3.92 (bs, 10.4 H, H-4, H-4_{Gal}), 3.85-3.40 (m, 1013 H, OCH_2CH_2, CH_2-6, $NHCH_2CH_2O$, 6 x S=CCNHH_2, C$H_2CH_2S_{Cyst}$, H-1_{Pent}, H-3_{Pent}, H-3_{Gal}, H-5_{Gal}, H-$6a_{Gal}$, H-$6b_{Gal}$, H-2), 3.15 (m, 70 H, CH_2CH_2NH_2, H-6a, H-6b), 2.89 (m, 34 H, CH_2CH_2NHCS, $CH_2CH_2S_{Cyst}$, H-5_{Pent}), 2.50-2.20 (m, 28 H, CH_2CO), 1.94 (m, .6.8 H, $^3J_{H,H}$ = 6.5 Hz, H-4_{Pent}), 1.64 (m, 28 H, CH_2CH_2CO), 1.60-1.40 (m, 9 H, 4 x CH_2), 1.37 (m, 56 H, CH_3CH_2, $CH_3CH_2CH_2$), 0.95, 0.94 (2 t, 42 H, $^3J_{H,H}$ = 7.2 Hz, CH_3) (**Scheme 3**)(**Fig. 3_13**).

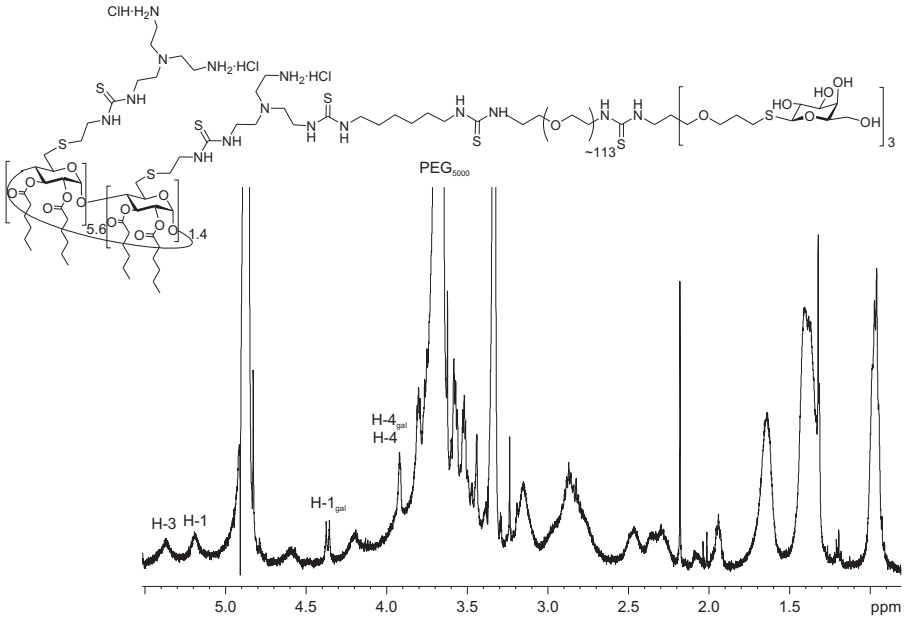

Figure 3_13. ^1H NMR spectra (500 MHz, CD_3OD) of **conjugate 4 (GalPEGCDs)**.

pDNA production

Heat-competent *E. coli* transformed with the gWIZ-GFP plasmid (GeneTherapy Systems, San Diego, California), pGEM4Z-EGFP-A64 plasmid (previously described by Rejman *et al.*[39]) or pBlue-Luc-A50 plasmid (previously described by Rejman *et al.*[39]) were grown in LB medium with respectively kanamycin and ampicillin at 37 °C for 20 h. pDNA was isolated and purified with the Qiafilter Plasmid Giga Kit (Qiagen, Venlo, The Netherlands) according to the manufacturer's instructions.

pDNA labeling

For fluorescence microscopy the pDNA was labeled with YOYO-1 (Molecular Probes, Merelbeke, Belgium) according to the manufacturer's instructions. Briefly, for a 10:1 base pair to dye ratio, 150 µl of 10 µM of YOYO-1 was mixed with 50 µl of 0.2 µg/µl pDNA. This was incubated in the dark for 1 h at RT and afterward the labeled pDNA was precipitated with a salt/ethanol solution which was followed by a 70% ethanol wash to remove free YOYO-1.

mRNA production

To produce mRNA by *in vitro* transcription, the pGEM4Z-EGFP-A64 or pBlue-Luc-A50 plasmids were first purified using a QIAquick PCR purification kit (Qiagen, Venlo, The Netherlands). The plasmids were linearized using SpeI and DraI restriction enzymes, respectively and then used as templates for the *in vitro* transcription reaction using a T7 mMessage mMachine kit (Ambion-Invitrogen, Merelbeke, Belgium) according to the manufacturer's instructions. mRNAs were purified by DNase I digestion, which was followed by LiCl precipitation and 70% ethanol wash. The produced mGFP and mLuc were both capped and polyadenylated. mRNA was stored in small aliquots at -80 °C.

CDplexes and transfection

pDNA

Different amounts of modified reference CDs were diluted in HEPES buffer (50 µl) to obtain the wanted N/P ratio (the ratio of moles of the amine groups of the specific cyclodextrin to those of the phosphate groups of the nucleic acids). They were mixed with pDNA (1 µg) diluted in HEPES buffer (50 µl). After 10 min of incubation, 400 µl OPTIMEM (Gibco-Invitrogen, Merelbeke, Belgium) were added and the mixture was added to HepG2 cells. After 4 h, the transfection medium was replaced by fresh culture medium.

mRNA

Different amounts of modified reference CDs were diluted in OPTIMEM (50 µl). They were mixed with mRNA (1 µg) diluted in OPTIMEM (50 µl). After 10 min of incubation, 400 µl OPTIMEM or full culture medium containing serum were added and the mixture was added to HepG2 cells. After 4 h, the transfection medium was replaced by fresh culture medium.

jetPEI-Hepatocyte polyplexes

jetPEI-Hepatocyte DNA transfection agent (Polyplus Transfection, Leuven, Belgium) was chosen as positive control transfection agent since it has been developed for specific gene delivery to hepatocytes. PEI-polyplexes with 1 µg pDNA or mRNA were prepared according to the manufacturer's instructions.

Complex destabilization

The ability of the CDplexes to escape out of the early endosomes was investigated as previously described by Xu and Szoka[40]. CDplexes were made as described earlier and then the free pDNA was labeled by adding PicoGreen (Molecular Probes, Merelbeke, Belgium) (λ_{em} 502nm, λ_{ex} 520 nm) to the suspensions. Then, liposomes with the same lipid composition as early endosomal membranes, phosphatidylcholine (PC) :

phosphatidylethanolamine (PE) : phosphatidylserine (PS) in a molar ratio 6:3:1 (Avanti Polar Lipids, Delfzijl, The Netherlands), were added. The fluorescence of free pDNA was measured over time with a spectrometer (SLM-Aminco Bowman Series 2, Thermo Fisher Scientific, Erembodegem-Aalst, Belgium). To know the maximal release of pDNA out of the CDplexes, 200 µl of 10% zwittergent (3-(N,N-dimethylmyristylammonio)propanesulfonate; Sigma-Aldrich, Bornem, Belgium) was added and the fluorescence of free pDNA was measured.

Cell culture conditions

HepG2 cells (Human Hepatoblastoma, ATCC-HB-8065, Molsheim Cedex, France) were cultured in Dulbecco's Modified Eagle's Medium (DMEM) (Gibco-Invitrogen, Merelbeke, Belgium) containing 2 mM glutamine (Gibco-Invitrogen, Merelbeke, Belgium), 10% heat-inactivated fetal bovine serum (FBS) (Hyclone/Perbio, Thermo Fisher Scientific, Erembodegem-Aalst, Belgium) and 100 U/ml penicillin-streptomycin liquid (Gibco-Invitrogen, Merelbeke, Belgium) at 37 °C in a humidified atmosphere containing 5% CO_2. For the expression experiments, HepG2 cells were plated 1 day prior to the experiment onto 12-well plates ($2x10^5$ cells/well) or 24-well plates ($1x10^5$ cells/well).

Flow cytometry

Flow cytometry (BD FACSCalibur, Erembodegem, Belgium) was used to determine the percentage of GFP-positive cells. For expression efficiencies, the fraction of cells expressing GFP (pGFP or mGFP) and the fluorescence intensities per positive cell were assessed. This was done 24 and 48 h after transfection for pDNA and after 24 h after transfection for mRNA.

Luciferase assay

The culture medium was removed and the cells were washed twice with PBS (Gibco-Invitrogen, Merelbeke, Belgium). This was followed by adding 100 µl of Cell Culture

Lysis Reagent (Promega, Leiden, The Netherlands). After 30 min the samples were centrifuged (12000 rpm at 4 °C for 5 min). 40 µl of the supernatants were transferred to a 96-well plate. Luciferase activity of each sample was assayed in a GloMax 96 Luminometer (Promega, Leiden, The Netherlands) by adding 100 µl of the substrate solution in each well. The emitted light was measured over a 10s-period. The protein content of each sample was determined by a standard Bradford assay (Biorad, Nazareth Eke, Belgium). The results are expressed as relative light units per mg of protein (RLU/mg).

Photochemical internalization (PCI)

The night before transfection, the cells were incubated with 250 µl photosensitizer (PhSen) meso-tetraphenylporphine disulfonate (TPPS2a) (PCI Biotech, Lysaker, Norway) (0.4 µg/ml in regular culture medium). Fresh culture medium was administered to the cells 1 h before transfection to remove non-associated PhSen. Following 4 h of incubation, the pDNA-CDplexes were removed, fresh culture medium was added and the cells were illuminated for 40 s with blue light (375-450 nm) emitted by LumiSource. After another incubation of 24 h, the expression efficiency was measured by flow cytometry.

Inhibition of uptake through the ASGPr

Preceding transfection, rabbit polyclonal antibodies to ASGPr1 (Abcam, Cambridge, UK) were applied to the HepG2 cells in order to assess to which extent the uptake of CDplexes carrying galactose is accounted by the ASGPrs. The cells were washed once in 2% FBS in PBS and then unspecific binding was blocked by incubation with 2% goat serum (in PBS, 30 min, at 37 °C in cell incubator). Then the cells were incubated for another 2 h at 37 °C (cell incubator) with 4 µg of ASGPr1-antibodies and washed twice with 2% FBS in PBS followed by transfection.

Viability test

The viability of the cells 24 h after transfection with mRNA-CDplexes was assayed with the Cell Proliferation Kit I (MTT) (Roche, Vilvoorde, Belgium) according to the manufacturer's instructions. To that end, HepG2 cells were seeded in 12-well plates ($2x10^5$ cells/well) one day before transfection. The absorbance was measured at 600 nm with a spectrophotometer (UV-1800, Shimadzu Corporation, Deurne-Antwerpen, Belgium) or Nanodrop 2000c (Thermo Fisher Scientific, Erembodegem-Aalst, Belgium).

Confocal microscopy

To study the uptake of CDplexes, HepG2 cells ($3x10^5$ cells) were plated onto sterile glass-bottom culture dishes (MatTek Corporation, Ashland, MA, USA) and allowed to adhere for 1 day. Transfections were performed with reference CDplexes at N/P ratio 10. The pDNA was labeled beforehand with YOYO-1. After 4 h of transfection, pictures were taken with a Nikon EZC1-si (Nikon Belux, Brussels, Belgium).

RESULTS

Synthesis

Design criteria

Previous attempts to formulate glycosylated CDplexes using different ratios of a paCD and a neutral glycoamphiphilic CD (GaCD) led to disruption of the complexes even at very low proportion of the GaCD-component. This was probably due to a destabilizing effect of neutral microdomains. Installing the sugar functional elements and the cationic groups as regular arrangements onto the CD-platform restored the capacity to form stable CDplexes, but implied a high synthetic cost[20]. To overcome this limitation, we have now adopted a much more straightforward and flexible approach. It consists of the coupling of the reference CD (**Fig. 1: Hex-CD-N_{21}**), a C_7-symmetrical β-cyclodextrin derivative with isothiocyanate-armed β-D-galactopyranosyl ligands. The incorporation of PEG-chains was considered to prevent aggregation in the

presence of serum proteins. The new CD derivatives shown in **figure 1** were thus prepared.

The thiourea-forming reaction was favored as the ligation method because thiourea-segments have been shown to contribute to pDNA complexation through hydrogen bonding[14, 41]. Nevertheless, we anticipated that extensive functionalization of the reference CD may compromise the pDNA complexing abilities, since an amino group is deactivated at every coupling event. To overcome this problem trivalent galactose-dendrons were used as the basic ligand units. This strategy offers a very convenient manner to control the density of the sugar epitopes at the surface of the resulting CDplexes after interaction with nucleic acids.

Synthesis strategy

The synthesis of the tri-antennary galactose ASGPr-recognition element involved the radical addition of the per-*O*-acetylated 1-thio-β-D-galactopyranose **6**[36] to the tri-*O*-allylated pentaerythritol derivative **5**[37]. The hydroxyl group in the resulting conjugate **7** was then replaced by azide **8** via a trifluoromethanesulfonate ester intermediate (87%, 2 steps). After deacetylation (→**9**), the azido group was reduced under Staudinger conditions to amine **10**, which was subsequently coupled with an excess of 1,6-hexamethylenediisothiocyanate **11**[38] to yield the isothiocyanate-armed glycodendron **12** in quantitative yield. Base-catalyzed reaction of variable proportions of **12** with reference CD in DMF using long reaction times yielded Gal10CD and Gal12CD, in which 10 and 12% of the primary amine groups incorporate the glycol-dendron, respectively, in 75-78% yields (**Scheme 1**). Higher proportions of the glycol-dendron resulted in compounds with poor pDNA complexing capacity (data not shown) and were not further considered.

PEGylation of reference CDs also relied in the thiourea-forming ligation strategy (**Scheme 2**). Incorporation of PEG_{5000} elements were considered in view of its higher stabilization effect against serum proteins in comparison to lower-weighted analogues[42]. The preparation of the non-glycosylated PEGCDs involved the *O*-methyl-

PEG_{5000}-NCS derivative **14**, prepared by reaction of commercially available *O*-methyl-PEG_{5000}-NH_2·HCl **13** with an excess of diisothiocyanate **11**. The formation of the thiourea linker was confirmed by MS spectrometry and ^{1}H NMR. Subsequent conjugation of **14** with reference CDs was carried out in DMF to yield PEGCDs having 13% of the primary amino groups substituted with PEG_{5000} chains as determined from the ratio of the ^{1}H NMR signal integration for the terminal methyl group in *O*-methyl-PEG and the anomeric proton of the D-glucopyranose units in the β-cyclodextrin core. The synthesis of GalPEGCDs required the isothiocyanate-armed PEG_{5000}-glycodendron **19.** Its preparation was accomplished in five steps from azide **8**. Isothiocyanation by treatment with triphenylphosphine (TPP) and carbon disulfide afforded isothiocyanate **15** (68% yield), which was coupled with commercial H_2N-PEG_{5000}-NHBoc **16** to yield the *N*-Boc-protected PEGylated glycodendron **17**. Deacetylation of **17** with NaOMe/MeOH followed by acid-catalyzed Boc cleavage afforded the unprotected galactopyranose dendron-PEG_{5000}-NH_2 **18** that, after reaction with excess of **11**, provided the key precursor **19**. Final coupling of **Hex-CD-N_{21}** and **19** was carried out in DMF/Et_3N at 40 °C for two days and the crude was purified by dialysis (**Scheme 3**). Integration of ^{1}H NMR anomeric signals from βCD and β-D-galactopyranose units evidenced that 10% of the amino groups have been transformed into thiourea segments bearing the PEG-dendron element, meaning 1.4 galactopyranose dendron-PEG_{5000} units per CD.

pDNA

Transfection efficiencies of pDNA-CDplexes

The potential of CDs to deliver pDNA to HepG2 cells, resulting in reporter gene expression, was determined. pDNA encoding GFP was complexed with reference CDs, Gal10CDs or Gal12CDs at N/P ratios varying from 10 to 30. The gel retardation assay demonstrated that the reference CDs efficiently complex pDNA at N/P ≥ 2.5 (**Fig. 4**). The same was observed for Gal10CDs and Gal12CDs (data not shown).

The fraction of GFP-positive cells was assessed 24 and 48 hours after transfection. As shown in **figure 5**, levels of transfection obtained by pDNA-CDplexes were very low. The most efficient CDplexes transfected maximally 4% of the cells. Remarkably, transfection efficiencies obtained by jetPEI-Hepatocyte, a cationic polymer specifically designed to transfect hepatocytes, were quite modest. Only a maximum of 6% GFP-positive HepG2 cells was reached.

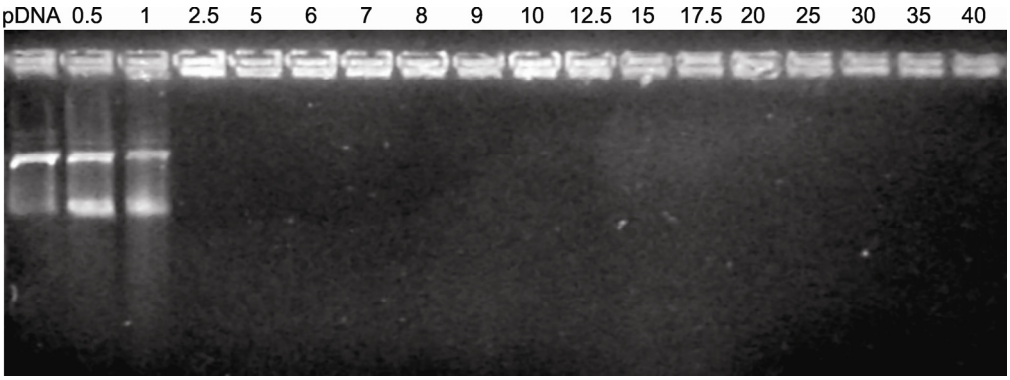

Figure 4. Gel retardation assay. Reference CDs were mixed with pDNA at different N/P ratios: 0, 0.5, 1, 2.5, 5, 6, 7, 8, 9, 10, 12.5, 15, 17.5, 20, 25, 30, 35 and 40. The formed pDNA-CDplexes were applied on a 1% agarose gel.

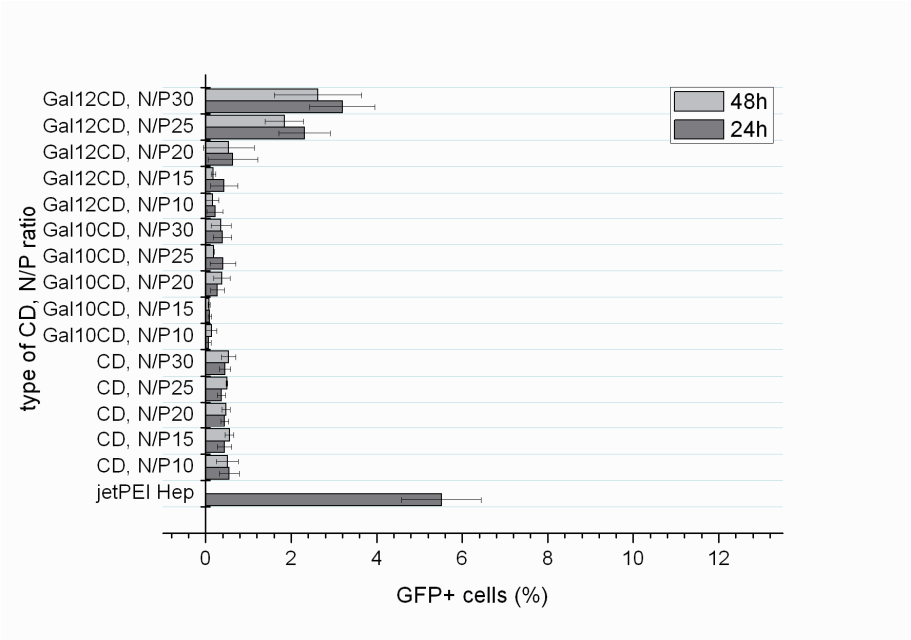

Figure 5. The fraction (%) of GFP-positive HepG2 cells after transfection with pDNA-CDplexes. The complexes were prepared by mixing reference CDs, Gal10CDs or Gal12CDs with pDNA at different N/P ratios. The results are compared with the transfection efficiency obtained by jetPEI-Hepatocyte/pDNA-complexes. 1 µg of pDNA was added per well. An increase to 2 µg/well did not yield larger fractions of GFP-positive HepG2 cells, neither did the use of OPTIMEM instead of HEPES buffer to prepare the CDplexes. (Mean ± SD)

To ascertain at what stage in the process from uptake to translation the pDNA-CDplexes fail, we focused individually on the different potential intracellular barriers, in the order of their appearance in the process. The results are presented in the following paragraphs.

Uptake of pDNA-CDplexes

First, we verified if CDplexes attach to the plasma membrane and are subsequently internalized by cells. To that end, fluorescently labeled CDplexes were incubated with HepG2 cells and analyzed by means of confocal microscopy. As shown in **figure 6**, HepG2 cells efficiently internalized fluorescently labeled CDplexes. These results

demonstrate that interaction with the plasma membrane and subsequent internalization do not present an obstacle for transfection mediated by CDplexes.

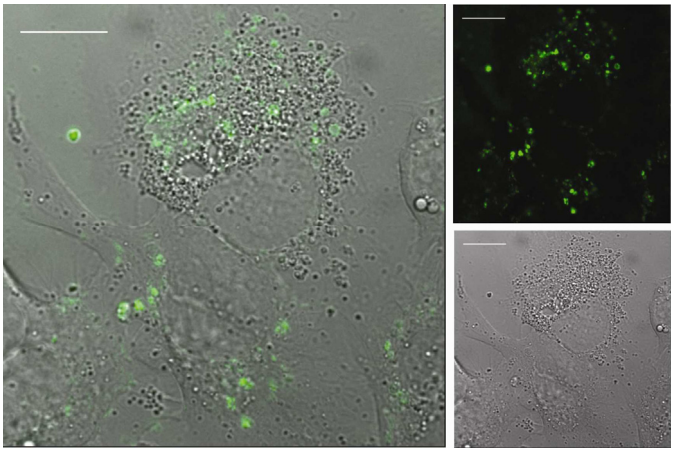

Figure 6. Representative confocal images of HepG2 cells which internalized pDNA-CDplexes. pDNA and reference CDs were mixed at an N/P ratio of 10. Scalebars = 15 µm

Photochemical internalization

In order to determine whether the endosomal entrapment limits the transfection potential of CDplexes, a technique called photochemical internalization (PCI) was used. PCI causes disruption of the endosomal membrane and thus facilitates release of material, which is localized in this compartment. If the CDplexes are trapped in the endosomes and further on degraded in the lysosomes, there should be no gene expression. When PCI is applied, the trapped CDplexes should be released from the endosomes which could result in an elevated gene expression, provided there are no other obstacles on the delivery path to the nucleoplasm. As shown in **figure 7**, there is no significant difference between fractions of GFP-positive cells or mean fluorescence intensities per GFP-positive cell for illuminated and non-illuminated HepG2 cells transfected with reference CD-, Gal10CD- or Gal12CDplexes. This lack of effect of PCI on expression mediated by different CDplexes points out that the escape

of the complexes from the endosomes is not responsible for the low level of gene expression.

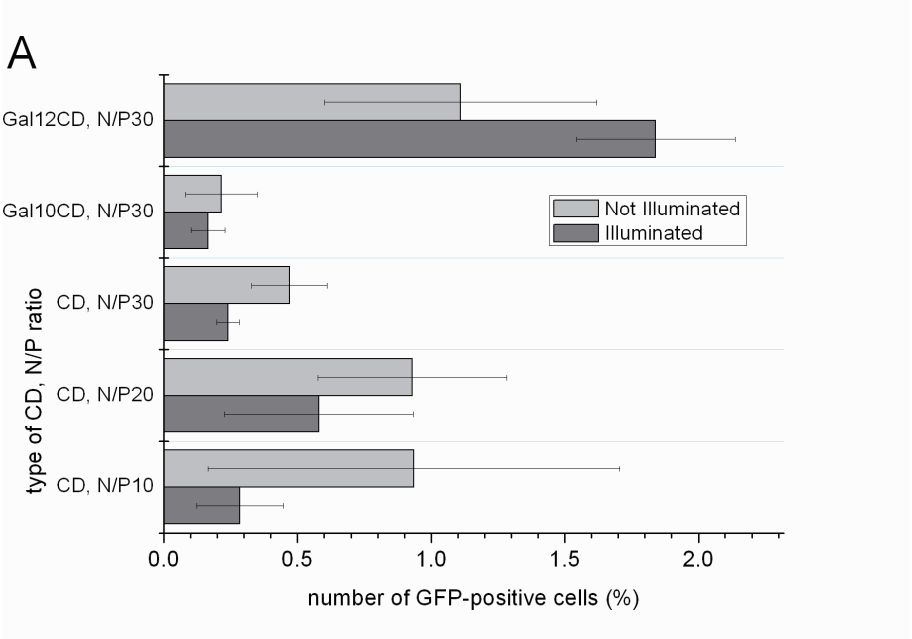

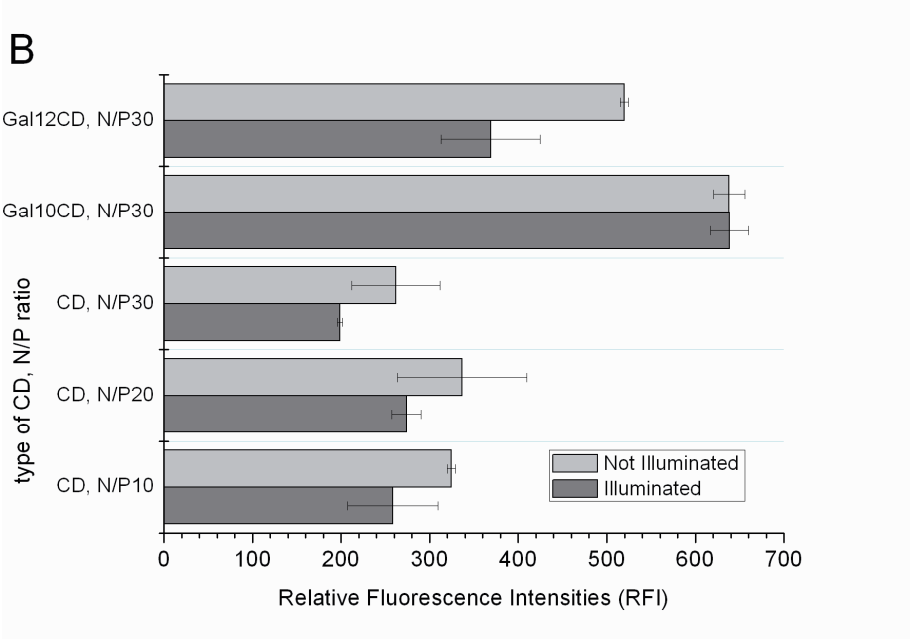

Figure 7. (A) The fraction (%) and **(B)** Mean Relative Fluorescence Intensities (RFI) of GFP-positive HepG2 cells after exposure to the PCI treatment. The complexes were prepared by mixing reference CDs, Gal10CDs or Gal12CDs with pDNA at different N/P ratios. 1 μg of pDNA was added per well (increase to 2 μg/well did not yield larger fractions of GFP-positive HepG2 cells). (Mean ± SD)

Release of pDNA from CDplexes

In a subsequent series of experiments we investigated the possibility that the low expression level is related to insufficient release of the plasmid from the complex. Therefore, we followed the approach earlier described by Xu and Szoka[40]. pDNA-CDplexes were added to a PicoGreen solution followed by addition of negatively charged liposomes with the same lipid composition as early endosomal membranes. The changes in fluorescence, indicating an increase in the amount of free pDNA as only free pDNA is accessible for PicoGreen, were measured with a fluorometer. As demonstrated in **figure 8**, the development of the fluorescence signal, which represents release of pDNA, occurs during the first 2-3 minutes and then reaches plateau values. We can conclude from these experiments that the low levels of transfection achieved by pDNA-CDplexes can neither be attributed to the lack of release of free pDNA from the CDplexes.

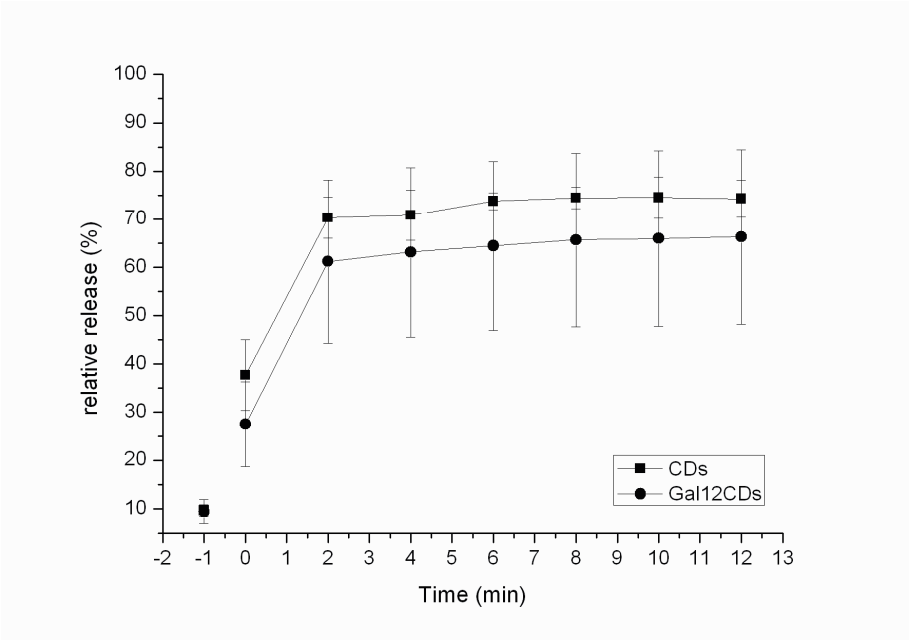

Figure 8. Accessibility of pDNA toward PicoGreen in pDNA-CDplexes. pDNA was complexed with reference CDs or Gal12CDs at N/P ratio 10 (time point -1). The complexes were mixed with negatively charged liposomes (time point 0) and the release of free pDNA interacting with PicoGreen was monitored over time. The relative release is plotted over a period of 12 min and shown as a fraction of the maximal release which was reached with zwittergent (100%). (Mean ± SD)

Taken together, these results suggest that the translocation of the pDNA into the nucleus represents the main obstacle for pDNA-CDplexes to become efficient. To verify that, we transfected HepG2 cells with mRNA-CDplexes. The results are presented in the next section.

mRNA

Transfection efficiency of mRNA-CDplexes

Our experiments strongly pointed out the nuclear envelope as the main obstacle for efficient transfection of HepG2 cells. To verify that, we transfected the cells with mRNA, which only needs to reach the cytosol to result in biological activity, instead of pDNA. Different CDs also efficiently complex mRNA. **Figure 9A** presents levels of transfection obtained for two galactosylated CD species (Gal10CDs and Gal12CDs) mixed with mRNA at different N/P ratios, expressed as fractions of GFP-positive cells. The results were compared with those obtained with complexes made of mRNA and jetPEI-Hepatocyte. The results clearly demonstrate that, in contrast to the cationic polymer, modified CDs mixed with mRNA at higher N/P ratios (>20) were efficient in transfecting HepG2 cells. The fractions of GFP-positive cells obtained with Gal12CDplexes were well above 20%. Moreover, as shown in **Figure 9B** transfection efficiencies obtained by the Gal10CDplexes incubated with the cells in full culture medium containing serum were equal or even higher than in OPTIMEM.

We further studied transfection capacities of PEG-modified CDs: PEGCDs and GalPEGCDs. The expression efficiency was expected to drop for PEGCDplexes because the PEG was expected to prevent or diminish the interaction with the cellular membrane. The presence of galactose at the tip of PEG-moieties was expected to restore the uptake as a result of specific interaction with the ASGPr. Complexes based on PEGCDs or GalPEGCDs alone were not active. This could be due to the lack of a sufficient number of cationic groups in these derivatives[14]. Therefore the complexes were made by premixing PEGCDs or GalPEGCDs with reference CDs at a ratio of 7:3, which were then added to mRNA. **Figure 9C** represents fractions of GFP-positive cells obtained for these complexes. As expected, there was a minimal expression of GFP in HepG2 cells transfected with PEGCDplexes. Interestingly, GalPEGCDplexes restored levels of transfection to values up to 31%.

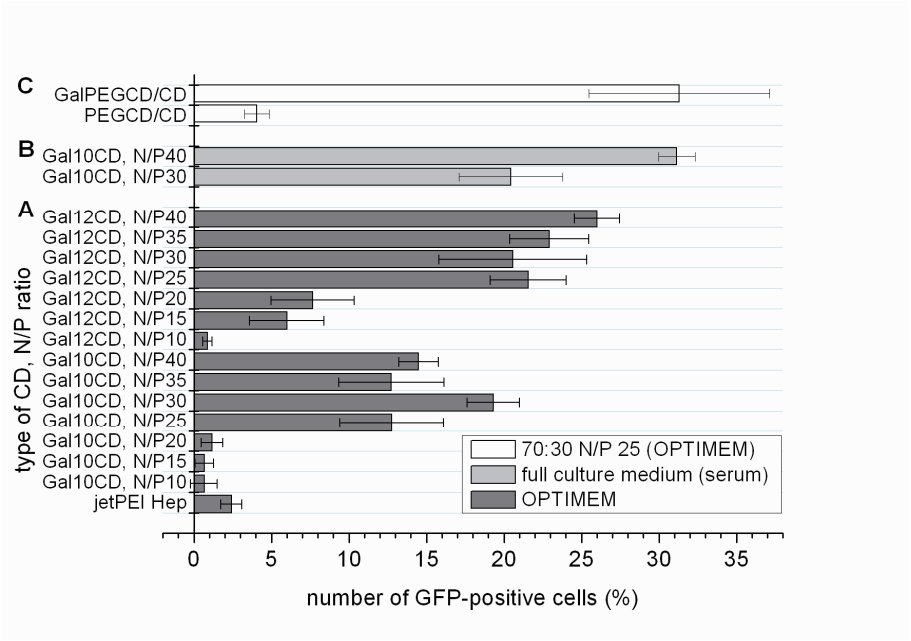

Figure 9. The fraction of GFP-positive HepG2 cells after transfection with mRNA-CDplexes. **(A and B)** The complexes were prepared by mixing Gal10CDs or Gal12CDs with mRNA at different N/P ratios or **(C)** they were prepared by mixing PEGCDs or GalPEGCDs and reference CDs at a ratio of 70:30 with mRNA at N/P ratio 25. Transfection efficiencies were determined 24 h after transfection by flow cytometry. The cells were seeded in 24-well plates. 1 µg of mRNA was added per well. Complexes were incubated with the cells for 4 h in OPTIMEM **(A and C)** or full culture medium containing 10% FBS **(B)**. The results are compared with the transfection efficiency obtained by jetPEI-Hepatocyte/mRNA-complexes. (Mean ± SD)

ASGPr-mediated endocytosis of galactosylated CDplexes

Since the ideal carrier for mRNA delivery to hepatocytes needs to be specific, we verified whether galactosylated CDplexes are internalized via the mechanism that involves the ASGPrs. To that end, the ASGPrs were blocked with anti-ASGPr1 antibodies prior to transfection with Gal12CDplexes or GalPEGCD/CDplexes carrying mRNA encoding luciferase. As shown in **figure 10**, relative levels of luciferase activity in HepG2 cells, in which ASGPr-mediated uptake was blocked, decreased significantly compared to the levels in the untreated cells.

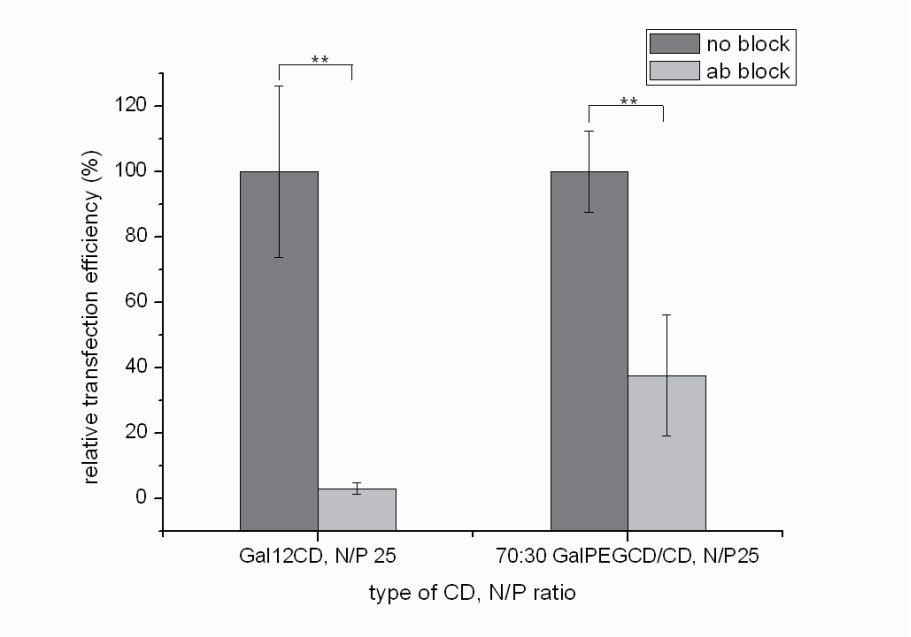

Figure 10. Inhibition of internalization of galactosylated reference CDs complexed with mRNA by blocking ASGPrs. ASGPrs were blocked by incubation with rabbit polyclonal antibodies against ASGPr1 (2 h, 37 °C). Gal12CDs or GalPEGCDs/CDs (70:30) were complexed with mRNA encoding luciferase at N/P 25 and incubated with HepG2 cells for 4 h. Luciferase activity was measured 6 h later with a luminometer. Relative light units per mg of protein were calculated for each sample. The data are presented as percentages of transfection levels obtained for control cells. The results were analyzed for the statistical significance: ** $p \leq 0.001$. (Mean ± SD)

Viability of HepG2 cells after mRNA transfection

The viability of the HepG2 cells was determined 24 hours after transfection with mRNA-CDplexes using an MTT cell proliferation assay. The viability of HepG2 cells treated with CDplexes was around 80% which is comparable with the viability after transfection with jetPEI-Hepatocyte (**Fig. 11**).

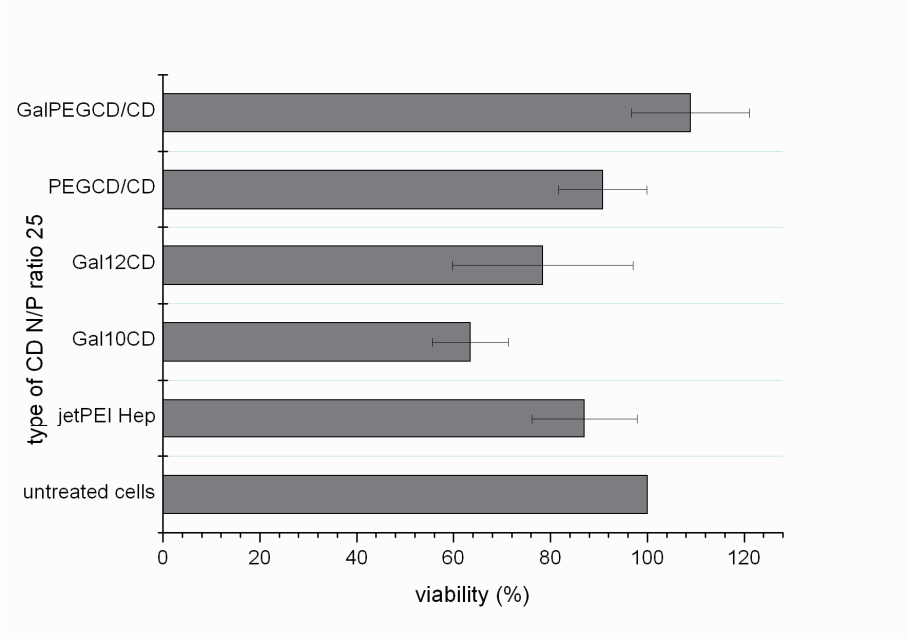

Figure 11. Viability of HepG2 cells after transfection with mRNA-CDplexes at an N/P ratio of 25. The viability of the transfected cells is compared with untreated cells (100 %) and with cells transfected with jetPEI-Hepatocyte polyplexes. (Mean ± SD)

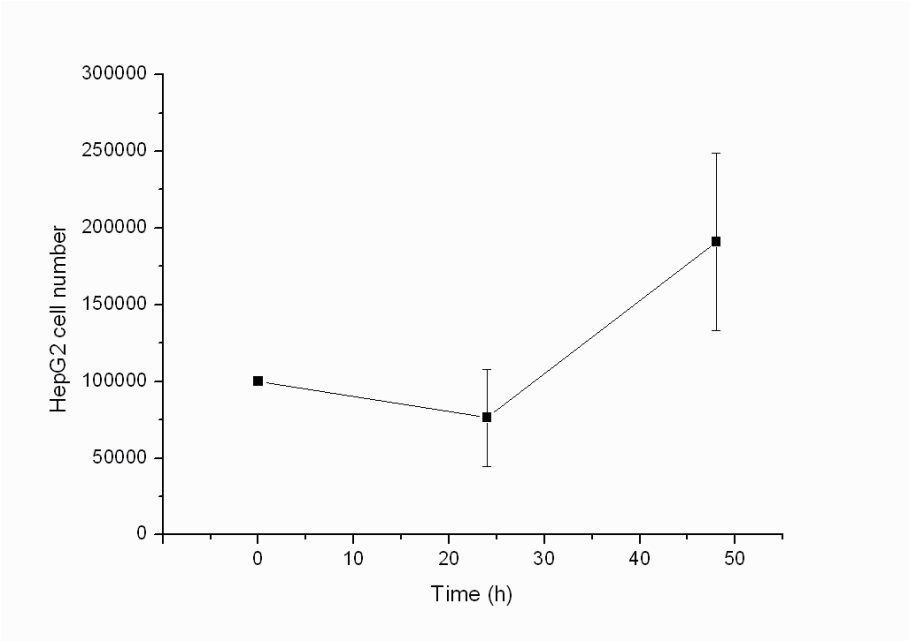

Figure 12. HepG2 cell count. $1x10^5$ HepG2 cells were plated per well in a 24-well plate. The cells were counted 24 and 48 h later. (Mean ± SD)

DISCUSSION

HepG2 cells in culture display a certain polarity and are morphologically and functionally differentiated to a certain extent, which makes them resemble the human hepatocytes in the *in vivo* situation and thus renders them an interesting and relevant model system. HepG2 cells are polarized and divide very slowly. The doubling time of HepG2 cells used in this study was 48 hours. It should be noted, however, that the number of cells in culture did not change during the first 24 hours (**Fig. 12**). For that reason, these cells are difficult to transfect with cationic carrier/pDNA complexes (CDplexes and polyplexes), as shown in the present work. Results reported by Kichler *et al.*[43] are compatible with this observation. These authors demonstrated that luciferase activity detected in HepG2 cells was

significantly lower than in epithelial 293 cells transfected with polyethylene imine (PEI)-complexes.

To pinpoint the cause of this failure, we performed a set of experiments to detect at which point(s) along the transfection pathway the CDplexes fail. We first determined whether or not the pDNA-CDplexes are internalized by HepG2 cells. Although we confirmed that they are taken up it is conceivable that this occurs through an unproductive pathway. Díaz-Moscoso *et al.*[15] have shown that in Vero cells ligand-devoid pDNA-CDplexes were internalized by both clathrin-dependent and clathrin-independent endocytosis. The largest fraction of pDNA-CDplexes was taken up by the transfection-ineffective clathrin-dependent route. The CDplexes taken up this way end up in acidic late endosomes/lysosomes and therefore do not lead to expression of the reporter gene. It is the smaller fraction which is internalized via caveolae-mediated endocytosis that is predominantly responsible for productive transfection in these cells. Also for PEI/pDNA polyplexes it has been shown that it is predominantly the fraction which is taken up via caveolae-mediated endocytosis which leads to gene expression[44-46]. In this context it is important to stress that HepG2 cells lack endogenous caveolins which causes their inability to carry out caveolae-mediated endocytosis[47]. This implies that complexes carrying pDNA enter HepG2 cells via other pathways. Indeed, it has been reported that histidylated-polylysine/pDNA complexes enter these cells via clathrin-mediated endocytosis and a macropinocytosis-like mechanism[46].

The next step was to investigate if the transfection-limiting factor is the escape of CDplexes out of the endosomes. We provided evidence that this is also not the main problem by showing that the disruption of endosomes by PCI following uptake of CDplexes does not lead to enhanced transfection. Third, we demonstrated the ability of pDNA to be released from the CDplexes by conditions that mimic the endosomal environment. This suggests also that inside the cell the pDNA is likely to be released from the complexes. Therefore the nuclear envelope is remaining as the major

barrier standing in the way of successful transfection of HepG2 cells with the pDNA-CDplexes. To obtain experimental evidence in favor of this hypothesis, we transfected HepG2 cells with mRNA instead of pDNA. As mRNA is translated in the cytoplasm, no transport step of the mRNA into the nucleus is required. We found up to 31% of GFP-positive cells upon transfection in OPTIMEM and in culture medium containing serum with mRNA-CDplexes, which is significantly higher even than with the jetPEI-Hepatocyte polymer which is especially developed for *in vitro* hepatocyte transfections. By showing that mRNA-mediated transfection by the galactosylated CDplexes was effectively blocked by antibodies to ASGPr, we confirmed the involvement of this receptor in the transfection process.

The results obtained for mRNA-CDplexes indicate that even though they are internalized by receptor-mediated endocytosis they lead to efficient transfection. This is likely due to the fact that the translation of mRNA occurs in the cytosol. In contrast to pDNA, its release from the endosomal compartment does not have to coincide with cell division to ensure its translation. In the case of pDNA-complexes, the release from the endosomal compartment should occur not long before cell division, in order to prevent the pDNA present in the cytosol from degradation by cytosolic nucleases. As reported by Lechardeur *et al.*[48] the half-life of pDNA in the cytosol does not exceed 90 min. This leaves a narrow window for pDNA to enter the nucleus during mitosis.

Ideally, transfection of cells with mRNA-complexes should result in 100% positive cells, but this number was not even approached. This might be explained by the occurrence of two distinct populations of ASGP receptors, which operate through two parallel but kinetically distinct endocytic pathways. Interestingly, the rate of ligand degradation is much faster in the State 1 receptor-mediated pathway and starts almost immediately after internalization. Differently, a distinct lag period between internalization and lysosomal localization was observed for ligand taken up via the State 2-dependent mechanism. In addition, recycling of ligand-receptor complex to

the cell surface was only observed for the State 1 receptor-subtype[49, 50]. These marked differences between the two receptor subpopulations lead us believe that only those mRNA-CDplexes that bind to State 2 receptors lead to successful transfection basically because there is a larger time window for these complexes to timely escape from the endosomal compartment.

The less impressive performance of jetPEI-Hepatocyte complexed to mRNA could be explained by the fact that the polymer's affinity to mRNA is so strong it does not allow its release from once-formed complexes as demonstrated in our earlier work[39].

A potential problem that may arise when applying our ASGPr-targeted CDplexes *in vivo* by intravenous administration is severe competition by other cell types, such as macrophages. PEGylation of particles has been shown to be quite effective in preventing or reducing the latter process and coupling of a ligand to the distal end of the PEG-molecule has been reported to improve cell-specific targeting[51-53]. Therefore, we also coupled the galactose-moieties to the distal end of the PEG-chain and showed that interaction with the ASGPr was fully restored after it was nearly abolished by just coupling the unmodified PEG to the CDplexes. We speculate that the distal coupling of galactose-moieties to the PEG-chains in our CDplexes will also improve the selective uptake by hepatocytes upon intravenous application.

In conclusion, our results show that the modified paCDs may serve as a valuable mRNA delivery platform for the transient transfection of hepatocytes, further widening the potential of cyclodextrin-based vectors in gene therapy[54]. Using mRNA instead of pDNA would be a solution to the major problem associated with hepatocyte transfection, i.e. their low proliferation state, which is quite unfavorable for effective pDNA-mediated transfection[1, 55]. Moreover, the use of mRNA would ensure no danger of introducing irreversible genetic modifications in the genome, often leading to oncogenesis or deactivation of vital genes. Therefore it is expected that mRNA will prove its value in a broad range of therapeutic applications as well as in basic research.

REFERENCES

1. Nguyen, T.H. & Ferry, N. Liver gene therapy: advances and hurdles. *Gene Ther.* **11 Suppl 1**, S76-84 (2004).
2. Suda, T., Kamimura, K., Kubota, T., Tamura, Y., Igarashi, M., Kawai, H., Aoyagi, Y. & Liu D. Progress toward liver-based gene therapy. *Hepatol. Res.* **39**, 325-340 (2009).
3. Braeckmans, K., Buyens, K., Bouqet, W., Vervaet, C., Joye, P., De Vos, F., Plawinski, L., Doeuvre, L., Angles-Cano, E., Sanders, N.N., Demeester, J. & De Smedt, S.C. Sizing nanomatter in biological fluids by fluorescence single particle tracking. *Nano Lett.* **10**, 4435-4442 (2010).
4. Jooss, K., Ertl, H.C. & Wilson, J.M. Cytotoxic T-lymphocyte target proteins and their major histocompatibility complex class I restriction in response to adenovirus vectors delivered to mouse liver. *J. Virol.* **72**, 2945-2954 (1998).
5. Mingozzi, F., Liu, Y.L., Dobrzynski, E., Kaufhold, A., Liu, J.H., Wang, Y., Arruda, V.R., High, K.A. & Herzog, R.W. Induction of immune tolerance to coagulation factor IX antigen by in vivo hepatic gene transfer. *J. Clin. Invest.* **111**, 1347-1356 (2003).
6. Follenzi, A., Battaglia, M., Lombardo, A., Annoni, A., Roncarolo, M.G. & Naldini, L. Targeting lentiviral vector expression to hepatocytes limits transgene-specific immune response and establishes long-term expression of human antihemophilic factor IX in mice. *Blood* **103**, 3700-3709 (2004).
7. Wu, G.Y. & Wu, C.H. Receptor-mediated gene delivery and expression in vivo. *J. Biol. Chem.* **263**, 14621-14624 (1988).
8. Ryan, S.M., Mantovani, G., Wang, X., Haddleton, D.M. & Brayden, D.J. Advances in PEGylation of important biotech molecules: delivery aspects. *Expert Opin. Drug. Deliv.* **5**, 371-383 (2008).
9. Mintzer, M.A. & Simanek, E.E. Nonviral vectors for gene delivery. *Chem. Rev.* **109**, 259-302 (2009).
10. Kay, M.A., Glorioso, J.C. & Naldini, L. Viral vectors for gene therapy: the art of turning infectious agents into vehicles of therapeutics. *Nat. Med.* **7**, 33-40 (2001).
11. Nayak, S. & Herzog, R.W. Progress and prospects: immune responses to viral vectors. *Gene Ther.* **17**, 295-304 (2010).
12. Kasuya, T. & Kuroda, S. Nanoparticles for human liver-specific drug and gene delivery systems: in vitro and in vivo advances. *Expert Opin. Drug. Deliv.* **6**, 39-52 (2009).
13. Diaz-Moscoso, A., Balbuena, P., Gomez-Garcia, M., Ortiz Mellet, C., Benito, J.M., Le Gourrierec, L., Di Giorgio, C., Vierling, P., Mazzaglia, A., Micali, N., Defaye, J. & Garcia Fernandez, J.M. Rational design of cationic cyclooligosaccharides as efficient gene delivery systems. *Chem. Commun.*, 2001-2003 (2008).
14. Diaz-Moscoso, A., Le Gourrierec, L., Gomez-Garcia, M., Benito, J.M., Balbuena, P., Ortega-Caballero, F., Guilloteau, N., Di Giorgio, C., Vierling, P., Defaye, J.,

Ortiz Mellet, C. & Garcia Fernandez, J.M. Polycationic amphiphilic cyclodextrins for gene delivery: synthesis and effect of structural modifications on plasmid DNA complex stability, cytotoxicity, and gene expression. *Chem. Eur. J.* **15**, 12871-12888 (2009).

15. Diaz-Moscoso, A., Vercauteren D., Rejman, J., Benito, J.M., Ortiz Mellet, C., De Smedt, S.C. & Garcia Fernandez, J.M. Insights in cellular uptake mechanisms of pDNA-polycationic amphiphilic cyclodextrin nanoparticles (CDplexes). *J. Control. Release* **143**, 318-325.
16. Mendez-Ardoy, A., Urbiola, K., Aranda, C., Ortiz Mellet, C., Garcia Fernandez, J.M. & Tros de Ilarduya, C. Polycationic amphiphilic cyclodextrin-based nanoparticles for therapeutic gene delivery. *Nanomedicine* **6**, 1697-1707.
17. Mislick, K.A. & Baldeschwieler, J.D. Evidence for the role of proteoglycans in cation-mediated gene transfer. *Proc. Natl. Acad. Sci. USA* **93**, 12349-12354 (1996).
18. Baeuerle, P.A. & Huttner, W.B. Chlorate--a potent inhibitor of protein sulfation in intact cells. *Biochem. Biophys. Res. Commun.* **141**, 870-877 (1986).
19. Mounkes, L.C., Zhong, W., Cipres-Palacin, G., Heath, T.D. & Debs, R.J. Proteoglycans mediate cationic liposome-DNA complex-based gene delivery in vitro and in vivo. *J. Biol. Chem.* **273**, 26164-26170 (1998).
20. Diaz-Moscoso, A., Guilloteau, N., Bienvenu, C., Mendez-Ardoy, A., Blanco, J.L., Benito, J.M., Le Guirrerec, L., Di Giorgio, C., Vierling, P., Defaye, J., Ortiz Mellet, C. & Garcia Fernandez, J.M. Mannosyl-coated nanocomplexes from amphiphilic cyclodextrins and pDNA for site-specific gene delivery. *Biomaterials* **32**, 7263-7273.
21. Bernardes, G.J., Kikkeri, R., Maglinao, M., Laurino, P., Collot, M., Hong, S.Y., Lepenies, B. & Seeberger, P.H. Design, synthesis and biological evaluation of carbohydrate-functionalized cyclodextrins and liposomes for hepatocyte-specific targeting. *Org. Biomol. Chem.* **8**, 4987-4996 (2010).
22. Bianucci, A.M. & Chiellini, F. A 3D model for the human hepatic asialoglycoprotein receptor (ASGP-R). *J. Biomol. Struct. Dyn.* **18**, 435-451 (2000).
23. Wragg, S. & Drickamer, K. Identification of amino acid residues that determine pH dependence of ligand binding to the asialoglycoprotein receptor during endocytosis. *J. Biol. Chem.* **274**, 35400-35406 (1999).
24. Novikoff, P.M., Cammer, M., Tao, L., Oda, H., Stockert, R.J., Wolkoff, A.W. & Satir, P. Three-dimensional organization of rat hepatocyte cytoskeleton: relation to the asialoglycoprotein endocytosis pathway. *J. Cell Sci.* **109 (Pt 1)**, 21-32 (1996).
25. Geuze, H.J., Slot, J.W., Strous, G.J., Lodish, H.F. & Schwartz, A.L. Intracellular site of asialoglycoprotein receptor-ligand uncoupling: double-label immunoelectron microscopy during receptor-mediated endocytosis. *Cell* **32**, 277-287 (1983).
26. Schwartz, A.L. Trafficking of asialoglycoproteins and the asialoglycoprotein receptor. *Targeted Diagn. Ther.* **4**, 3-39 (1991).

27. Signoret, N., Christophe, T., Oppermann, M. & Marsh, M. pH-independent endocytic cycling of the chemokine receptor CCR5. *Traffic* **5**, 529-543 (2004).
28. DiPaola, M. & Maxfield, F.R. Conformational changes in the receptors for epidermal growth factor and asialoglycoproteins induced by the mildly acidic pH found in endocytic vesicles. *J. Biol. Chem.* **259**, 9163-9171 (1984).
29. Clarke, B.L., Oka, J.A. & Weigel, P.H. Degradation of asialoglycoproteins mediated by the galactosyl receptor system in isolated hepatocytes. Evidence for two parallel pathways. *J. Biol. Chem.* **262**, 17384-17392 (1987).
30. Sarkar, M., Liao, J., Kabat, E.A., Tanabe, T. & Ashwell, G. The binding site of rabbit hepatic lectin. *J. Biol. Chem.* **254**, 3170-3174 (1979).
31. Rice, K.G. & Lee, Y.C. Oligosaccharide valency and conformation in determining binding to the asialoglycoprotein receptor of rat hepatocytes. *Adv. Enzymol. Relat. Areas Mol. Biol.* **66**, 41-83 (1993).
32. Khorev, O., Stokmaier, D., Schwardt, O., Cutting, B. & Ernst, B. Trivalent, Gal/GalNAc-containing ligands designed for the asialoglycoprotein receptor. *Bioorg. Med. Chem.* **16**, 5216-5231 (2008).
33. Biessen, E.A., Bakkeren, H.F., Beuting, D.M., Kuiper, J. & Van Berkel, T.J. Ligand size is a major determinant of high-affinity binding of fucose- and galactose-exposing (lipo)proteins by the hepatic fucose receptor. *Biochem. J.* **299 (Pt 1)**, 291-296 (1994).
34. Zegers, M.M. & Hoekstra, D. Mechanisms and functional features of polarized membrane traffic in epithelial and hepatic cells. *Biochem. J.* **336 (Pt 2)**, 257-269 (1998).
35. Knowles, B.B., Howe, C.C. & Aden, D.P. Human hepatocellular carcinoma cell lines secrete the major plasma proteins and hepatitis B surface antigen. *Science* **209**, 497-499 (1980).
36. Haque, M.B., Roberts, B.P. & Tocher, D.A. Enantioselective radical-chain hydrosilylation of alkenes using homochiral thiols as polarity-reversal catalysts. *J. Chem. Soc. Perk. T 1*, 2881-2889 (1998).
37. Lubineau, A., Malleron, A. & Le Narvor, C. Chemo-enzymatic synthesis of oligosaccharides using a dendritic soluble support. *Tetrahedron Lett.* **41**, 8887-8891 (2000).
38. Li, G., Tajima, H. & Ohtani, T. An Improved Procedure for the Preparation of Isothiocyanates from Primary Amines by Using Hydrogen Peroxide as the Dehydrosulfurization Reagent. *J. Org. Chem.* **62**, 4539-4540 (1997).
39. Rejman, J., Tavernier, G., Bavarsad, N., Demeester, J. & De Smedt, S.C. mRNA transfection of cervical carcinoma and mesenchymal stem cells mediated by cationic carriers. *J. Control. Release* **147**, 385-391 (2010).
40. Xu, Y. & Szoka, F.C., Jr. Mechanism of DNA release from cationic liposome/DNA complexes used in cell transfection. *Biochem.* **35**, 5616-5623 (1996).
41. Breton, M., Leblond, J., Seguin, J., Midoux, P., Scherman, D., Herscovici, J., Pichon, C. & Mignet, N. Comparative gene transfer between cationic and thiourea lipoplexes. *J. Gene Med.* **12**, 45-54 (2010).

42. Gref, R., Luck, M., Quellec, P., Marchand, M., Dellacherie, E., Harnisch, S., Blunk, T. & Muller, R.H. 'Stealth' corona-core nanoparticles surface modified by polyethylene glycol (PEG): influences of the corona (PEG chain length and surface density) and of the core composition on phagocytic uptake and plasma protein adsorption. *Colloids Surf. B. Biointerfaces* **18**, 301-313 (2000).
43. Kichler, A., Leborgne, C., Coeytaux, E. & Danos, O. Polyethylenimine-mediated gene delivery: a mechanistic study. *J. Gene Med.* **3**, 135-144 (2001).
44. Rejman, J., Bragonzi, A. & Conese, M. Role of clathrin- and caveolae-mediated endocytosis in gene transfer mediated by lipo- and polyplexes. *Mol. Ther.* **12**, 468-474 (2005).
45. Rejman, J., Conese, M. & Hoekstra, D. Gene transfer by means of lipo- and polyplexes: role of clathrin and caveolae-mediated endocytosis. *J. Liposome Res.* **16**, 237-247 (2006).
46. Goncalves, C., Mennesson, E., Fuchs, R., Gorvel, J.P., Midoux, P. & Pichon, C. Macropinocytosis of polyplexes and recycling of plasmid via the clathrin-dependent pathway impair the transfection efficiency of human hepatocarcinoma cells. *Mol. Ther.* **10**, 373-385 (2004).
47. Fujimoto, T., Kogo, H., Nomura, R. & Une, T. Isoforms of caveolin-1 and caveolar structure. *J. Cell Sci.* **113 Pt 19**, 3509-3517 (2000).
48. Lechardeur, D., Sohn, K.J., Haardt, M., Joshi, P.B., Monck, M., Graham, R.W., Beatty, B., Squire, J., O'Brodovich, H. & Lukacs, G.L. Metabolic instability of plasmid DNA in the cytosol: a potential barrier to gene transfer. *Gene Ther.* **6**, 482-497 (1999).
49. Oka, J.A. & Weigel, P.H. Recycling of the asialoglycoprotein receptor in isolated rat hepatocytes. Dissociation of internalized ligand from receptor occurs in two kinetically and thermally distinguishable compartments. *J. Biol. Chem.***258**, 10253-10262 (1983).
50. Weigel, P.H., Clarke, B.L. & Oka, J.A. The hepatic galactosyl receptor system: two different ligand dissociation pathways are mediated by distinct receptor populations. *Biochem. Biophys. Res. Commun.* **140**, 43-50 (1986).
51. Guo, W. & Lee, R.L. Receptor-targeted gene delivery via folate-conjugated polyethylenimine. *AAPS Pharm. Sci.* **1**, E19 (1999).
52. Brown, M.D., Gray, A.I., Tetley, L., Santovena, A., Rene, J., Schatzlein, A.G. & Uchegbu, I.F. In vitro and in vivo gene transfer with poly(amino acid) vesicles. *J. Control. Release* **93**, 193-211 (2003).
53. Frisch, B., Carriere, M., Largeau, C., Mathey, F., Masson, C., Schuber, F., Scherman, D. & Escriou, V. A new triantennary galactose-targeted PEGylated gene carrier, characterization of its complex with DNA, and transfection of hepatoma cells. *Bioconjug. Chem.* **15**, 754-764 (2004).
54. Ortiz Mellet, C., Garcia Fernandez, J.M. & Benito, J.M. Cyclodextrin-based gene delivery systems. *Chem. Soc. Rev.* **40**, 1586-1608 (2011).
55. Nguyen, T.H., Pages, J.C., Farge, D., Briand, P. & Weber, A. Amphotropic retroviral vectors displaying hepatocyte growth factor-envelope fusion

proteins improve transduction efficiency of primary hepatocytes. *Hum. Gene Ther.* **9**, 2469-2479 (1998).

SUMMARY

Theoretically, gene therapy could cure any genetic disease. This notion gave hope to all the patients which cannot be cured by current conventional therapies. Cystic fibrosis (CF), for example, is a severe chronic disease which harshly restricts patients' quality of life. The average life expectancy of CF patients increased over the years and lies between 40 and 50 years now. CF is a recessive genetic disorder caused by a mutation in the cystic fibrosis transmembrane conductance regulator (*CFTR)* gene. The most common mutation is a deletion of three nucleotides which leads to the loss of phenylalanine at position 508 of the protein. Since the disease is caused by a single mutation, CF was one of the first diseases investigated as a potential target of a gene-therapeutic strategy. The very simple concept of introducing a normal healthy copy of the *CFTR* gene into affected cells, turned out to be more challenging than expected. Different viral vectors have been tested for their possible application in CF gene therapy. The use of adenoviral vectors was restricted by the immune responses they evoked. Sendai virus-derived vectors ensured only transient transfection and repeated administration led to production of neutralizing antibodies against the vector. Lentiviral vectors pseudotyped with the vesicular stomatitis virus glycoprotein G (VSV-G) failed to efficiently transfer genetic material into murine epithelia *in vivo*. It has been suggested that immune response-related concerns could be overcome by employing non-viral carriers. It should be stressed, however, that even though they have been developed and characterized for decades now, they are still far less efficient than their viral counterparts. The initial 'trial and error' approach did not result in development of efficient non-viral carriers. It was realized soon that only a rational design based on thorough and detailed knowledge of cell biology, molecular biology, immunology and virology could lead to the design of safe and efficient non-viral carriers.

This thesis focuses on better understanding of the intracellular barriers involved in the process of non-viral delivery of plasmid DNA (pDNA) and potential approaches to overcome them. The first step in the transfection process is the interaction of non-viral particles carrying pDNA with the plasma membrane, followed by their endocytic uptake by the cells. Since endocytosis eventually delivers the internalized material to the acidic lysosomal compartment where it will be degraded, the pDNA-containing complexes have to escape from the endosomal compartment before this starts to acidify. In addition, the pDNA needs to be released from the complexes. Once released from the complexes, pDNA needs to travel through the crowded and viscous cytoplasm, where it is prone to degradation by DNases, toward the nucleus. For that reason it would be ideal if the pDNA-carrying nanoparticles or the pDNA are only

released from the endosomal compartment once they reach the perinuclear region. Since pDNA cannot be transported through the nuclear pore complexes (NPCs) due to its size limitations, cell division is needed to lead to successful delivery of the pDNA to the nucleoplasm. Even then, however, transcription of the DNA into mRNA is not guaranteed. For the introduced gene to be properly expressed, pDNA enclosed in the daughter nuclei should still be able to reach transcription-active sites.

Chapter 1 reviews current knowledge on the intracellular partitioning of cell organelles (endosomal vesicles, Golgi apparatus, endoplasmic reticulum and nucleus), foreign macromolecules (dextrans and pDNA), inert nanoparticles (gold, quantum dot, polystyrene and iron oxide) and gene delivery nanoparticles (lipid- or polymer-based) during mitosis. Moreover, it provides an overview on means by which some retroviruses make use of mitosis to deliver their genome into the nucleus and on how latent DNA viruses segregate their episomes to the progeny of host cells. This knowledge is employed to reflect on possible strategies for the improvement of nuclear inclusion of exogenous pDNA or nanoparticles in dividing cells. We propose to exploit the mitotic spindle, the NPCs, the inner nuclear membrane (INM) elements or the nuclear lamina to ensure inclusion of pDNA or nanoparticles in the newly formed daughter nuclei. Another strategy involves the development of cell division-responsive nanoparticles which would be able to release their pDNA at the onset of mitosis. This approach would guarantee pDNA protection until the moment it gets a chance to be enclosed in the nucleus. Another approach implies coupling of viral or non-viral chromatin-targeting peptides which could allow nanoparticles or pDNA to be strongly bound to the condensed chromosomes during mitosis and eventually be enclosed in the daughter nuclei.

We evaluated the latter strategy in **chapter 2**. First, the nuclear inclusion of polystyrene beads with different sizes (100, 200 and 500 nm) and charges (positively or negatively charged or coated with polyethylene glycol (PEG)) was assessed in the *Xenopus* nuclear envelope reassembly (XNER) model. In this model, functional artificial nuclei are formed by mixing cytosolic extract, chromatin, membrane extract and an energy-providing solution. We observed that the combination of small size and positive charge results in the most effective nuclear inclusion. Therefore, we chose to modify the polystyrene beads of 100 nm with the chromatin-binding peptide sequences of Mel-28 (maternal effect lethal 28) or HMGA2β (high mobility group AT-hook 2 isoform β). Also polyethylene imine (PEI), which is the reference polymer to complex pDNA in non-viral gene delivery modalities, was modified with these peptides. This modification improved the inclusion of the polystyrene beads and the PEI/pDNA polyplexes in the artificial nuclei by two- to three-fold. When these

nanoparticles were microinjected in the cytoplasm of living HeLa cells, however, inclusion in the nuclei of dividing cells was never observed. Both types of nanoparticles accumulated in lysosomes located at the perinuclear region. The nature of the mechanism that prevents the nuclear inclusion of nanoparticles in living cells is a topic that requires further research. This additional barrier, which appears to be a protection mechanism of the cell against foreign material, should be overcome before the potential of the chromatin-binding peptides could be evaluated in living cells.

In **chapter 3**, another strategy to improve non-viral mediated transfection efficiency was evaluated. We demonstrated that coding pDNA within Lipofectamine lipoplexes can be partly replaced by non-coding pDNA without a drop in transfection efficiency. We observed that non-coding pDNA without immunogenic unmethylated CpG motives had even a slightly higher positive effect. However, the use of non-coding salmon DNA instead had an antagonistic effect on the transfection levels. Also linearized and partly digested non-coding pDNA had a negative effect. Consequently, we concluded that only the co-delivery of supercoiled non-coding pDNA with the coding pDNA within lipoplexes results in increased transfection efficiencies. Further, we investigated why this supercoiled non-coding pDNA increases transfection efficiency while non-coding salmon DNA decreases it. To that end we studied in detail the events which occur at each single step of the transfection process. Our data indicated that, the release of coding pDNA from the endosomal compartment continues over a longer period of time if the lipoplexes co-deliver supercoiled non-coding pDNA. Knowing that the cytosolic half-life of naked pDNA hardly exceeds ninety minutes, this sustained release increases the chance that intact pDNA is present in the cytoplasm when cell division occurs. This results in the transfection of a larger fraction of the cell population. By contrast, the endosomal release of coding pDNA from lipoplexes co-delivering non-coding salmon DNA seems to be much faster and therefore of shorter duration so that only a relatively small fraction of the cells is transfected.

In **chapter 4**, we addressed a more application-oriented aspect of this thesis, i.e. the evaluation of galactosylated polycationic amphiphilic cyclodextrins (paCDs) as non-viral pDNA-carriers to specifically transfect hepatocytes. We chose HepG2 cells as model cells for *in vivo* hepatocytes. In first experiments, attempts to transfect these cells with pDNA complexed to different CDs (CDplexes) resulted in hardly any transfection. To identify a cause of this failure, we performed a series of additional experiments. These allowed us to conclude that HepG2 cells efficiently internalize the CDplexes and that these CDplexes do not end up in the endosomal compartment but

that they are released into the cytosol, as required. Further, we showed that the problem also does not reside in a lack of release of pDNA from the CDplexes. This left us with the option that the nuclear envelope is the major obstacle for efficient transfection of HepG2 cells with pDNA. To confirm this hypothesis, we transfected HepG2 cells with mRNA-CDplexes instead of pDNA-CDplexes. As mRNA only needs to reach the cytosol to be translated, there is no need for the mRNA-CDplexes to reach the nucleoplasm. Within this approach, we transfected up to 31% of the HepG2 cells. Moreover, we showed that the galactosylated mRNA-CDplexes are specifically taken up via asialoglycoprotein receptor (ASGPr)-mediated endocytosis. Therefore, we believe that mRNA-CDplexes may represent a promising platform for specific and efficient transfection of hepatocytes *in vivo*. Moreover, mRNA presented itself as an alternative to pDNA to ensure efficient transfection of non-dividing or slowly dividing cells.

CONCLUSIONS

In conclusion, the work described in this thesis on one hand has broadened our knowledge about the processes of cell transfection by non-viral means, but on the other hand raised new important questions about intracellular barriers in non-viral gene delivery. Our results repeatedly pointed at **the nuclear envelope as a major barrier for efficient delivery of nanoparticles or pDNA to the nucleoplasm**. It became apparent that there is a mechanism which prevents that nanoparticles are enclosed in the newly formed nuclei of dividing cells. Moreover, we observed that **not only the total concentration of delivered pDNA determines transfection efficiency, but also the way this pDNA is released into the cell cytoplasm**. It appears that to ensure high levels of transfection, **pDNA should be released from the endosomal compartment in a continuous, slow manner over a long period of time**. Further, we showed that **galactosylated paCDs are efficient carriers of mRNA to specifically transfect hepatocytes**. The use of mRNA instead of pDNA presented a good alternative to transfect slowly dividing cells.

SAMENVATTING

In theorie zou gentherapie elke genetische aandoening moeten kunnen genezen. Dit gegeven geeft hoop aan alle patiënten die niet genezen kunnen worden met de huidige traditionele behandelingen. Een voorbeeld van zo'n genetische aandoening die nog niet genezen kan worden, is de ernstige chronische ziekte cystische fibrose (CF). CF vermindert de levenskwaliteit van de patiënt sterk. Hun gemiddelde levensverwachting is gaandeweg toegenomen en ligt nu tussen 40 en 50 jaar. CF is een recessieve genetische aandoening die veroorzaakt wordt door een mutatie in het gen coderend voor de 'cystic fibrosis transmembrane conductance regulator' (CFTR). De meest voorkomende mutatie is een deletie van drie nucleotiden waardoor het aminozuur phenylalanine ontbreekt op plaats 508 van het eiwit. Omdat CF wordt veroorzaakt door slechts één mutatie, was het een van de eerste ziekten die bestudeerd werd als mogelijke kandidaat voor gentherapie. Het lijkt heel eenvoudig om het gezonde gen toe te dienen aan de zieke cellen, maar dit blijkt een grotere uitdaging te zijn dan verwacht. Verschillende virale vectoren werden getest op hun potentiële gebruik in gentherapie bij CF. Het gebruik van adenovirale vectoren werd beperkt omdat deze immuunreacties uitlokken. Vectoren afgeleid van het Sendaivirus konden enkel een tijdelijke transfectie garanderen en herhaalde toediening leidde tot de aanmaak van neutraliserende antilichamen tegen de vector. Lentivirale vectoren, die een pseudotypering met het 'vesicular stomatitis virus glycoprotein G (VSV-G)' ondergingen, slaagden er niet in het genetische materiaal efficiënt over te brengen in *in vivo* epithelia van de muis. Er werd toen gesuggereerd dat het gebruik van niet-virale vectoren de ongerustheid en de problemen gerelateerd aan de ongewilde immuunreacties zou kunnen overwinnen. Hierbij moet benadrukt worden dat deze niet-virale vectoren ondanks de tientallen jaren van ontwikkeling en karakterisering helemaal nog niet zo efficiënt zijn als virale vectoren. De initiële 'trial and error' benadering resulteerde niet in de ontwikkeling van efficiënte niet-virale vectoren. Men zag al snel in dat enkel een weldoordachte aanpak gebaseerd op een grondige kennis van de celbiologie, moleculaire biologie, immunologie en virologie zou kunnen leiden tot de ontwikkeling van veilige en efficiënte niet-virale vectoren.

Dit proefschrift stelt zich tot doel een beter inzicht te krijgen in de intracellulaire barrières bij het niet-virale toedieningsproces van plasmide DNA (pDNA), alsook de verschillende manieren om deze barrières te overwinnen. De eerste stap van het transfectieproces is de interactie van de niet-virale partikels, die het pDNA bevatten, met de plasmamembraan van de cel. Hierop volgt de opname van de pDNA-partikels in de cel waardoor die zich in endosomen bevinden. Omdat het opgenomen materiaal uiteindelijk naar de zure lysosomen wordt geleid waar het zal worden

afgebroken, moeten de pDNA-partikels of het pDNA uit de endosomen kunnen ontsnappen vooraleer die verzuring optreedt. Daarbovenop moet het pDNA ook worden vrijgesteld van zijn niet-virale dragers. Waarna het pDNA zich moet begeven naar de nucleus van de cel doorheen het dichte cytoplasma waar het ook is blootgesteld aan afbraak door DNasen. Daarom zou het ideaal zijn als de pDNA-partikels slechts werden vrijgesteld uit de endosomen eenmaal ze de perinucleaire regio hebben bereikt. Het pDNA kan niet doorheen de nucleaire poriecomplexen (NPCs) worden getransporteerd omwille van de gelimiteerde poriegrootte. Er is dus een celdeling nodig opdat het pDNA het nucleoplasma kan bereiken, maar zelfs dan is de transcriptie van het pDNA naar mRNA niet gegarandeerd. Het geïntroduceerde gen moet namelijk transcriptie-actieve regio's in dat nucleoplasma kunnen bereiken om tot expressie te worden gebracht.

Hoofdstuk 1 geeft een overzicht van de huidige kennis over de intracellulaire verdeling van celorganellen (endosomale vesikels, Golgi-apparaat, endoplasmatisch reticulum en nucleus), oneigen macromoleculen (dextranen en pDNA), inerte nanopartikels (goud, 'quantum dot', polystyreen en ijzeroxide) en gentherapienanopartikels (lipide- of polymeergebaseerd) gedurende mitose. Ook wordt beschreven op welke manier sommige retrovirussen gebruik maken van de mitose van hun gastheercel om hun genoom in de nucleus te brengen. Tevens komt aan bod hoe latente DNA-virussen hun episomen verdelen over de dochtercellen van de gastheercel. Deze kennis is nodig om strategieën te ontwikkelen om de nucleaire insluiting van exogene nanopartikels of pDNA in delende cellen te verbeteren. We stellen voor gebruik te maken van de mitotische spilfiguur, de NPCs, de elementen van de binnenste membraan van de nucleus of de nucleaire lamina om de insluiting van nanopartikels of pDNA in de nieuwgevormde dochternuclei te kunnen verzekeren. Een ander voorstel is het ontwikkelen van celdelingsgevoelige nanopartikels die hun pDNA vrijstellen aan de start van de mitose. Op die manier zou het pDNA beschermd worden tot op het moment dat het een kans krijgt om ingesloten te worden in de nucleus. Een andere strategie is het koppelen van virale of niet-virale chromatinebindende peptiden aan de nanopartikels of het pDNA. Dit zou ervoor zorgen dat de nanopartikels of het pDNA sterk binden met de gecondenseerde chromosomen tijdens de mitose zodat ze uiteindelijk worden ingesloten in de dochternuclei.

Deze laatste strategie evalueerden we in **hoofdstuk 2**. Eerst werd de nucleaire insluiting van polystyreensfeertjes met verschillende groottes (100, 200 en 500 nm) en ladingen (positief of negatief geladen of gecoat met polyethyleenglycol (PEG)) bepaald in het '*Xenopus* nuclear envelope reassembly' (XNER) model. Hierbij worden

functionele artificiële nuclei gevormd door het mengen van cytosolisch extract, chromatine, membraanextract en een energieleverende oplossing. We observeerden dat de combinatie van de kleinste grootte en een positieve lading leidden tot de meeste nucleaire insluiting. Daarom besloten we de polystyreensfeertjes van 100 nm te modificeren met de chromatinebindende peptidesequenties van Mel-28 ('maternal effect lethal 28') of HMGA2β ('high mobility group AT-hook 2 isoform β'). Ook polyethyleenimine (PEI), dat het referentiepolymeer is om pDNA te complexeren in niet-virale gentherapie, werd gemodificeerd met deze peptiden. Deze modificatie verbeterde de nucleaire insluiting van polystyreensfeertjes en PEI/pDNA-partikels met een factor twee tot drie. Hierna werden deze twee types nanopartikels geïnjecteerd in het cytoplasma van levende HeLa-cellen. Insluiting van de nanopartikels in de nuclei van delende cellen werd echter nooit vastgesteld. De twee types nanopartikels accumuleerden in lysosomen in de perinucleaire regio. Het mechanisme dat verhindert dat de nanopartikels worden ingesloten in de nuclei van levende cellen vereist verder onderzoek. Deze bijkomende barrière, die een beschermingsmechanisme van de cel tegenover oneigen materiaal blijkt te zijn, zal overwonnen moeten worden vooraleer het potentieel van de chromatinebindende peptiden in levende cellen kan worden beoordeeld.

Een andere strategie om niet-virale transfectie-efficiëntie te verhogen werd geëvalueerd in **hoofdstuk 3**. We toonden aan dat coderend pDNA in Lipofectamine-partikels deels kan worden vervangen door niet-coderend pDNA zonder dat de transfectie-efficiëntie daalt. We observeerden dat niet-coderend pDNA zonder de immunogene niet-gemethyleerde CpG-motieven zelfs een enigszins hoger positief effect had. Het gebruik van niet-coderend zalm-DNA, daarentegen had een antagonistisch effect op de transfectie-efficiëntie. Ook lineair en gefragmenteerd niet-coderend pDNA hadden een negatief effect. Bijgevolg concluderen we dat enkel de gezamenlijke toediening van 'supercoiled' niet-coderend pDNA met het coderend pDNA leidt tot hogere transfectie-efficiënties. Verder onderzochten we waarom het supercoiled niet-coderend pDNA de transfectie-efficiëntie verhoogt terwijl het niet-coderend zalm-DNA de transfectie-efficiëntie verlaagt. We bestudeerden daartoe in detail wat er gebeurt tijdens elke stap van het transfectieproces. Onze resultaten wijzen uit dat de vrijstelling van het coderend pDNA uit de endosomen wellicht plaatsvindt over een langere periode als de partikels supercoiled niet-coderend pDNA mee toedienen. Als er rekening wordt gehouden met de cytosolische halfwaardetijd van pDNA die hoogstens negentig minuten is, dan verhoogt de langdurige vrijstelling van pDNA de kans dat er intact pDNA aanwezig is in het cytosol op het moment dat een celdeling plaatsvindt. Dit heeft de transfectie van een grotere fractie van de

celpopulatie tot gevolg. Een merkwaardig contrast daarmee wordt gezien indien de partikels niet-coderend zalm-DNA mee toedienen. De vrijstelling uit de endosomen blijkt in dat geval veel sneller te zijn en daardoor van kortere duur zodat slechts een relatief kleine fractie van de cellen getransfecteerd wordt.

Hoofdstuk 4 is meer toepassingsgericht. We evalueerden polykationische amfifiele cyclodextrines (paCDs) gemodificeerd met galactose als niet-virale pDNA-dragers voor de specifieke transfectie van hepatocyten. We maakten de keuze om HepG2-cellen te gebruiken als modelcellen voor *in vivo* hepatocyten. Tijdens de eerste experimenten resulteerden de pogingen om deze cellen te transfecteren met pDNA gecomplexeerd met verschillende paCDs (CDplexen) nauwelijks in transfectie. Om de oorzaak van dit falen te achterhalen voerden we een serie van additionele experimenten uit. Daaruit concludeerden we dat HepG2-cellen op een efficiënte manier CDplexen opnemen en dat deze CDplexen niet vast blijven zitten in de endosomen maar dat ze zoals vereist vrijgesteld worden in het cytoplasma. Verder zagen we dat ook de vrijstelling van het pDNA uit de CDplexen geen probleem vormt. Dit deed ons geloven dat de nucleaire membraan de belangrijkste barrière vormt voor efficiënte transfectie van HepG2-cellen met pDNA. Om dit te bevestigen transfecteerden we HepG2-cellen met mRNA-CDplexen in plaats van pDNA-CDplexen. Omdat mRNA enkel het cytosol hoeft te bereiken om getransleerd te worden, is er geen reden voor de mRNA-CDplexen om het nucleoplasma te bereiken. Op deze manier slaagden we erin 31% van de HepG2-cellen te transfecteren. Bovendien toonden we aan dat mRNA-CDplexen gemodificeerd met galactose specifiek worden opgenomen in de HepG2-cellen via 'asialoglycoprotein receptor (ASGPr)'-gemedieerde endocytose. Daarom nemen we aan dat mRNA-CDplexen veelbelovend zijn voor de specifieke en efficiënte transfectie van *in vivo* hepatocyten. mRNA werd bovendien als alternatief gepresenteerd voor pDNA om een efficiënte transfectie te garanderen van niet-delende of traag-delende cellen.

BESLUITEN

We concluderen dat het werk beschreven in deze thesis enerzijds onze kennis over de processen tijdens de niet-virale transfectie van cellen heeft vergroot, maar anderzijds nieuwe belangrijke vragen heeft doen rijzen over intracellulaire barrières in niet-virale gentherapie. Onze resultaten toonden meermaals aan dat **de nucleaire membraan een voorname barrière vormt voor de efficiënte toediening van nanopartikels of pDNA aan het nucleoplasma**. Het werd duidelijk dat er een mechanisme is dat verhindert dat nanopartikels worden ingesloten in de

nieuwgevormde kernen van delende cellen. Bovendien observeerden we dat niet alleen **de totale concentratie van toegediend pDNA de transfectie-efficiëntie bepaalt, maar dat ook de manier waarop het pDNA wordt vrijgesteld in het cytoplasma van belang is**. Onze resultaten indiceren dat **pDNA moet worden vrijgesteld vanuit de endosomen op een continue langzame manier over een lange periode om hoge transfectie-efficiëntie te verzekeren**. Verder toonden we aan dat **paCDs gemodificeerd met galactose efficiënte niet-virale vectoren zijn van mRNA voor de specifieke transfectie van hepatocyten**. Het gebruik van mRNA in plaats van pDNA kwam naar voren als een goed alternatief om traag-delende cellen te transfecteren.

CURRICULUM VITAE

PERSONALIA

Nathalie Symens
12 augustus 1984 in Torhout (Belgium)

Ichtegemsestraat 2, 8211 Aartrijke, Belgium
Mobile phone: (+32)494 04 87 72
symensnathalie@hotmail.com

EDUCATION

Ph.D. Student in Pharmaceutical Sciences (2007-present)
Laboratory for General Biochemistry and Physical Pharmacy (Ghent University)
Promoter: Prof. dr. Stefaan De Smedt
Co-promoters: dr. Katrien Remaut and dr. Joanna Rejman

Additional certificate
FELASA C: Laboratory Animal Science I and II (Ghent University) (academic year 2010-2011)

Bioscience Engineer Cell and Gene Biotechnology (2002 - 2007) (Ghent University)

Master thesis (July 2006 – June 2007)
Laboratory for Cytogenetics (Center for Medical Genetics - University Hospital Ghent)
'Hoge resolutie moleculair-cytogenetisch onderzoek van patiënten met een proportionele kleine gestalte'
Promoters: Prof. dr. Godelieve Gheysen and Prof. dr. Franki Speleman
Supervisor: dr. Karen Buysse

Internship (September 2005)
General analytical laboratory Chemiphar N.V. (Bruges)
'Validatie en optimalisatie van het gebruik van de MicroSeq 500 16S rDNA bacterial identification kit (Applied Biosystems)'
Supervisors: Prof. dr. Mieke Uyttendaele and Lic. Yves De Bleecker

INTERNATIONAL PEER REVIEWED PUBLICATIONS

K. Remaut, N. Symens, B. Lucas, J. Demeester & S.C. De Smedt. Efficient delivery of intact phosphodiester oligonucleotides by poly-β-amino esters. *Journal of Controlled Release* (2010), **144** (1), 65-74.
http://dx.doi.org/10.1016/j.jconrel.2010.01.028. (IF_{2011} 6.499)

N. Symens, R. Walczak, J. Demeester, I. Mattaj, S.C. De Smedt and K. Remaut. Nuclear inclusion of nontargeted and chromatin-targeted polystyrene beads and plasmid DNA-containing nanoparticles. *Molecular Pharmaceutics* (2011), **8** (5), 1757-1766. http://dx.doi.org/10.1021/mp200120v. (IF_{2011} 4.782)

N. Symens, S.J. Soenen, J. Rejman, K. Braeckmans, S.C. De Smedt and K. Remaut. Intracellular partitioning of cell organelles and extraneous nanoparticles during mitosis. *Advanced Drug Delivery Reviews* (2012), **64** (1), 78-94. http://dx.doi.org/10.1016/j.addr.2011.11.012. (IF_{2011} 11.502)

N. Symens, A. Méndez-Ardoy, A. Díaz-Moscoso, E. Sánchez-Fernández, K. Remaut, J. Demeester, J.M. García Fernández, S.C. De Smedt and J. Rejman. Efficient transfection of hepatocytes mediated by mRNA complexed to galactosylated cyclodextrins. *Bioconjugate Chemistry* (2012), **23** (6), 1276-1289 http://dx.doi.org/10.1021/bc3001003. (IF_{2011} 4.930)

N. Symens, J. Rejman, B. Lucas, J. Demeester, S.C. De Smedt and K. Remaut. How does non-coding DNA increase lipofection efficiency in HeLa cells? *(submitted manuscript).*

INTERNATIONAL PEER REVIEWED ABSTRACTS

N. Symens, R. Walczak, J. Demeester, I. Mattaj, S.C. De Smedt and K. Remaut. Nuclear inclusion of inert and chromatin-targeted polystyrene beads and plasmid DNA containing particles. *Drug Discovery Today* (2010), **12** (23-23), 1082-1083. http://dx.doi.org/10.1016/j.drudis.2010.09.360. (CDTM Cardiff)

N. Symens, R. Walczak, J. Demeester, I. Mattaj, S.C. De Smedt and K. Remaut. Nuclear inclusion of inert and chromatin-targeted polystyrene spheres and plasmid DNA containing particles. *Journal of Controlled Release* (2010), **148** (1), E96-E98. http://dx.doi.org/10.1016/j.jconrel.2010.07.071. (CRS Portland)

N. Symens, A. Méndez-Ardoy, J.M. García Fernández, S.C. De Smedt and J. Rejman. Galactosylated polycationic amphiphilic cyclodextrins for transfection of hepatocytes. *Human Gene Therapy* (2011), **22** (10), A122-A123. (ESGCT/BSGT Brighton)

ORAL OR POSTER PRESENTATIONS (presenting author)

N. Symens, R. Walczak, J. Demeester, I. Mattaj, S.C. De Smedt and K. Remaut. Enclosure of inert nanospheres in artificial nuclei, a matter of size or zeta-potential? 2nd ESF/UB European Summer School in Nanomedicine, Cascais (Portugal), 12th-16th June 2009.

N. Symens, R. Walczak, J. Demeester, I. Mattaj, S.C. De Smedt and K. Remaut. Nuclear inclusion of inert and chromatin-targeted polystyrene beads and plasmid DNA containing nanoparticles. 8th International Conference and Workshop on Biological

Barriers: *in vitro* Tools, Nanotoxicology and Nanomedicine (Meditrans conference). Saarbrücken (Germany), 21th March-1st April 2010.

N. Symens, R. Walczak, J. Demeester, I. Mattaj, S.C. De Smedt and K. Remaut. Nuclear inclusion of inert and chromatin-targeted polystyrene beads and plasmid DNA containing nanoparticles. 11th European Symposium on Controlled Drug Delivery, Egmond aan Zee (The Netherlands), 7th-9th April 2010. (**Jan Feijen Poster award)**

N. Symens, R. Walczak, J. Demeester, I. Mattaj, S.C. De Smedt and K. Remaut. Nuclear inclusion of inert and chromatin-targeted polystyrene beads and plasmid DNA containing nanoparticles. 3th International symposium: Cellular delivery of therapeutic molecules (CDTM), Cardiff (Wales), 26th-29th June 2010.

N. Symens, R. Walczak, J. Demeester, I. Mattaj, S.C. De Smedt and K. Remaut. Nuclear inclusion of inert and chromatin-targeted polystyrene beads and plasmid DNA containing nanoparticles. 37th annual meeting and exposition of the controlled release society (CRS), Portland (Oregon, USA), 10th-14th July 2010.

N. Symens, R. Walczak, J. Demeester, I. Mattaj, S.C. De Smedt and K. Remaut. Nuclear inclusion of inert and chromatin-targeted polystyrene beads and plasmid DNA containing nanoparticles. Advanced light microscopy symposium (ALM), Ghent (Belgium), 23th-24th September 2010.

K. Remaut, N. Symens, R. Vandenbroucke, B. Lucas and S.C. De Smedt, Plasmid transfer to the nucleus. ESF-UB conference: Nanomedicine, Sant Feliu de Guixols (Spain), 23th-28th October 2010.

N. Symens, R. Walczak, J. Demeester, I. Mattaj, S.C. De Smedt and K. Remaut. Nuclear inclusion of inert and chromatin-targeted polystyrene beads and plasmid DNA containing nanoparticles. 15th International Symposium on Recent Advances in Drug Delivery Systems: Drug delivery 's New Directions in a New Decade, Salt Lake City (Utah, USA), 13th-16th February 2011.

N. Symens, R. Walczak, J. Demeester, I. Mattaj, S.C. De Smedt and K. Remaut. Nuclear inclusion of non-targeted and chromatin-targeted nanoparticles. 15th Forum of Pharmaceutical Sciences (Belgian Society of Pharmaceutical Sciences), Spa (Belgium), 12th-13th May 2011.

N. Symens, A. Méndez-Ardoy, J.M. García Fernández, S.C. De Smedt and J. Rejman. Galactosylated polycationic amphiphilic cyclodextrins for transfection of hepatocytes. The European Society of Gene and Cell Therapy and British Society of Gene Therapy Collaborative Congress (ESGCT/BSGT), Brighton (UK), 26th-31th October 2011.

RESEARCH VISIT

14th-18th January 2008: Mattaj Group (EMBL, Heidelberg, Germany) to learn the *Xenopus* nuclear envelope reassembly (XNER) assay